FINDING SUITABLE FEATURE EXTRACTION METHOD FOR CONDITION MONITORING OF ELECTRICAL EQUIPMENT

By

Synthia Hossain Karobi
Student ID: 17121049
Tahmidur Rahman
Student ID: 17121071
Md Shoaib Khoshnabish
Student ID: 17121078
Swarup Kumar Dey
Student ID: 16221022

A thesis submitted to the Department of Electrical and Electronic Engineering in partial
fulfillment of the requirements for the degree of
Bachelor of Science in Electrical and Electronic Engineering

Department of Electrical and Electronic Engineering
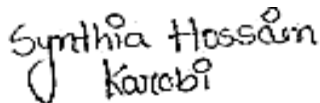Brac University
June, 2021

i

Declaration

It is hereby declared that

1. The thesis submitted is our own original work while completing degree at Brac University.

2. The thesis does not contain material previously published or written by a third party, except where this is appropriately cited through full and accurate referencing.

3. The thesis does not contain material which has been accepted, or submitted, for any other degree or diploma at a university or other institution.

4. We have acknowledged all main sources of help.

Student's Full Name & Signature:

Synthia Hossain Karobi	**Tahmidur Rahman**
Student ID: 17121049	Student ID: 17121071
Md Shoaib Khoshnabish	**Swarup Kumar Dey**
Student ID: 17121078	Student ID: 16221022

Approval

The thesis titled "Finding Suitable Feature Extraction Method for Condition Monitoring of Electrical Equipment" submitted by

1. Synthia Hossain Karobi (Student ID: 17121049)
2. Tahmidur Rahman (Student ID: 17121071)
3. Shoaib Khoshnabish (Student ID: 17121078)
4. Swarup Kumar Dey (Student ID: 16221022)

of Spring, 2021 has been accepted as satisfactory in partial fulfillment of the requirement for the degree of Bachelor of Science in Electrical and Electronic Engineering on June 9, 2021.

Examining Committee:

Supervisor:
(Member)

_____
Dr. A. S. Nazmul Huda
Assistant Professor, Department Of
Electrical and Electronic Engineering
Brac University

Thesis Coordinator:
(Member)

_____
Dr. Abu S.M. Mohsin
Assistant Professor, Department Of
Electrical and Electronic Engineering
Brac University

Departmental Head:
(Chair)

_____
Dr. Md. Mosaddequr Rahman
Professor and Chairperson, Department Of
Electrical and Electronic Engineering
Brac University

Abstract

The degradation of electrical equipment caused by excessive temperature rise leading to the failure of a total electrical system can be reduced by the thermal monitoring of the equipment. Manual analysis of thermal images is time-consuming, cost-effective and can cause injuries or health damages. Therefore, building an automated fault diagnosis system plus selecting the suitable features for developing that system is essential. As there are several feature extraction methods and applying all of them to identify suitable features is time-consuming and creates extra loads on the automated system, choosing one efficient method for feature extraction is necessary. This study actually shows the comparison among different texture feature extraction techniques and find the best one by using Machine Learning. After extracting different features using different methods from thermal images of electrical equipment, firstly, supervised learning was used along with Random Forest as a classifier and then training-testing data were used to train the machine and predict the segmented regions of the pictures. The study result shows that using Gray-Level Co-Occurrence Matrix as feature extracting method gave the most accuracy and less error in the performance analysis algorithm. Finally, the condition of the electrical equipment is also predicted whether it was faulty or normal in addition to which feature extracting method provides most accuracy.

Keywords: Infrared Thermography; Texture Analysis; Co-occurrence Matrix; Condition Monitoring; Region of Interest; Feature Extraction; Auto Regression; Moment Binary; Gradient; Level Run-length Matrix.

Dedication

We would like to dedicate our thesis to all the teachers we have faced till now, without their

love, support, help and encouragement we could not reach this far.

Acknowledgement

Table of Contents

List of Tables

List of Figures

List of Acronyms

GLCM   Gray-Level Co-Occurrence Matrix

GLRLM Gray-Level Run-Length Matrix

AR   Auto Regression

ML   Machine Learning

IRT   Infrared Thermography

ROI   Region of Interest

TPR   True Positive Rate

FPR   False Positive Rate

CNN   Convolutional Neural Network

AI   Artificial Intelligence

Chapter 1

Introduction

1.1 Background

Electricity is a blessing to this modern world. We cannot even think about spending a single day without it. All of the daily equipment that we use, starting from our home to office or school is connected to electricity one way or another. Electricity has made our life easier and flexible. The biggest advantage of electricity is industrial automation. With the combination of mechanical and electrical power, people have managed to build huge machines which can do most of the works with perfection that even human being are incapable of achieving. Those machines are faster, can do more heavy and dedicated work, and are more accurate. In a nutshell, industrial automation is a big step for past motorization, it is approximately utilizing control frameworks and innovation to replace physical and mental work of human within the fabricating and designing segment. Human labor is erroneous and while machines are not fail-proof but they are less prone to make mistakes. In industrial automation environment, the work is physically demanding and dangerous. The machinery doing the heavy-dangerous works should be monitored carefully to avoid any kind of accidents in work or to the people. A malfunctioning machine can cause injuries to the workers, other machineries and eventually lead to expensive compensation. The reason behind malfunction is mostly of damaged electrical components within that machine. Human monetarization is not always a full-proof way to go while handling those machineries. Replacing the hardware in time can prevent that failure but it is not always possible to predict the faults in a machine. The fault can be in a sensor or in a wire or in a circuit breaker. An intelligent system that can detect these faults within time and determine whether a replacement is needed to the component or not can be

very useful. This can reduce human labor and ensure the security of the worker and the machine.

In short, by using an intelligent system built by Machine learning, the faulty state of those electrical equipment can be pre-determined that can save the machinery and lower the power consumptions in industrial automation. That is why, extracted texture features from those machineries are needed for feeding them to the intelligent system so that an automatic system with IRT Camera can continuously check this electrical equipment and compare them with the standard ones and inform the user if there is any fault occurring in the system. Since, there are many ways to extract features from the thermal images of electrical equipment, choosing the most accurate technique is hereby needed. Hence, the study is conducted in this thesis work which is to determine the best technique for feature extraction for regular monitoring the condition of electrical equipment.

1.2 Literature Review

Electrical equipment inspections are extremely important for home, office or power plant's reliability and stability towards the system. Faulty wiring or equipment can lead to power failure as well as catastrophic damages to the electrical system. It can cause potentially life-threatening situations if devices are not well maintained. However, manual inspection or monitoring of electrical equipment is time consuming and cost-ineffective, therefore, an intelligent system where regular features found from the thermal images of electrical equipment can be fed to detect faults at very primary stages would be useful detecting the faulty parts within equipment as well.

As an emerging and most demanding topic, the study of ML is used in every sector of science as well as the applications on different field leads numerous students and researchers to work with enthusiasm which propagate new doors for them.

There are numerous researches and studies regarding the image analysis field. By doing different experiments and using different methods, this field is explored theoretically and physically. Numerous books and papers are published about the feature extraction methods and image processing using ML. Before digging deep into feature extraction methods and image analysis, some papers and books were gone through to gain knowledge in this field.

"Recent progress in diagnosing the reliability of electrical equipment by using infrared thermography" written by two researchers named Jadin, M. S., & Taib where the authors tried to portray how IRT based inspection techniques can further be improved. They also emphasized that for developing automated system, it is necessary to find out the heat signature area from the ROI and hereby good thresholding methods are required, though it was not mentioned which thresholding technique gives the most accurate result.

"Texture Feature Extraction Techniques for Image Recognition" by Jyotismita Chaki and Nilanjan Dey is a book from Springer Briefs in Applied Sciences and Technology series was modified last in 2020 had illustrated 19 different feature extraction methods that helped to learn about the algorithms and mathematical formulas related to image recognition.

"Comparison of thresholding techniques for extraction of electrical hotspots from infrared images" written by Asaduzzaman Abir, Md Rifat Islam Joy, Mobtasim Fuad & Nafiul Ahmed Emon discusses seven different thresholding techniques (Iso-Data, MaxEntropy/Kapur, MET, Otsu, Moments, Renyi-Entropy and Yen) on different electrical devices (Transformer, Circuit Breaker, PFI Board, Induction Motor) to know which of these particular thresholding techniques can perform the best for implementing an automatic inspection of electrical equipment. Among above-mentioned thresholding techniques, this paper comes to an illation that 'Moment' thresholding method is the most feasible segmentation method based on

comparison of TPR, FPR, Accuracy, Precision, Matthew's Correlation Coefficient (MCC), Dice Index, Jaccard Index and Error Rate.

"Suitable features selection for monitoring thermal condition of electrical equipment using infrared thermography" was published in the 2013 Infrared Physics & Technology journal. The following research portrays three set of features, called first order histogram based statistical, co-occurrence matrix and component-based intensity feature as inputs in four different neural network algorithms likely Resilient Back Propagation, Bayesian Regulazation, Levenberg–Marquardt and Scale Conjugate Gradient that are used to classify the condition of electrical equipment. On the whole, component-based intensity feature with Levenberg–Marquardt algorithm provides the best outcome in order to distinguish the normal and defected components.

"Texture Image Analysis and Texture Classification Methods - A Review" by Laleh Armi and Shervan Fekri-Ershad was published in International Online Journal of Image Processing and Pattern Recognition 2019. The journal contained information about the suitable texture extraction method for certain types of texture analysis.

"Textural Features for Image Classification" by Robert M. Haralick, Karthikeyan Shanmugam, and Its' Hak Dinstein, is the research paper which explain how texture analysis is important to identify objects or ROI of an image. Later "A Comparative Study of Texture Measures for Terrain Classification" written by Joan S. Weszka, Charles R. Dyer, and Azriel Rosenfeld was published on IEEE Transactions on Systems, Man, and Cybernetics, VOL. SMC-6, NO. 4, April 1976, which was based on the previous paper, contains the information of how GLCM is one of the most accurate method to do terrain analysis. In addition, all the statistical approach of texture analysis method was mentioned along with the algorithms in this paper.

Lastly, a paper which was published in First International Conference on Advanced Algorithms and Control Engineering 2018 named "Feature Extraction and Image Recognition with Convolutional Neural Networks" by Yu Han LIU provided the modern technical solution of image recognition by applying CNN which is an algorithm of ML. Moreover, this paper also includes the detailed step by step process of Convolutional Neural Network (CNN) for extracting potential features without much computational cost from the input images.

1.3 Aim and Objective

The main focus of our study is to determine the best feature extraction method and to predict the defective component of the electrical equipment so that we can take proper actions before it malfunctions. First and foremost, we use thermal Cameras to detect temperature by apprehending various levels of inferred lights of the machinery. Radiation is a way of emitting heat, our camera records that heat radiating from the object then assigns a shade of RGB color to it. The blue to purple shade indicates lesser temperature on the other hand, yellow to red shade means higher temperature. Image processing comes in handy in this place. For this study, 24 thermal images were collected from Opex Garments Ltd as input in the image processing system. By segmenting those pictures using 'Moment Binary' thresholding technique, the ROIs of the pictures are determined. From them, features are extracted using five different feature extracting methods: GLCM, GLRLM, Auto Regression, Histogram and Gradient. Those features are later fed into the ML, then using linear regression as classifier and testing-training and cross validation as algorithms, the most accurate feature extraction method is diagnosed along with the prediction of the defective component of the equipment.

1.4 Thesis Organization

The research work in this thesis paper has been categorized in six chapters based on chronological activities done for the thesis work.

In Chapter 1, mainly the significance, importance and inspiration of feature extraction methods analysis have been discussed. Also, the books or papers needed for the primary study are also mentioned with a briefed review.

In Chapter 2, a detailed description of the normal and thermal images collected from the Opex Garments Ltd. is presented.

In Chapter 3, different texture feature analysis techniques are discussed. Each technique is shown with a complete demonstration using different software plus all the feature-pictures are shown including the numerical values which are got during the extraction of features.

In Chapter 4, applying machine learning on the extracted features are mainly discussed and how it is used to predict the faulty region in addition to finding the best feature extracting techniques.

In Chapter 5, the results and limitation of the thesis work has been declared.

Finally, in Chapter 6, the thesis work concludes with the future prospective of this thesis work.

Chapter 2

Infrared Thermography (IRT) and Thermal Images Collection

2.1 Overview

Industrial Automation is one of the greatest gifts to mankind. With the help of industrial automation, one can accomplish any work without difficulty or effort. Mechanical computerization is a step for past motorization, it is utilizing control systems and development to supplant human's physical and mental work inside the creating and planning section. Though these pieces of machinery make our life easier, they are not error-free. One of the main reasons for the malfunctioning of the machine is the failure of the electrical components. To prevent the malfunctioning beforehand, infrared thermography can be utilized to distinguish and analyze warm irregularities of machines. An intelligent system using Machine Learning can help us to predict the faulty part of the machine and allow us to remove it quickly before it can do any further damage to the main part of the equipment. To train ML for prediction, input features play a very important part. Exact and accurate features have a vital role in training in this case. The more samples and features the user have, the more accurate results the user will get. Some features might also be unnecessary and can increase the error in prediction. For that, the best feature extraction technique has been determined in this thesis work where the highest accuracy is found. Here, not only the best feature extraction technique is determined by analyzing the performance but also the faulty part of the machinery using ML from the thermal picture is predicted.

2.2 Infrared Radiation

Infrared Radiation is also known as IR is a type of electromagnetic radiation. From most noteworthy to lowest frequency, electromagnetic radiation incorporates gamma-rays, X-rays, ultra-violate radiation, visible light, infrared, microwaves, and radio waves. One can feel it as

heat but is invisible to the naked human eye. All the things in the world emit some level of IR radiation. The main root of IR radiation is the sun and fire. It was discovered in 1800 by a British astronomer named William Herschel. William Herschel conducted an experiment in which he measured the temperature of different colors in the visible spectrum. As a result, he observed an increase in temperature when the color changes from blue to red. As the color goes from blue to red, the temperature increases, he also discovered a warmer temperature just past the red color in the visible spectrum [1].

Violate color has the shortest and red has the longest visible light wavelength in that spectrum, similarly inferred radiation has its range of wavelengths in which the shorter wavelengths are closer visible to on EM spectrum plus do not emit any noticeable heat (i.e., the heat discharged from the TV remote control). The longer IR wavelengths that are closer to the microwave part of the EM spectrum emit an intense heat that also is felt like the heat of sunlight. According to the research conducted by the team of California Institute of Technology (Caltech), IR wavelengths range between 1000µm to 760nm, though these values are not absolute. The frequencies range from 300GHz up to 400THz. Among the electromagnetic spectrum, these frequencies are above microwaves and below the red visible light, thus the name inferred was given.

As per the University of Tennessee, everything that is below 5K (Kelvin) radiates IR ray. And one can transfer the heat from one place to another using IR bedsides conduction and convection. Moreover, the sun emits half of its total energy as IR. One of the practical uses of IR is detection and sensation. As all the items in the universe emit IR in formation of heat, it can be detected by thermal cameras, night vision goggles or sensors.

2.3 Laws of IR Radiation

There are four basic laws of IR radiation [2].

- **Kirchhoff's Law of Thermal Radiation:**

  This law is dependent on the emission by a fixed wavelength of a material when it is in thermal equilibrium. Let's say, there is an object that emits and absorbs the radiation when thermal equilibrium is fully established. It is the ratio of power to its coefficient of absorption which equals to a universal function only of radiative wavelength and temperature.

  $$\alpha_\lambda = \varepsilon_\lambda$$

- **Plank's Law:**

  It describes the spectral density of EM radiation. The emission is caused by a black body when thermal equilibrium is established for any particular temperature. In this case, net energy flowing should be zero between the body and environment. For an increasing temperature the radiated energy increases and the peak of emitted spectrum converts to short wavelengths.

  $$B(v,T) = \frac{2hv^3}{c^2} \frac{1}{e^{\frac{hv}{k_B T}} - 1}$$

- **Stefan-Boltzmann Law:**

  The law states that total energy that is radiated per unit surface area of a black body among all the wavelength in per unit time is proportional to the fourth power of that body's thermodynamic temperature. It is also known as Blackbody radiation since the power is radiated in terms of temperature.

  $$j = \sigma T^4$$

- **Wien's Displacement Law:**

    It describes that the curve for the radiation of a black body for various temperatures will

    peak different wavelengths which is inversely proportional to the temperature.

$$\lambda_{peak} = \frac{b}{T}$$
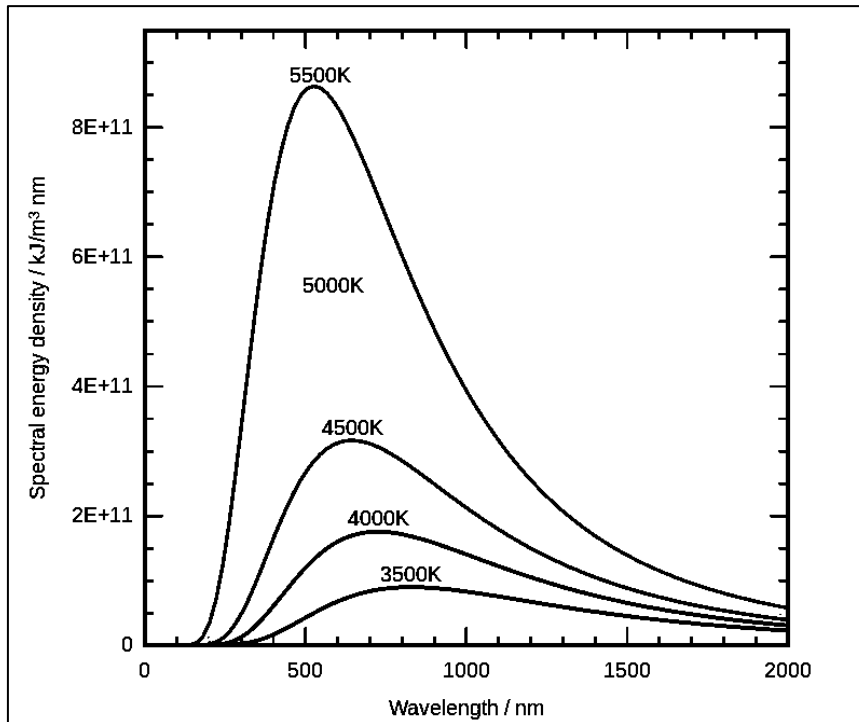
Figure 2.1: Graph of a Black-body Radiation

Depending on those laws the IR radiation happens which is utilized in thermal cameras.

2.4 Thermal Camera and its Working Principle

An inferred camera or a thermography camera is a non-contact device that is used to detect the

heat radiating from the object using IR and capture it as image in monochromatic form. Just

like visible light cameras, it detects wavelengths but of 1µm to 1400nm. Though the camera

can detect wavelength of a certain band, it cannot distinguish between them, so pictures come

out in monochromatic form. Sometimes those monochromatic images are displayed in pseudo

colors so that a human eye can easily detect it. For measuring the temperature, the dark colors as in black is the coolest temperature, red to yellow is the intermediate temperature and white has the highest temperature.

The hotter any object is, the more IR ray it produces. Thermal camera captures those IR radiation from the image and converts them to pictures. For doing that, there is a microbolometer which captures the temperature and assigns that pixel an appropriate color. The picture resolution of the thermal camera is really low for that reason.

In this thesis work, Fluke Thermal Camera had been used for capturing thermal images of the electrical equipment and it was able to detect some irregularities among the electrical components. After getting those pictures, it was hard to detect which were faulty or normal among those components. So, a fixation and image segmentation were required for further image processing.

2.5 Collection of Thermal Images for Samples

To conduct this thesis work, thermal images of electrical equipment were needed. Initially, Opex Garments Ltd was visited to inspect some machineries used for garments purposes. There were several types of electrical equipment, such as Circuit Breakers, Transformers, PFI Boards and Induction Motors. Among all the machineries, only 24 were chosen for this thesis work. The images were captured with a Thermal Camera that later was processed by Fluke Connect Software for further dealings with them.

2.5.1 Visible Representation of Collected Images

Figure 2.2: Visible Representation of Collected Images

Serial	Equipment	Location	Problem
1	Circuit Breaker	Main Distribution Board (MDB), Factory 3	Among three phases (R, Y, B), Y-Phase is connected to the higher load, therefore showing high heat signature.
2	Circuit Breaker	Distribution Board, Factory 3	[No Defect]
3	Circuit Breaker	Distribution Board, Factory 3	Imbalanced Load
4	Circuit Breaker	Distribution Board, Factory 3	R-Phase stays at Overload
5	Circuit Breaker	Distribution Board, Factory 3	R-Phase contains Overload
6	Transformer	1st Floor, Factory 3	Y-Phase contains Overload
7	Transformer	1st Floor, Factory 3	B-Phase contains Overload
8	Transformer	1st Floor, Factory 3	B-Phase contains Overload
9	Transformer	1st Floor, Factory 3	[No Defect]
10	Circuit Breaker	Main Distribution Board (MDB), Factory 3	R-Phase contains Overload
11	Circuit Breaker	Main Distribution Board (MDB), Factory 3	B-Phase contains Overload
12	Circuit Breaker	Main Distribution Board (MDB), Factory 3	B-Phase contains Overload
13	Circuit Breaker	Main Distribution Board (MDB), Factory 3	B-Phase contains Overload
14	PFI Board	Main Distribution Board (MDB), Factory 3	To maintain power factor of the inductive loads, capacitors inject apparent power causes heat signature.
15	Circuit Breaker	Main Distribution Board (MDB), Factory 3	R-Phase contains Overload
16	Circuit Breaker	Main Distribution Board (MDB), Factory 3	R-Phase contains Overload
17	Ceiling Fan	Cutting Section, Factory 3	Ceiling fan produces heat signature due to its mechanical energy.
18	Induction Moton	Water Supply, Factory 3	Due to excessive current, it shows heat signature.
19	Induction Moton	Production Line, Factory 3	Releasing energy as a large amount of current passing through it.
20	Induction Moton	Production Line, Factory 3	The motor is releasing energy as a large amount of current passing through it.
21	Circuit Breaker	Distribution Board, Factory 2	Y-Phase stays at Overload
22	Circuit Breaker	Factory 2	Transformer core shows excessive heat due to its incapacity of dissipating heat of high current.
23	Transformer	Factory 2	Transformer core shows excessive heat due to its incapacity of dissipating heat of high current.
24	Circuit Breaker	Distribution Board, Factory 2	Corrosion in the incoming contact causes current not to flow normally, eventually causes excessive heat.

Table 2.1: Report of Collected Thermal Images

2.5.2 Thermal Representation of Collected Images
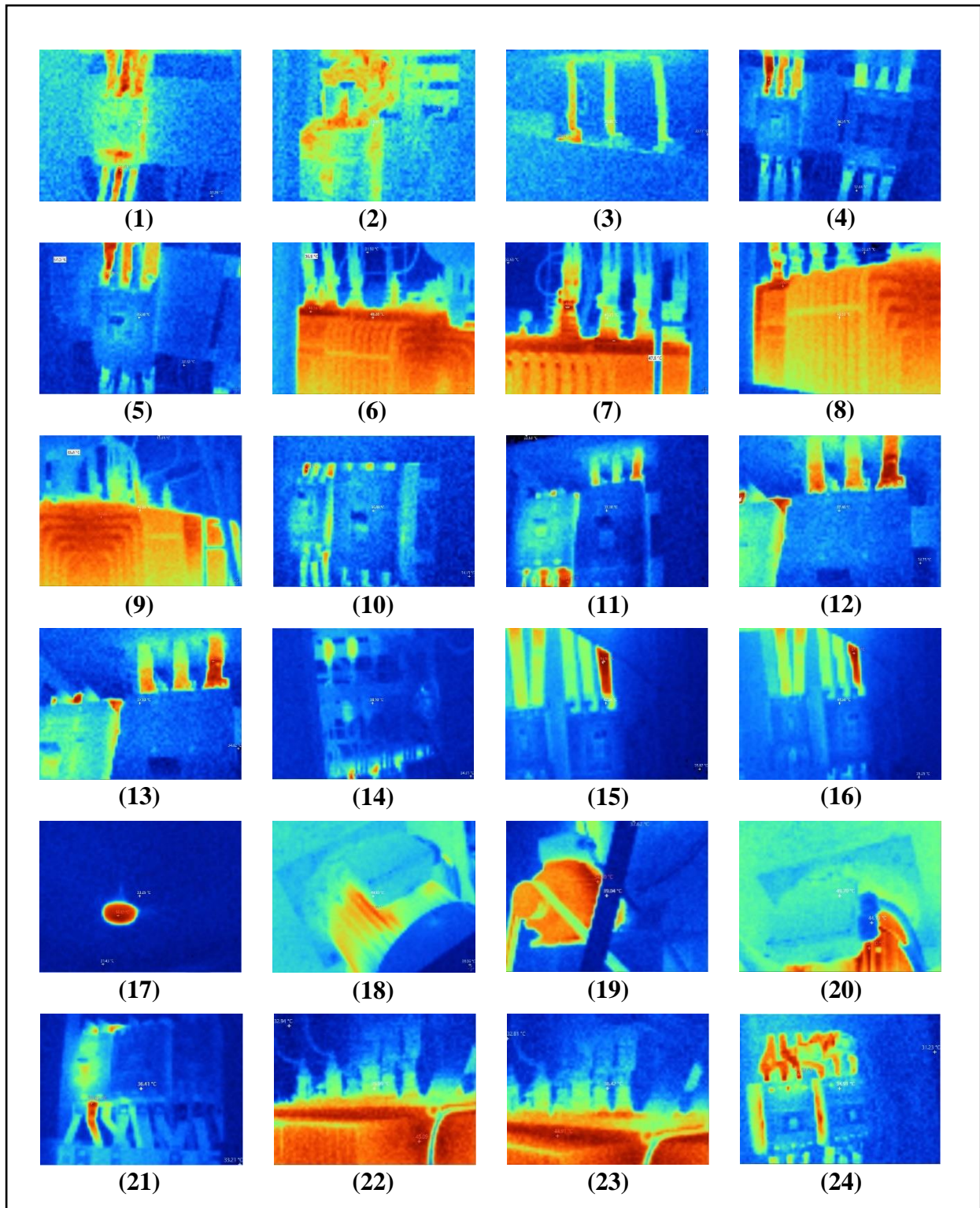
Figure 2.3: Thermal Representation of Collected Images

2.5.3 Gray-Scale Representation of Collected Images
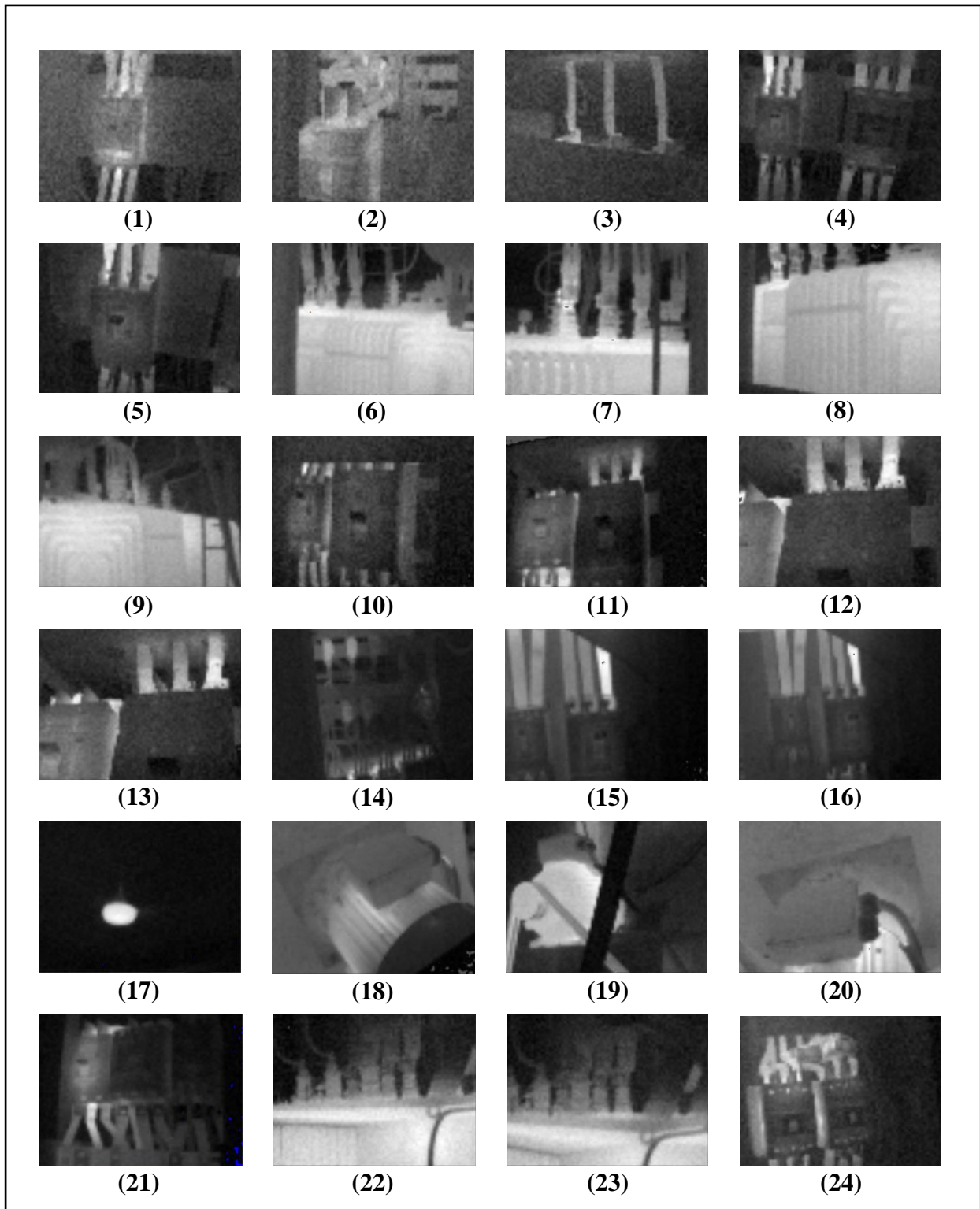
Figure 2.4: Gray-Scale Representation of Collected Images

2.6 Image Segmentation

For extracting features, image segmentation is one of the most important tasks to do for image processing. It is basically the way of partitioning an image into many meaningful parts which are known as segments. The significance of using this technique is for object recognition or image compression. Therefore, image segmentation is done to segment the parts from the original images for additional processing [3]. There are several techniques to segment images. These techniques are called Thresholding Techniques. The process is normally done with the grayscale images. In this thesis, 'Moments Binary' method had been chosen for segmentation and ImageJ software was used as a tool.

2.6.1 Flowchart of Image Segmentation

Opening **ImageJ**
Software

↓

Opening
Grayscale Image

↓

Converting Image
to 8 bit

↓

Selecting
Thresholding Method

↓
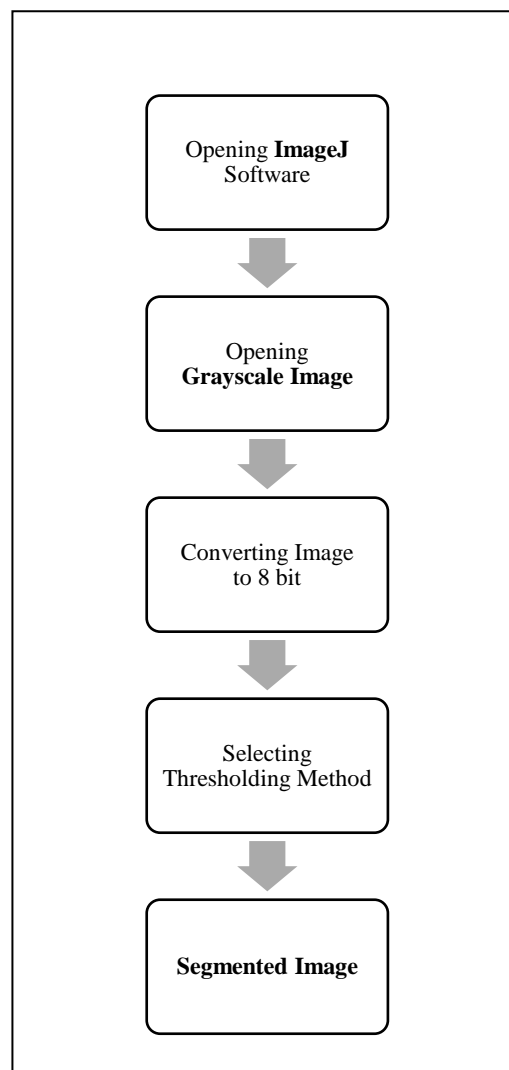
Segmented Image

Figure 2.5: Flowchart of Image Segmentation

2.6.2 Software Usage (ImageJ) for Image Segmentation

(a) Opening ImageJ Software

(b) Clicking File>Open

(c) Opening Grayscale Image

(d) Clicking Image>Type>8 bit

(e) Clicking Image>Adjust>Auto Threshold

(f) Selecting 'Moment' as Method

(h) Segmented Image using Moments Method
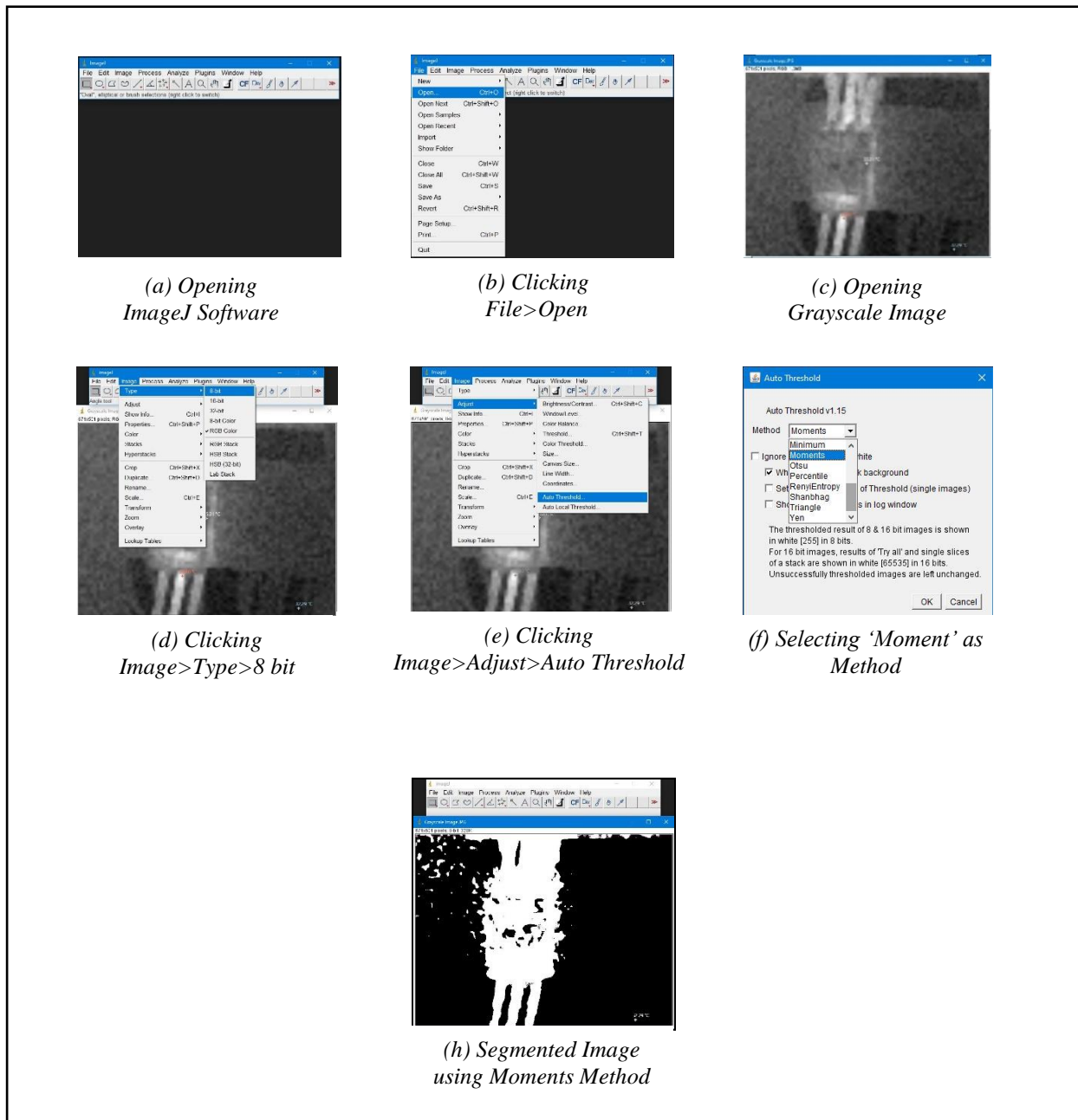
Figure 2.6: Software Usage (ImageJ) for Image Segmentation

2.6.3 Segmented Representation of Collected Images (Moments Binary)
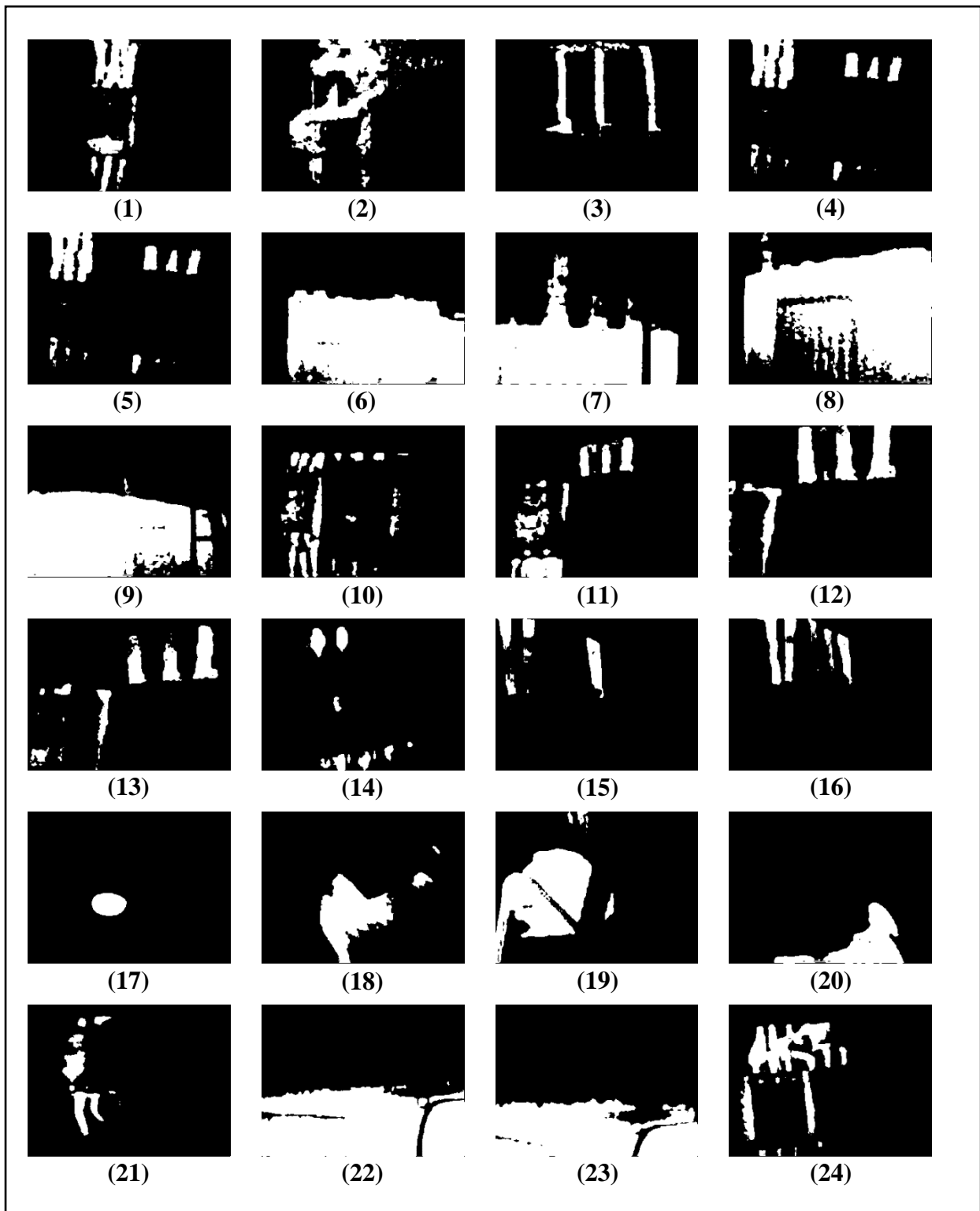
Figure 2.7: Segmented Representation of Collected Images (Moments Binary)

Chapter 3

Feature Extraction from Collected Images

3.1 Feature Extraction Techniques

Features are basically the characteristics of images that had been aimed to extract to analyze properly so that they can be of useful finding best feature extraction technique by feeding these features to the intelligent system. Total 5 feature extraction techniques (GLCM, GLRLM, Gradient, Histogram, Auto-Regression) had been applied on the 24 collected thermal images using MaZda Software. Used Feature Extraction Technique and name of the features with description have been given below.

3.1.1 Gray-Level Co-Occurrence Matrix (GLCM) Technique

Gray-Level Co-Occurrence distribution is a matrix that displays the various combinations of gray levels that can be contained in an image. Moreover, a Co-Occurrence Matrix is generated by comparing the pixel values of adjacent pixels in grayscale image [9]. Furthermore, the number of rows and columns is the same as the number of brightness values in pixels in gray level. However, Co-Occurrence is a second-order statistical texture function computing approach that considers the relationship between two pixels for mathematical calculations, namely the reference pixel and the neighboring pixel [10].

$$Angular\ second\ moment\ = \sum_{i,j} P_{ij}^2$$

$$Contrast\ = \sum_{i,j} P_{i,j}\ (i-j)^2$$

$$Correlation\ = \sum_{i,j} P_{i,j} \left[\frac{(i-\mu_i)(j-\mu_j)}{\partial_i\ \partial_j} \right]$$

$$Variance\ = \sum_{i,j} P_{i,j}\ (i-\mu_i)^2$$

$$Inverse\ Difference\ Moment\ = \sum_{i,j} \frac{P_{i,j}}{1 + (i-j)^2}$$

$$Sum\ Average\ =\ f_{12} = \sum_{i=2}^{2N_g} iP_{x+y}(i)$$

$$Sum\ Entropy\ = f_{14}\ = -\sum_{i=2}^{2N_g} P_{x+y}(i)log(P_{x+y}(i))$$

$$Sum\ Variance\ = f_{13} = \sum_{i=2}^{2N_g} (i - f_{14})^2 P_{x-y}(i)$$

$$Sum\ of\ Square = \sum_{i-1}^{N_k} \sum_{j-1}^{N_k} (i - \mu_x)^2 p(i,j)$$

$$Entropy\ = -\sum_{i,j} P_{ij}\ Log\ (P\_(i,j))$$

$$Difference\ Variance\ = -\sum_{i=0}^{N_g-1} (i - f_6)^2 P_{x-y}(i)\ ; \qquad f_6 = \sum_{i,j} |i - j| P_{ij}$$

$$Difference\ Entropy\ = f_{16}\ = -\sum_{i=0}^{N_g-1} P_{x-y}(i)\ log\ (P_{x-y}(i))$$

$$Information\ Measure\ of\ Correlation\ 1 = \frac{-\sum_{i,j} P_{i,j}((\ log\ (P_{i,j})) -\ log\ (P_x(i))}{max(HX, HY)}$$

$$Information\ measure\ of\ Correlation\ 2 = f_{18} = \sqrt{1 - e^{-2(a-b)}}\ ;$$

$$a = -\sum_{i,j} P_x(i)P_y(i)\ log(P_x(i)P_y(i))$$

$$b = -\sum_{i,j} P_{i,j}\ log(P_x(i)P_y(i))$$

where,

$P_{(i,j)}$ *gives the statistical probability values for changes between gray levels i and j*

at a given distance d and angle θ.

3.1.2 Gray-Level Run-Length Matrix (GLRLM) Technique

Gray-Level Run-Length Matrix is known as higher-order statistical method of texture feature extraction which aims to calculate the number of consecutive pixels in a given direction that has the same gray-level intensity [5]. It is a group of pixels with the same gray-level intensity value in a specific direction and as a result, relatively long runs will dominate a coarse texture, while a fine texture will be dominated by much shorter runs [6]. In thesis work, the gray-level run-length matrix's parameters are computed in two separate directions: horizontal and vertical. A number of consecutive pixels with the same gray-level value are defined by the run-length focus. Depending on the number of consecutive pixels in the chosen direction with the same gray-level value, it may be appropriately referred to as long-run or short-run focus. The disorderliness in pixel and pixel gray-level runs is defined by run-length and gray-level non-uniformity. The fraction of the image in runs simply refers to run percentages which is calculated as a percentage, the ratio of the total number of runs in the image to the total number of pixels in the image [7]. Galloway was the first who introduces the use of run-length texture analysis technique [8]. However, it has yet to achieve widespread acceptance as a reliable method of texture calculation. As a result, it is not popular among researchers working to develop diagnostic tools for medical applications. If $P(i,j)$ represents the frequency of a run of length j with a grey-level intensity i, Ng represents the number of gray-level intensities, and Nr represents the number of runs, then using the equations below, the parameters for the run-length matrix can be determined.

$$Short\ Run\ Emphasis = \frac{\left(\sum_{i=1}^{Ng} \sum_{j=1}^{Nr} \frac{p(i,j)}{j^2} \right)}{\left(\sum_{i=1}^{Ng} \sum_{j=1}^{Nr} j\, p(i,j) \right)}$$

$$Long\ Run\ Emphasis = \frac{\left(\sum_{i=1}^{Ng} \sum_{j=1}^{Nr} j^2 p(i,j) \right)}{\left(\sum_{i=1}^{Ng} \sum_{j=1}^{Nr} j\, p(i,j) \right)}$$

$$Gray\ Level\ Nonuniformity = \frac{\left(\sum_{i=1}^{Ng}\sum_{j=1}^{Nr} p(i,j)^2\right)}{\left(\sum_{i=1}^{Ng}\sum_{j=1}^{Nr} j\ p(i,j)\right)}$$

$$Run\ Length\ Nonuniformity = \frac{\left(\sum_{i=1}^{Ng}\sum_{j=1}^{Nr} p(i,j)^2\right)}{\left(\sum_{i=1}^{Ng}\sum_{j=1}^{Nr} j\ p(i,j)\right)}$$

$$Fraction\ of\ Image\ in\ Runs = \frac{\left(\sum_{i=1}^{Ng}\sum_{j=1}^{Nr} p(i,j)\right)}{\left(\sum_{i=1}^{Ng}\sum_{j=1}^{Nr} j\ p(i,j)\right)}$$

3.1.3 Gradient Technique

Gradient Method is used as one of the most common statistical approaches. A particular point about the image is the rate of the difference between the gray-level and its neighborhood pixel. However, the gradient values are calculated by taking the discrete derivative which means finite difference.

$$G_x = (\partial I(x,y))/\partial x \approx I(x+1,y) - I(x,y)$$

$$G_y = \partial I/\partial y\ (x,y) \approx I(x,y+1) - I(x,y)$$

$$G_z = \nabla I(x,y) \approx I(x+1,y+1) - I(x,y)$$

Furthermore, the gradient values generally are in the direction of most rapid increase in intensity of pixel and its neighborhood, which is often considered as 3×3 pixels. It contains the absolute gradient value at each point of the analyzed image region [11].

$$Gradient_{Min} = Min\ (G_x, G_y, G_z)$$

$$Gradient_{Max} = Max\ (G_x, G_y, G_z)$$

$$Gradient_{Average} = Mean\ (G_x, G_y, G_z)$$

Moreover, Gradient features also can be derived from a gradient matrix after calculating its histogram (His) which is determined for gradient values extended along the range of values [-255, 255]. Therefore, the determined gradient features are as follows:

$$Mean = \sum_{v} \frac{His(v + 256).v}{Total\ number\ of\ pixel}$$

$$\left[Where\ v\ is\ the\ gradient\ value\ which\ is\ extended\ within\ the\ range\ [-255,255]\right]$$

$$Variance = \sum_{v} \frac{His(v + 256)(v - \mu)^2}{Total\ number\ of\ pixel}$$

$$Skewness = \sum_{v} \frac{His(v + 256)(v - \mu)^3}{Total\ number\ of\ pixel}$$

$$Kurtosis = \sum_{v} \frac{His(v + 256)(v - \mu)^4}{Total\ number\ of\ pixel}$$

3.1.4 Histogram Technique

This method is basically a first-order statistical analysis which uses pixel occurrence probability to calculate texture. Assuming that the grey levels in an image are in the range $0 \leq i \leq Ng - 1$, where Ng is the total number of specific grey levels, to demonstrate the histogram approach to texture analysis. If $N(i)$ is the total number of pixels with intensity i and M is the total number of pixels in the image, then the pixel occurrence probability $P(i)$ is given by, $P(i) = \frac{N(i)}{M}$. Histogram is the probability of occurrence of a pixel of particular grey intensity. Also, it does not consider the spatial relationships, and correlations, between pixels. Furthermore, **t**he key benefit of the histogram is its simplicity, which is achieved by using standard descriptors to describe texture data, such as mean and variance. However, mean, variance, skewness, kurtosis, percentile 01, percentile 10, percentile 50, percentile 90, and percentile 99 are all characteristics that can be derived from the histogram [12]. The equations represent some of the features from the histogram that are used to describe texture:

$$Mean\ (\mu) = \sum_{i=0}^{N-1} ip(i)$$

$$Variance\ (\sigma^2) = \sum_{i=0}^{N-1} (i - \mu)^2\, p(i)$$

$$Skewness\ (\mu_3) = \sigma^{-3} \sum_{i=0}^{N-1} (i - \mu)^3\, p(i)$$

$$Kurtosis\ (\mu_4) = \sigma^{-4} \sum_{i=0}^{N-1} (i - \mu)^4\, p(i) - 3$$

3.1.5 Auto Regression (AR) Technique

The auto-regressive (AR) predicts a local interaction between image pixels in that pixel intensity and a weighted sum of neighboring pixel intensities. Assuming image f is a zero-mean random field, an AR causal model can be defined as:

$$f_s = \sum_{r \in N_s} \theta_r f_r + e_s$$

Where, f_s represents image intensity at site s, e_s represents independent and identically distributed noise, Ns represents a neighborhood of s and θ which are the vector of model parameters.

Using the AR model for image segmentation consists in identifying the model parameters for a given image region and then using the obtained parameter values for texture discrimination. Moreover, there are 5 unknown model parameters in the simple pixel neighborhood seen in Figure 4, which consists of 4 immediate pixel neighbors: the standard deviation σ of the driving noise e_s and the model parameter vector θ= [θ_1 , θ_2 , θ_3 , θ_4]. However, the parameters can be estimated by minimizing the sum of squared error.

$$\sum_{s} e_s^2 = \sum_{s}(f_s - \theta v_s)^2$$

$$\theta = \left(\sum_{s} w_s w_s^T\right)^{-1} \left(\sum_{s} w_s f_s\right) \partial^2 = N^{-2} \sum_{s}(f_s - \theta v_s)^2$$

where $w_s = \text{col}[f_i, i \in N_s]$, and the square N×N image is assumed. For each ROI of interest, the above set of equations is numerically solved in Mazda. As an example, AR model parameters were used in for unsupervised texture segmentation. Finally, the complexity of the computations to determine the model parameters is the key drawback of the model-based approach to texture analysis.

3.2 Flowchart of Feature Extraction
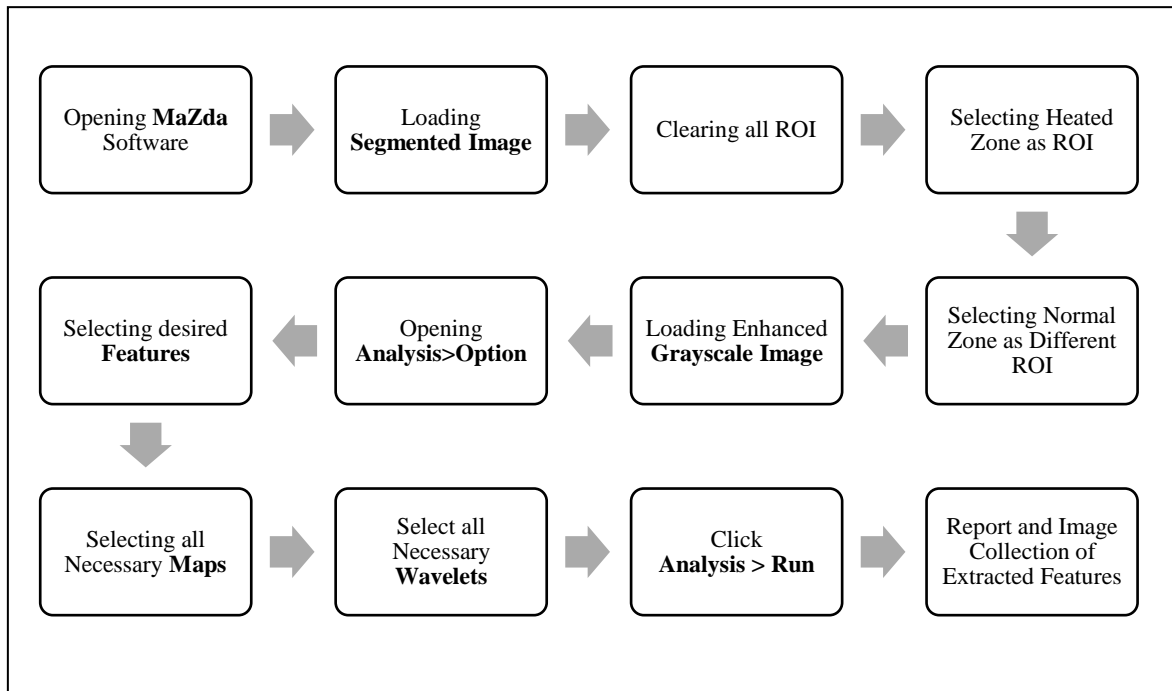
Figure 3.1: Flowchart of Feature Extraction

3.3 Software Usage (MaZda) for Feature Extraction

(a) Opening
MazDa Software

(b) Clicking
File>Load Image

(c) Loading Segmented
Image

(d) Clicking
Edit>Clear ROI

(e) Selecting Heated
and Normal Zone as
different ROI

(f) Clicking
File>Load Image

(g) Loading enhanced
Grayscale Image

(h) Clicking
Analysis>Options

(i) Selecting desired
Features
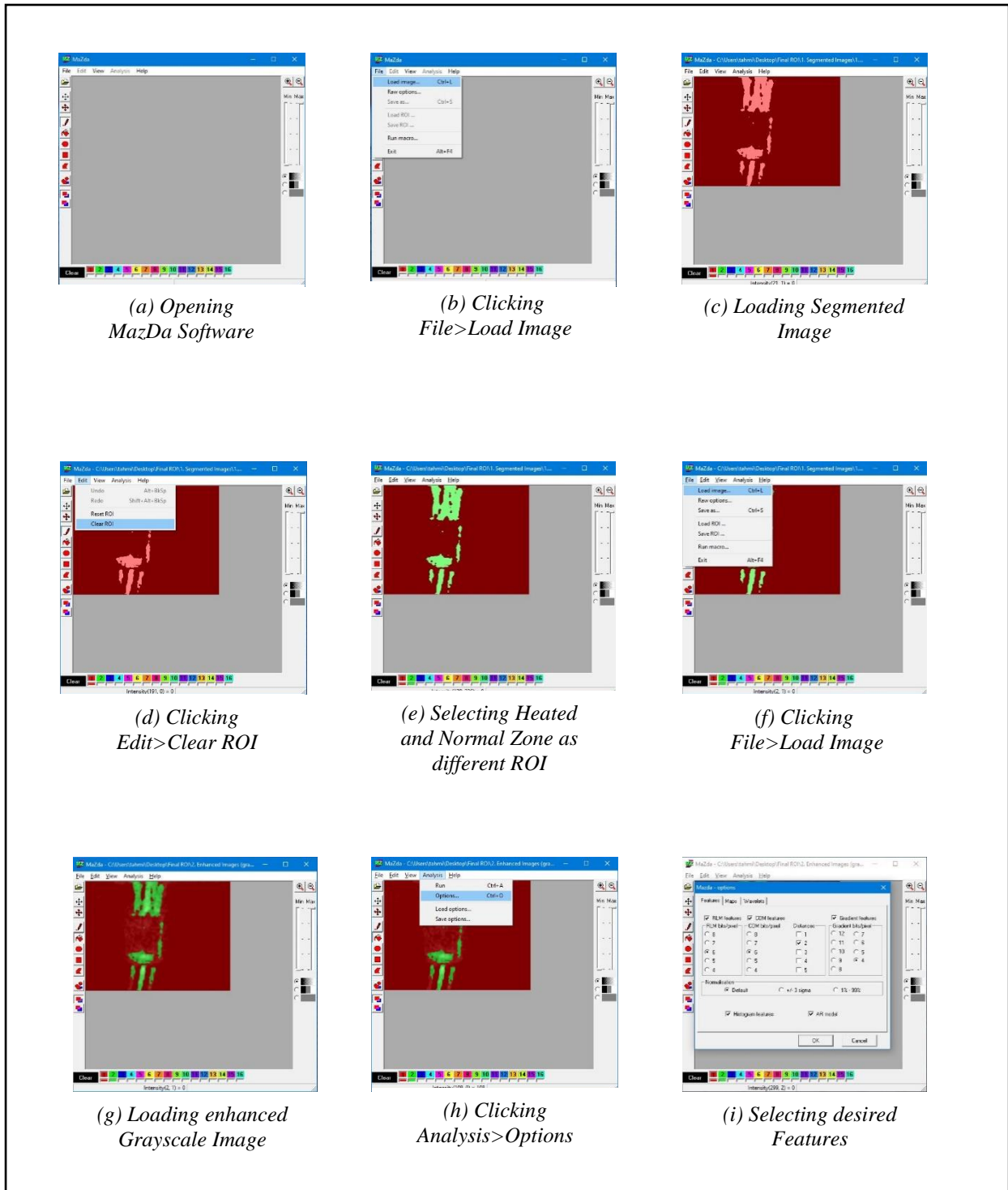
Figure 3.2: Software Usage (MaZda) for Feature Extraction (a)
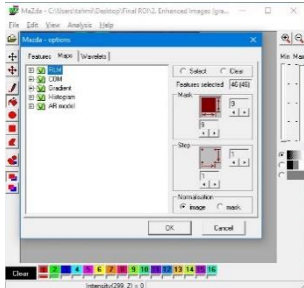
(j) Selecting necessary Maps
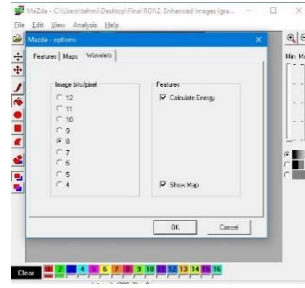
(k) Selecting necessary Wavelets
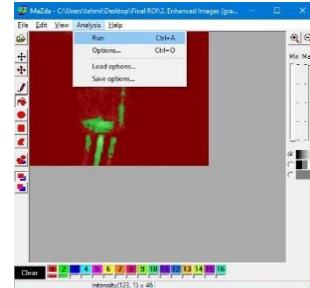
(l) Clicking Analysis>Run
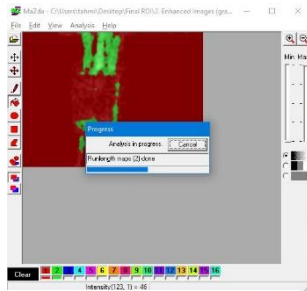
(m) Progressing
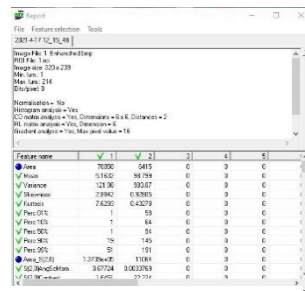
(n) Feature Report
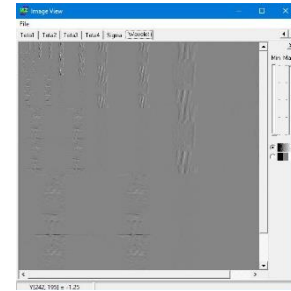
(o) Feature Images

Figure 3.3: Software Usage (MaZda) for Feature Extraction (b)

3.4.1 Collected Feature Images from Sample Image-1:

Figure 3.4: Feature Images for Sample Image-1 (Part-1)

(a) GrKurtosis4b, (b) GrMean4b, (c) GrNonZeros4b, (d) GrSkewness4b,

(e) GrVariance4b, (f) Horzl_Fraction6b, (g) Horzl_GLevNonU6b,

(h) Horzl_LngREmph6b, (i) Horzl_RLNonUni6b, (j) Horzl_ShrtREmp6b,

(k) Kurtosis, (l) Mean, (m) S(0,2)AngScMom6b, (n) S(0,2)Contrast6b ,

(o) S(0,2)Correlat6b, (p) S(0,2)DifEntrp6b

Figure 3.5: Feature Images for Sample Image-1 (Part-2)

(a) S(0,2)DifVarnc6b, (b) S(0,2)Entropy6b, (c) S(0,2)InvDfMom6b,

(d) S(0,2)SumAverg6b, (e) S(0,2)SumEntrp6b, (f) S(0,2)SumOfSqs6b,

(g) S(0,2)SumVarnc6b, (h) S(2,0)AngScMom6b, (i) S(2,0)Contrast6b,

(j) S(2,0)Correlat6b, (k) S(2,0)DifEntrp6b, (l) S(2,0)DifVarnc6b,

(m) S(2,0)Entropy6b, (n) S(2,0)InvDfMom6b ,

(o) Vertl_ShrtREmp6b, (p) S(2,0)SumAverg6b

Figure 3.6: Feature Images for Sample Image-1 (Part-3)

(a) S(2,0)SumEntrp6b, (b) S(2,0)SumOfSqs6b, (c) S(2,0)SumVarnc6b, (d) Sigma,

(e) Skewness, (f) Teta1, (g) Teta2, (h) Teta3, (i) Teta4, (j) Variance, (k) Vertl_Fraction6b,

(l) Vertl_GLevNonU6b, (m) Vertl_LngREmph6b, (n) Vertl_RLNonUni6b

3.4.2 Collected Feature Images from Sample Image-2:

Figure 3.7: Feature Images for Sample Image-2 (Part-1)

(a) GrKurtosis4b, (b) GrMean4b, (c) GrNonZeros4b, (d) GrSkewness4b,

(e) GrVariance4b, (f) Horzl_Fraction6b, (g) Horzl_GLevNonU6b,

(h) Horzl_LngREmph6b, (i) Horzl_RLNonUni6b, (j) Horzl_ShrtREmp6b,

(k) Kurtosis, (l) Mean, (m) S(0,2)AngScMom6b, (n) S(0,2)Contrast6b ,

(o) S(0,2)Correlat6b, (p) S(0,2)DifEntrp6b

31

Figure 3.8: Feature Images for Sample Image-2 (Part-2)

(a) S(0,2)DifVarnc6b, (b) S(0,2)Entropy6b, (c) S(0,2)InvDfMom6b,

(d) S(0,2)SumAverg6b, (e) S(0,2)SumEntrp6b, (f) S(0,2)SumOfSqs6b,

(g) S(0,2)SumVarnc6b, (h) S(2,0)AngScMom6b, (i) S(2,0)Contrast6b,

(j) S(2,0)Correlat6b, (k) S(2,0)DifEntrp6b, (l) S(2,0)DifVarnc6b,

(m) S(2,0)Entropy6b, (n) S(2,0)InvDfMom6b ,

(o) Vertl_ShrtREmp6b, (p) S(2,0)SumAverg6b

Figure 3.9: Feature Images for Sample Image-2 (Part-3)

(a) S(2,0)SumEntrp6b, (b) S(2,0)SumOfSqs6b, (c) S(2,0)SumVarnc6b, (d) Sigma,

(e) Skewness, (f) Teta1, (g) Teta2, (h) Teta3, (i) Teta4, (j) Variance, (k) Vertl_Fraction6b,

(l) Vertl_GLevNonU6b, (m) Vertl_LngREmph6b, (n) Vertl_RLNonUni6b

3.4.3 Collected Feature Images from Sample Image-3:

Figure 3.10: Feature Images for Sample Image-3 (Part-1)

(a) GrKurtosis4b, (b) GrMean4b, (c) GrNonZeros4b, (d) GrSkewness4b,

(e) GrVariance4b, (f) Horzl_Fraction6b, (g) Horzl_GLevNonU6b,

(h) Horzl_LngREmph6b, (i) Horzl_RLNonUni6b, (j) Horzl_ShrtREmp6b,

(k) Kurtosis, (l) Mean, (m) S(0,2)AngScMom6b, (n) S(0,2)Contrast6b ,

(o) S(0,2)Correlat6b, (p) S(0,2)DifEntrp6b

Figure 3.11: Feature Images for Sample Image-3 (Part-2)

(a) S(0,2)DifVarnc6b, (b) S(0,2)Entropy6b, (c) S(0,2)InvDfMom6b,

(d) S(0,2)SumAverg6b, (e) S(0,2)SumEntrp6b, (f) S(0,2)SumOfSqs6b,

(g) S(0,2)SumVarnc6b, (h) S(2,0)AngScMom6b, (i) S(2,0)Contrast6b,

(j) S(2,0)Correlat6b, (k) S(2,0)DifEntrp6b, (l) S(2,0)DifVarnc6b,

(m) S(2,0)Entropy6b, (n) S(2,0)InvDfMom6b ,

(o) Vertl_ShrtREmp6b, (p) S(2,0)SumAverg6b

Figure 3.12: Feature Images for Sample Image-3 (Part-3)

(a) S(2,0)SumEntrp6b, (b) S(2,0)SumOfSqs6b, (c) S(2,0)SumVarnc6b, (d) Sigma,

(e) Skewness, (f) Teta1, (g) Teta2, (h) Teta3, (i) Teta4, (j) Variance, (k) Vertl_Fraction6b,

(l) Vertl_GLevNonU6b, (m) Vertl_LngREmph6b, (n) Vertl_RLNonUni6b

3.4.4 Collected Feature Images from Sample Image-4:

Figure 3.13: Feature Images for Sample Image-4 (Part-1)

(a) GrKurtosis4b, (b) GrMean4b, (c) GrNonZeros4b, (d) GrSkewness4b,

(e) GrVariance4b, (f) Horzl_Fraction6b, (g) Horzl_GLevNonU6b,

(h) Horzl_LngREmph6b, (i) Horzl_RLNonUni6b, (j) Horzl_ShrtREmp6b,

(k) Kurtosis, (l) Mean, (m) S(0,2)AngScMom6b, (n) S(0,2)Contrast6b ,

(o) S(0,2)Correlat6b, (p) S(0,2)DifEntrp6b

Figure 3.14: Feature Images for Sample Image-4 (Part-2)

(a) S(0,2)DifVarnc6b, (b) S(0,2)Entropy6b, (c) S(0,2)InvDfMom6b,

(d) S(0,2)SumAverg6b, (e) S(0,2)SumEntrp6b, (f) S(0,2)SumOfSqs6b,

(g) S(0,2)SumVarnc6b, (h) S(2,0)AngScMom6b, (i) S(2,0)Contrast6b,

(j) S(2,0)Correlat6b, (k) S(2,0)DifEntrp6b, (l) S(2,0)DifVarnc6b,

(m) S(2,0)Entropy6b, (n) S(2,0)InvDfMom6b ,

(o) Vertl_ShrtREmp6b, (p) S(2,0)SumAverg6b

Figure 3.15: Feature Images for Sample Image-4 (Part-3)

(a) S(2,0)SumEntrp6b, (b) S(2,0)SumOfSqs6b, (c) S(2,0)SumVarnc6b, (d) Sigma,

(e) Skewness, (f) Teta1, (g) Teta2, (h) Teta3, (i) Teta4, (j) Variance, (k) Vertl_Fraction6b,

(l) Vertl_GLevNonU6b, (m) Vertl_LngREmph6b, (n) Vertl_RLNonUni6b

3.4.5 Collected Feature Images from Sample Image-5:

Figure 3.16: Feature Images for Sample Image-5 (Part-1)

(a) GrKurtosis4b, (b) GrMean4b, (c) GrNonZeros4b, (d) GrSkewness4b,

(e) GrVariance4b, (f) Horzl_Fraction6b, (g) Horzl_GLevNonU6b,

(h) Horzl_LngREmph6b, (i) Horzl_RLNonUni6b, (j) Horzl_ShrtREmp6b,

(k) Kurtosis, (l) Mean, (m) S(0,2)AngScMom6b, (n) S(0,2)Contrast6b ,

(o) S(0,2)Correlat6b, (p) S(0,2)DifEntrp6b

Figure 3.17: Feature Images for Sample Image-5 (Part-2)

(a) S(0,2)DifVarnc6b, (b) S(0,2)Entropy6b, (c) S(0,2)InvDfMom6b,

(d) S(0,2)SumAverg6b, (e) S(0,2)SumEntrp6b, (f) S(0,2)SumOfSqs6b,

(g) S(0,2)SumVarnc6b, (h) S(2,0)AngScMom6b, (i) S(2,0)Contrast6b,

(j) S(2,0)Correlat6b, (k) S(2,0)DifEntrp6b, (l) S(2,0)DifVarnc6b,

(m) S(2,0)Entropy6b, (n) S(2,0)InvDfMom6b ,

(o) Vertl_ShrtREmp6b, (p) S(2,0)SumAverg6b

41

Figure 3.18: Feature Images for Sample Image-5 (Part-3)

(a) S(2,0)SumEntrp6b, (b) S(2,0)SumOfSqs6b, (c) S(2,0)SumVarnc6b, (d) Sigma,

(e) Skewness, (f) Teta1, (g) Teta2, (h) Teta3, (i) Teta4, (j) Variance, (k) Vertl_Fraction6b

, (l) Vertl_GLevNonU6b, (m) Vertl_LngREmph6b, (n) Vertl_RLNonUni6b

3.4.6 Collected Feature Images from Sample Image-6:

Figure 3.19: Feature Images for Sample Image-6 (Part-1)

(a) GrKurtosis4b, (b) GrMean4b, (c) GrNonZeros4b, (d) GrSkewness4b,

(e) GrVariance4b, (f) Horzl_Fraction6b, (g) Horzl_GLevNonU6b,

(h) Horzl_LngREmph6b, (i) Horzl_RLNonUni6b, (j) Horzl_ShrtREmp6b,

(k) Kurtosis, (l) Mean, (m) S(0,2)AngScMom6b, (n) S(0,2)Contrast6b ,

(o) S(0,2)Correlat6b, (p) S(0,2)DifEntrp6b

Figure 3.20: Feature Images for Sample Image-6 (Part-2)

(a) S(0,2)DifVarnc6b, (b) S(0,2)Entropy6b, (c) S(0,2)InvDfMom6b,

(d) S(0,2)SumAverg6b, (e) S(0,2)SumEntrp6b, (f) S(0,2)SumOfSqs6b,

(g) S(0,2)SumVarnc6b, (h) S(2,0)AngScMom6b, (i) S(2,0)Contrast6b,

(j) S(2,0)Correlat6b, (k) S(2,0)DifEntrp6b, (l) S(2,0)DifVarnc6b,

(m) S(2,0)Entropy6b, (n) S(2,0)InvDfMom6b ,

(o) Vertl_ShrtREmp6b, (p) S(2,0)SumAverg6b

44

Figure 3.21: Feature Images for Sample Image-6 (Part-3)

(a) S(2,0)SumEntrp6b, (b) S(2,0)SumOfSqs6b, (c) S(2,0)SumVarnc6b, (d) Sigma,

(e) Skewness, (f) Teta1, (g) Teta2, (h) Teta3, (i) Teta4, (j) Variance, (k) Vertl_Fraction6b,

(l) Vertl_GLevNonU6b, (m) Vertl_LngREmph6b, (n) Vertl_RLNonUni6b

3.4.7 Collected Feature Images from Sample Image-7:

Figure 3.22: Feature Images for Sample Image-7 (Part-1)

(a) GrKurtosis4b, (b) GrMean4b, (c) GrNonZeros4b, (d) GrSkewness4b,

(e) GrVariance4b, (f) Horzl_Fraction6b, (g) Horzl_GLevNonU6b,

(h) Horzl_LngREmph6b, (i) Horzl_RLNonUni6b, (j) Horzl_ShrtREmp6b,

(k) Kurtosis, (l) Mean, (m) S(0,2)AngScMom6b, (n) S(0,2)Contrast6b ,

(o) S(0,2)Correlat6b, (p) S(0,2)DifEntrp6b

Figure 3.23: Feature Images for Sample Image-7 (Part-2)

(a) S(0,2)DifVarnc6b, (b) S(0,2)Entropy6b, (c) S(0,2)InvDfMom6b,

(d) S(0,2)SumAverg6b, (e) S(0,2)SumEntrp6b, (f) S(0,2)SumOfSqs6b,

(g) S(0,2)SumVarnc6b, (h) S(2,0)AngScMom6b, (i) S(2,0)Contrast6b,

(j) S(2,0)Correlat6b, (k) S(2,0)DifEntrp6b, (l) S(2,0)DifVarnc6b,

(m) S(2,0)Entropy6b, (n) S(2,0)InvDfMom6b ,

(o) Vertl_ShrtREmp6b, (p) S(2,0)SumAverg6b

47

Figure 3.24: Feature Images for Sample Image-7 (Part-3)

(a) S(2,0)SumEntrp6b, (b) S(2,0)SumOfSqs6b, (c) S(2,0)SumVarnc6b, (d) Sigma,

(e) Skewness, (f) Teta1, (g) Teta2, (h) Teta3, (i) Teta4, (j) Variance, (k) Vertl_Fraction6b,

(l) Vertl_GLevNonU6b, (m) Vertl_LngREmph6b, (n) Vertl_RLNonUni6b
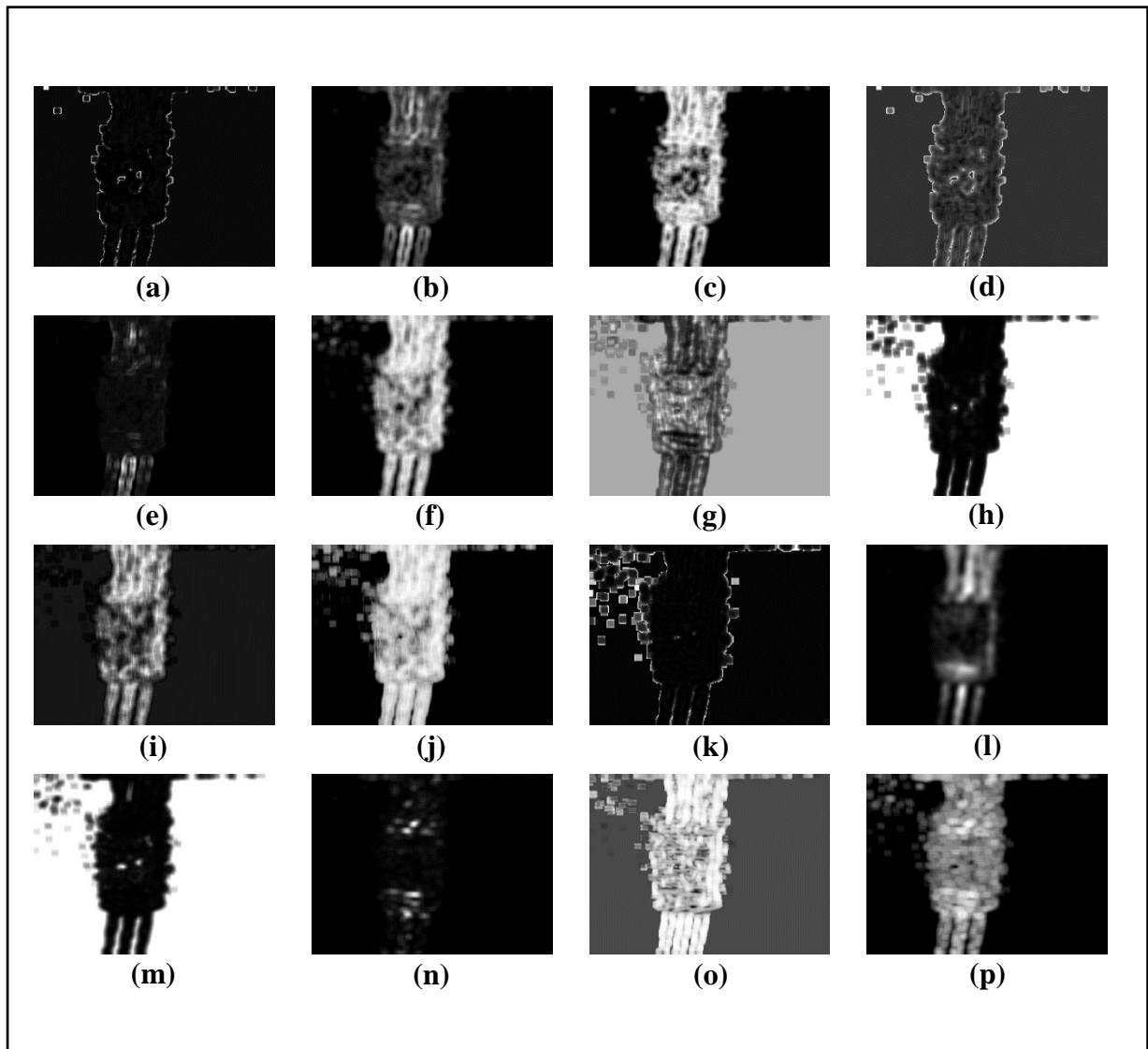
3.4.8 Collected Feature Images from Sample Image-8:

Figure 3.25: Feature Images for Sample Image-8 (Part-1)

(a) GrKurtosis4b, (b) GrMean4b, (c) GrNonZeros4b, (d) GrSkewness4b,

(e) GrVariance4b, (f) Horzl_Fraction6b, (g) Horzl_GLevNonU6b,

(h) Horzl_LngREmph6b, (i) Horzl_RLNonUni6b, (j) Horzl_ShrtREmp6b,

(k) Kurtosis, (l) Mean, (m) S(0,2)AngScMom6b, (n) S(0,2)Contrast6b ,
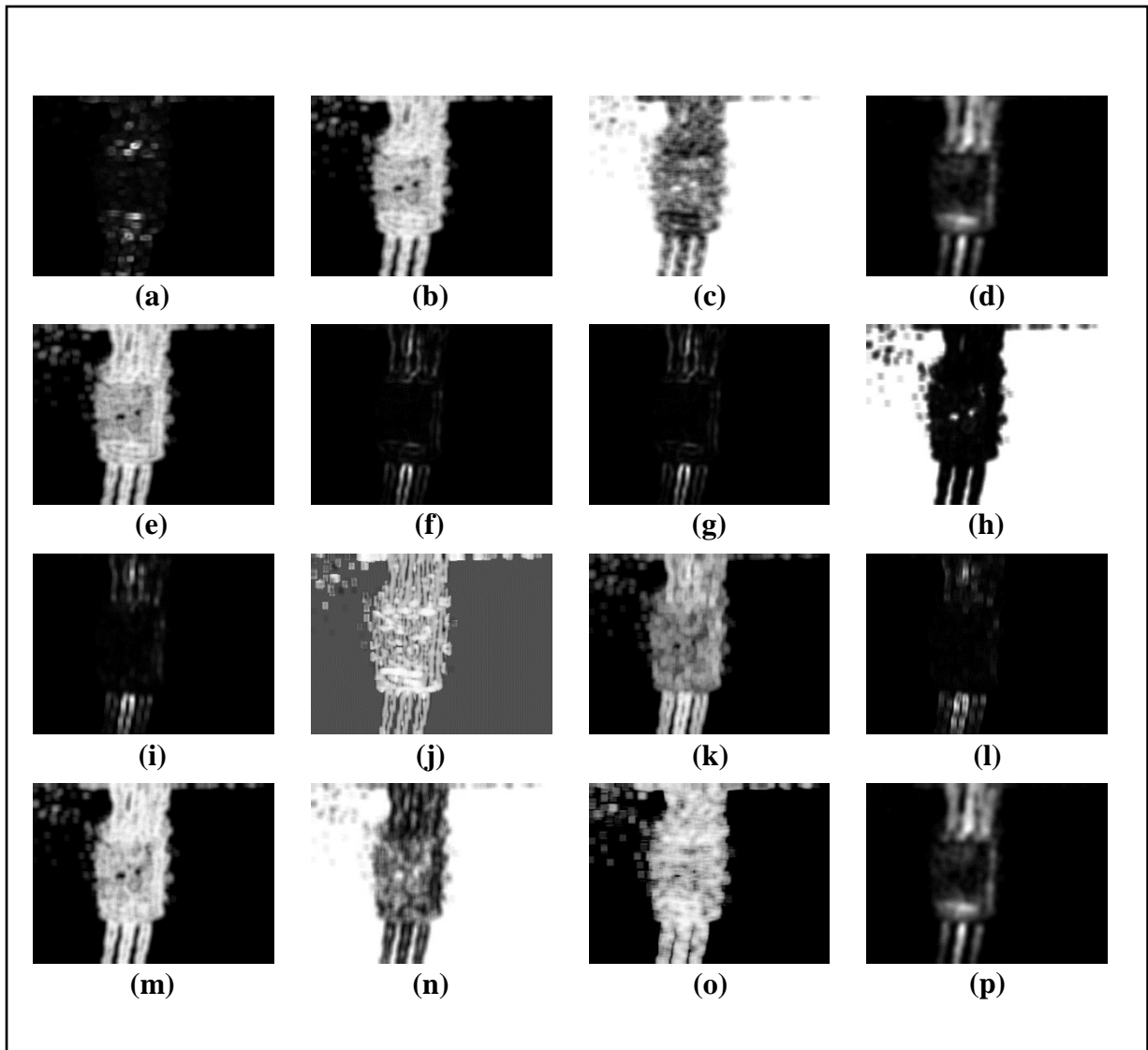
(o) S(0,2)Correlat6b, (p) S(0,2)DifEntrp6b

Figure 3.26: Feature Images for Sample Image-8 (Part-2)

(a) S(0,2)DifVarnc6b, (b) S(0,2)Entropy6b, (c) S(0,2)InvDfMom6b,

(d) S(0,2)SumAverg6b, (e) S(0,2)SumEntrp6b, (f) S(0,2)SumOfSqs6b,

(g) S(0,2)SumVarnc6b, (h) S(2,0)AngScMom6b, (i) S(2,0)Contrast6b,

(j) S(2,0)Correlat6b, (k) S(2,0)DifEntrp6b, (l) S(2,0)DifVarnc6b,

(m) S(2,0)Entropy6b, (n) S(2,0)InvDfMom6b ,
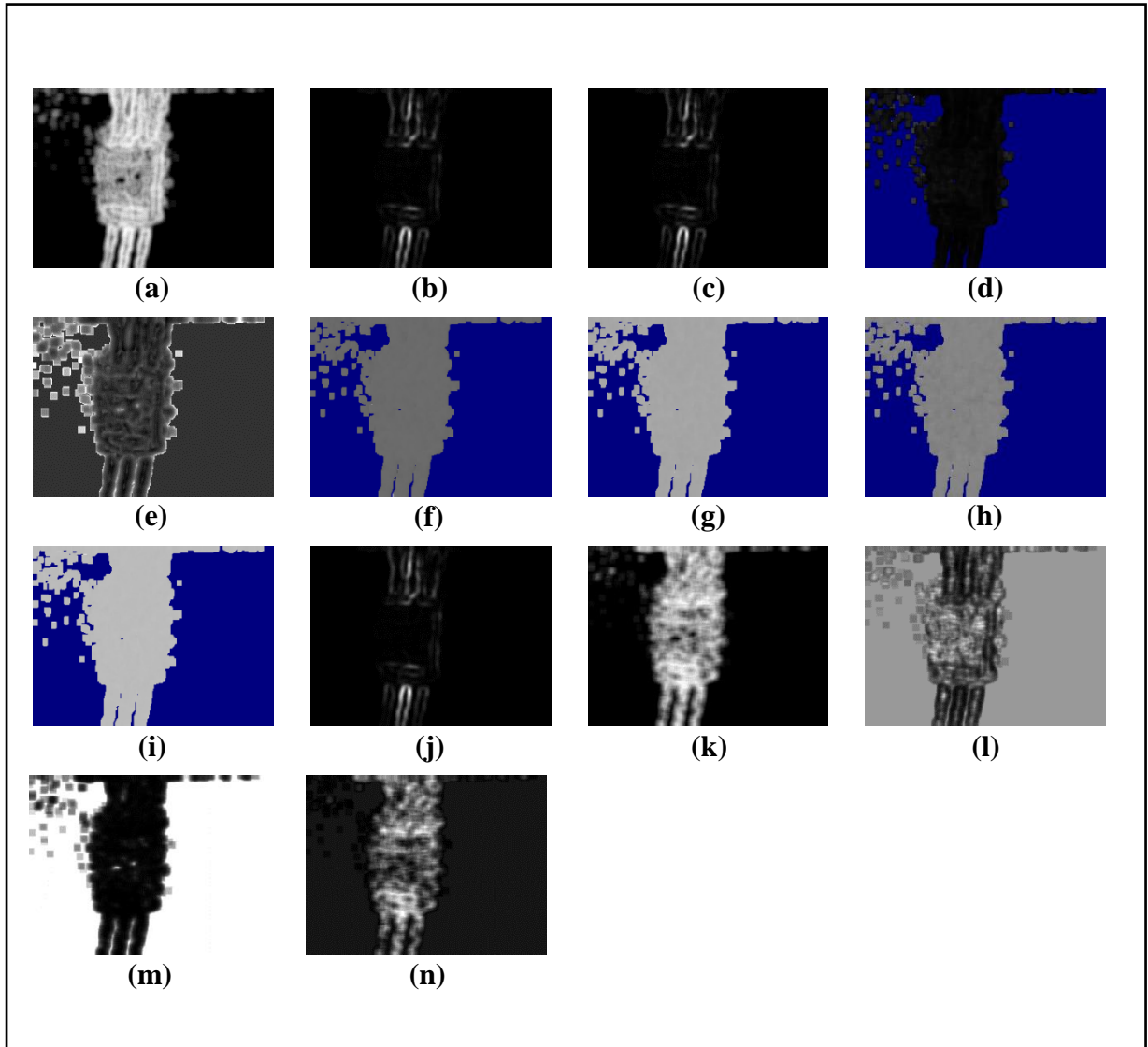
(o) Vertl_ShrtREmp6b, (p) S(2,0)SumAverg6b

Figure 3.27: Feature Images for Sample Image-8 (Part-3)

(a) S(2,0)SumEntrp6b, (b) S(2,0)SumOfSqs6b, (c) S(2,0)SumVarnc6b, (d) Sigma,

(e) Skewness, (f) Teta1, (g) Teta2, (h) Teta3, (i) Teta4, (j) Variance, (k) Vertl_Fraction6b,

(l) Vertl_GLevNonU6b, (m) Vertl_LngREmph6b, (n) Vertl_RLNonUni6b
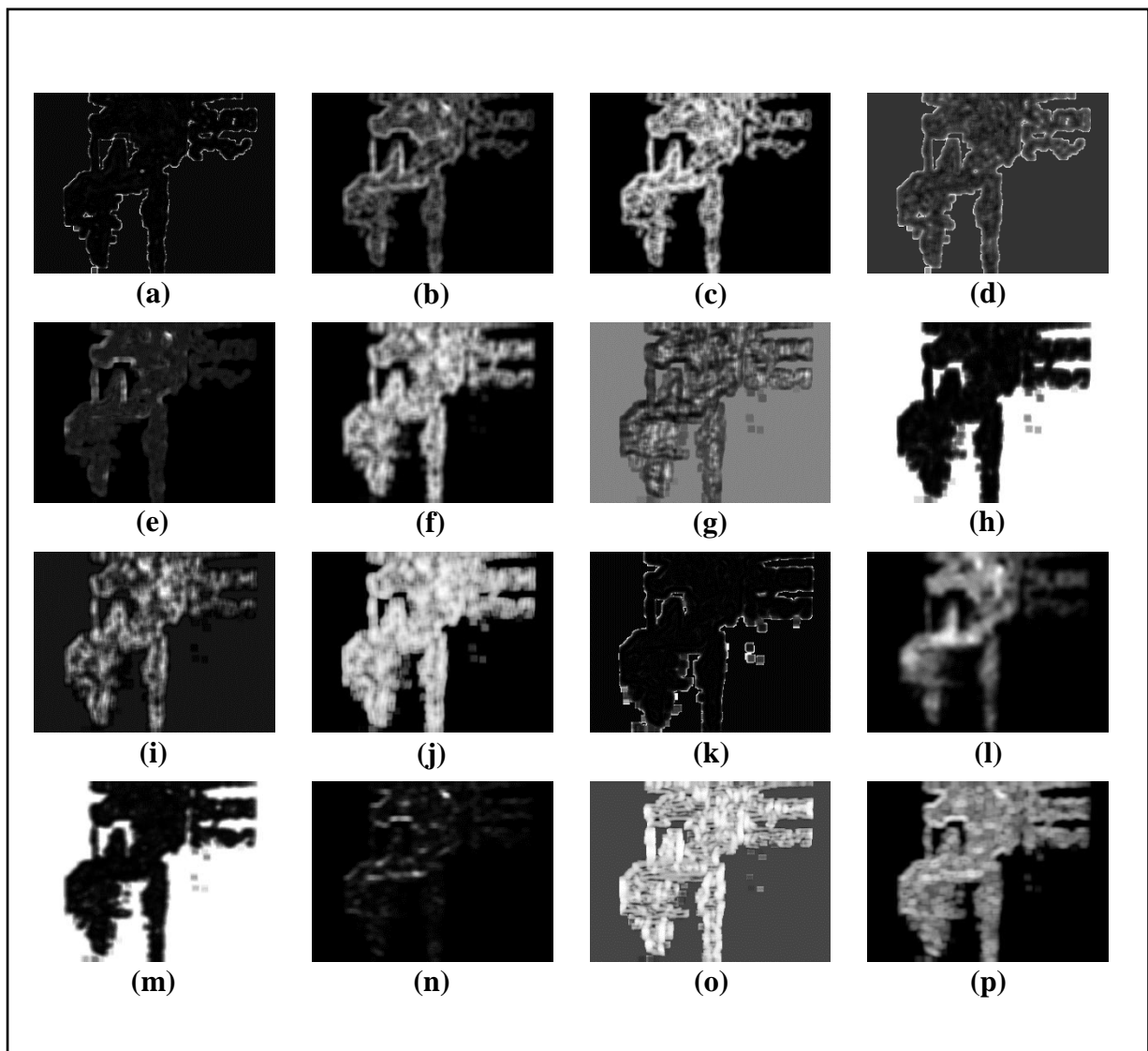
3.4.9 Collected Feature Images from Sample Image-9:

Figure 3.28: Feature Images for Sample Image-9 (Part-1)

(a) GrKurtosis4b, (b) GrMean4b, (c) GrNonZeros4b, (d) GrSkewness4b,

(e) GrVariance4b, (f) Horzl_Fraction6b, (g) Horzl_GLevNonU6b,

(h) Horzl_LngREmph6b, (i) Horzl_RLNonUni6b, (j) Horzl_ShrtREmp6b,

(k) Kurtosis, (l) Mean, (m) S(0,2)AngScMom6b, (n) S(0,2)Contrast6b ,
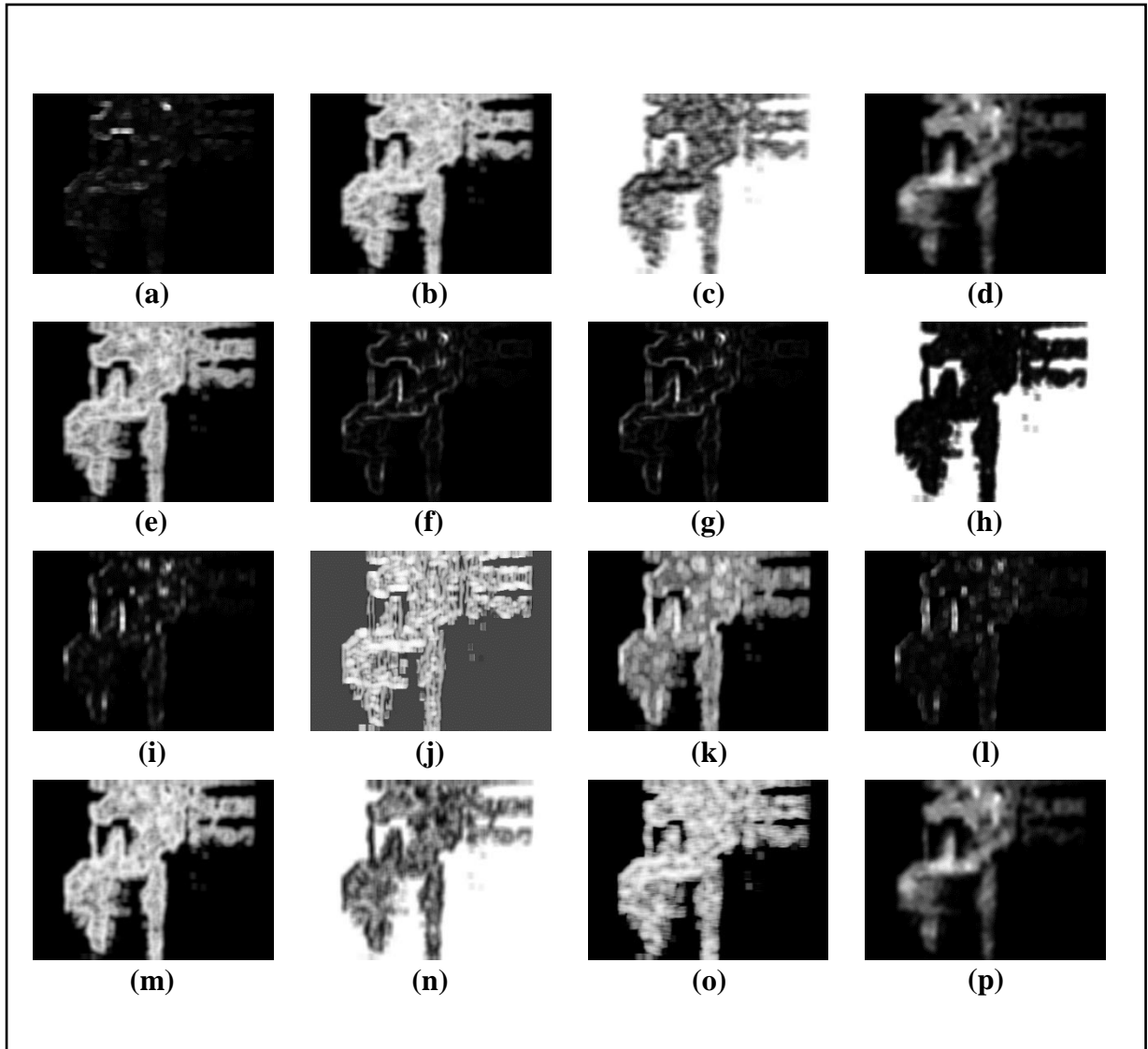
(o) S(0,2)Correlat6b, (p) S(0,2)DifEntrp6b

Figure 3.29: Feature Images for Sample Image-9 (Part-2)

(a) S(0,2)DifVarnc6b, (b) S(0,2)Entropy6b, (c) S(0,2)InvDfMom6b,

(d) S(0,2)SumAverg6b, (e) S(0,2)SumEntrp6b, (f) S(0,2)SumOfSqs6b,

(g) S(0,2)SumVarnc6b, (h) S(2,0)AngScMom6b, (i) S(2,0)Contrast6b,

(j) S(2,0)Correlat6b, (k) S(2,0)DifEntrp6b, (l) S(2,0)DifVarnc6b,

(m) S(2,0)Entropy6b, (n) S(2,0)InvDfMom6b ,

(o) Vertl_ShrtREmp6b, (p) S(2,0)SumAverg6b

Figure 3.30: Feature Images for Sample Image-9 (Part-3)

(a) S(2,0)SumEntrp6b, (b) S(2,0)SumOfSqs6b, (c) S(2,0)SumVarnc6b, (d) Sigma,

(e) Skewness, (f) Teta1, (g) Teta2, (h) Teta3, (i) Teta4, (j) Variance, (k) Vertl_Fraction6b,

(l) Vertl_GLevNonU6b, (m) Vertl_LngREmph6b, (n) Vertl_RLNonUni6b

3.4.10 Collected Feature Images from Sample Image-10:
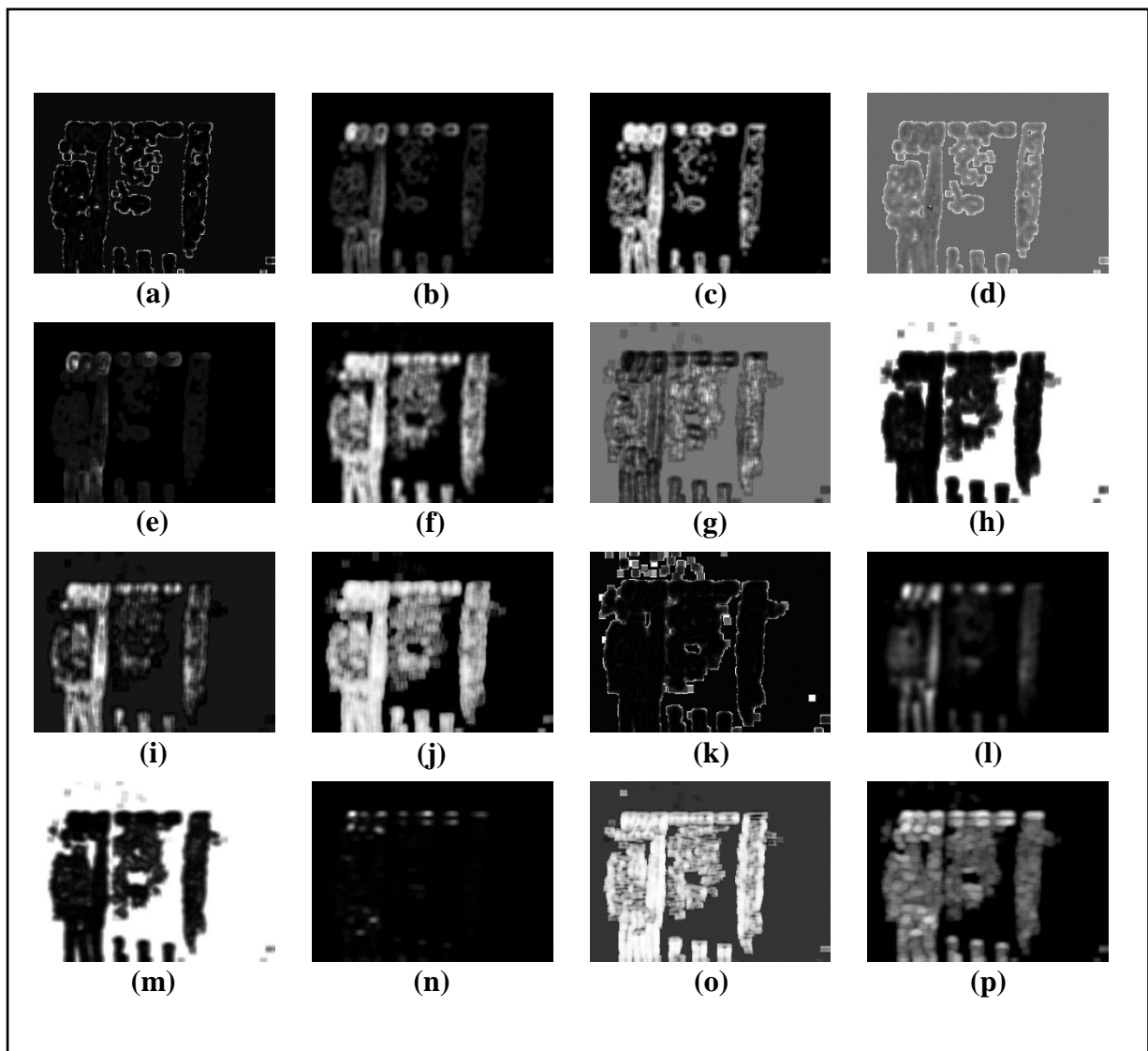
Figure 3.31: Feature Images for Sample Image-10 (Part-1)

(a) GrKurtosis4b, (b) GrMean4b, (c) GrNonZeros4b, (d) GrSkewness4b,

(e) GrVariance4b, (f) Horzl_Fraction6b, (g) Horzl_GLevNonU6b,

(h) Horzl_LngREmph6b, (i) Horzl_RLNonUni6b, (j) Horzl_ShrtREmp6b,

(k) Kurtosis, (l) Mean, (m) S(0,2)AngScMom6b, (n) S(0,2)Contrast6b ,

(o) S(0,2)Correlat6b, (p) S(0,2)DifEntrp6b

Figure 3.32: Feature Images for Sample Image-10 (Part-2)

(a) S(0,2)DifVarnc6b, (b) S(0,2)Entropy6b, (c) S(0,2)InvDfMom6b,

(d) S(0,2)SumAverg6b, (e) S(0,2)SumEntrp6b, (f) S(0,2)SumOfSqs6b,

(g) S(0,2)SumVarnc6b, (h) S(2,0)AngScMom6b, (i) S(2,0)Contrast6b,

(j) S(2,0)Correlat6b, (k) S(2,0)DifEntrp6b, (l) S(2,0)DifVarnc6b,

(m) S(2,0)Entropy6b, (n) S(2,0)InvDfMom6b ,
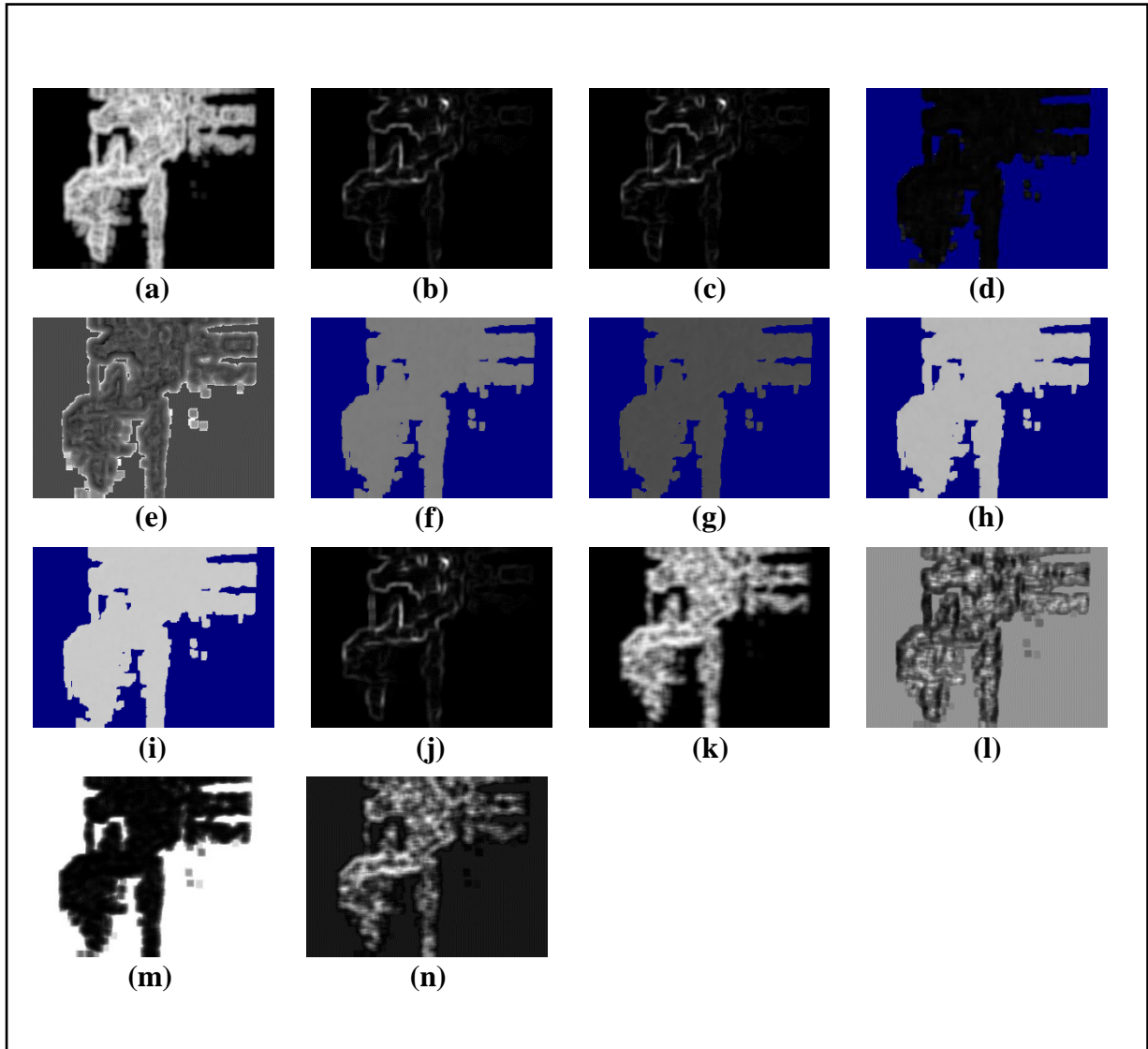
(o) Vertl_ShrtREmp6b, (p) S(2,0)SumAverg6b

Figure 3.33: Feature Images for Sample Image-10 (Part-3)

(a) S(2,0)SumEntrp6b, (b) S(2,0)SumOfSqs6b, (c) S(2,0)SumVarnc6b, (d) Sigma,

(e) Skewness, (f) Teta1, (g) Teta2, (h) Teta3, (i) Teta4, (j) Variance, (k) Vertl_Fraction6b,

(l) Vertl_GLevNonU6b, (m) Vertl_LngREmph6b, (n) Vertl_RLNonUni6b
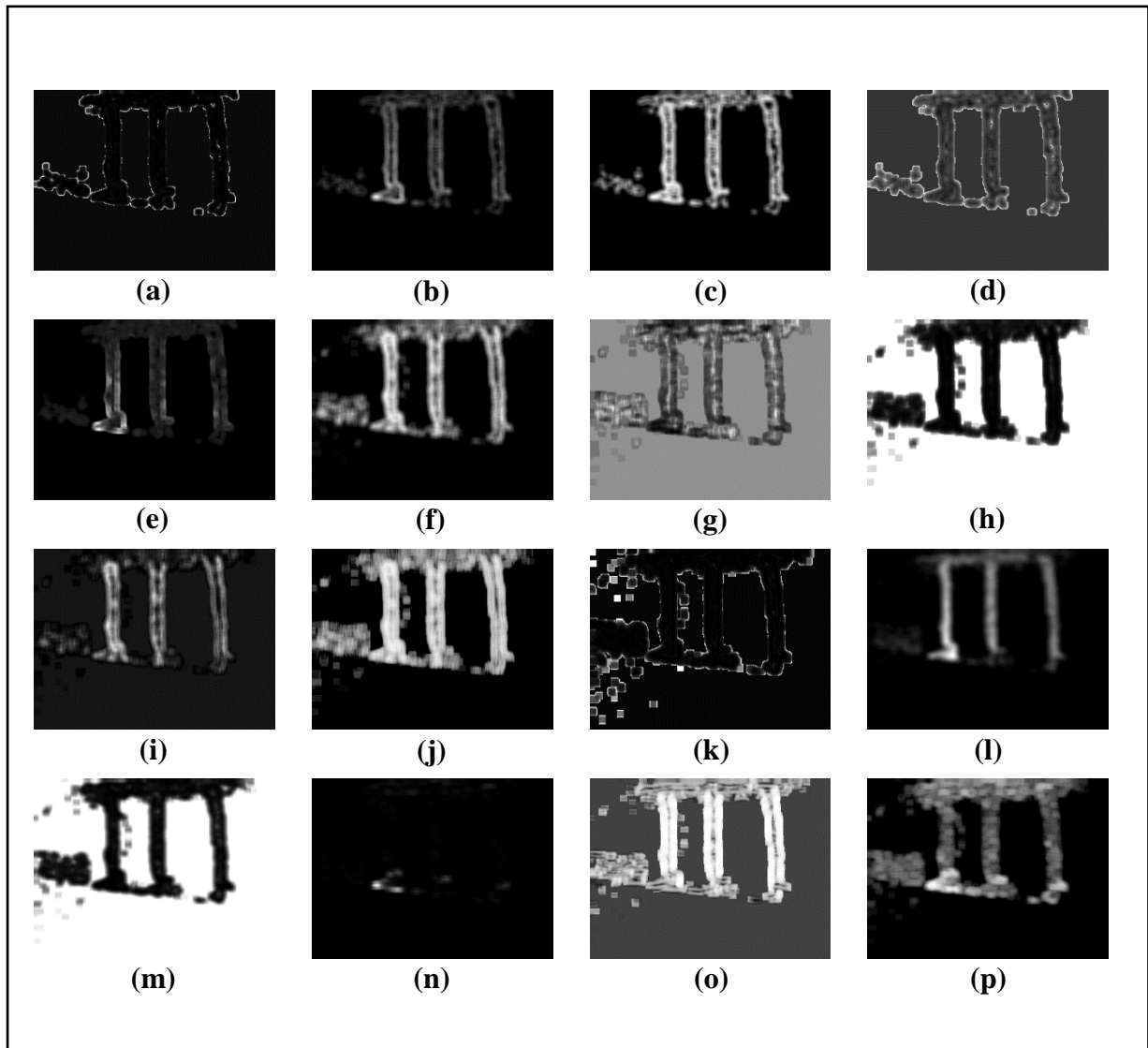
3.4.11 Collected Feature Images from Sample Image-11:

Figure 3.34: Feature Images for Sample Image-11 (Part-1)

(a) GrKurtosis4b, (b) GrMean4b, (c) GrNonZeros4b, (d) GrSkewness4b,

(e) GrVariance4b, (f) Horzl_Fraction6b, (g) Horzl_GLevNonU6b,

(h) Horzl_LngREmph6b, (i) Horzl_RLNonUni6b, (j) Horzl_ShrtREmp6b,

(k) Kurtosis, (l) Mean, (m) S(0,2)AngScMom6b, (n) S(0,2)Contrast6b ,
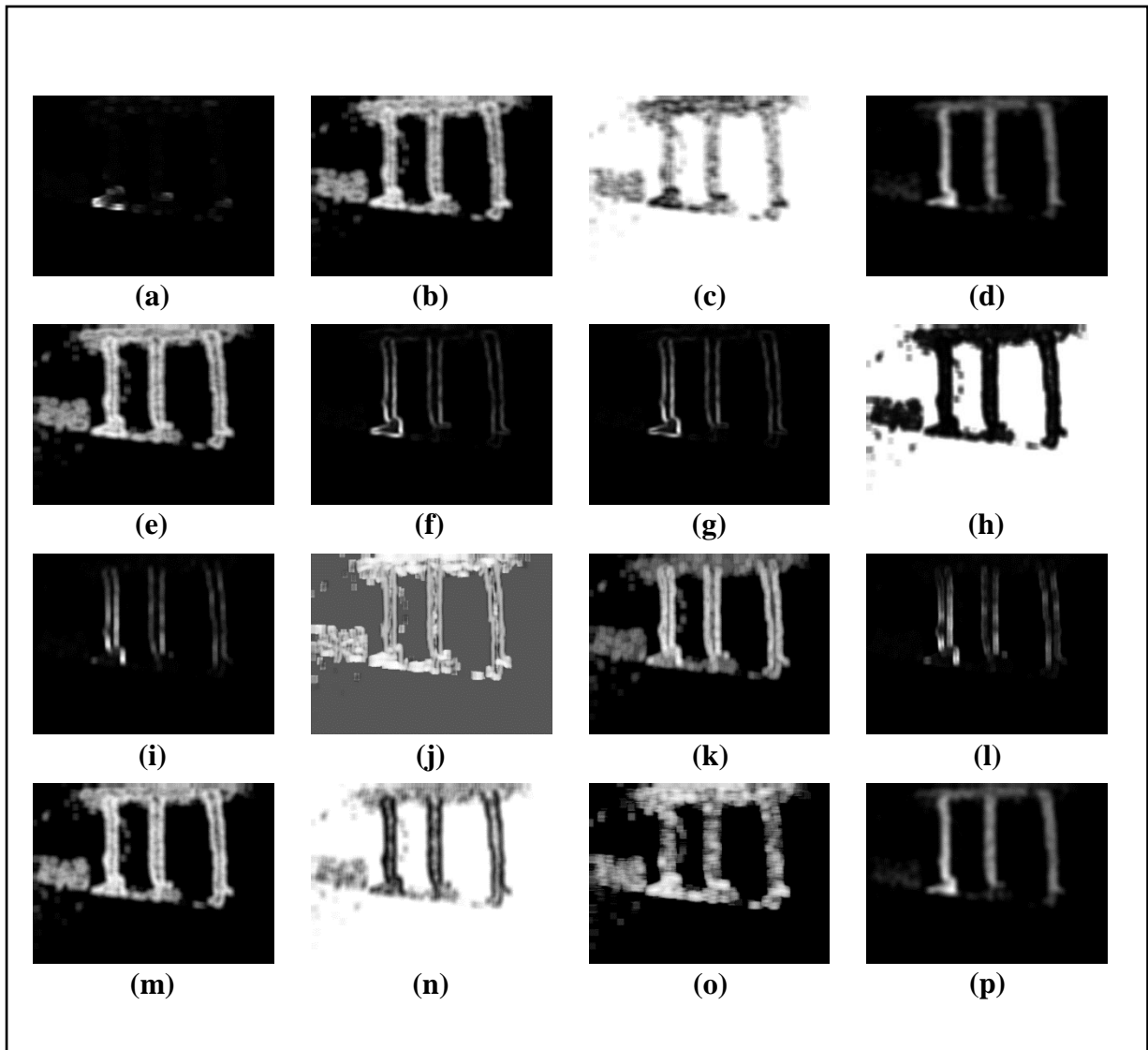
(o) S(0,2)Correlat6b, (p) S(0,2)DifEntrp6b

Figure 3.35: Feature Images for Sample Image-11 (Part-2)

(a) S(0,2)DifVarnc6b, (b) S(0,2)Entropy6b, (c) S(0,2)InvDfMom6b,

(d) S(0,2)SumAverg6b, (e) S(0,2)SumEntrp6b, (f) S(0,2)SumOfSqs6b,

(g) S(0,2)SumVarnc6b, (h) S(2,0)AngScMom6b, (i) S(2,0)Contrast6b,

(j) S(2,0)Correlat6b, (k) S(2,0)DifEntrp6b, (l) S(2,0)DifVarnc6b,

(m) S(2,0)Entropy6b, (n) S(2,0)InvDfMom6b ,
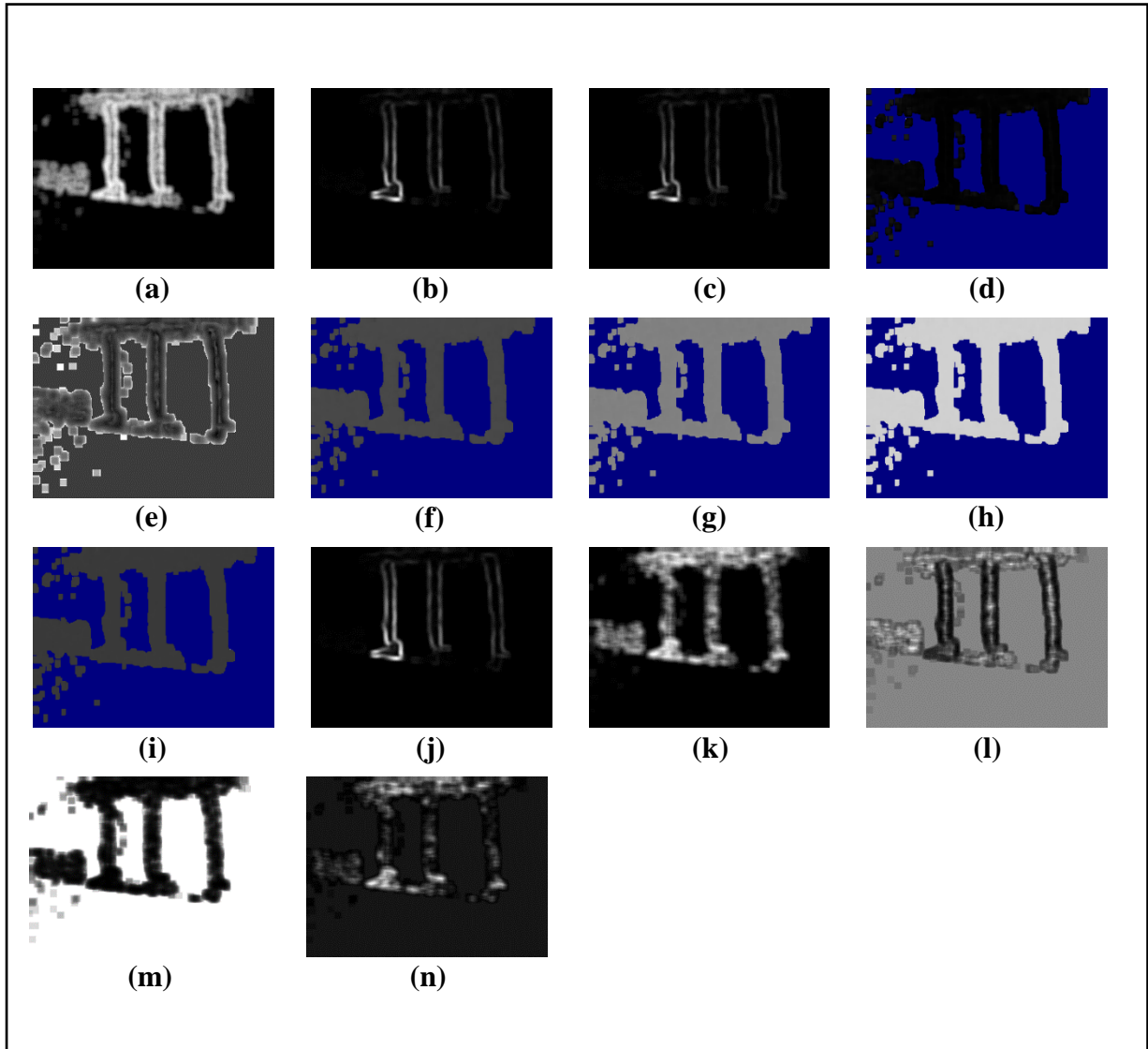
(o) Vertl_ShrtREmp6b, (p) S(2,0)SumAverg6b

Figure 3.36: Feature Images for Sample Image-11 (Part-3)

(a) S(2,0)SumEntrp6b, (b) S(2,0)SumOfSqs6b, (c) S(2,0)SumVarnc6b, (d) Sigma,

(e) Skewness, (f) Teta1, (g) Teta2, (h) Teta3, (i) Teta4, (j) Variance, (k) Vertl_Fraction6b,

(l) Vertl_GLevNonU6b, (m) Vertl_LngREmph6b, (n) Vertl_RLNonUni6b
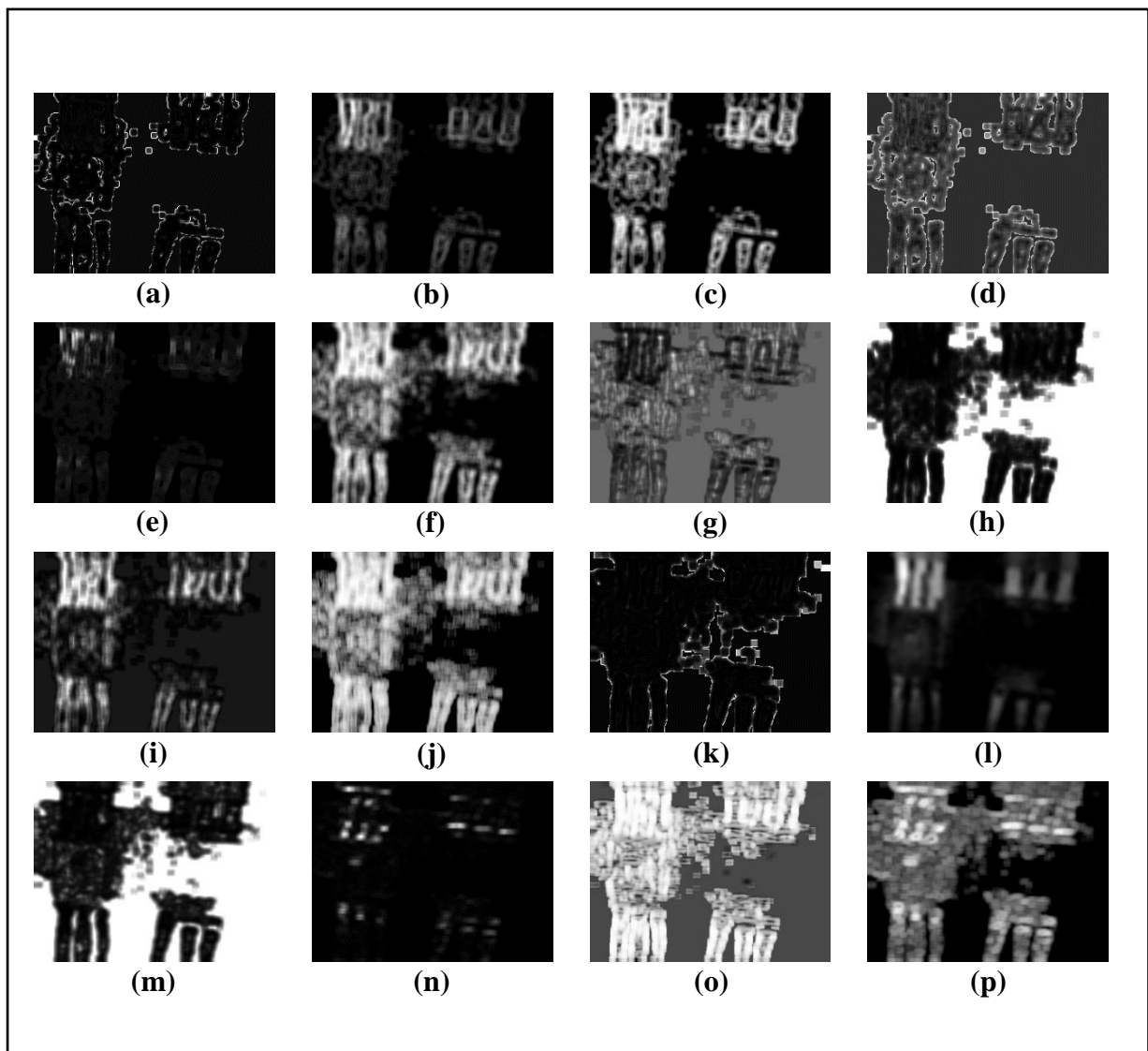
3.4.12 Collected Feature Images from Sample Image-12:

Figure 3.37: Feature Images for Sample Image-12 (Part-1)

(a) GrKurtosis4b, (b) GrMean4b, (c) GrNonZeros4b, (d) GrSkewness4b,

(e) GrVariance4b, (f) Horzl_Fraction6b, (g) Horzl_GLevNonU6b,

(h) Horzl_LngREmph6b, (i) Horzl_RLNonUni6b, (j) Horzl_ShrtREmp6b,

(k) Kurtosis, (l) Mean, (m) S(0,2)AngScMom6b, (n) S(0,2)Contrast6b ,
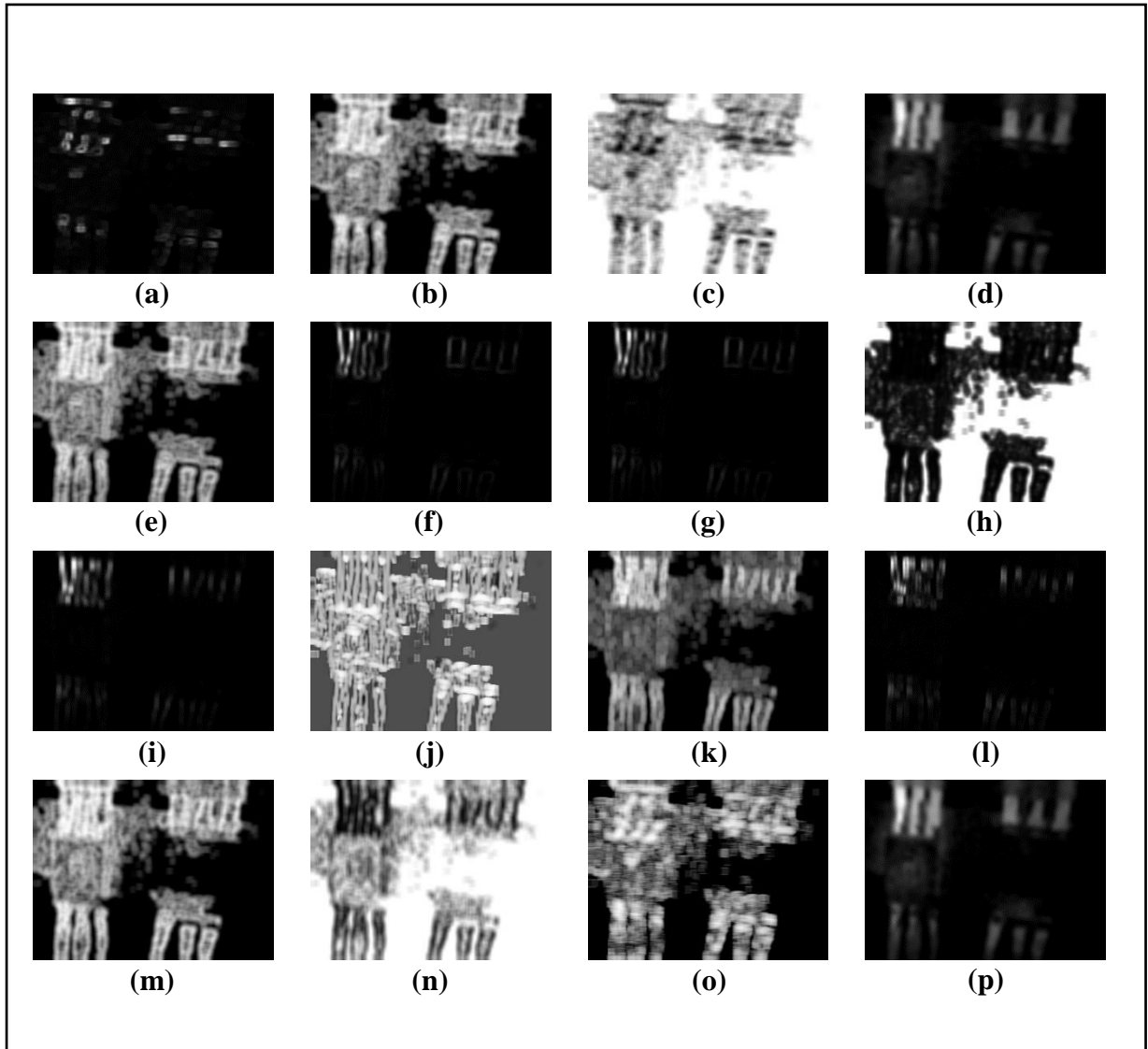
(o) S(0,2)Correlat6b, (p) S(0,2)DifEntrp6b

Figure 3.38: Feature Images for Sample Image-12 (Part-2)

(a) S(0,2)DifVarnc6b, (b) S(0,2)Entropy6b, (c) S(0,2)InvDfMom6b,

(d) S(0,2)SumAverg6b, (e) S(0,2)SumEntrp6b, (f) S(0,2)SumOfSqs6b,

(g) S(0,2)SumVarnc6b, (h) S(2,0)AngScMom6b, (i) S(2,0)Contrast6b,

(j) S(2,0)Correlat6b, (k) S(2,0)DifEntrp6b, (l) S(2,0)DifVarnc6b,

(m) S(2,0)Entropy6b, (n) S(2,0)InvDfMom6b ,
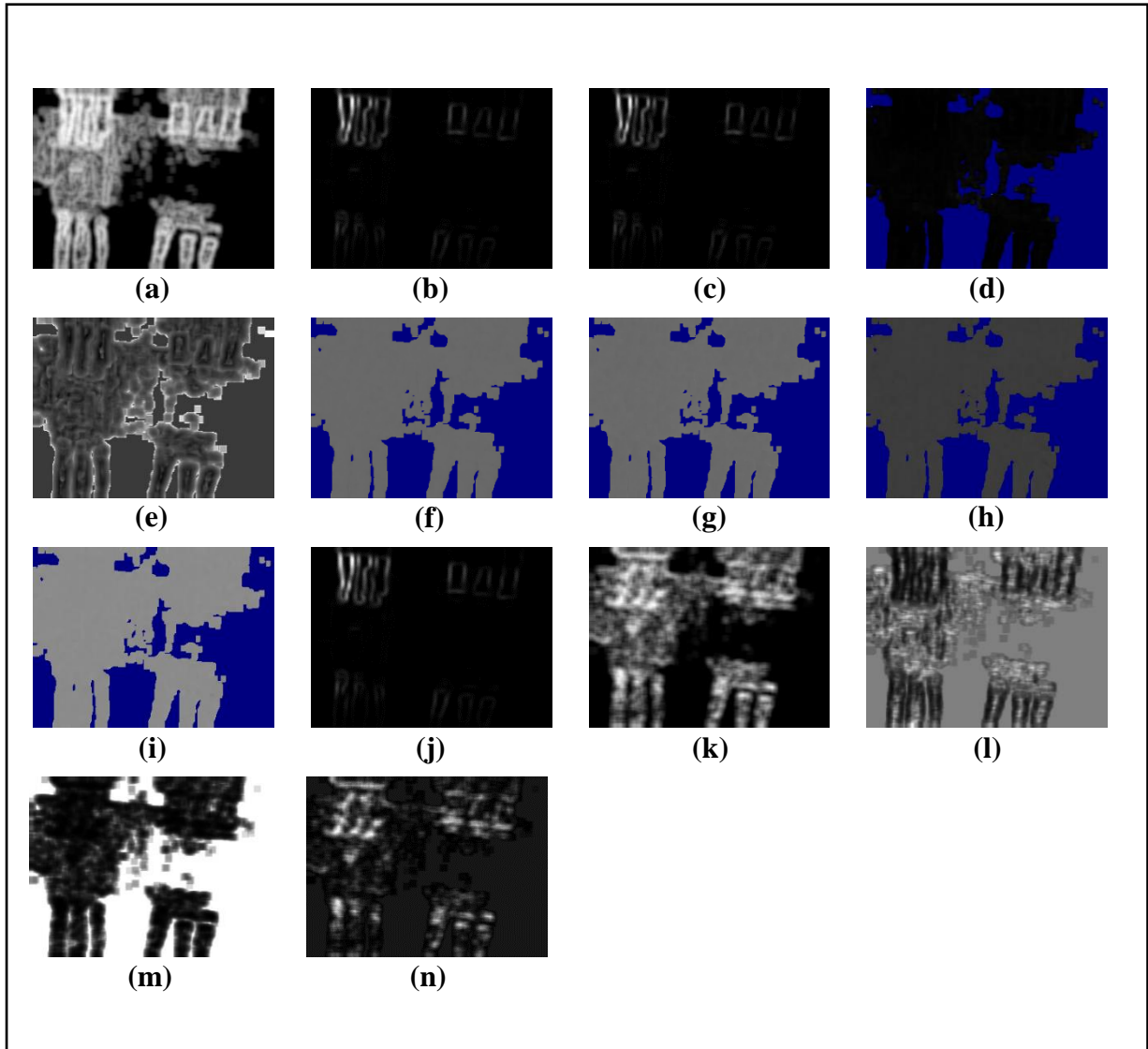
(o) Vertl_ShrtREmp6b, (p) S(2,0)SumAverg6b

Figure 3.39: Feature Images for Sample Image-12 (Part-3)

(a) S(2,0)SumEntrp6b, (b) S(2,0)SumOfSqs6b, (c) S(2,0)SumVarnc6b, (d) Sigma,

(e) Skewness, (f) Teta1, (g) Teta2, (h) Teta3, (i) Teta4, (j) Variance, (k) Vertl_Fraction6b,

(l) Vertl_GLevNonU6b, (m) Vertl_LngREmph6b, (n) Vertl_RLNonUni6b
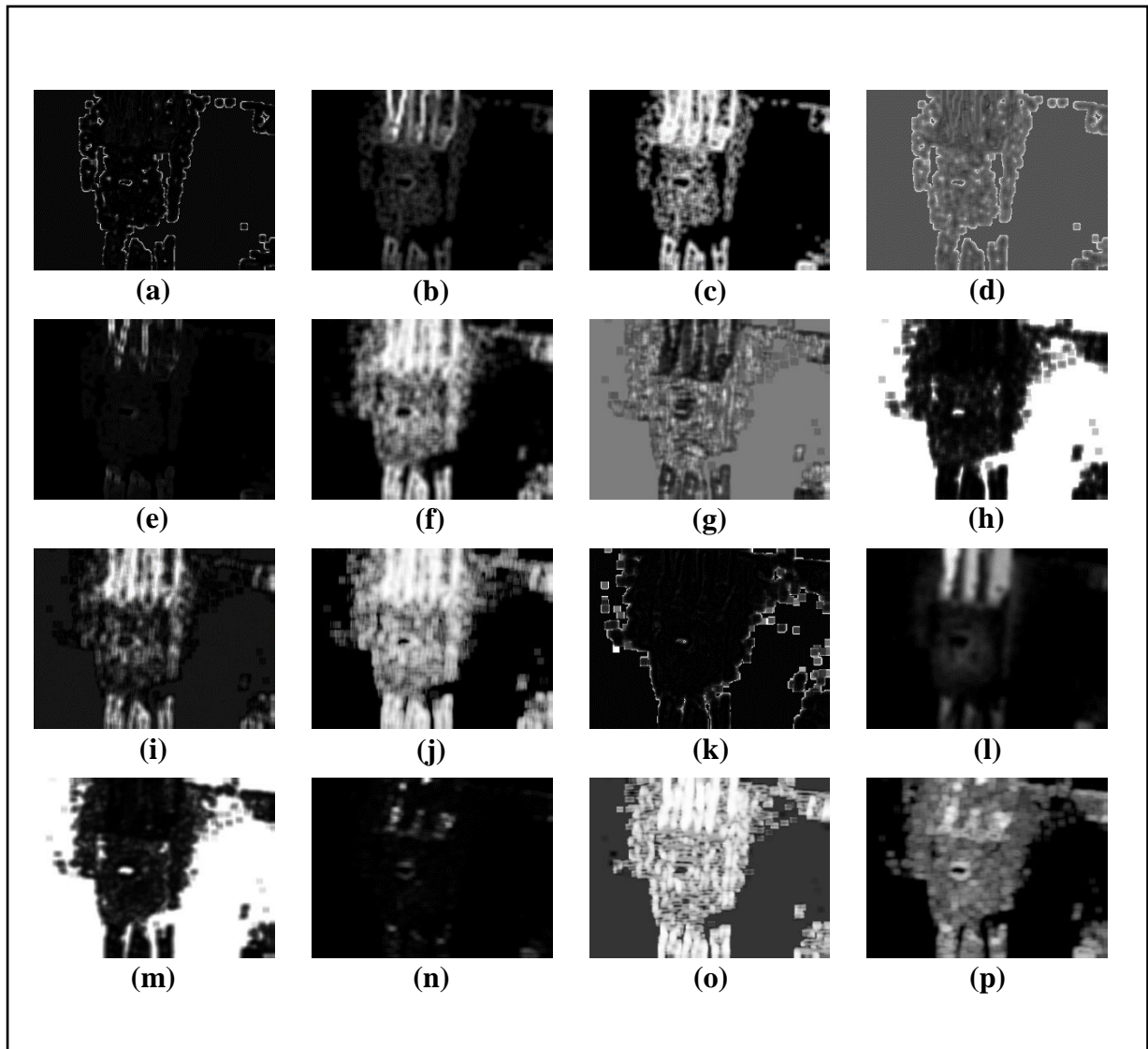
3.4.13 Collected Feature Images from Sample Image-13:
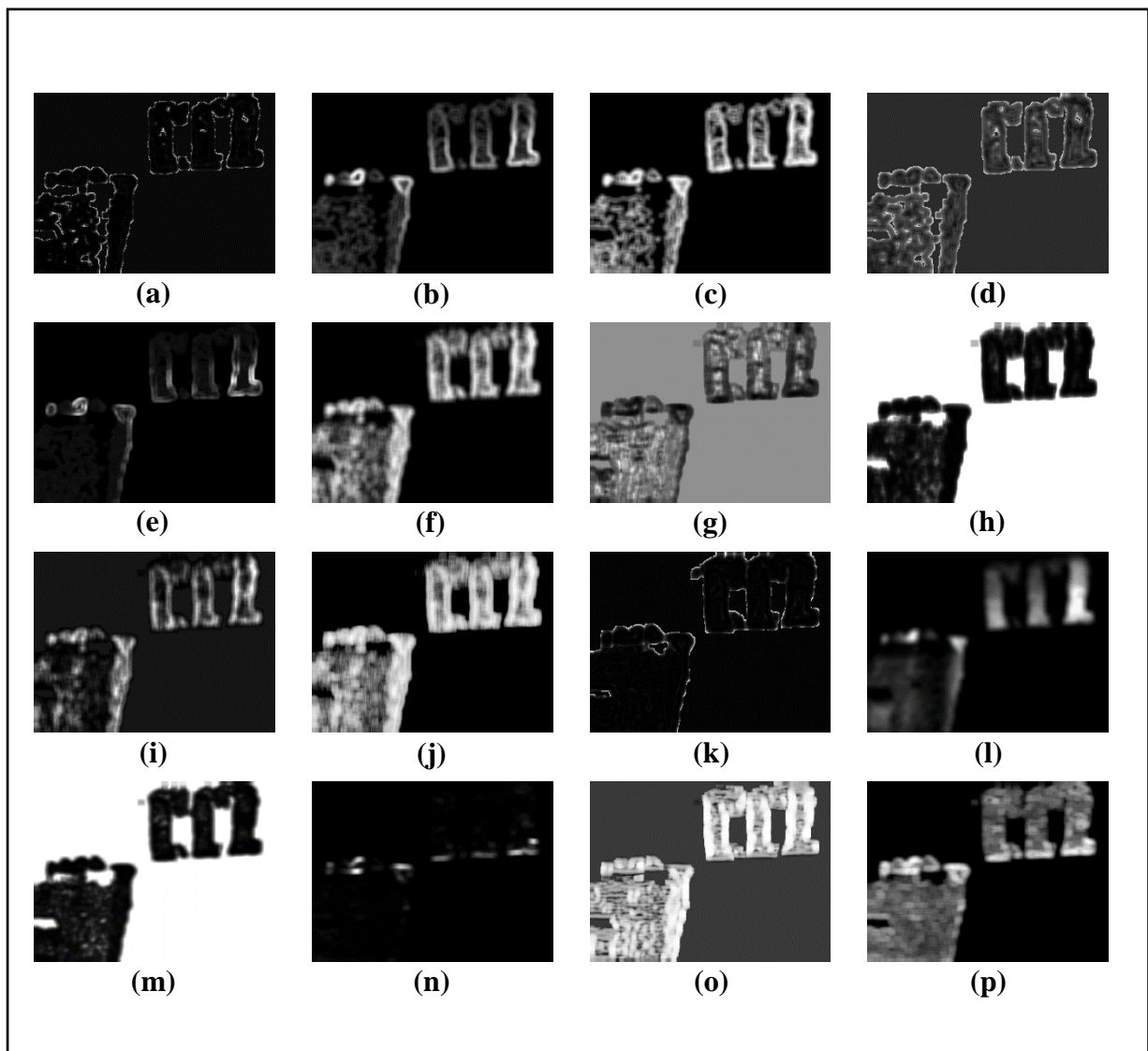
Figure 3.40: Feature Images for Sample Image-13 (Part-1)

(a) GrKurtosis4b, (b) GrMean4b, (c) GrNonZeros4b, (d) GrSkewness4b,

(e) GrVariance4b, (f) Horzl_Fraction6b, (g) Horzl_GLevNonU6b,

(h) Horzl_LngREmph6b, (i) Horzl_RLNonUni6b, (j) Horzl_ShrtREmp6b,

(k) Kurtosis, (l) Mean, (m) S(0,2)AngScMom6b, (n) S(0,2)Contrast6b ,
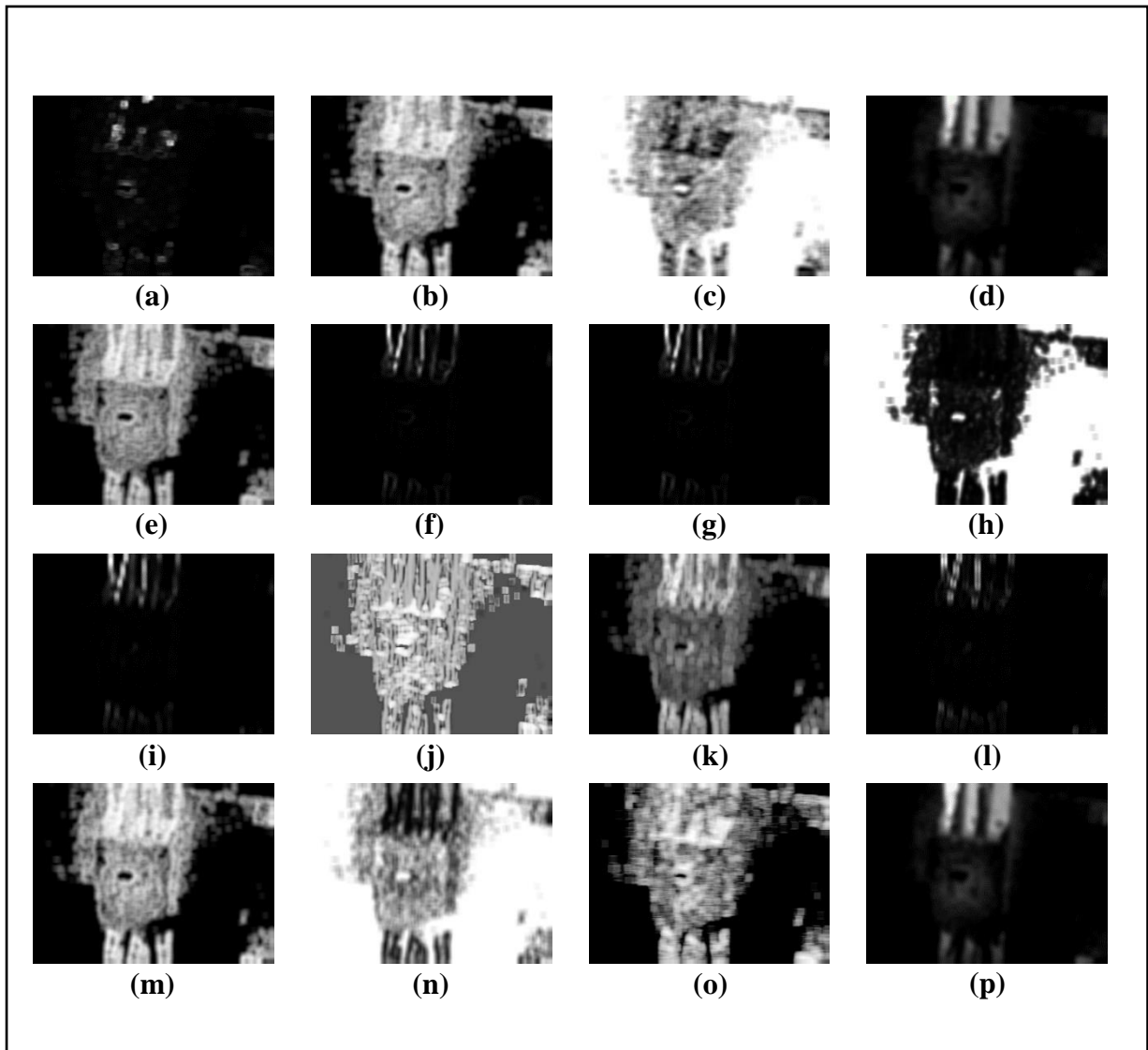
(o) S(0,2)Correlat6b, (p) S(0,2)DifEntrp6b

Figure 3.41: Feature Images for Sample Image-13 (Part-2)

(a) S(0,2)DifVarnc6b, (b) S(0,2)Entropy6b, (c) S(0,2)InvDfMom6b,

(d) S(0,2)SumAverg6b, (e) S(0,2)SumEntrp6b, (f) S(0,2)SumOfSqs6b,

(g) S(0,2)SumVarnc6b, (h) S(2,0)AngScMom6b, (i) S(2,0)Contrast6b,

(j) S(2,0)Correlat6b, (k) S(2,0)DifEntrp6b, (l) S(2,0)DifVarnc6b,

(m) S(2,0)Entropy6b, (n) S(2,0)InvDfMom6b ,
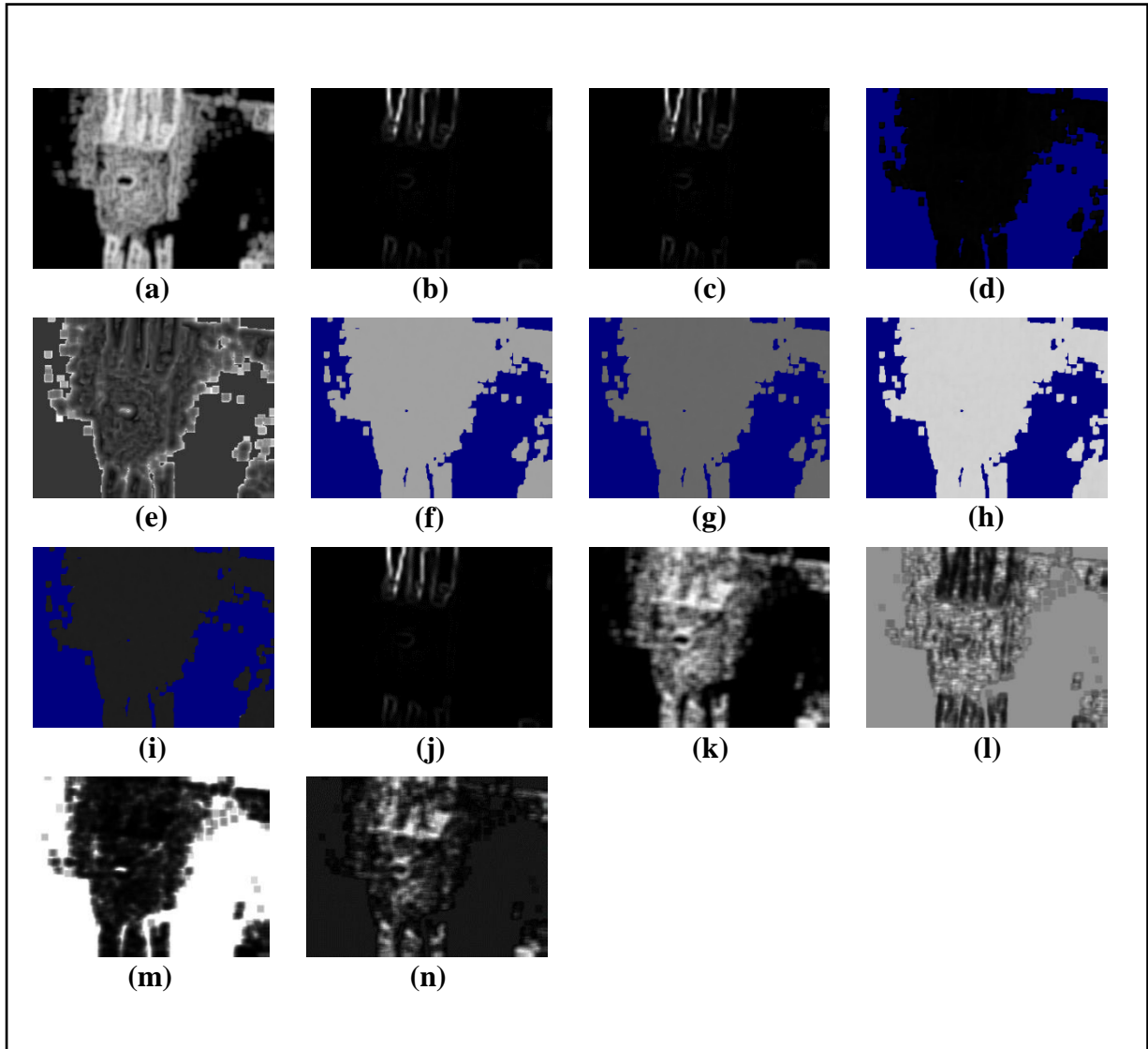
(o) Vertl_ShrtREmp6b, (p) S(2,0)SumAverg6b
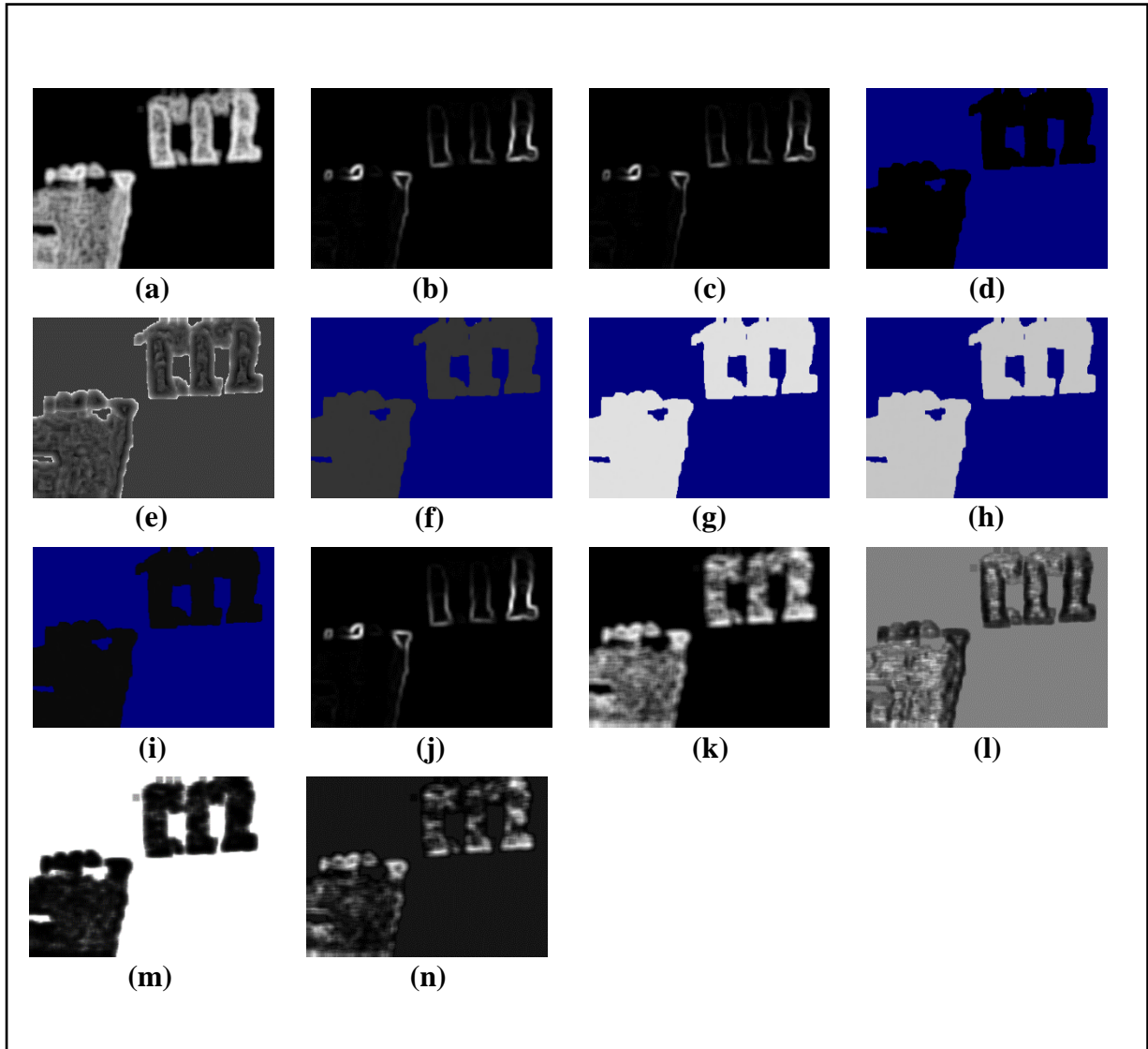
Figure 3.42: Feature Images for Sample Image-13 (Part-3)

(a) S(2,0)SumEntrp6b, (b) S(2,0)SumOfSqs6b, (c) S(2,0)SumVarnc6b, (d) Sigma,

(e) Skewness, (f) Teta1, (g) Teta2, (h) Teta3, (i) Teta4, (j) Variance, (k) Vertl_Fraction6b,

(l) Vertl_GLevNonU6b, (m) Vertl_LngREmph6b, (n) Vertl_RLNonUni6b
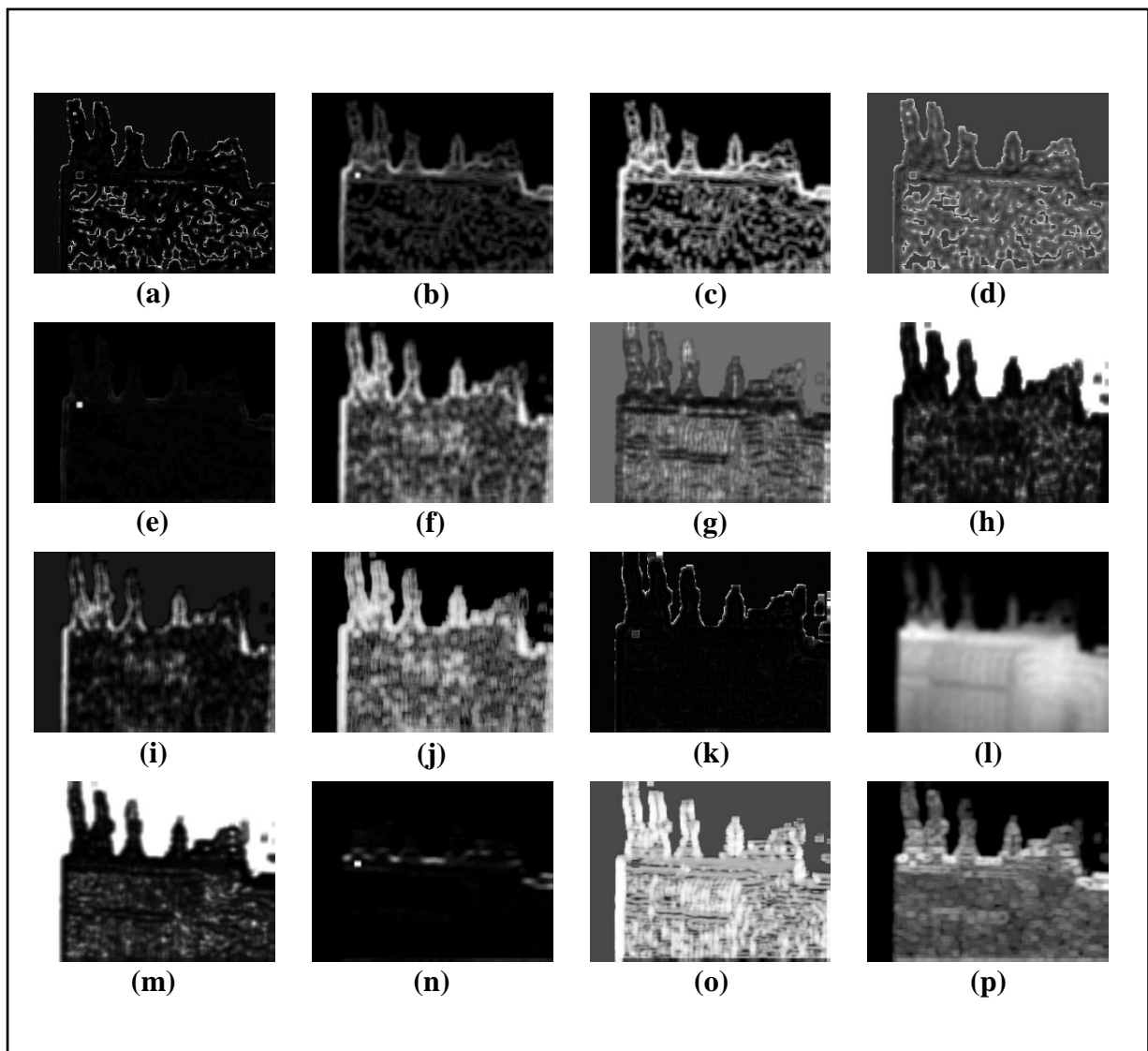
3.4.14 Collected Feature Images from Sample Image-14:
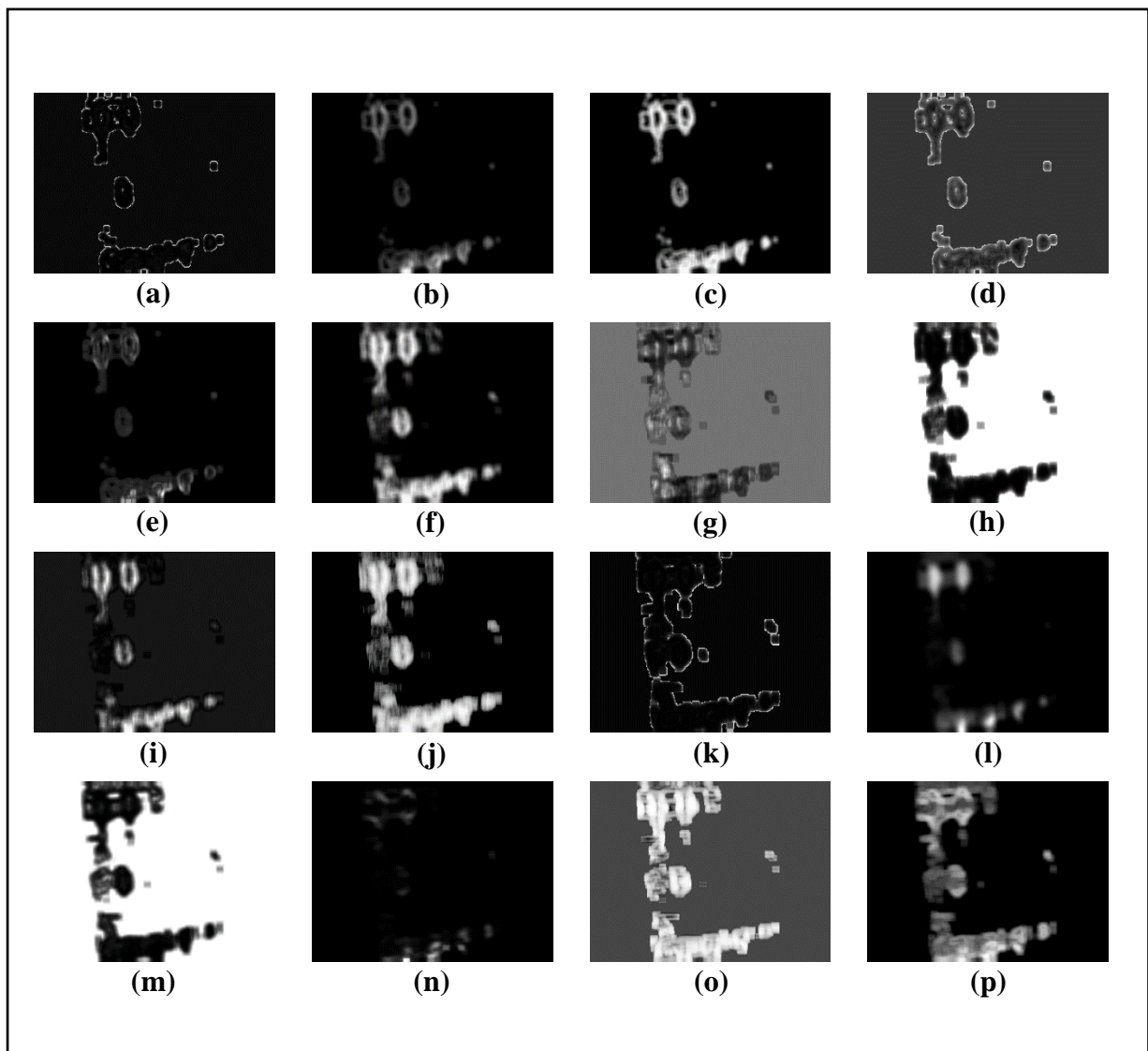
Figure 3.43: Feature Images for Sample Image-14 (Part-1)

(a) GrKurtosis4b, (b) GrMean4b, (c) GrNonZeros4b, (d) GrSkewness4b,

(e) GrVariance4b, (f) Horzl_Fraction6b, (g) Horzl_GLevNonU6b,

(h) Horzl_LngREmph6b, (i) Horzl_RLNonUni6b, (j) Horzl_ShrtREmp6b,

(k) Kurtosis, (l) Mean, (m) S(0,2)AngScMom6b, (n) S(0,2)Contrast6b ,

(o) S(0,2)Correlat6b, (p) S(0,2)DifEntrp6b
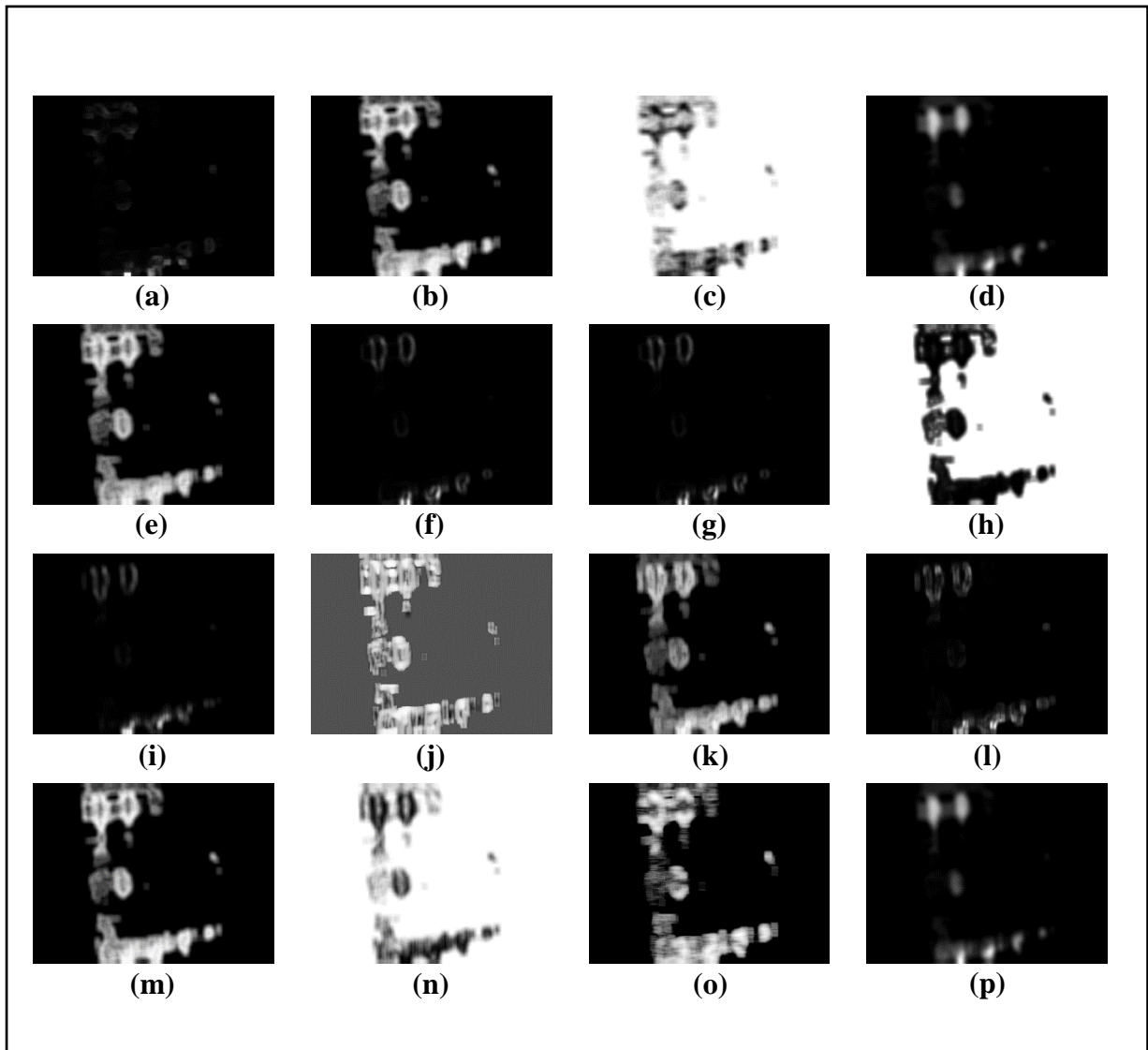
Figure 3.44: Feature Images for Sample Image-14 (Part-2)

(a) S(0,2)DifVarnc6b, (b) S(0,2)Entropy6b, (c) S(0,2)InvDfMom6b,

(d) S(0,2)SumAverg6b, (e) S(0,2)SumEntrp6b, (f) S(0,2)SumOfSqs6b,

(g) S(0,2)SumVarnc6b, (h) S(2,0)AngScMom6b, (i) S(2,0)Contrast6b,

(j) S(2,0)Correlat6b, (k) S(2,0)DifEntrp6b, (l) S(2,0)DifVarnc6b,

(m) S(2,0)Entropy6b, (n) S(2,0)InvDfMom6b ,

(o) Vertl_ShrtREmp6b, (p) S(2,0)SumAverg6b
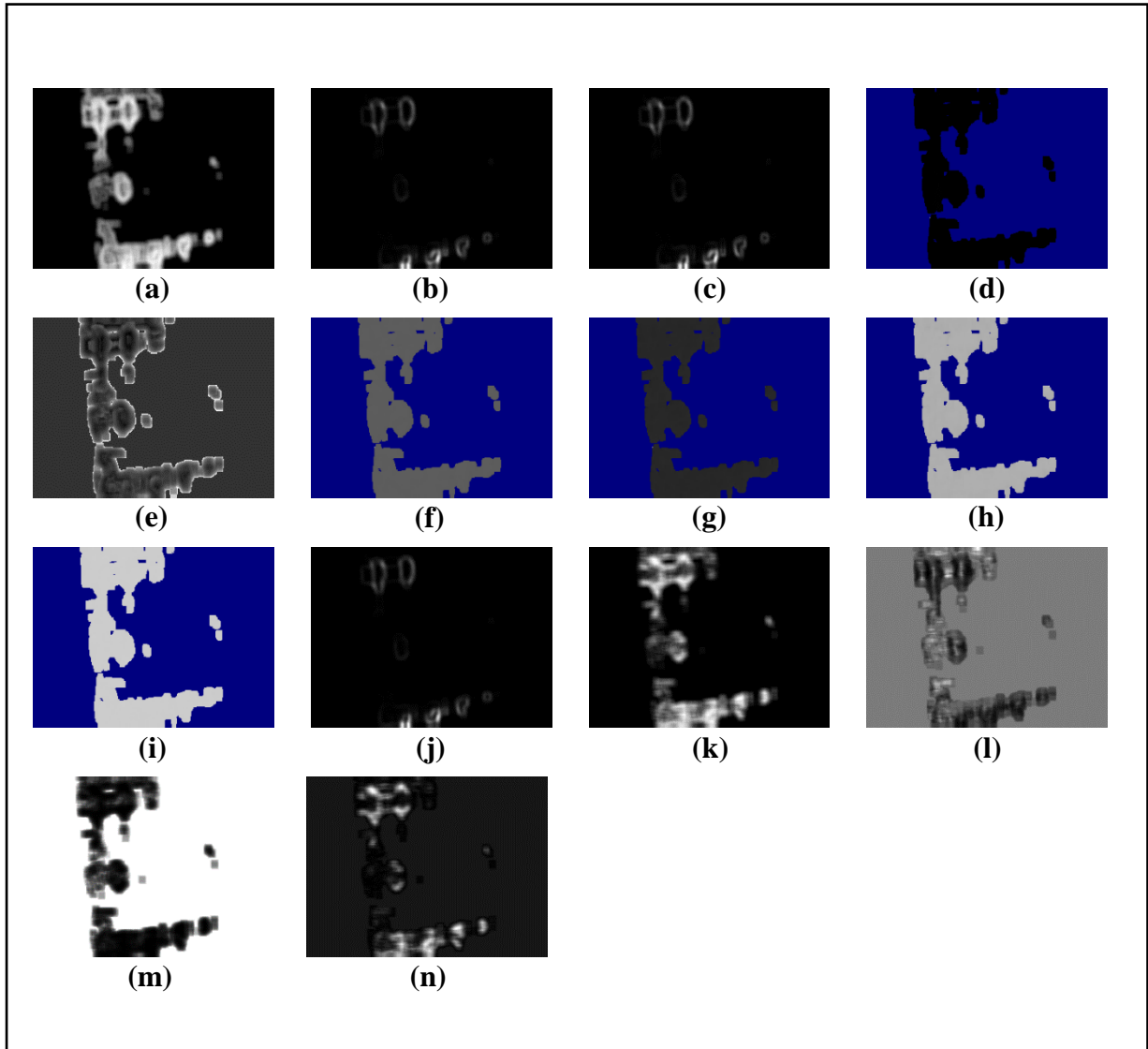
Figure 3.45: Feature Images for Sample Image-14 (Part-3)

(a) S(2,0)SumEntrp6b, (b) S(2,0)SumOfSqs6b, (c) S(2,0)SumVarnc6b, (d) Sigma,

(e) Skewness, (f) Teta1, (g) Teta2, (h) Teta3, (i) Teta4, (j) Variance, (k) Vertl_Fraction6b,

(l) Vertl_GLevNonU6b, (m) Vertl_LngREmph6b, (n) Vertl_RLNonUni6b

3.4.15 Collected Feature Images from Sample Image-15:
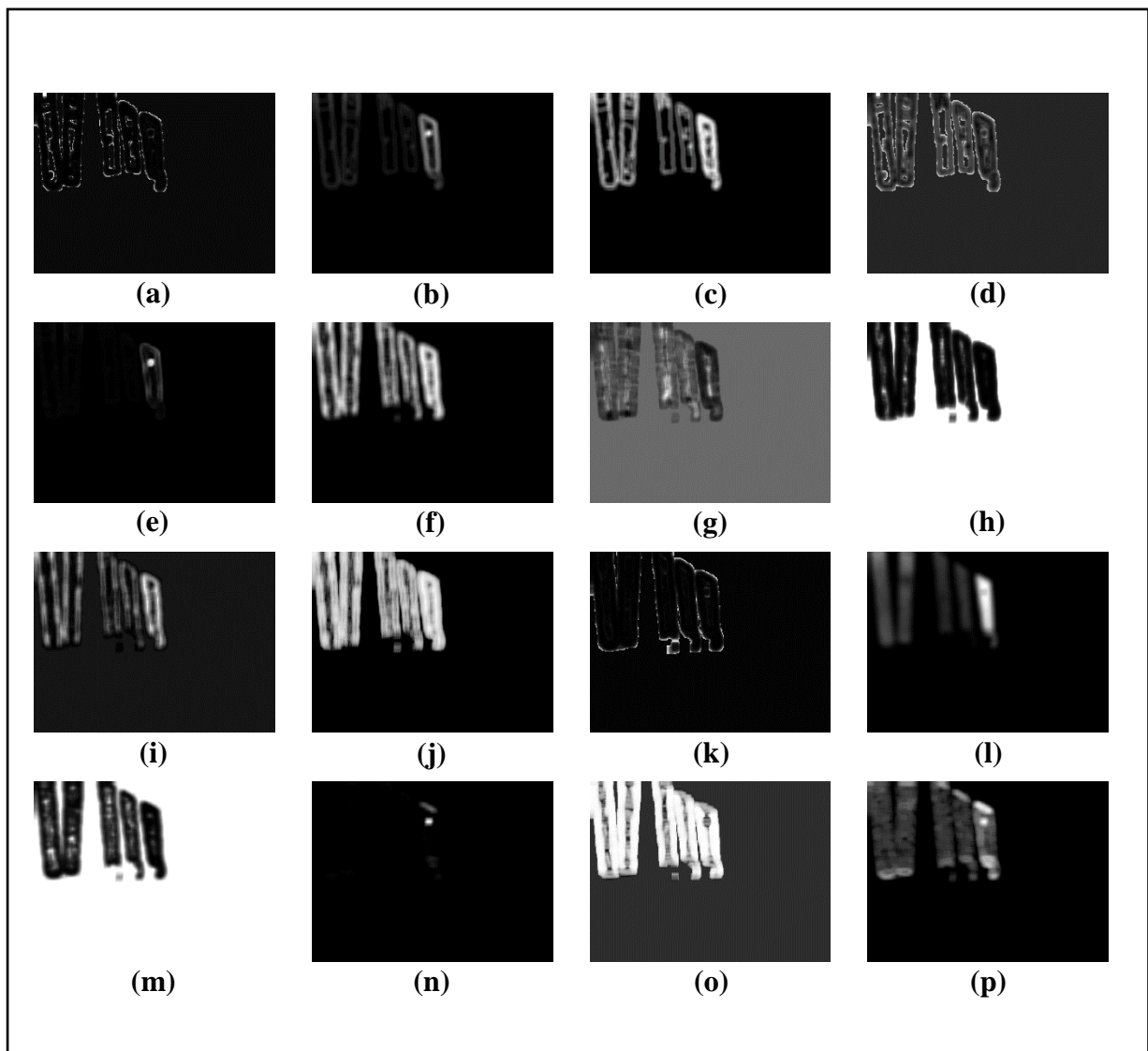
Figure 3.46: Feature Images for Sample Image-15 (Part-1)

(a) GrKurtosis4b, (b) GrMean4b, (c) GrNonZeros4b, (d) GrSkewness4b,

(e) GrVariance4b, (f) Horzl_Fraction6b, (g) Horzl_GLevNonU6b,

(h) Horzl_LngREmph6b, (i) Horzl_RLNonUni6b, (j) Horzl_ShrtREmp6b,

(k) Kurtosis, (l) Mean, (m) S(0,2)AngScMom6b, (n) S(0,2)Contrast6b ,
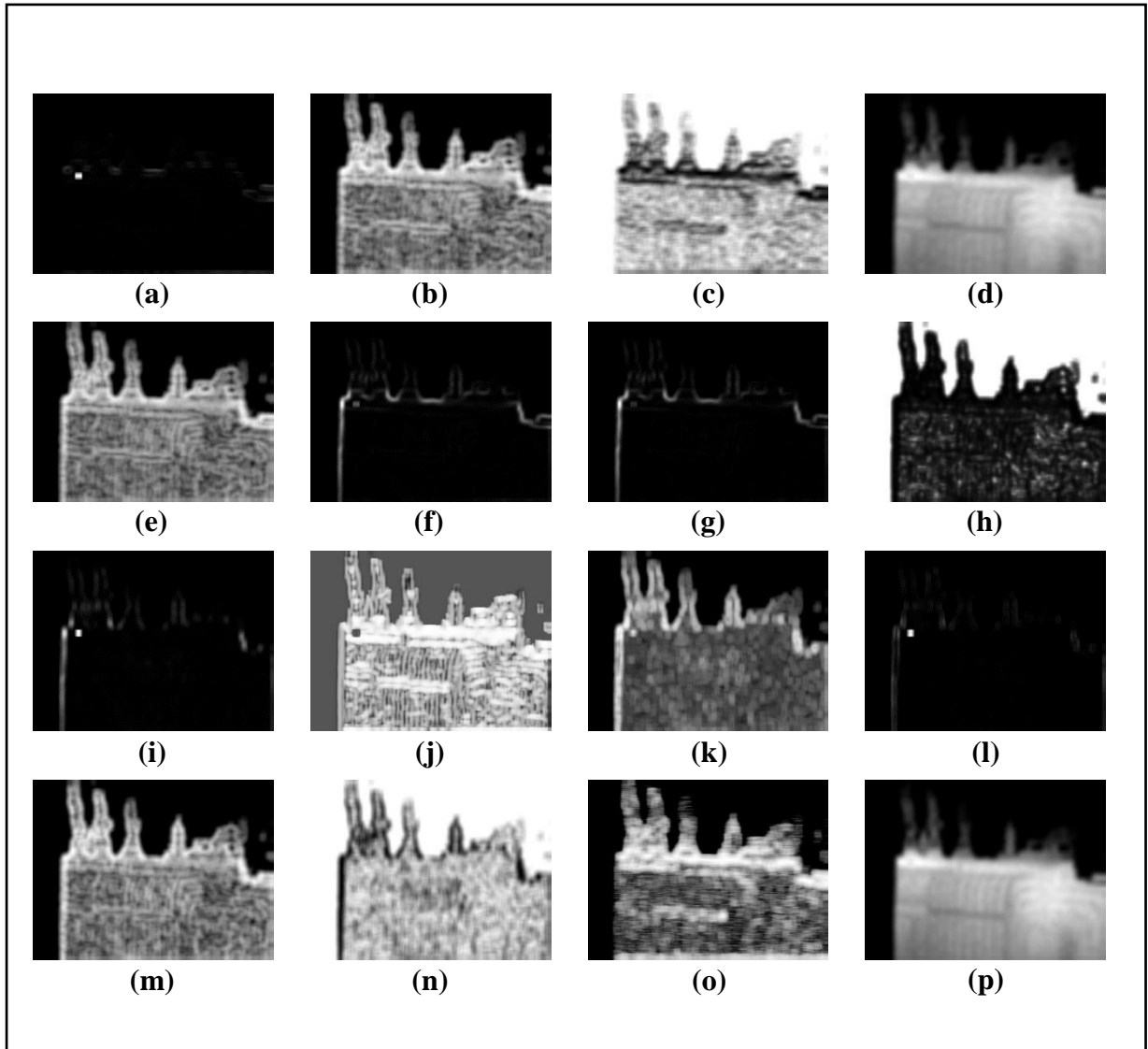
(o) S(0,2)Correlat6b, (p) S(0,2)DifEntrp6b
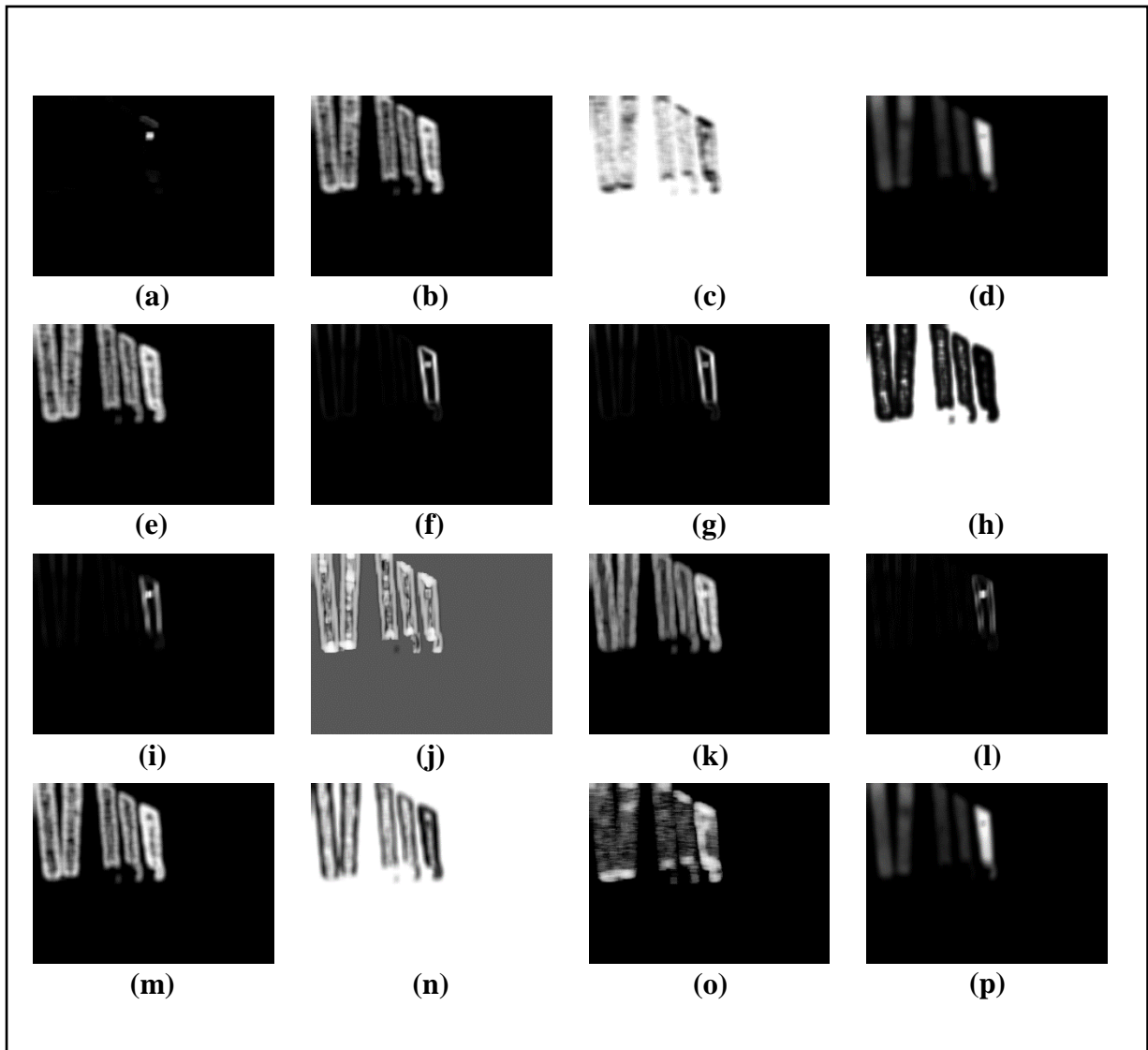
Figure 3.47: Feature Images for Sample Image-15 (Part-2)

(a) S(0,2)DifVarnc6b, (b) S(0,2)Entropy6b, (c) S(0,2)InvDfMom6b,

(d) S(0,2)SumAverg6b, (e) S(0,2)SumEntrp6b, (f) S(0,2)SumOfSqs6b,

(g) S(0,2)SumVarnc6b, (h) S(2,0)AngScMom6b, (i) S(2,0)Contrast6b,

(j) S(2,0)Correlat6b, (k) S(2,0)DifEntrp6b, (l) S(2,0)DifVarnc6b,

(m) S(2,0)Entropy6b, (n) S(2,0)InvDfMom6b ,
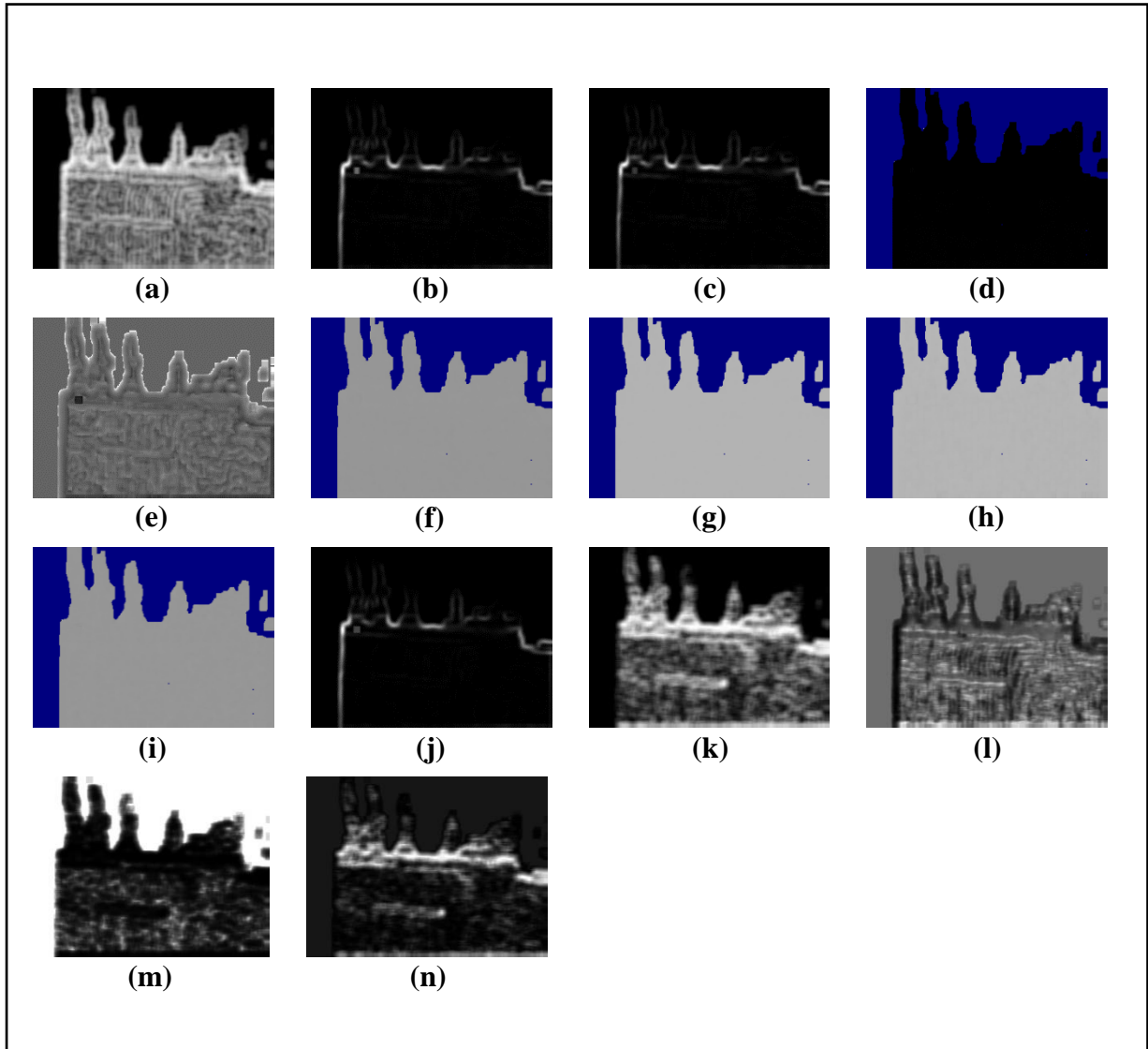
(o) Vertl_ShrtREmp6b, (p) S(2,0)SumAverg6b
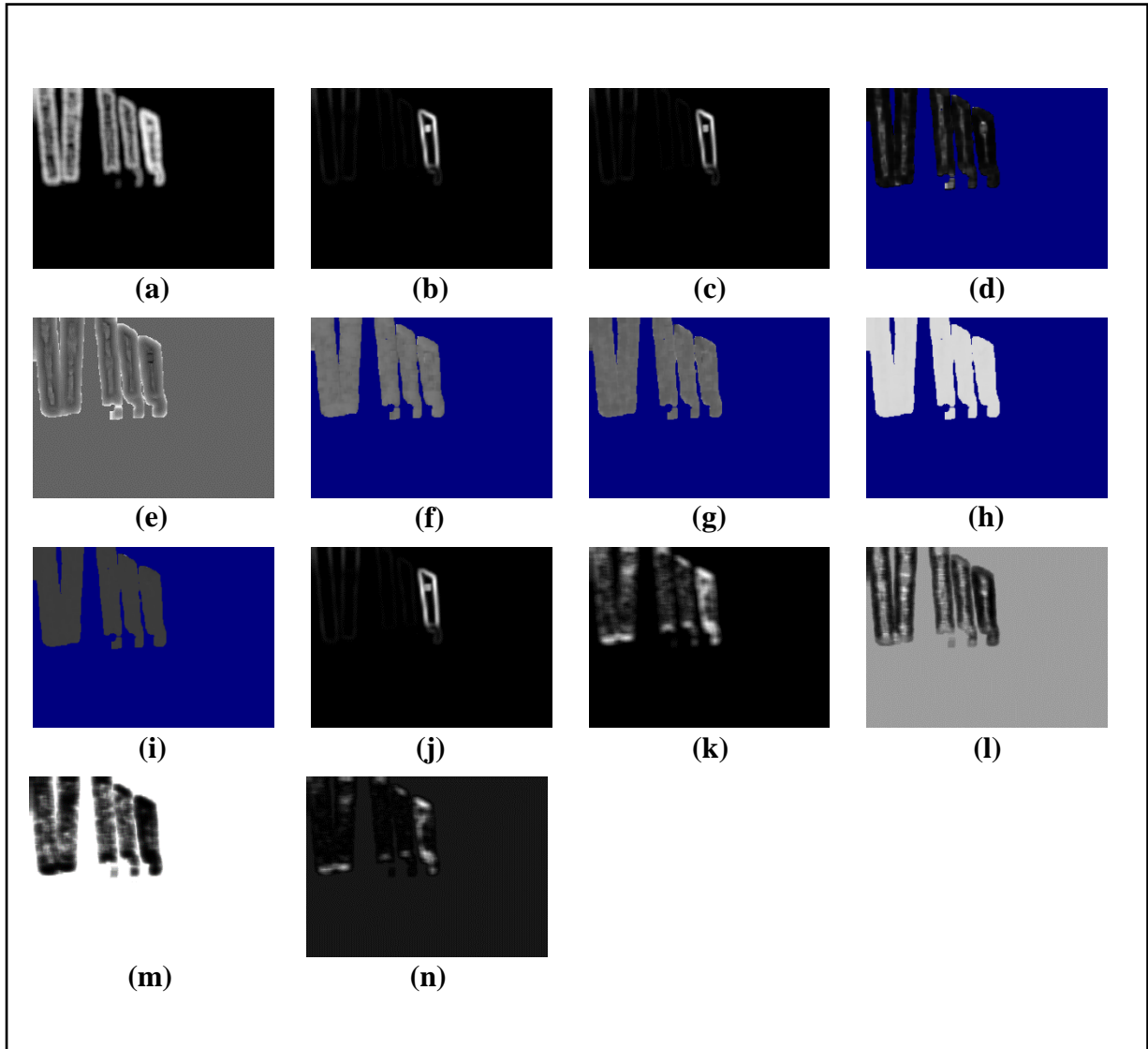
Figure 3.48: Feature Images for Sample Image-15 (Part-3)

(a) S(2,0)SumEntrp6b, (b) S(2,0)SumOfSqs6b, (c) S(2,0)SumVarnc6b, (d) Sigma,

(e) Skewness, (f) Teta1, (g) Teta2, (h) Teta3, (i) Teta4, (j) Variance, (k) Vertl_Fraction6b,

(l) Vertl_GLevNonU6b, (m) Vertl_LngREmph6b, (n) Vertl_RLNonUni6b
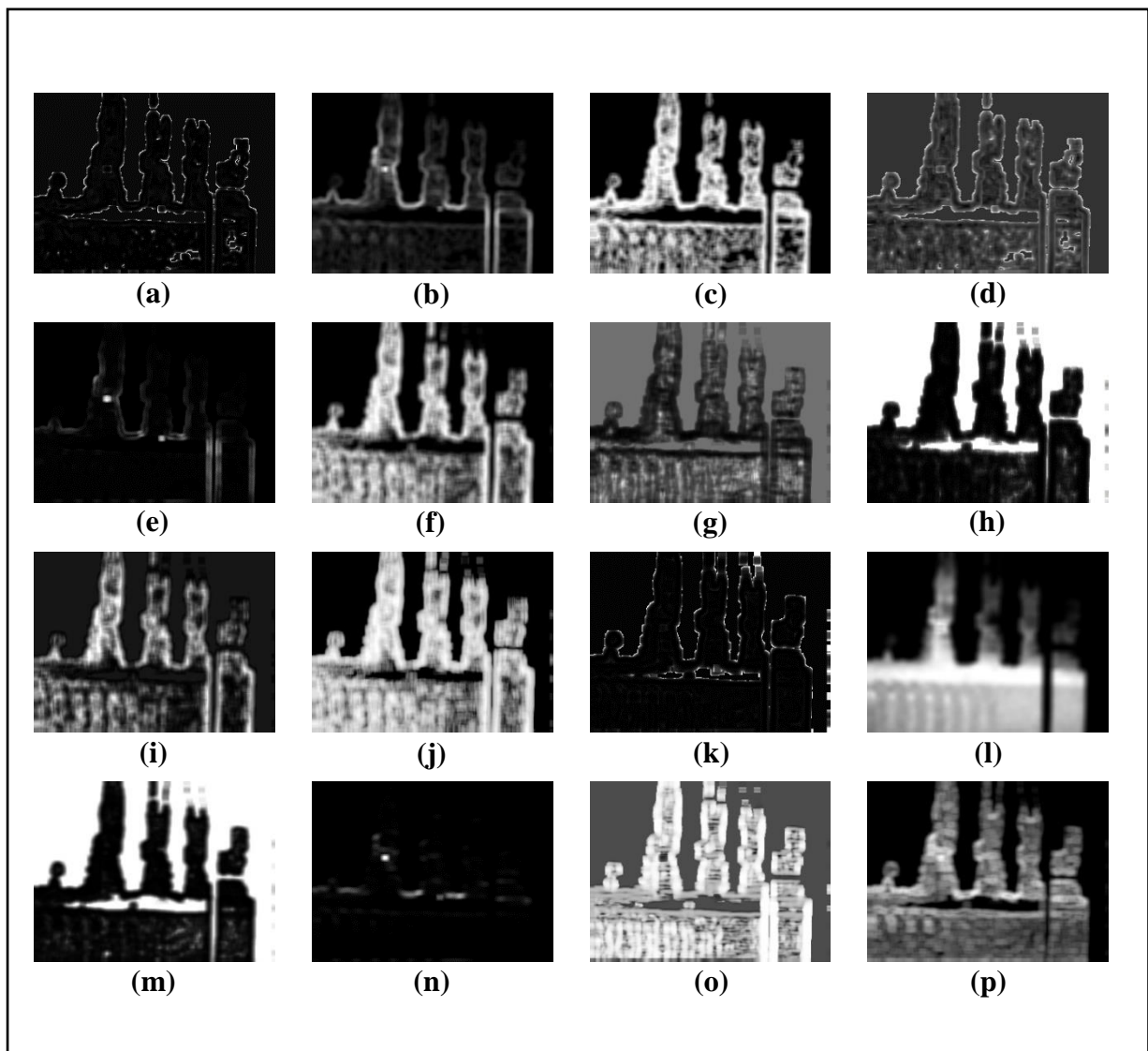
3.4.16 Collected Feature Images from Sample Image-16:
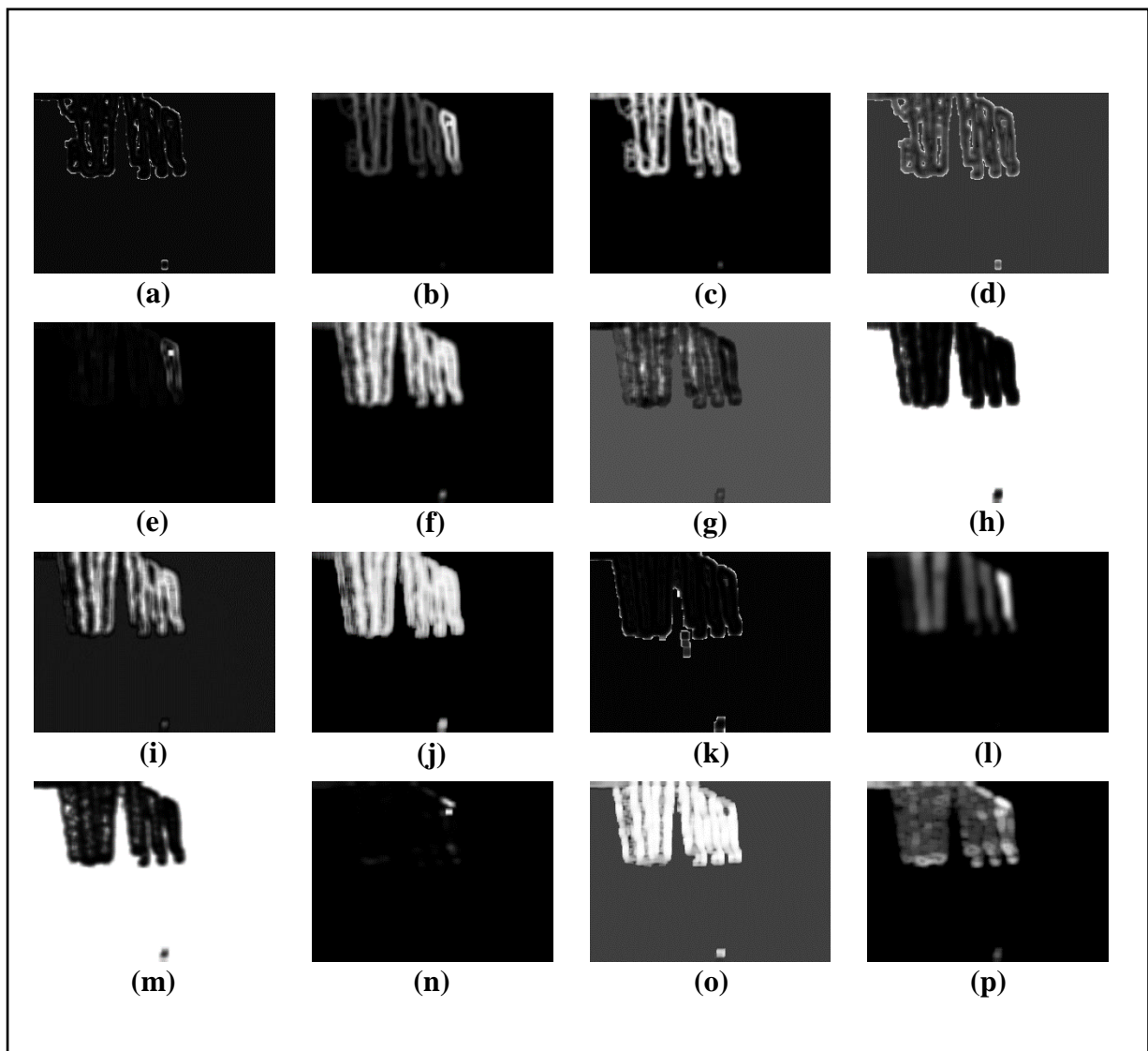
Figure 3.49: Feature Images for Sample Image-16 (Part-1)

(a) GrKurtosis4b, (b) GrMean4b, (c) GrNonZeros4b, (d) GrSkewness4b,

(e) GrVariance4b, (f) Horzl_Fraction6b, (g) Horzl_GLevNonU6b,

(h) Horzl_LngREmph6b, (i) Horzl_RLNonUni6b, (j) Horzl_ShrtREmp6b,

(k) Kurtosis, (l) Mean, (m) S(0,2)AngScMom6b, (n) S(0,2)Contrast6b ,
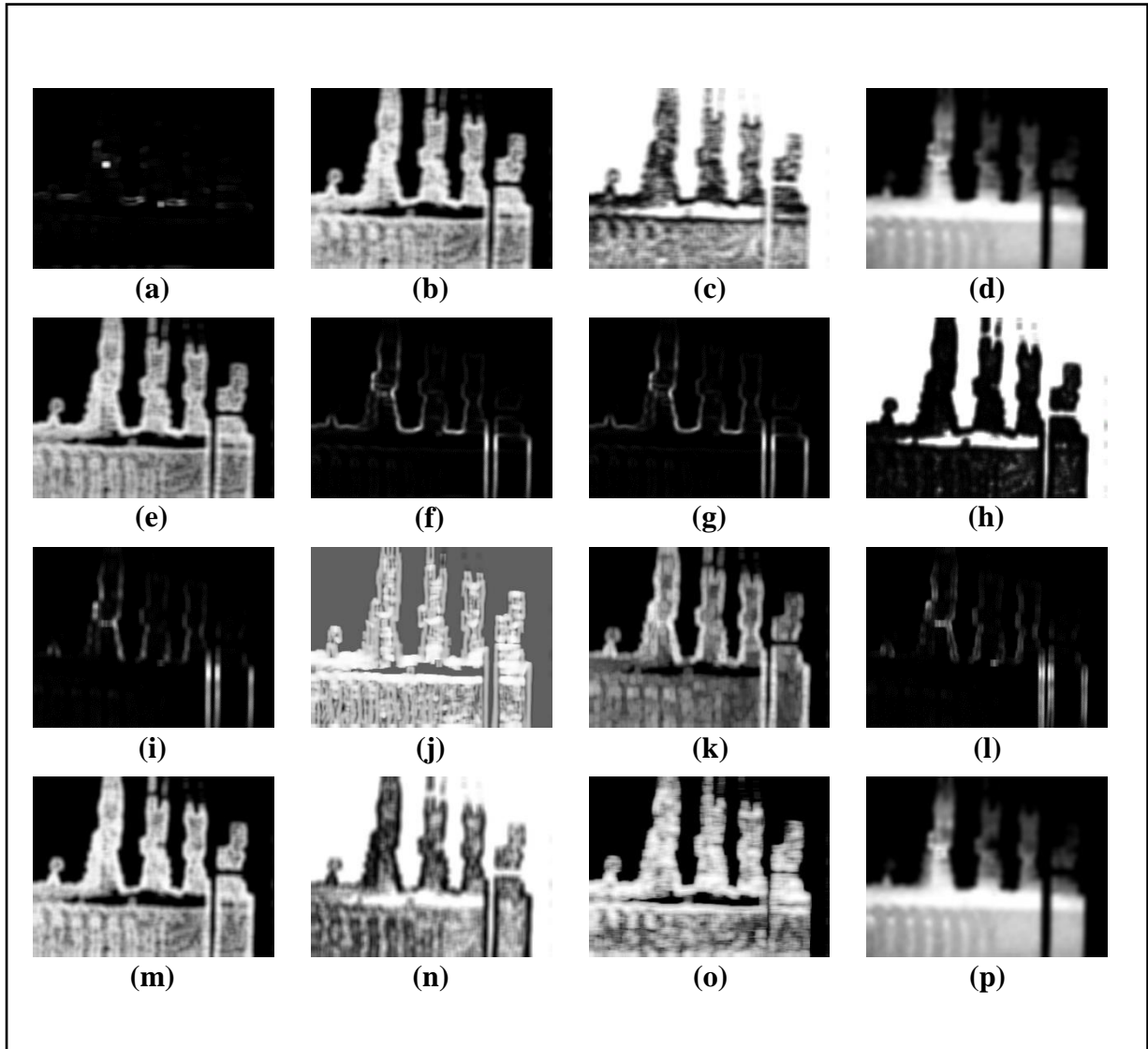
(o) S(0,2)Correlat6b, (p) S(0,2)DifEntrp6b
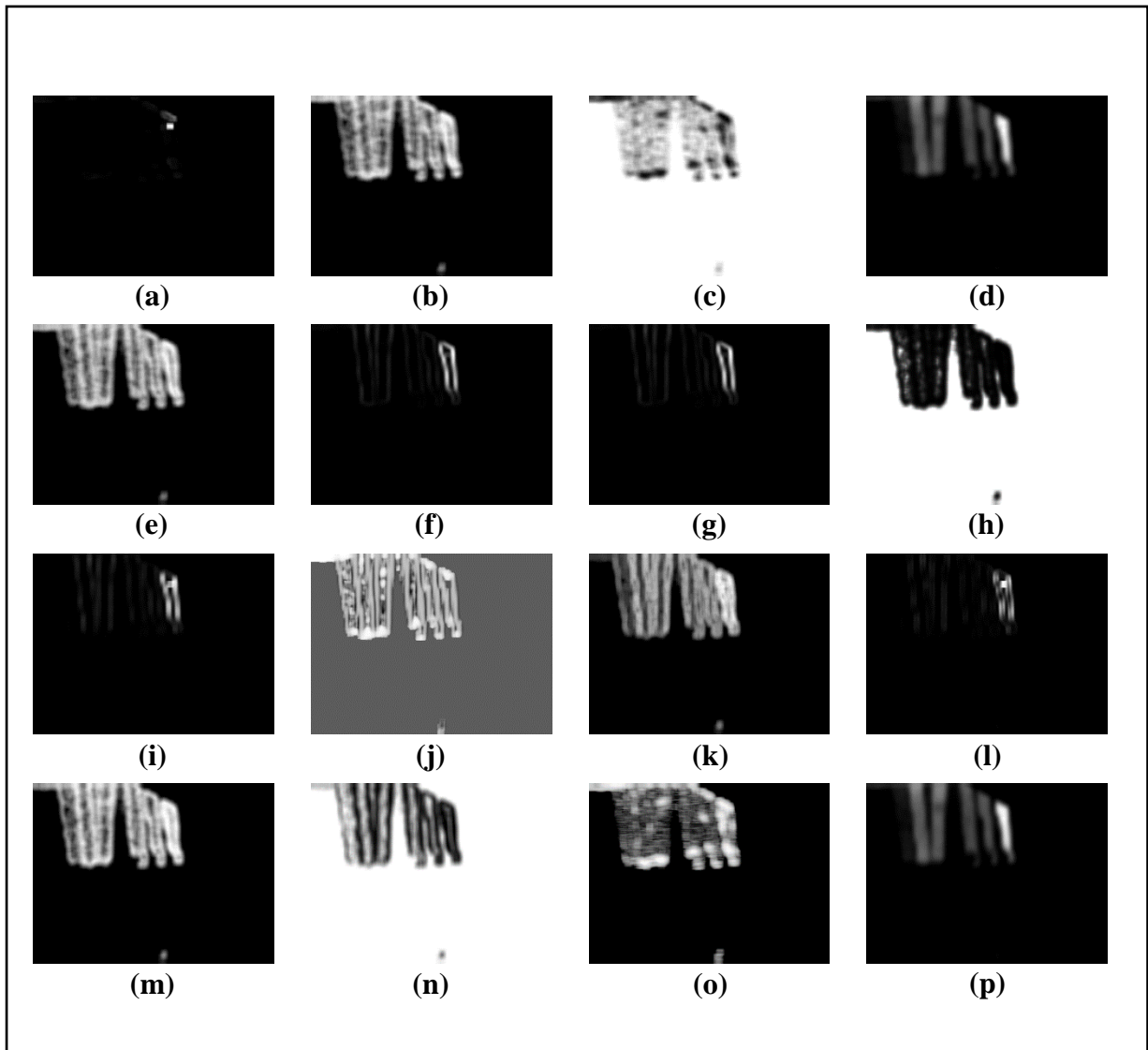
Figure 3.50: Feature Images for Sample Image-16 (Part-2)

(a) S(0,2)DifVarnc6b, (b) S(0,2)Entropy6b, (c) S(0,2)InvDfMom6b,

(d) S(0,2)SumAverg6b, (e) S(0,2)SumEntrp6b, (f) S(0,2)SumOfSqs6b,

(g) S(0,2)SumVarnc6b, (h) S(2,0)AngScMom6b, (i) S(2,0)Contrast6b,

(j) S(2,0)Correlat6b, (k) S(2,0)DifEntrp6b, (l) S(2,0)DifVarnc6b,

(m) S(2,0)Entropy6b, (n) S(2,0)InvDfMom6b ,
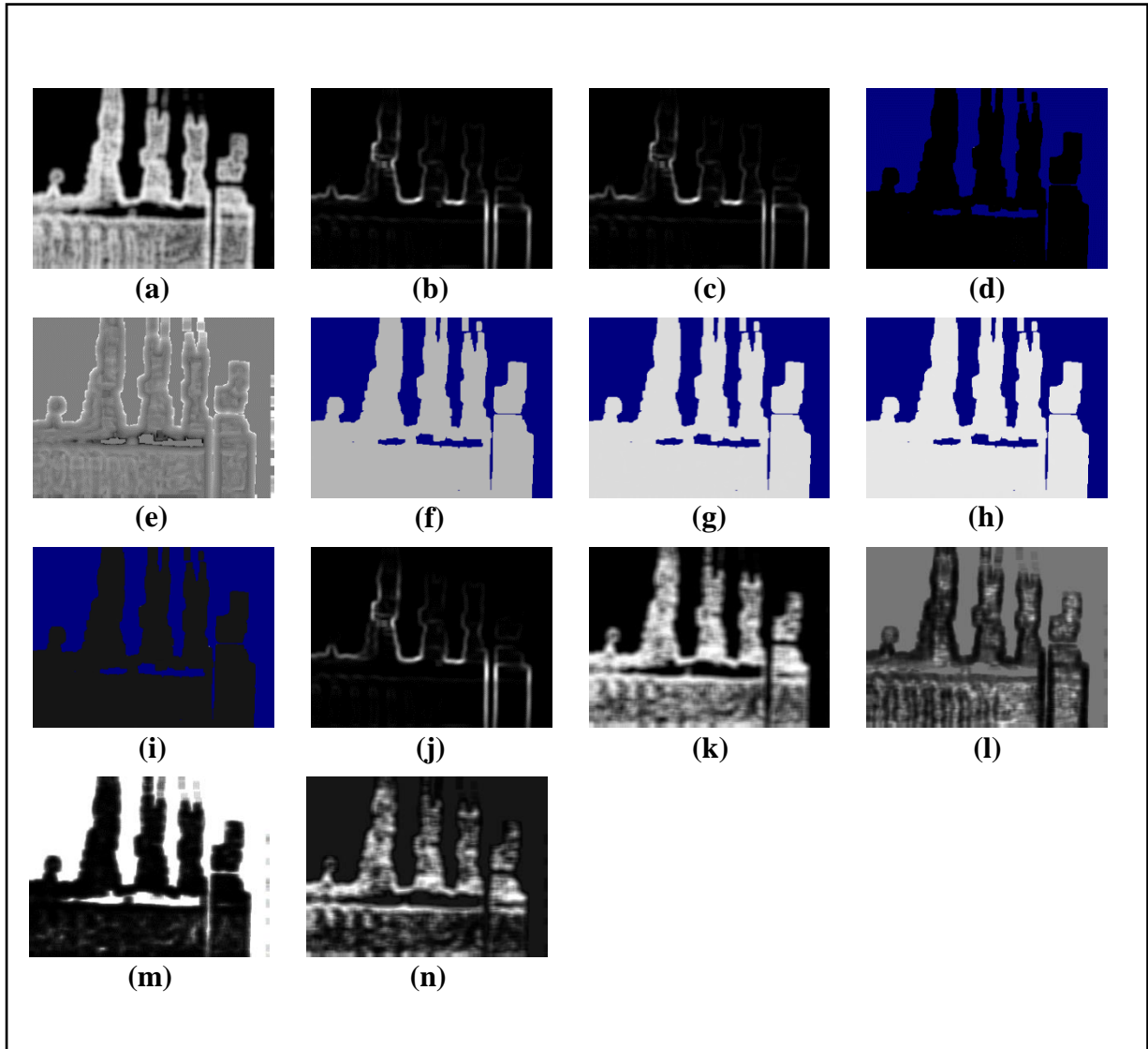
(o) Vertl_ShrtREmp6b, (p) S(2,0)SumAverg6b
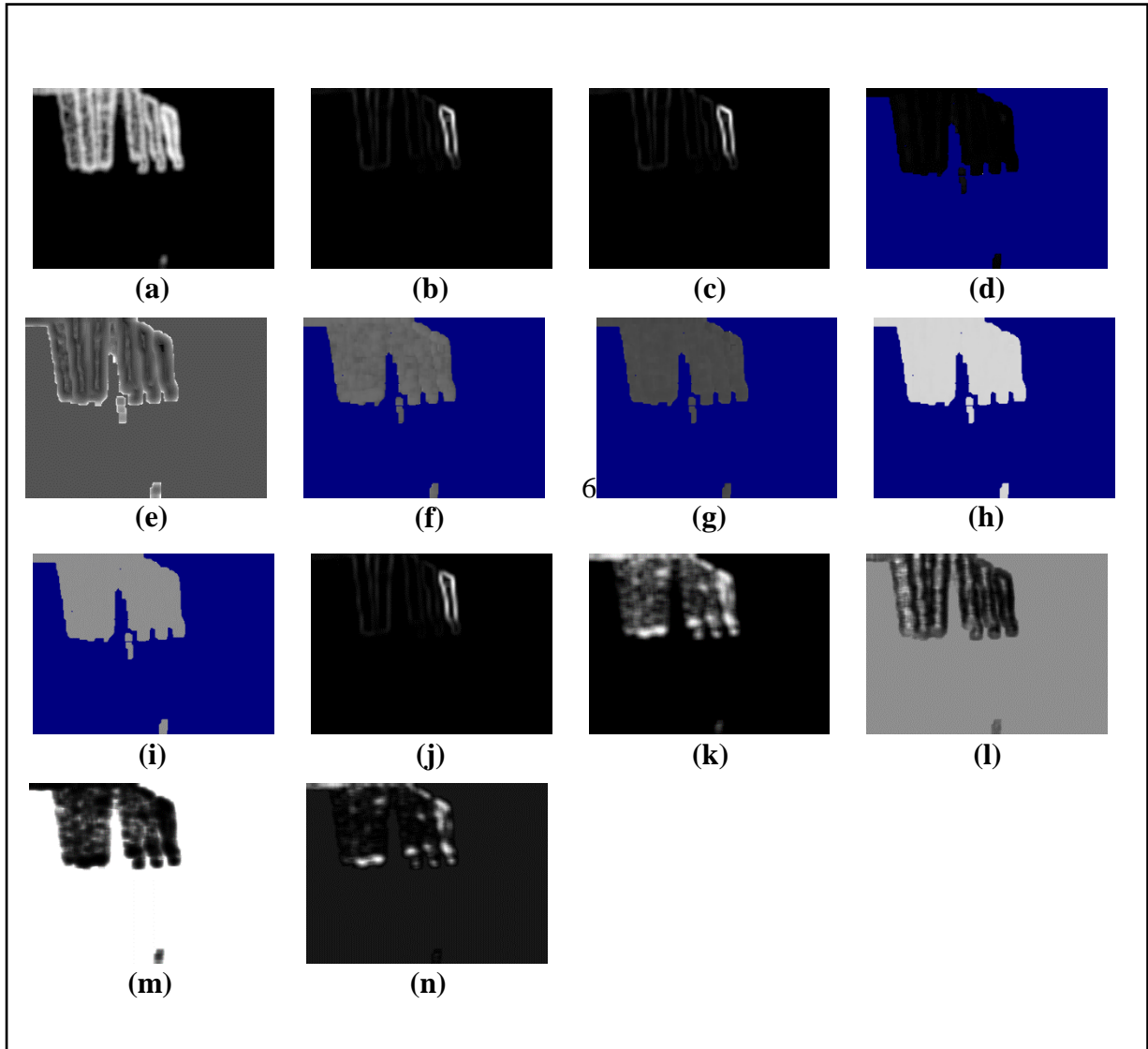
Figure 3.51: Feature Images for Sample Image-16 (Part-3)

(a) S(2,0)SumEntrp6b, (b) S(2,0)SumOfSqs6b, (c) S(2,0)SumVarnc6b, (d) Sigma,

(e) Skewness, (f) Teta1, (g) Teta2, (h) Teta3, (i) Teta4, (j) Variance, (k) Vertl_Fraction6b,

(l) Vertl_GLevNonU6b, (m) Vertl_LngREmph6b, (n) Vertl_RLNonUni6b
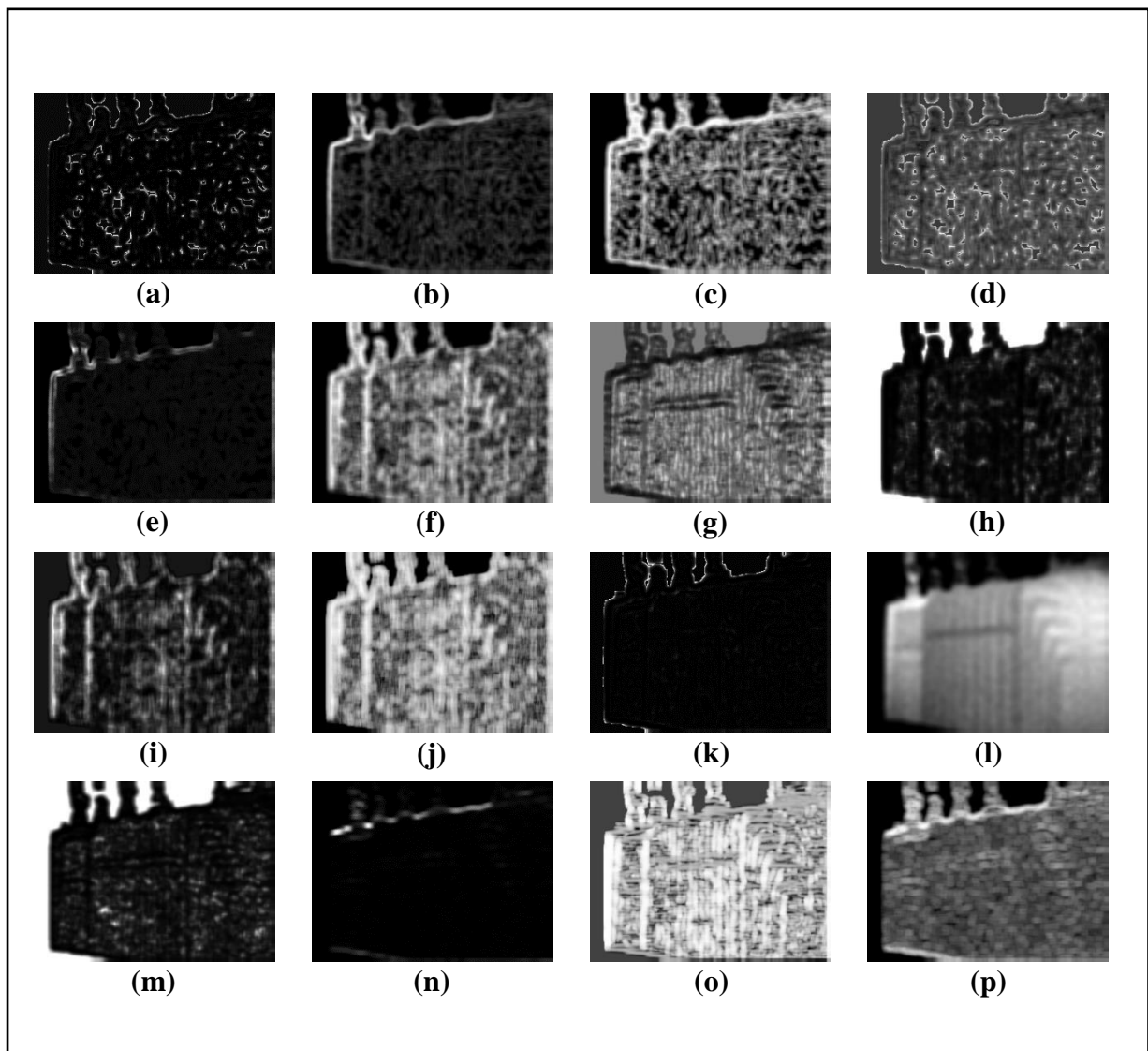
3.4.17 Collected Feature Images from Sample Image-17:
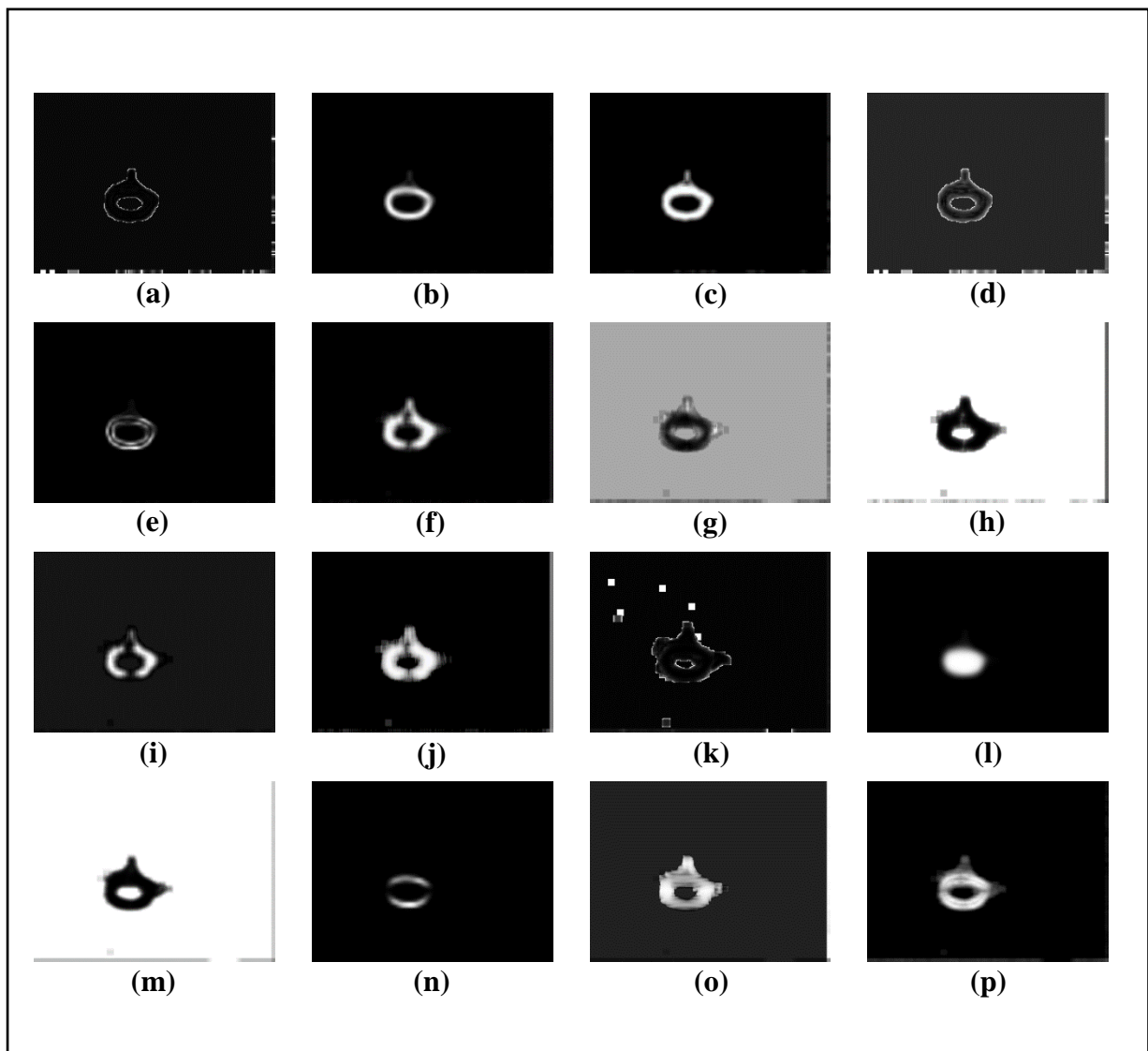
Figure 3.52: Feature Images for Sample Image-17 (Part-1)

(a) GrKurtosis4b, (b) GrMean4b, (c) GrNonZeros4b, (d) GrSkewness4b,

(e) GrVariance4b, (f) Horzl_Fraction6b, (g) Horzl_GLevNonU6b,

(h) Horzl_LngREmph6b, (i) Horzl_RLNonUni6b, (j) Horzl_ShrtREmp6b,

(k) Kurtosis, (l) Mean, (m) S(0,2)AngScMom6b, (n) S(0,2)Contrast6b ,
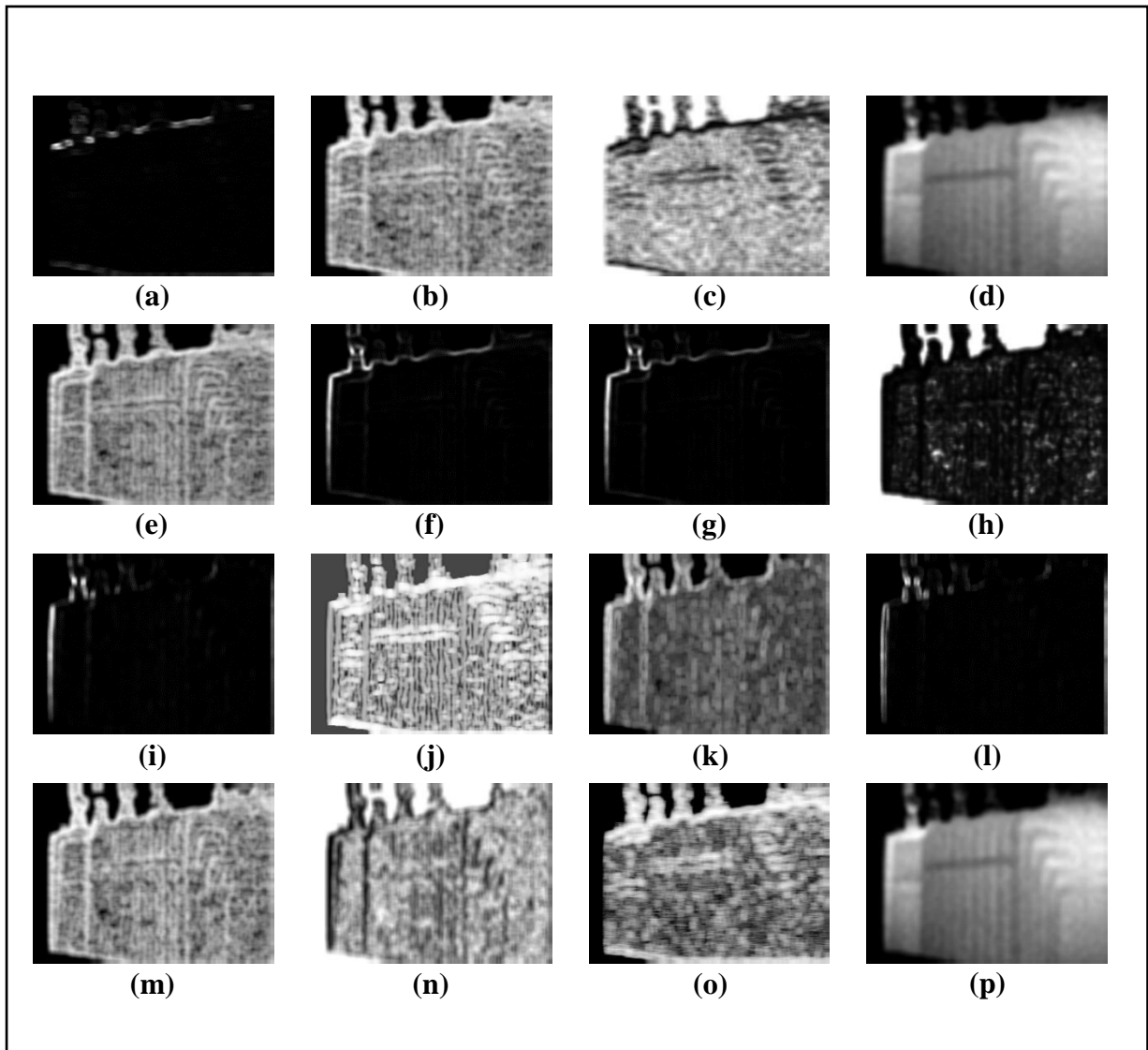
(o) S(0,2)Correlat6b, (p) S(0,2)DifEntrp6b
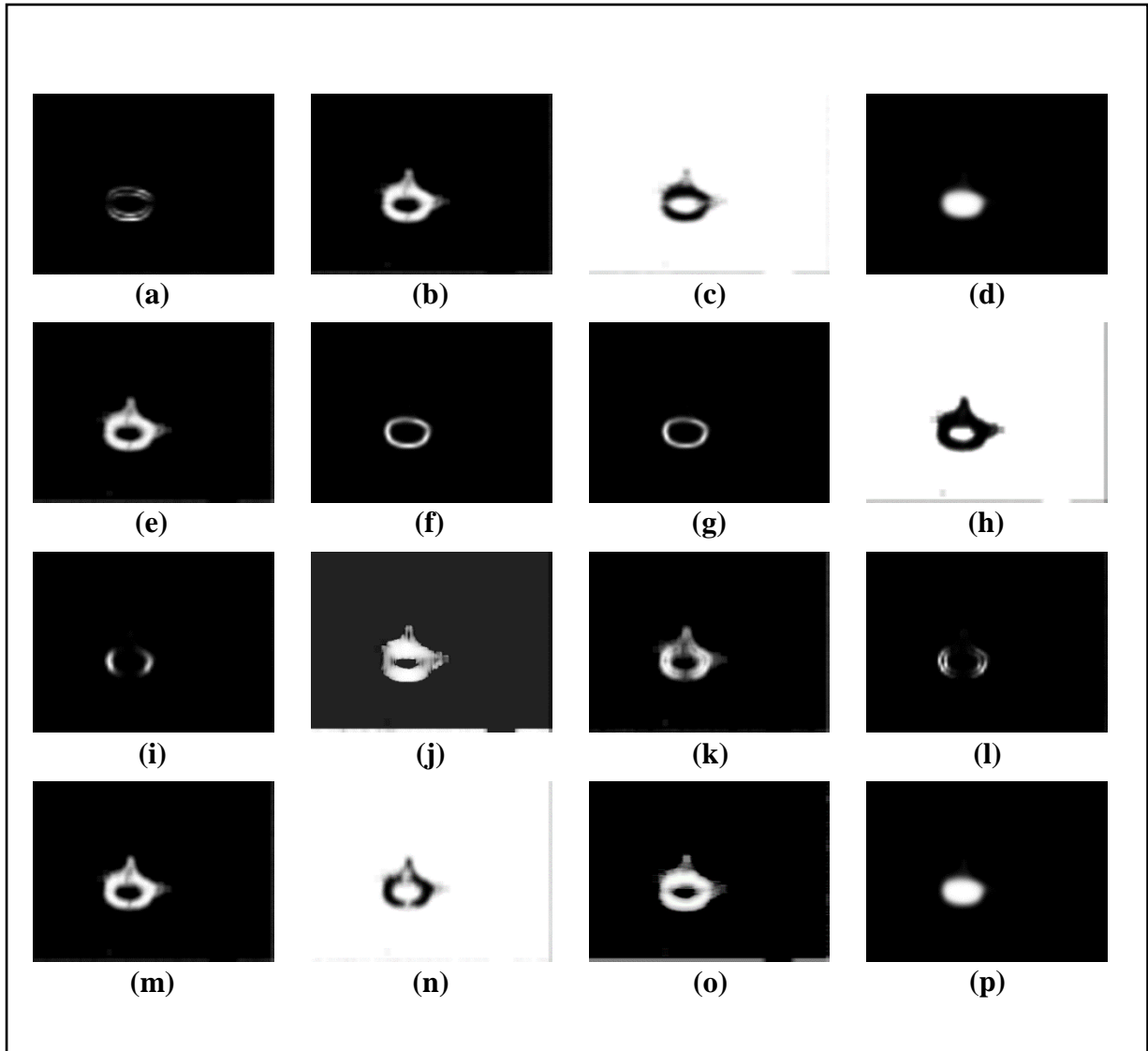
Figure 3.53: Feature Images for Sample Image-17 (Part-2)

(a) S(0,2)DifVarnc6b, (b) S(0,2)Entropy6b, (c) S(0,2)InvDfMom6b,

(d) S(0,2)SumAverg6b, (e) S(0,2)SumEntrp6b, (f) S(0,2)SumOfSqs6b,

(g) S(0,2)SumVarnc6b, (h) S(2,0)AngScMom6b, (i) S(2,0)Contrast6b,

(j) S(2,0)Correlat6b, (k) S(2,0)DifEntrp6b, (l) S(2,0)DifVarnc6b,

(m) S(2,0)Entropy6b, (n) S(2,0)InvDfMom6b ,
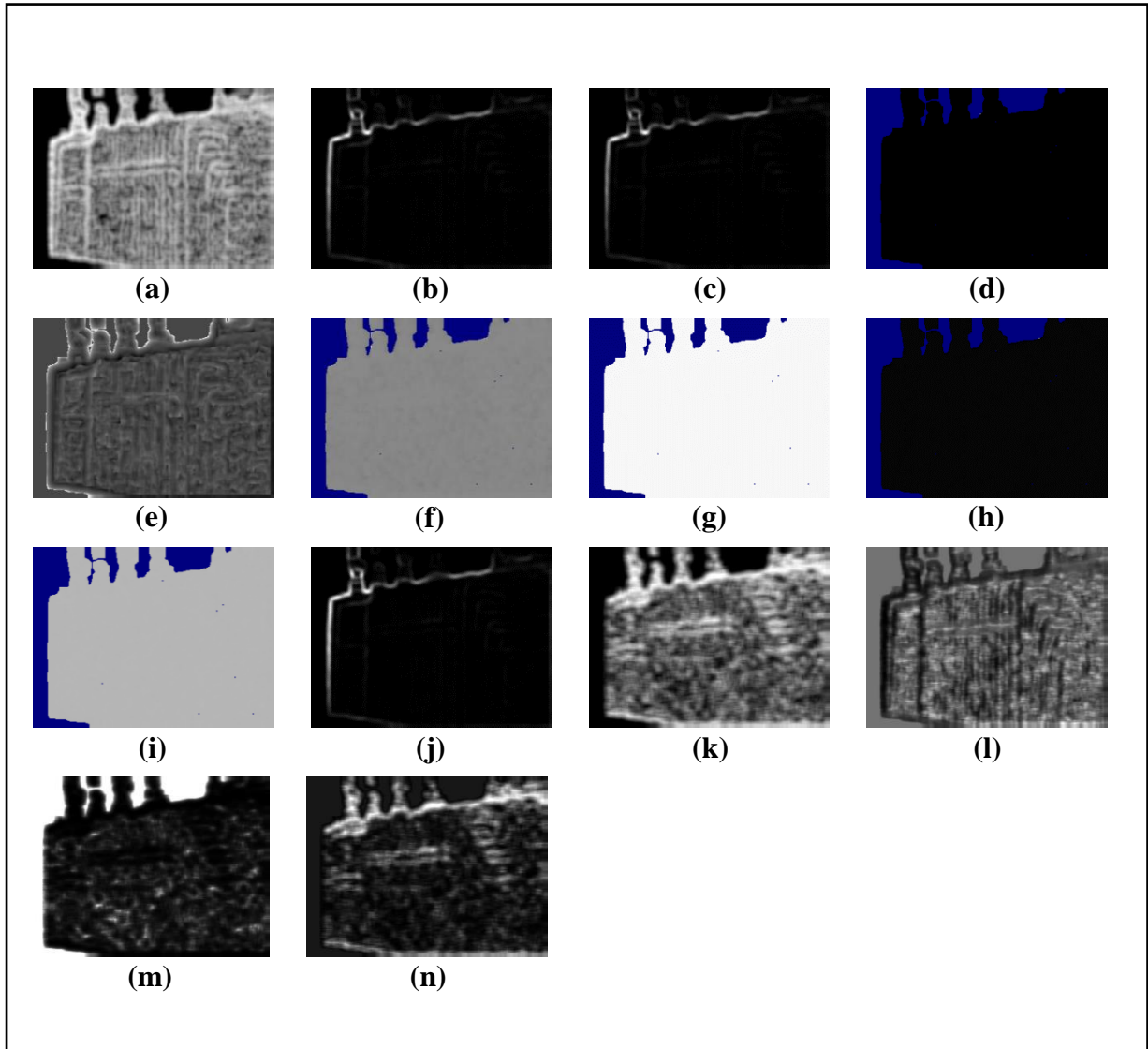
(o) Vertl_ShrtREmp6b, (p) S(2,0)SumAverg6b
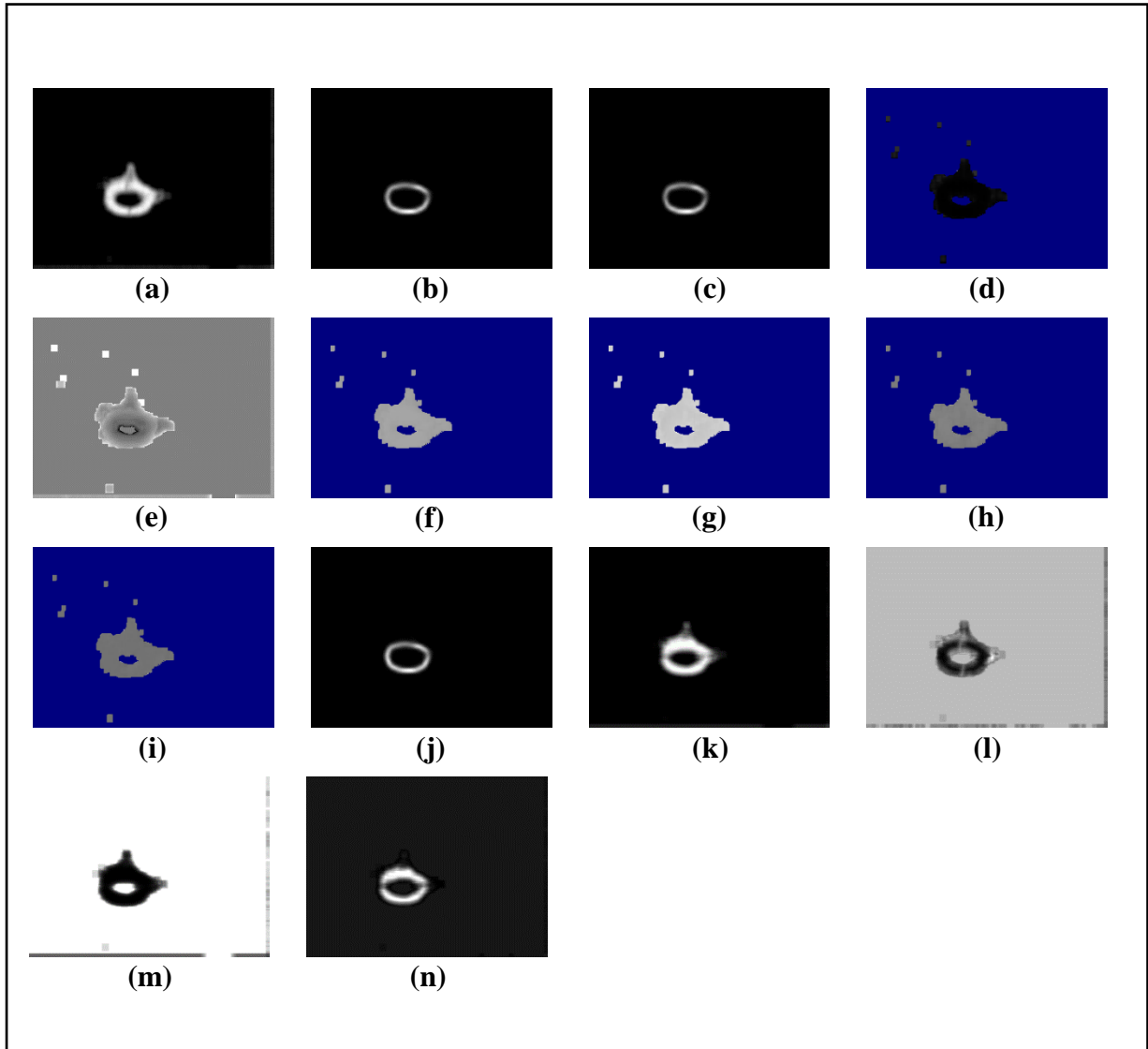
Figure 3.54: Feature Images for Sample Image-17 (Part-3)

(a) S(2,0)SumEntrp6b, (b) S(2,0)SumOfSqs6b, (c) S(2,0)SumVarnc6b, (d) Sigma,

(e) Skewness, (f) Teta1, (g) Teta2, (h) Teta3, (i) Teta4, (j) Variance, (k) Vertl_Fraction6b,

(l) Vertl_GLevNonU6b, (m) Vertl_LngREmph6b, (n) Vertl_RLNonUni6b
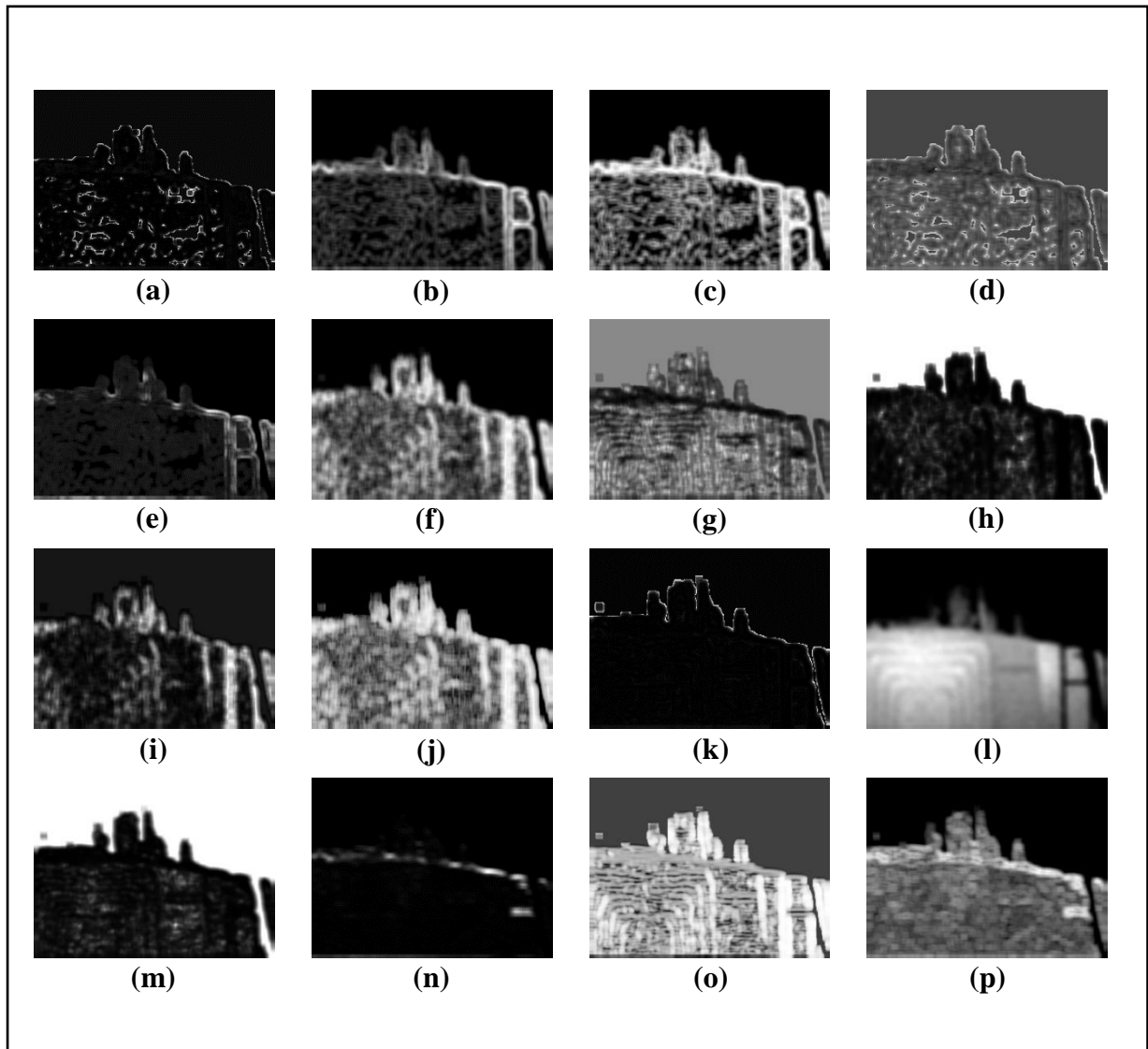
3.4.18 Collected Feature Images from Sample Image-18:
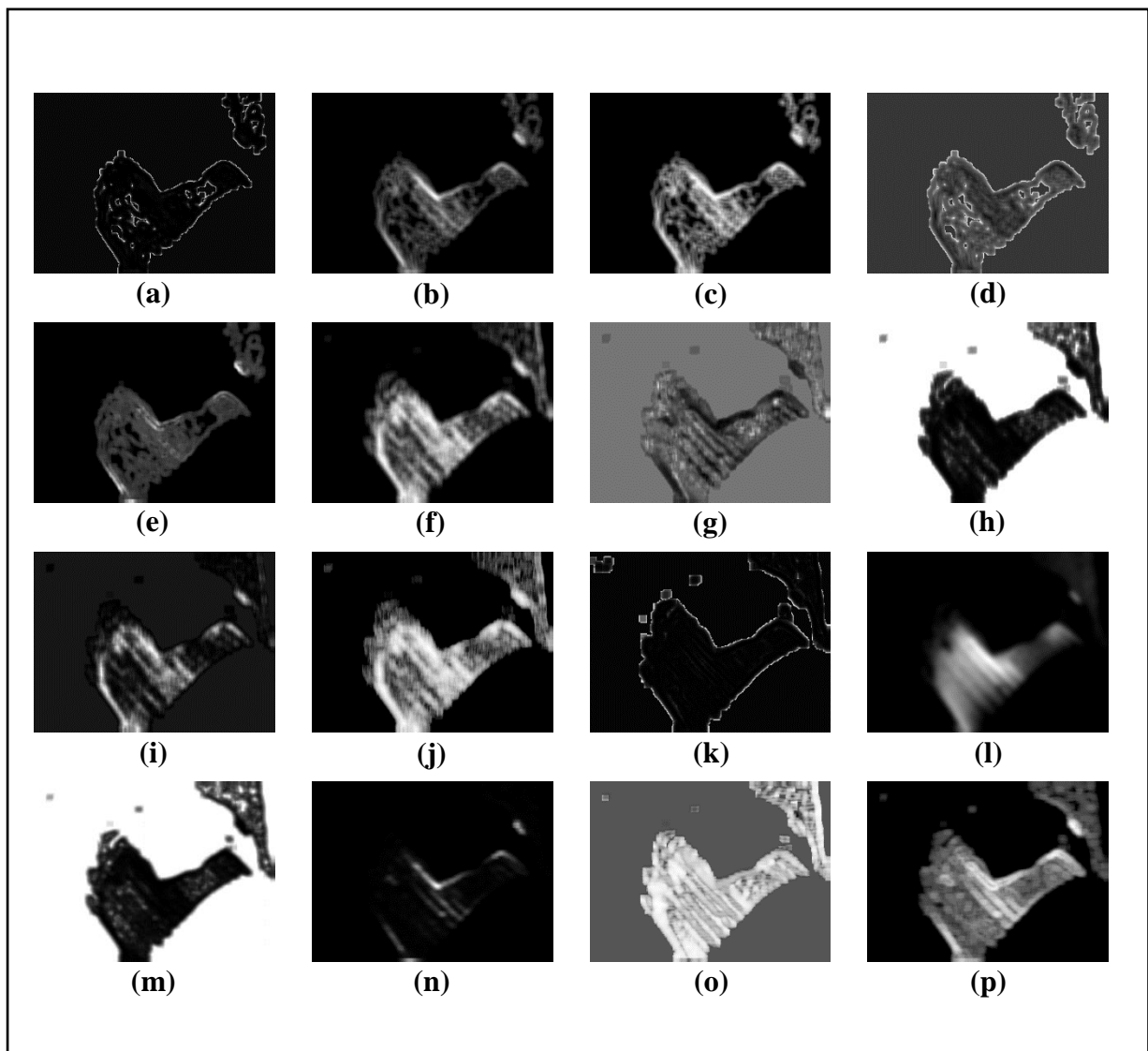
Figure 3.55: Feature Images for Sample Image-18 (Part-1)

(a) GrKurtosis4b, (b) GrMean4b, (c) GrNonZeros4b, (d) GrSkewness4b,

(e) GrVariance4b, (f) Horzl_Fraction6b, (g) Horzl_GLevNonU6b,

(h) Horzl_LngREmph6b, (i) Horzl_RLNonUni6b, (j) Horzl_ShrtREmp6b,

(k) Kurtosis, (l) Mean, (m) S(0,2)AngScMom6b, (n) S(0,2)Contrast6b ,
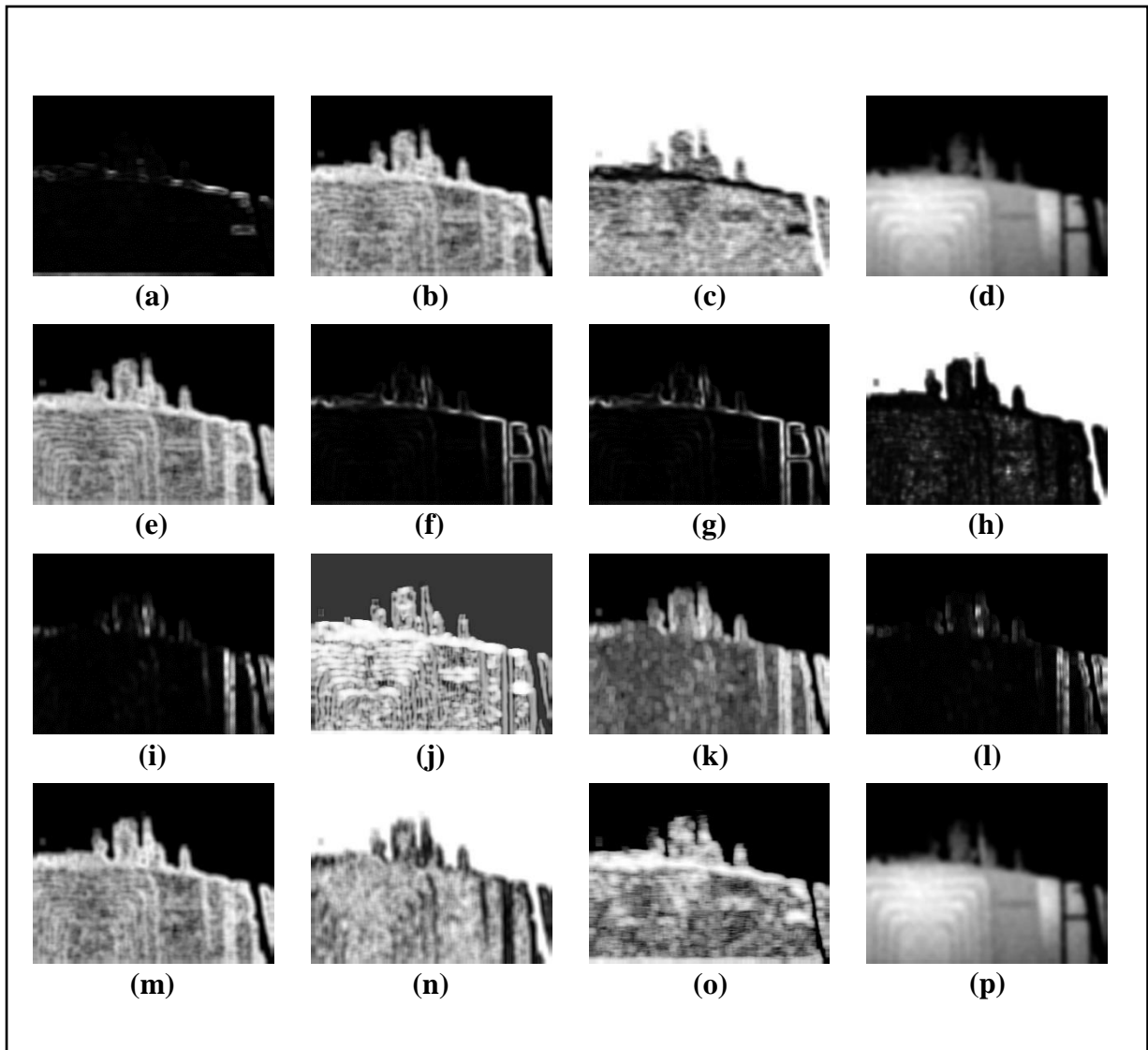
(o) S(0,2)Correlat6b, (p) S(0,2)DifEntrp6b
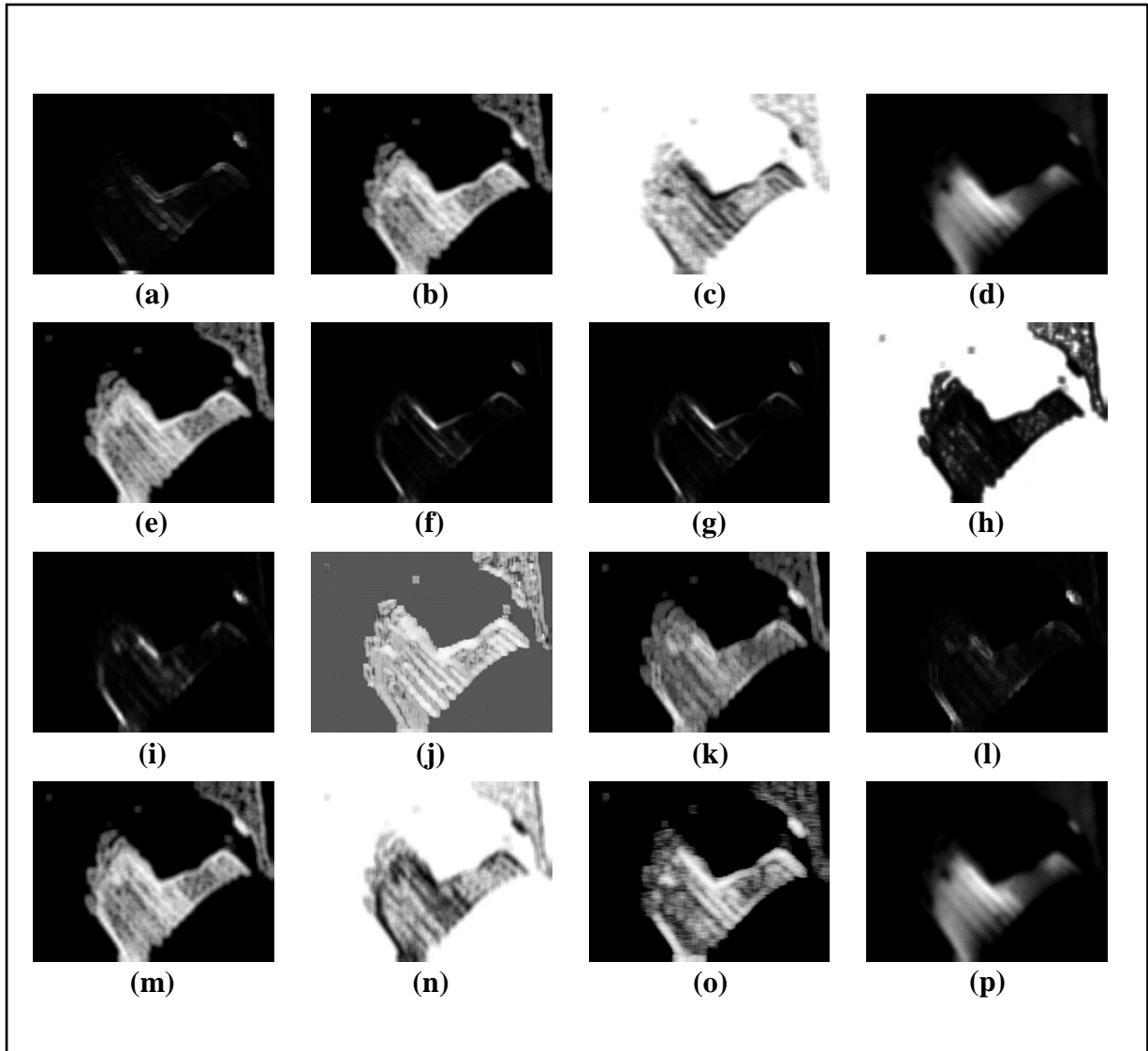
Figure 3.56: Feature Images for Sample Image-18 (Part-2)

(a) S(0,2)DifVarnc6b, (b) S(0,2)Entropy6b, (c) S(0,2)InvDfMom6b,

(d) S(0,2)SumAverg6b, (e) S(0,2)SumEntrp6b, (f) S(0,2)SumOfSqs6b,

(g) S(0,2)SumVarnc6b, (h) S(2,0)AngScMom6b, (i) S(2,0)Contrast6b,

(j) S(2,0)Correlat6b, (k) S(2,0)DifEntrp6b, (l) S(2,0)DifVarnc6b,

(m) S(2,0)Entropy6b, (n) S(2,0)InvDfMom6b ,

(o) Vertl_ShrtREmp6b, (p) S(2,0)SumAverg6b

80
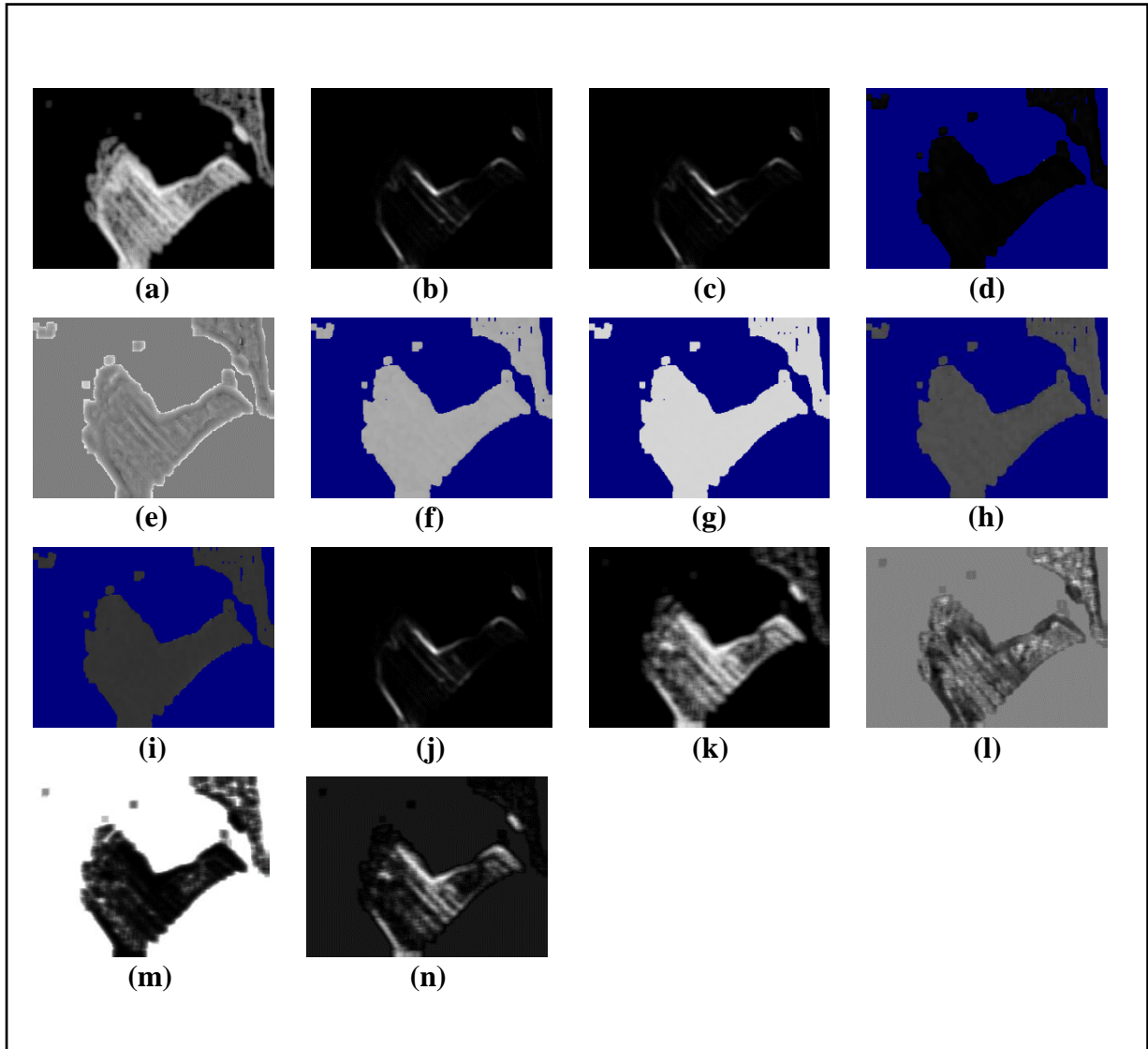
Figure 3.57: Feature Images for Sample Image-18 (Part-3)

(a) S(2,0)SumEntrp6b, (b) S(2,0)SumOfSqs6b, (c) S(2,0)SumVarnc6b, (d) Sigma,

(e) Skewness, (f) Teta1, (g) Teta2, (h) Teta3, (i) Teta4, (j) Variance, (k) Vertl_Fraction6b,

(l) Vertl_GLevNonU6b, (m) Vertl_LngREmph6b, (n) Vertl_RLNonUni6b

3.4.19 Collected Feature Images from Sample Image-19:
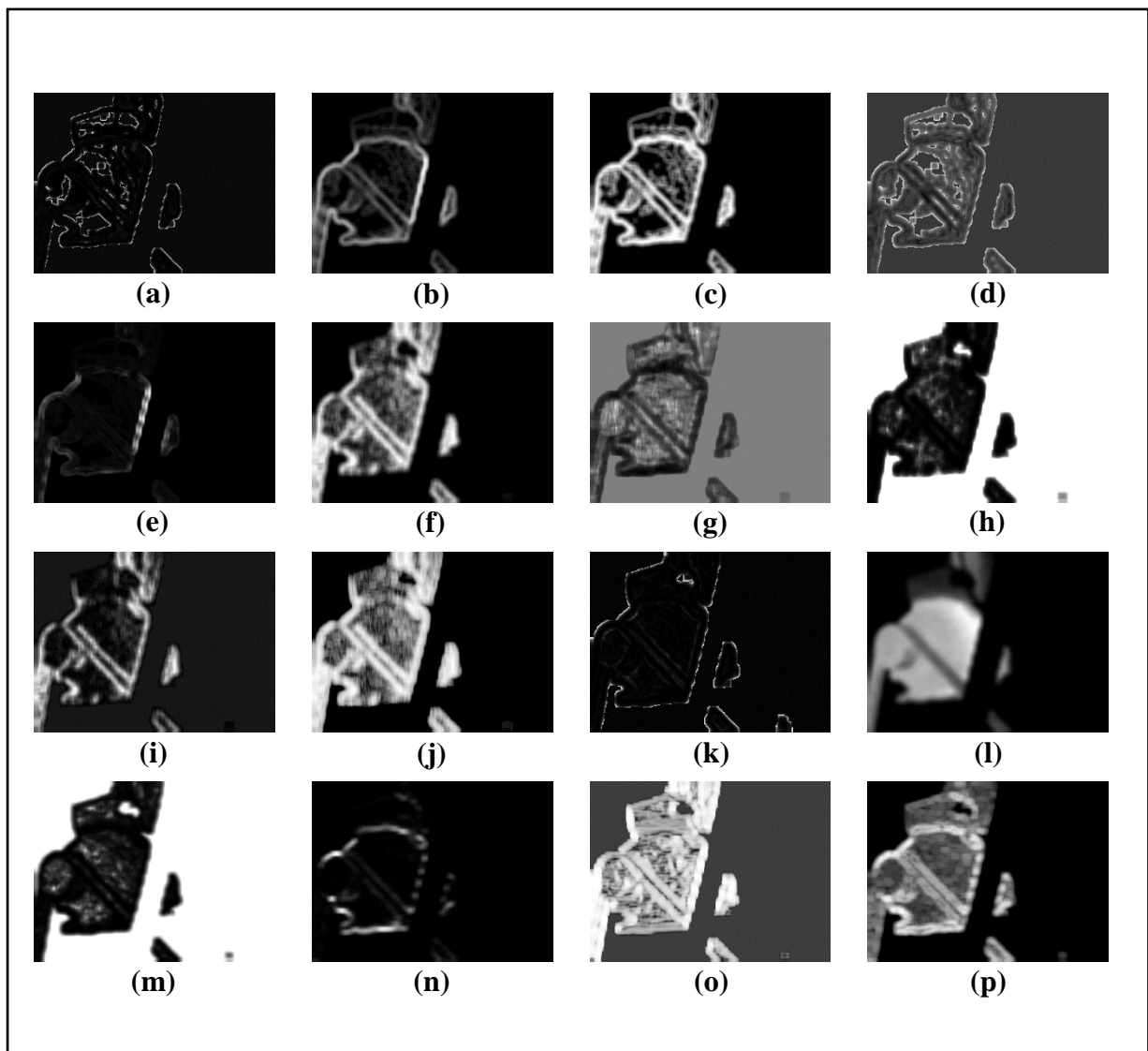
Figure 3.58: Feature Images for Sample Image-19 (Part-1)

(a) GrKurtosis4b, (b) GrMean4b, (c) GrNonZeros4b, (d) GrSkewness4b,

(e) GrVariance4b, (f) Horzl_Fraction6b, (g) Horzl_GLevNonU6b,

(h) Horzl_LngREmph6b, (i) Horzl_RLNonUni6b, (j) Horzl_ShrtREmp6b,

(k) Kurtosis, (l) Mean, (m) S(0,2)AngScMom6b, (n) S(0,2)Contrast6b ,

(o) S(0,2)Correlat6b, (p) S(0,2)DifEntrp6b
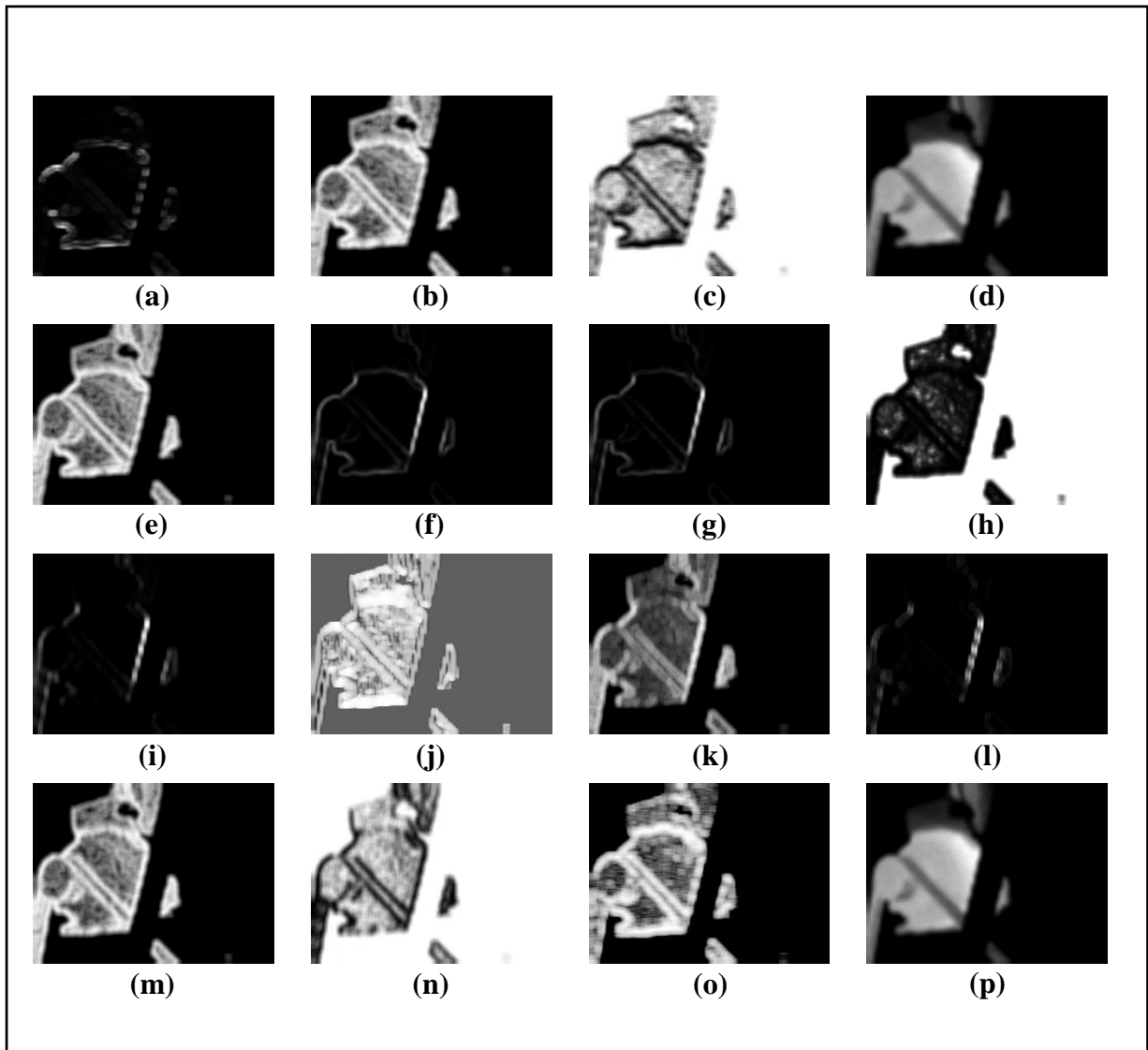
Figure 3.59: Feature Images for Sample Image-19 (Part-2)

(a) S(0,2)DifVarnc6b, (b) S(0,2)Entropy6b, (c) S(0,2)InvDfMom6b,

(d) S(0,2)SumAverg6b, (e) S(0,2)SumEntrp6b, (f) S(0,2)SumOfSqs6b,

(g) S(0,2)SumVarnc6b, (h) S(2,0)AngScMom6b, (i) S(2,0)Contrast6b,

(j) S(2,0)Correlat6b, (k) S(2,0)DifEntrp6b, (l) S(2,0)DifVarnc6b,

(m) S(2,0)Entropy6b, (n) S(2,0)InvDfMom6b ,
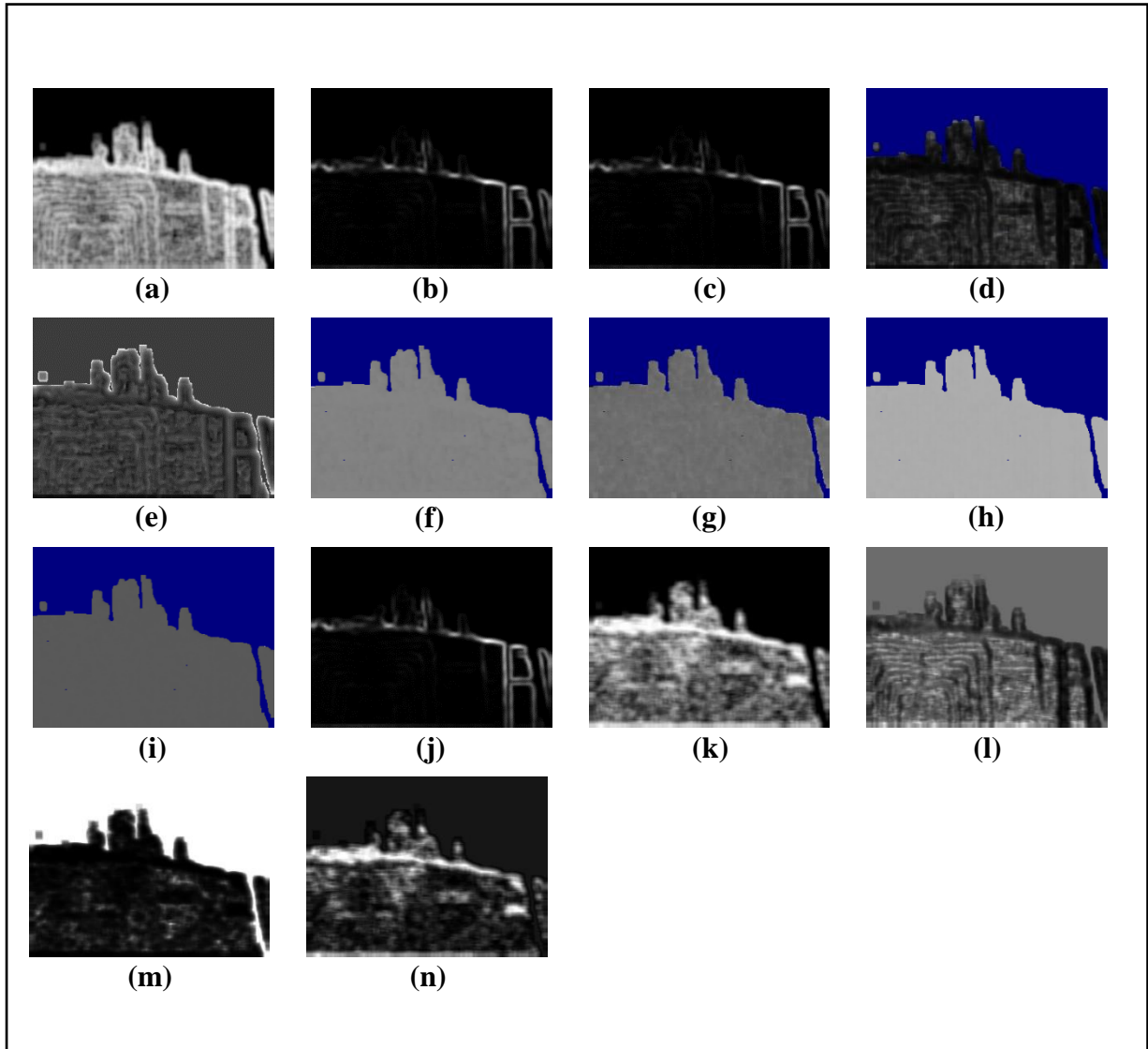
(o) Vertl_ShrtREmp6b, (p) S(2,0)SumAverg6b
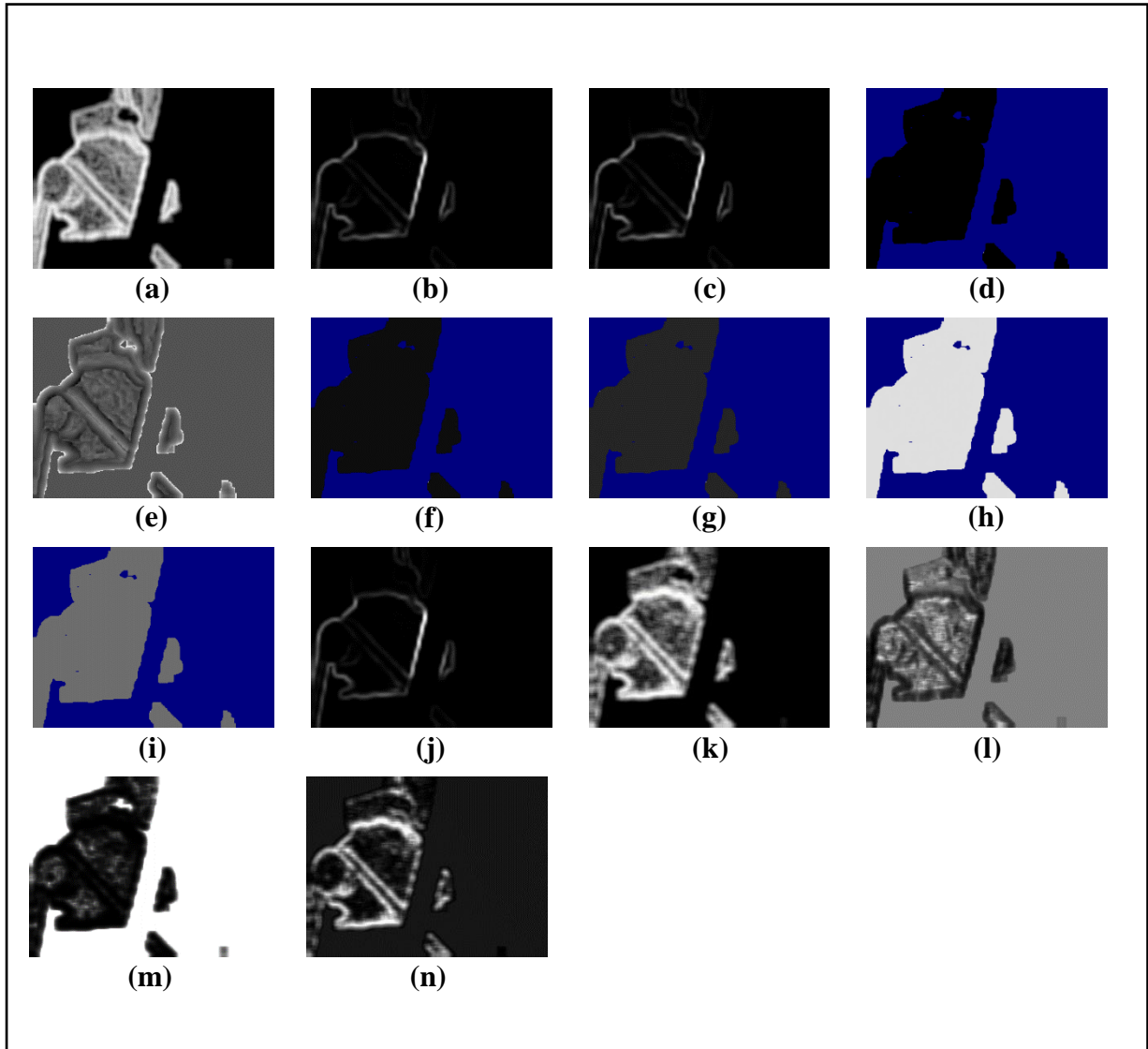
Figure 3.60: Feature Images for Sample Image-19 (Part-3)

(a) S(2,0)SumEntrp6b, (b) S(2,0)SumOfSqs6b, (c) S(2,0)SumVarnc6b, (d) Sigma,

(e) Skewness, (f) Teta1, (g) Teta2, (h) Teta3, (i) Teta4, (j) Variance, (k) Vertl_Fraction6b,

(l) Vertl_GLevNonU6b, (m) Vertl_LngREmph6b, (n) Vertl_RLNonUni6b

3.4.20 Collected Feature Images from Sample Image-20:
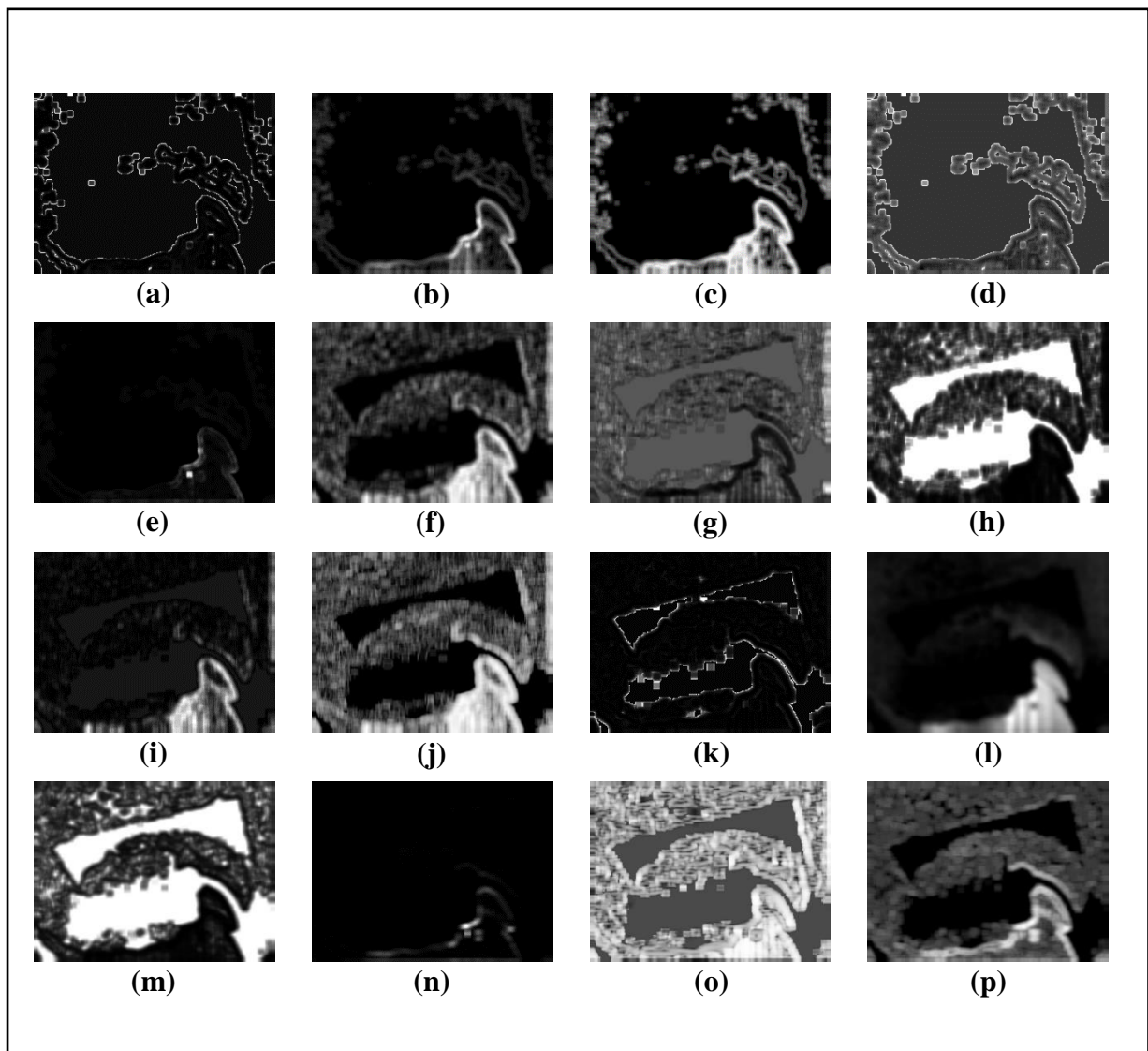
Figure 3.61: Feature Images for Sample Image-20 (Part-1)

(a) GrKurtosis4b, (b) GrMean4b, (c) GrNonZeros4b, (d) GrSkewness4b,

(e) GrVariance4b, (f) Horzl_Fraction6b, (g) Horzl_GLevNonU6b,

(h) Horzl_LngREmph6b, (i) Horzl_RLNonUni6b, (j) Horzl_ShrtREmp6b,

(k) Kurtosis, (l) Mean, (m) S(0,2)AngScMom6b, (n) S(0,2)Contrast6b ,
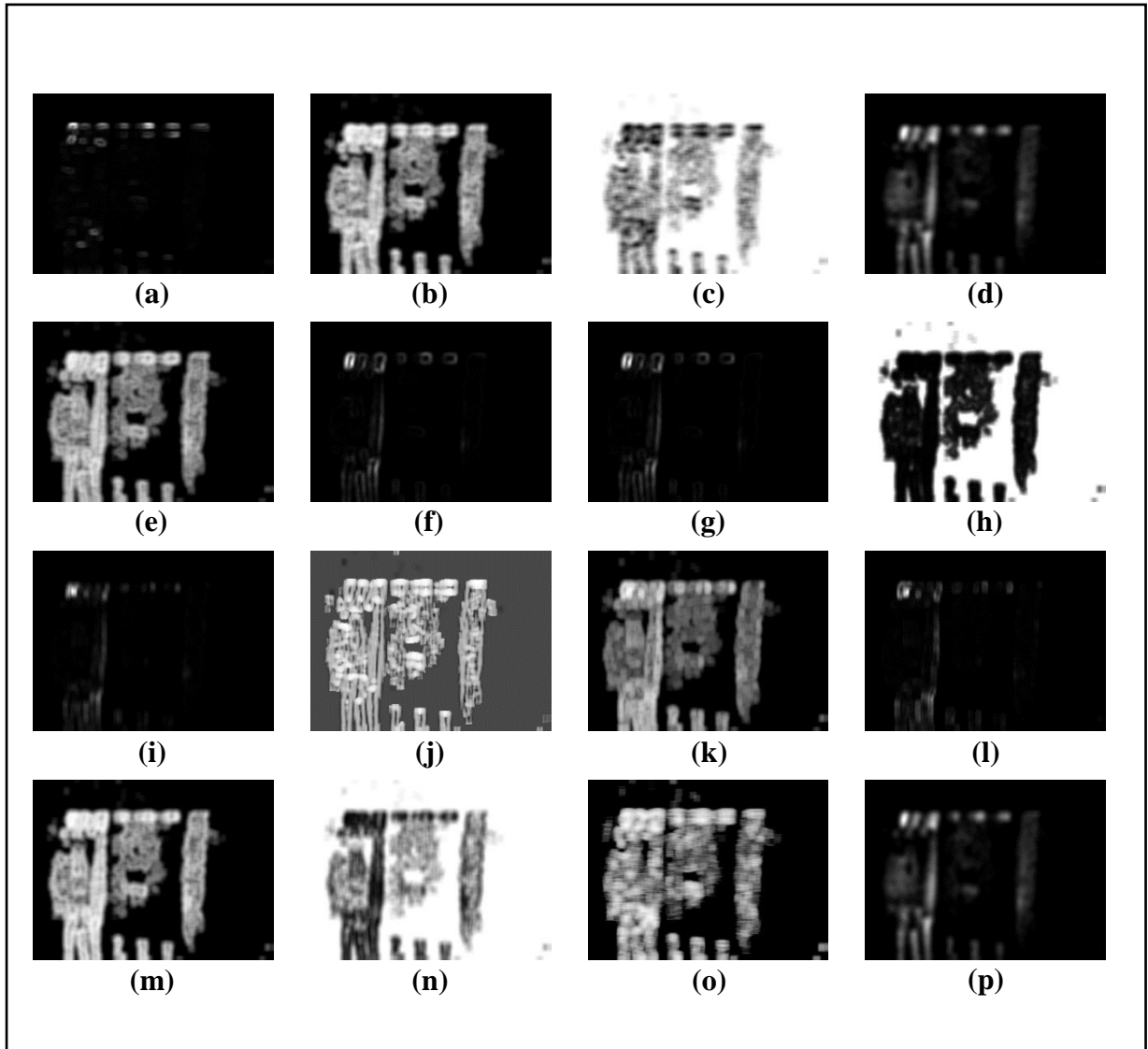
(o) S(0,2)Correlat6b, (p) S(0,2)DifEntrp6b
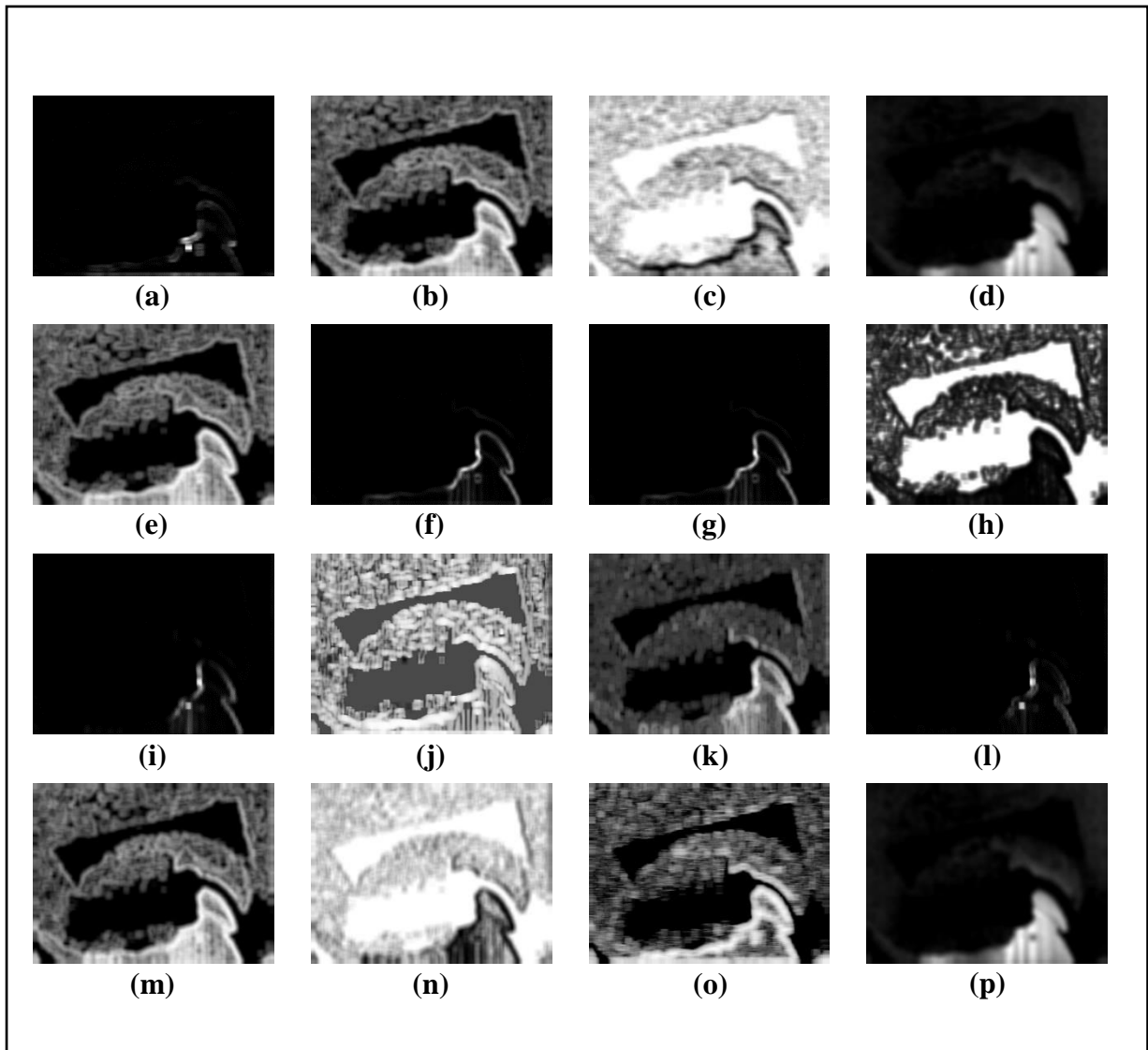
Figure 3.62: Feature Images for Sample Image-20 (Part-2)

(a) S(0,2)DifVarnc6b, (b) S(0,2)Entropy6b, (c) S(0,2)InvDfMom6b,

(d) S(0,2)SumAverg6b, (e) S(0,2)SumEntrp6b, (f) S(0,2)SumOfSqs6b,

(g) S(0,2)SumVarnc6b, (h) S(2,0)AngScMom6b, (i) S(2,0)Contrast6b,

(j) S(2,0)Correlat6b, (k) S(2,0)DifEntrp6b, (l) S(2,0)DifVarnc6b,

(m) S(2,0)Entropy6b, (n) S(2,0)InvDfMom6b ,
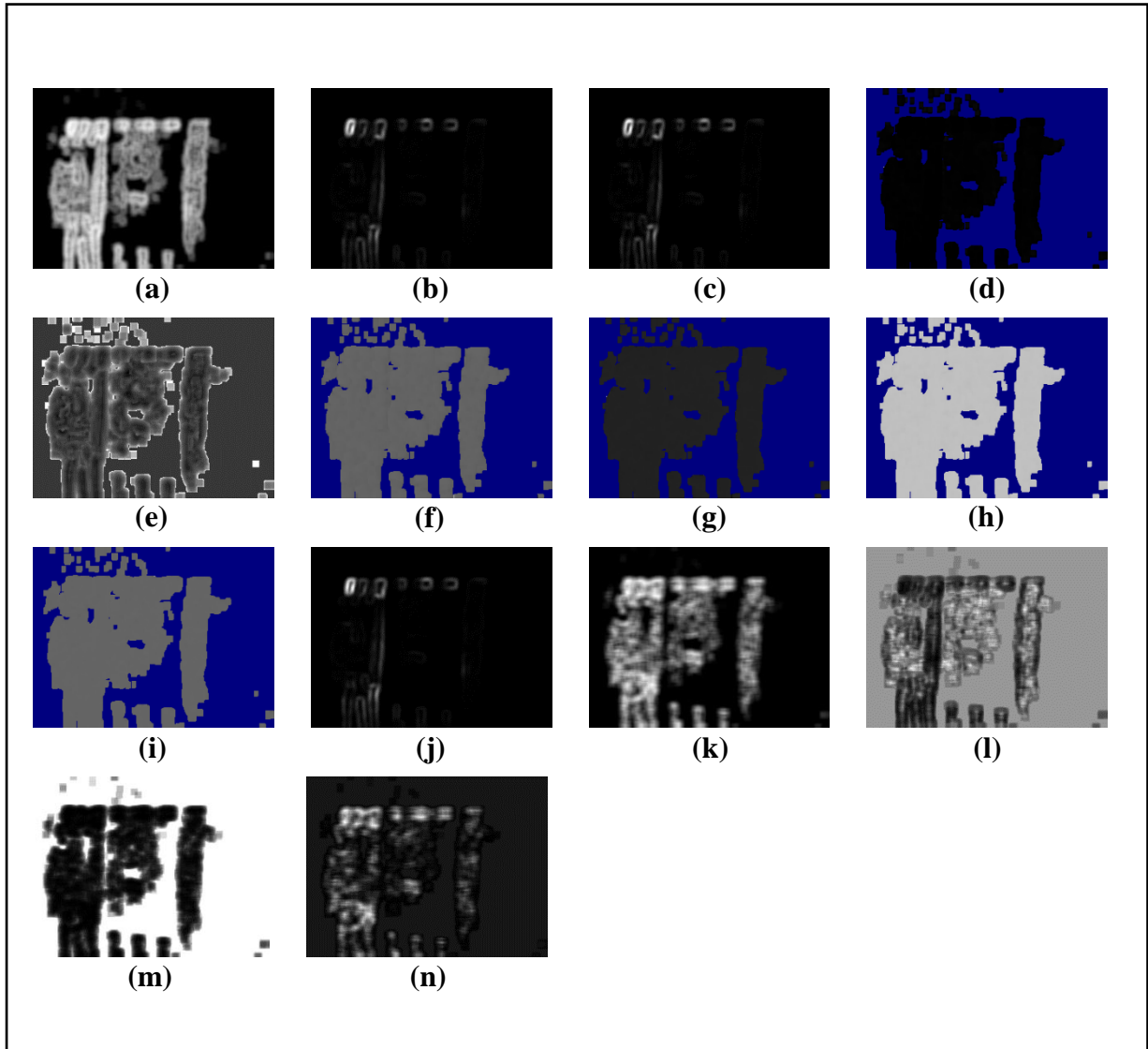
(o) Vertl_ShrtREmp6b, (p) S(2,0)SumAverg6b
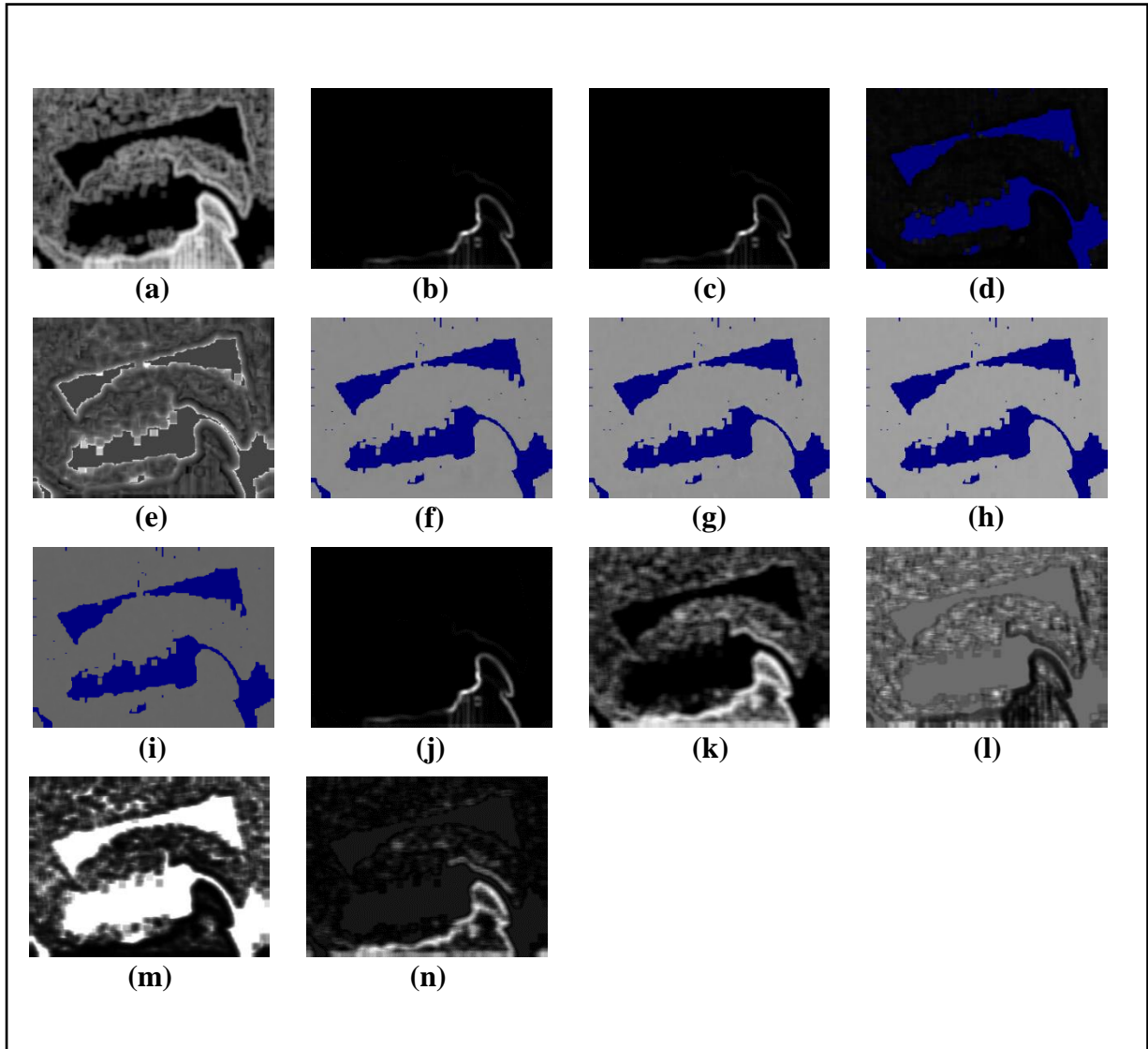
Figure 3.63: Feature Images for Sample Image-20 (Part-3)

(a) S(2,0)SumEntrp6b, (b) S(2,0)SumOfSqs6b, (c) S(2,0)SumVarnc6b, (d) Sigma,

(e) Skewness, (f) Teta1, (g) Teta2, (h) Teta3, (i) Teta4, (j) Variance, (k) Vertl_Fraction6b,

(l) Vertl_GLevNonU6b, (m) Vertl_LngREmph6b, (n) Vertl_RLNonUni6b
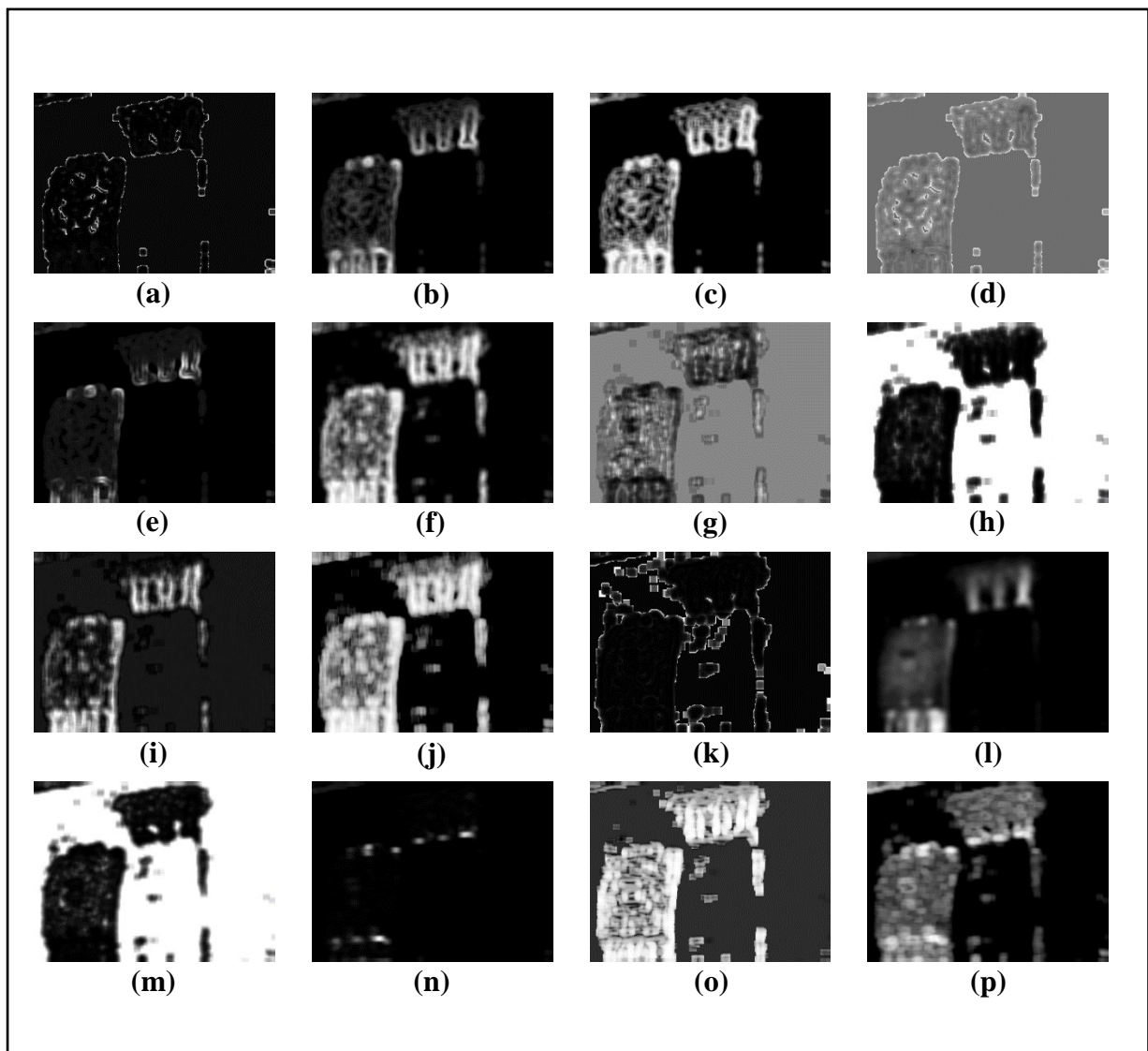
3.4.21 Collected Feature Images from Sample Image-21:
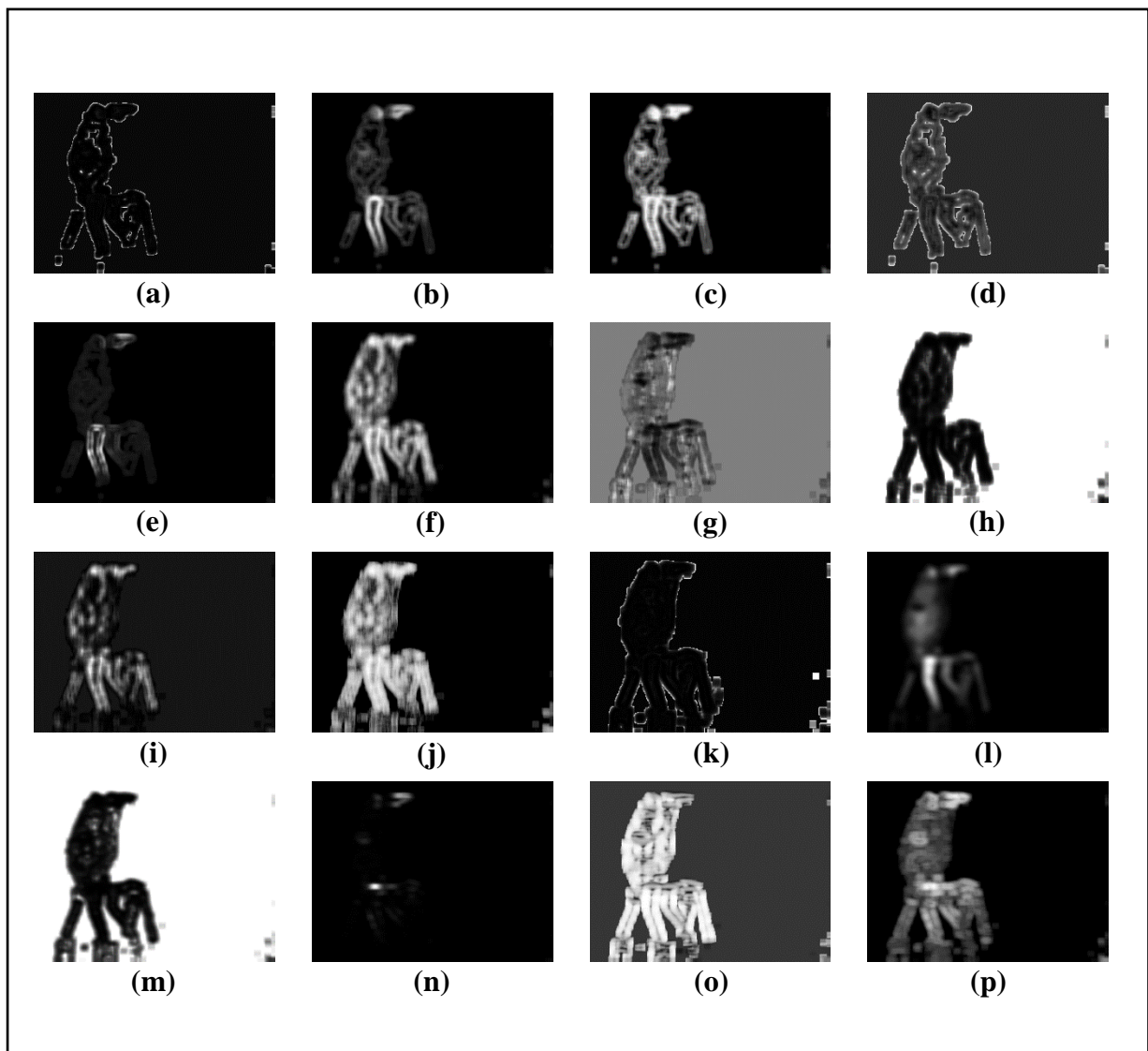
Figure 3.64: Feature Images for Sample Image-21 (Part-1)

(a) GrKurtosis4b, (b) GrMean4b, (c) GrNonZeros4b, (d) GrSkewness4b,

(e) GrVariance4b, (f) Horzl_Fraction6b, (g) Horzl_GLevNonU6b,

(h) Horzl_LngREmph6b, (i) Horzl_RLNonUni6b, (j) Horzl_ShrtREmp6b,

(k) Kurtosis, (l) Mean, (m) S(0,2)AngScMom6b, (n) S(0,2)Contrast6b ,
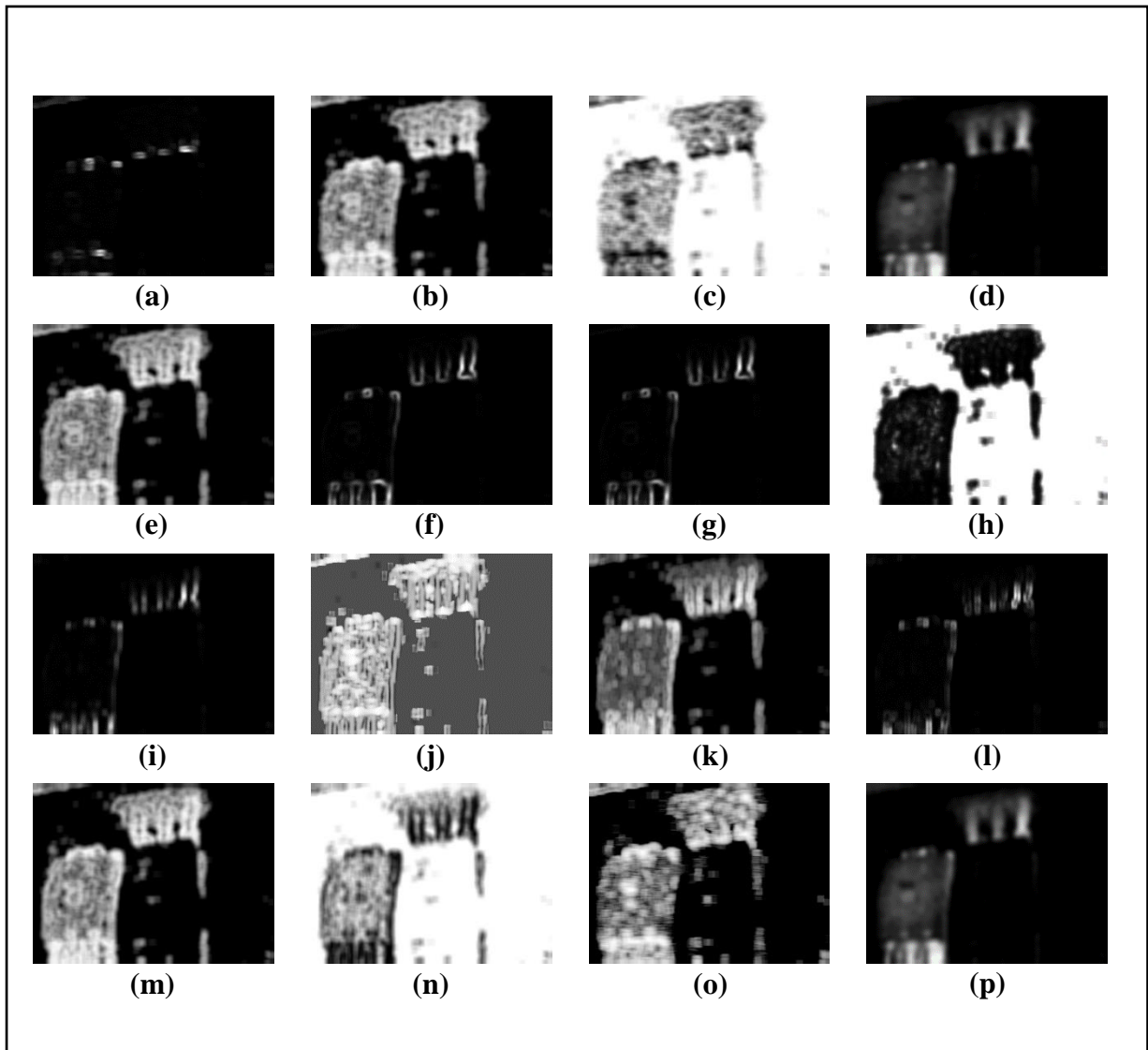
(o) S(0,2)Correlat6b, (p) S(0,2)DifEntrp6b
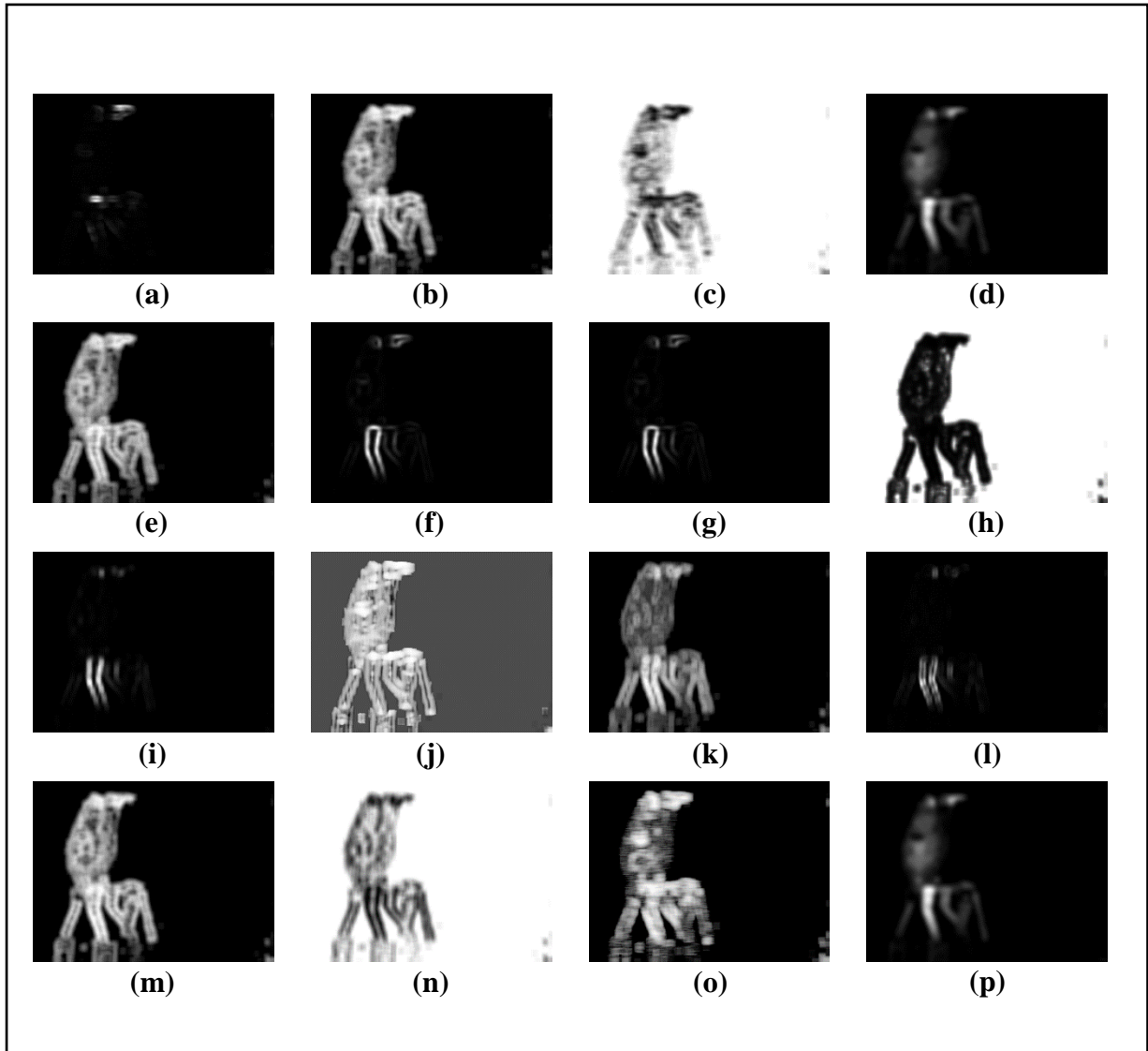
Figure 3.65: Feature Images for Sample Image-21 (Part-2)

(a) S(0,2)DifVarnc6b, (b) S(0,2)Entropy6b, (c) S(0,2)InvDfMom6b,

(d) S(0,2)SumAverg6b, (e) S(0,2)SumEntrp6b, (f) S(0,2)SumOfSqs6b,

(g) S(0,2)SumVarnc6b, (h) S(2,0)AngScMom6b, (i) S(2,0)Contrast6b,

(j) S(2,0)Correlat6b, (k) S(2,0)DifEntrp6b, (l) S(2,0)DifVarnc6b,

(m) S(2,0)Entropy6b, (n) S(2,0)InvDfMom6b ,
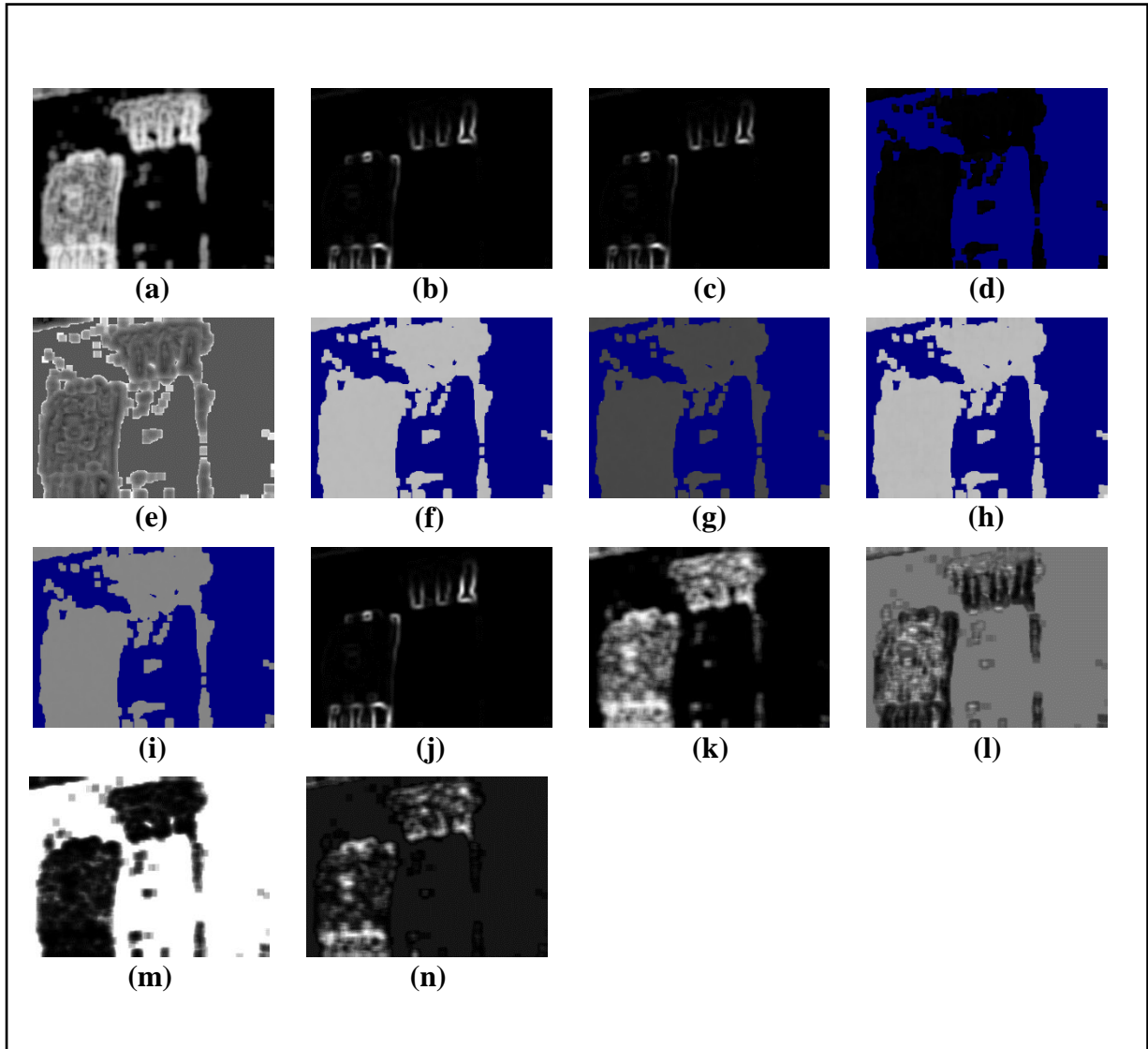
(o) Vertl_ShrtREmp6b, (p) S(2,0)SumAverg6b
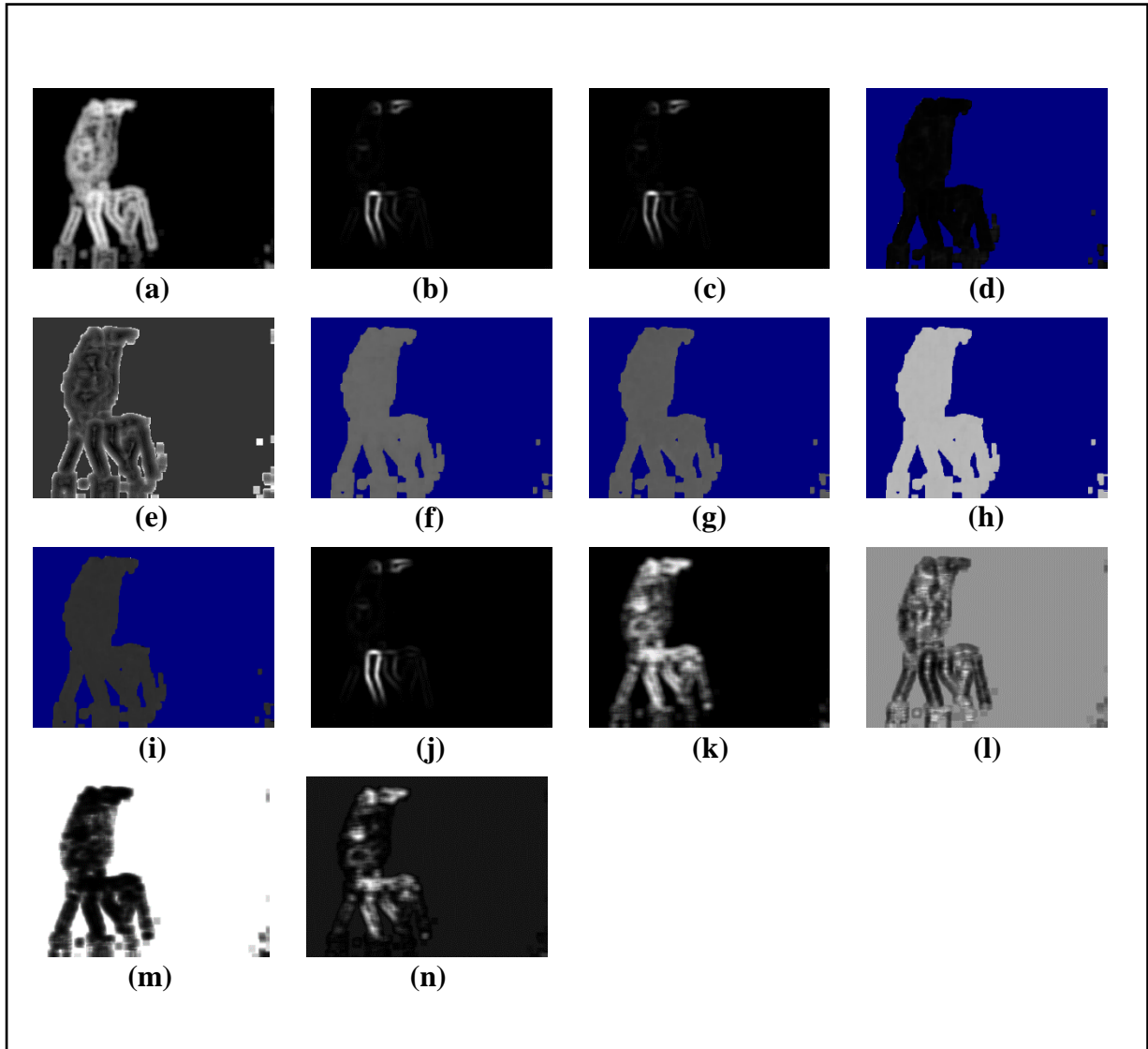
Figure 3.66: Feature Images for Sample Image-21 (Part-3)

(a) S(2,0)SumEntrp6b, (b) S(2,0)SumOfSqs6b, (c) S(2,0)SumVarnc6b, (d) Sigma,

(e) Skewness, (f) Teta1, (g) Teta2, (h) Teta3, (i) Teta4, (j) Variance, (k) Vertl_Fraction6b,

(l) Vertl_GLevNonU6b, (m) Vertl_LngREmph6b, (n) Vertl_RLNonUni6b
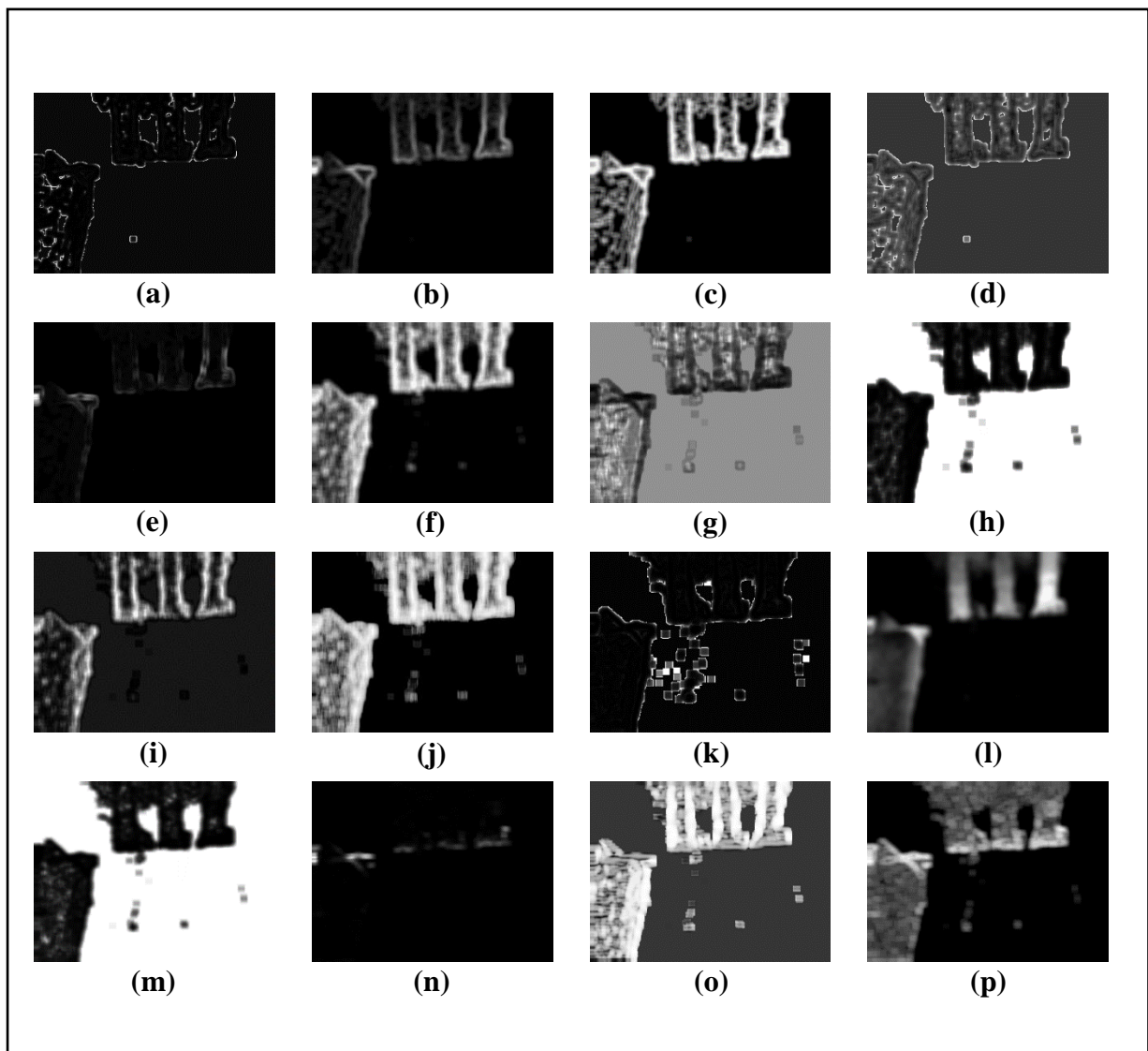
3.4.22 Collected Feature Images from Sample Image-22:
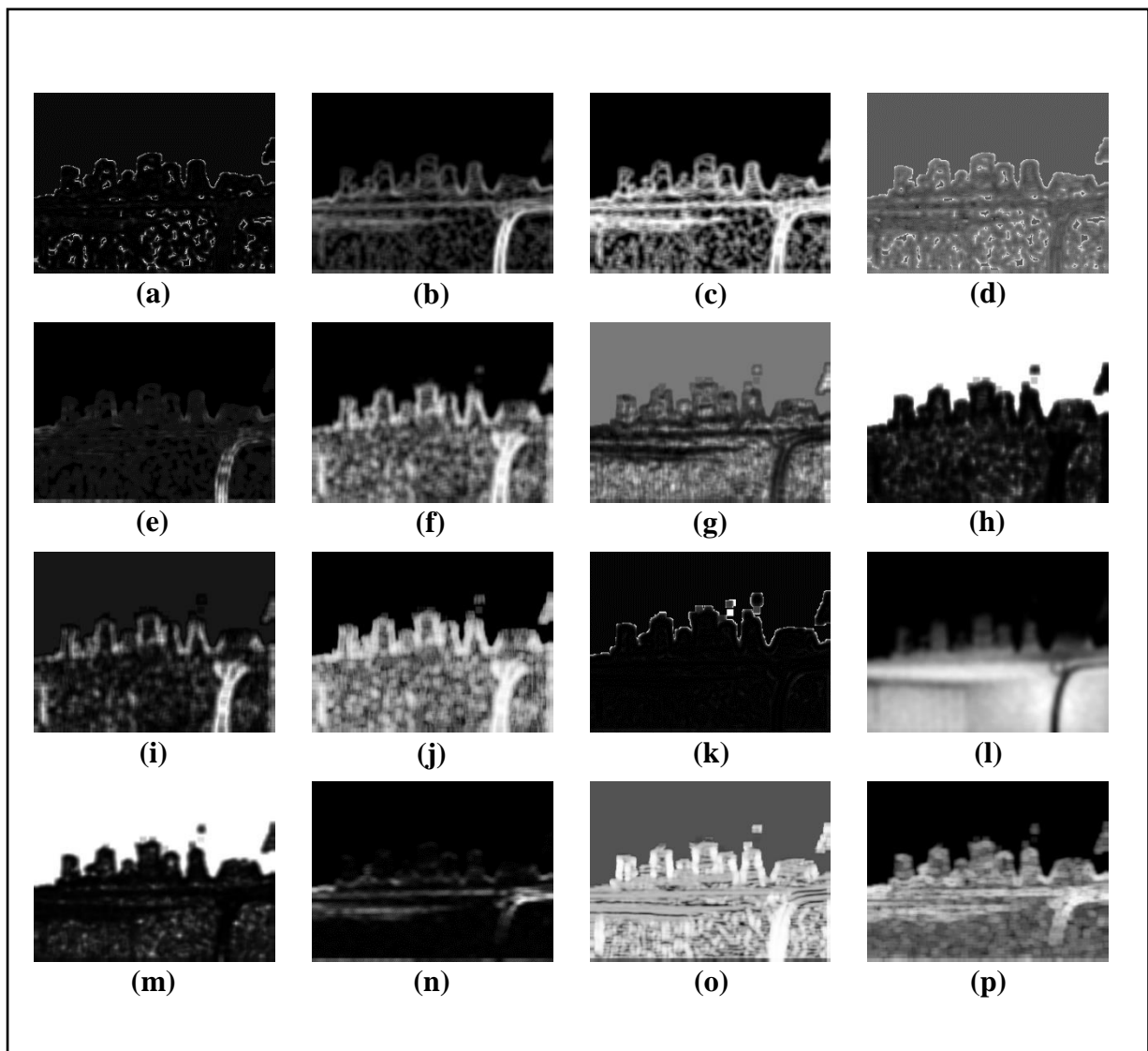
Figure 3.67: Feature Images for Sample Image-22 (Part-1)

(a) GrKurtosis4b, (b) GrMean4b, (c) GrNonZeros4b, (d) GrSkewness4b,

(e) GrVariance4b, (f) Horzl_Fraction6b, (g) Horzl_GLevNonU6b,

(h) Horzl_LngREmph6b, (i) Horzl_RLNonUni6b, (j) Horzl_ShrtREmp6b,

(k) Kurtosis, (l) Mean, (m) S(0,2)AngScMom6b, (n) S(0,2)Contrast6b ,
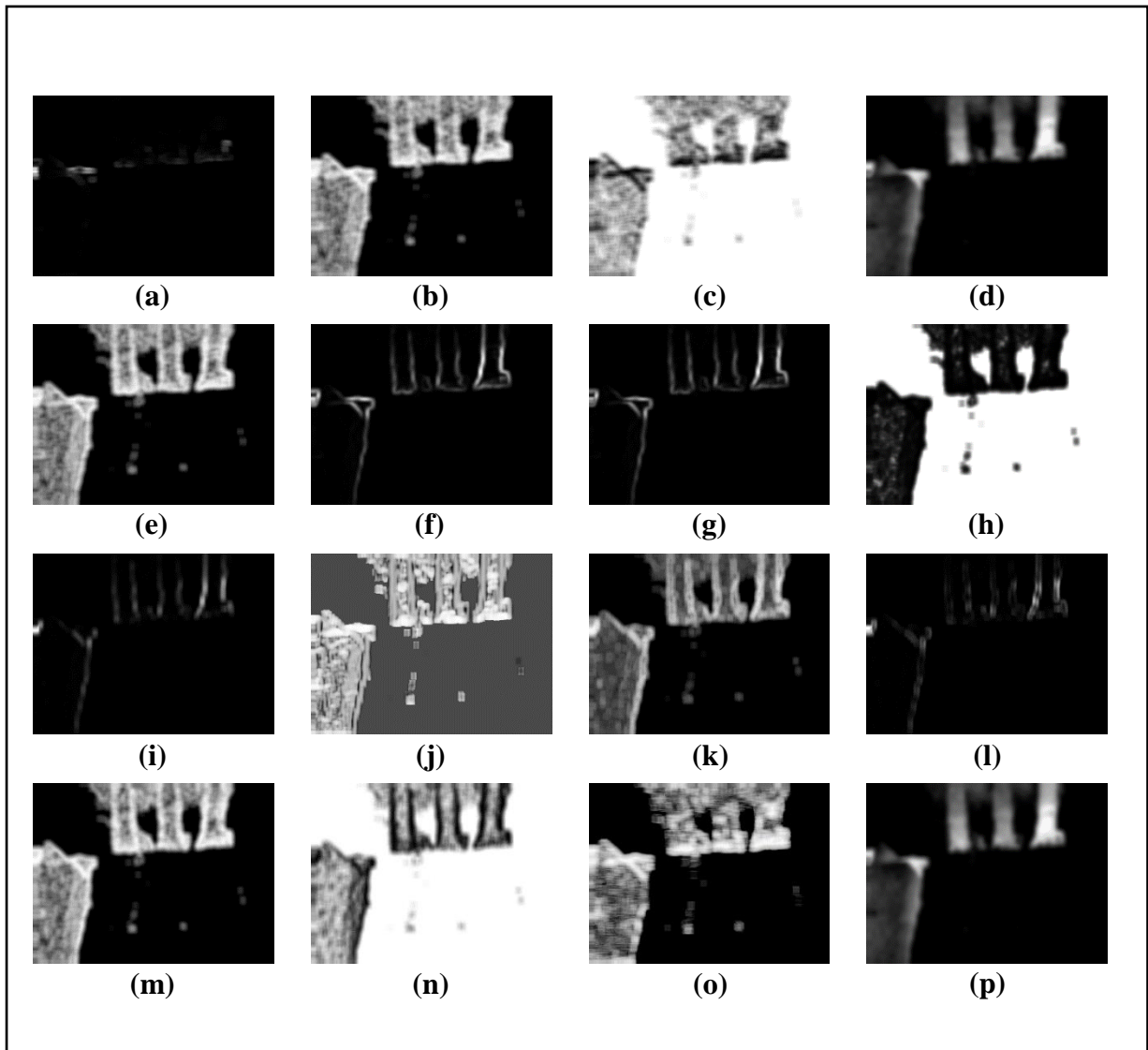
(o) S(0,2)Correlat6b, (p) S(0,2)DifEntrp6b
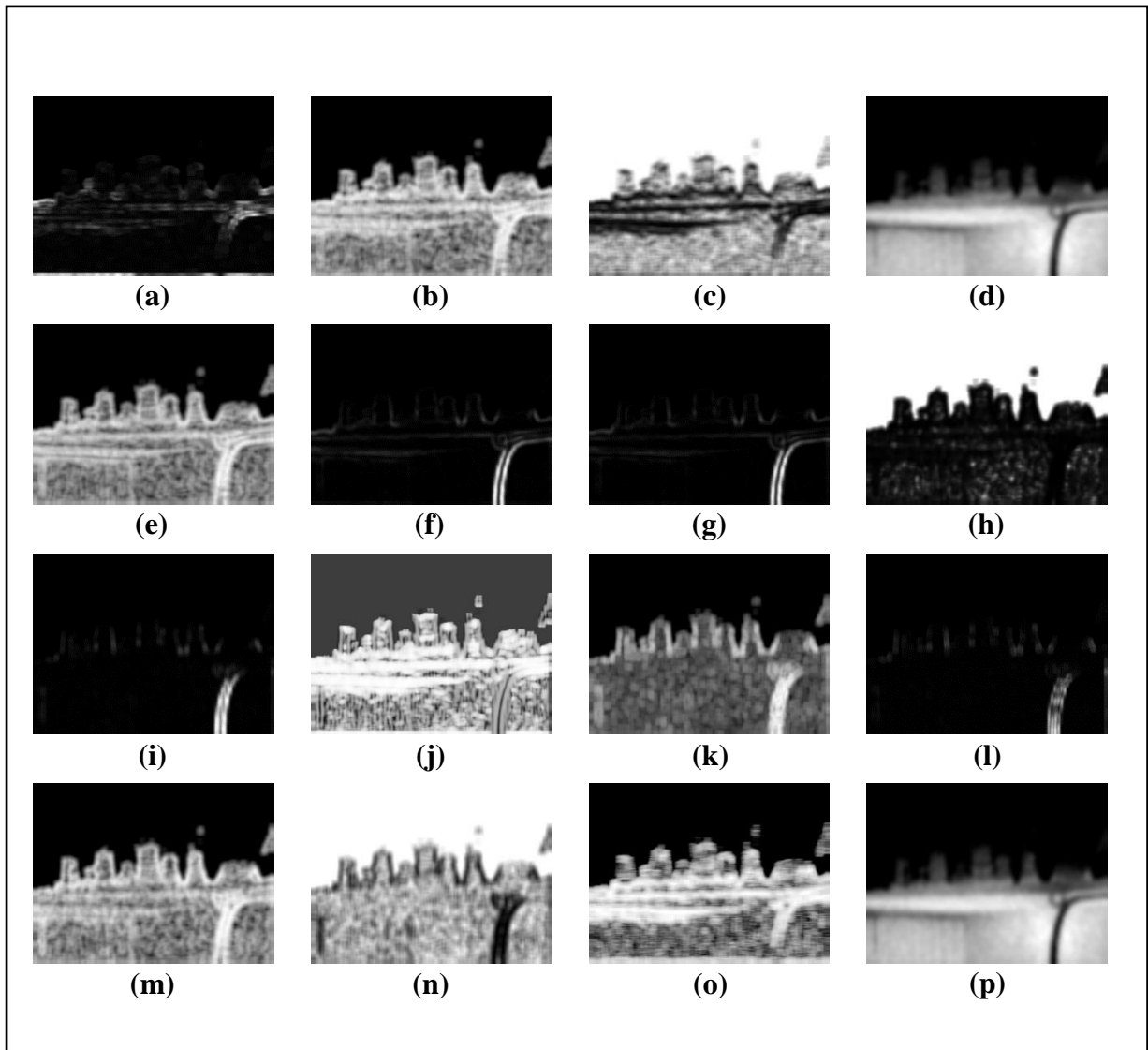
Figure 3.68: Feature Images for Sample Image-22 (Part-2)

(a) S(0,2)DifVarnc6b, (b) S(0,2)Entropy6b, (c) S(0,2)InvDfMom6b,

(d) S(0,2)SumAverg6b, (e) S(0,2)SumEntrp6b, (f) S(0,2)SumOfSqs6b,

(g) S(0,2)SumVarnc6b, (h) S(2,0)AngScMom6b, (i) S(2,0)Contrast6b,

(j) S(2,0)Correlat6b, (k) S(2,0)DifEntrp6b, (l) S(2,0)DifVarnc6b,

(m) S(2,0)Entropy6b, (n) S(2,0)InvDfMom6b ,

(o) Vertl_ShrtREmp6b, (p) S(2,0)SumAverg6b
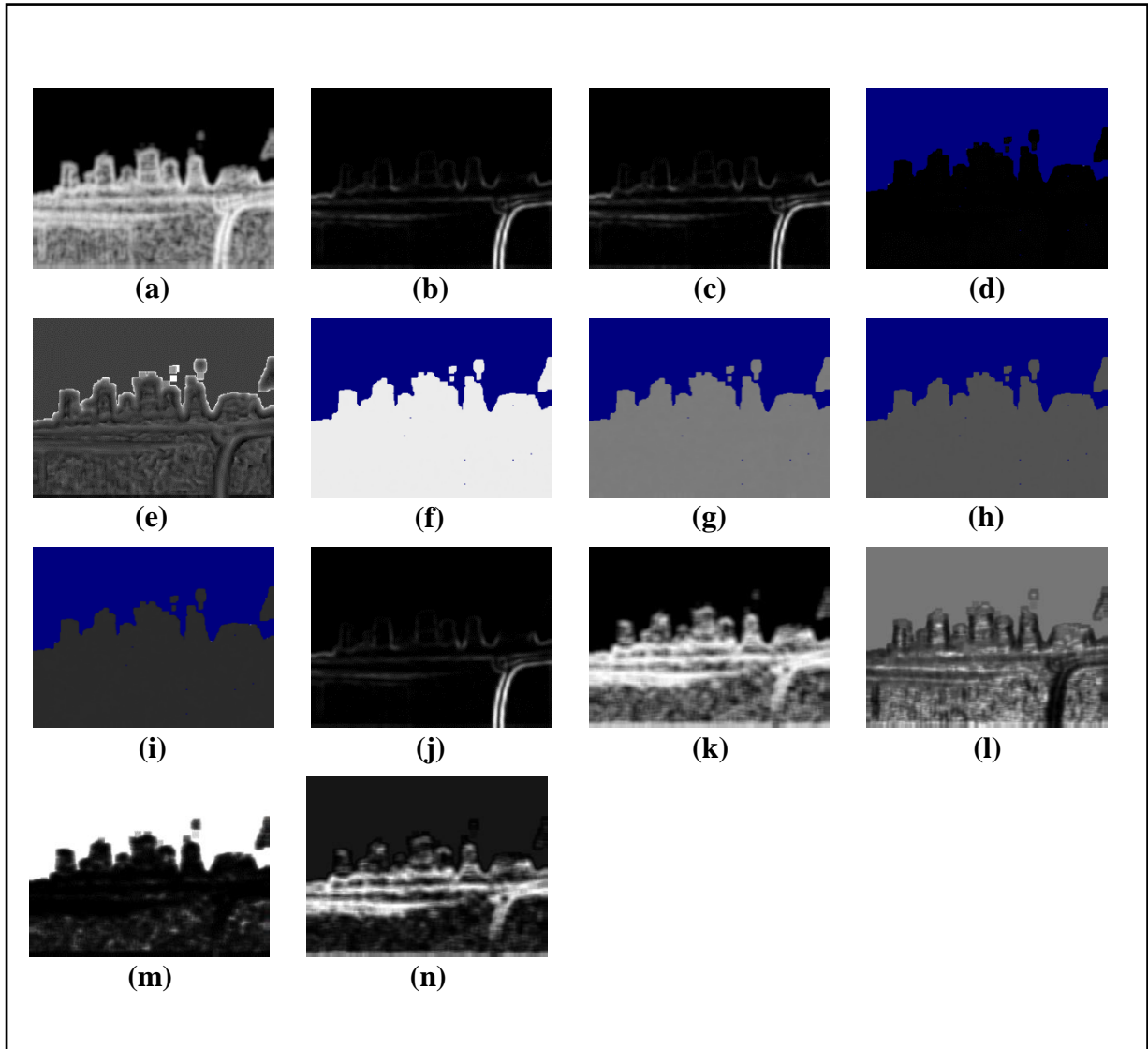
Figure 3.69: Feature Images for Sample Image-22 (Part-3)

(a) S(2,0)SumEntrp6b, (b) S(2,0)SumOfSqs6b, (c) S(2,0)SumVarnc6b, (d) Sigma,

(e) Skewness, (f) Teta1, (g) Teta2, (h) Teta3, (i) Teta4, (j) Variance, (k) Vertl_Fraction6b,

(l) Vertl_GLevNonU6b, (m) Vertl_LngREmph6b, (n) Vertl_RLNonUni6b

3.4.23 Collected Feature Images from Sample Image-23:
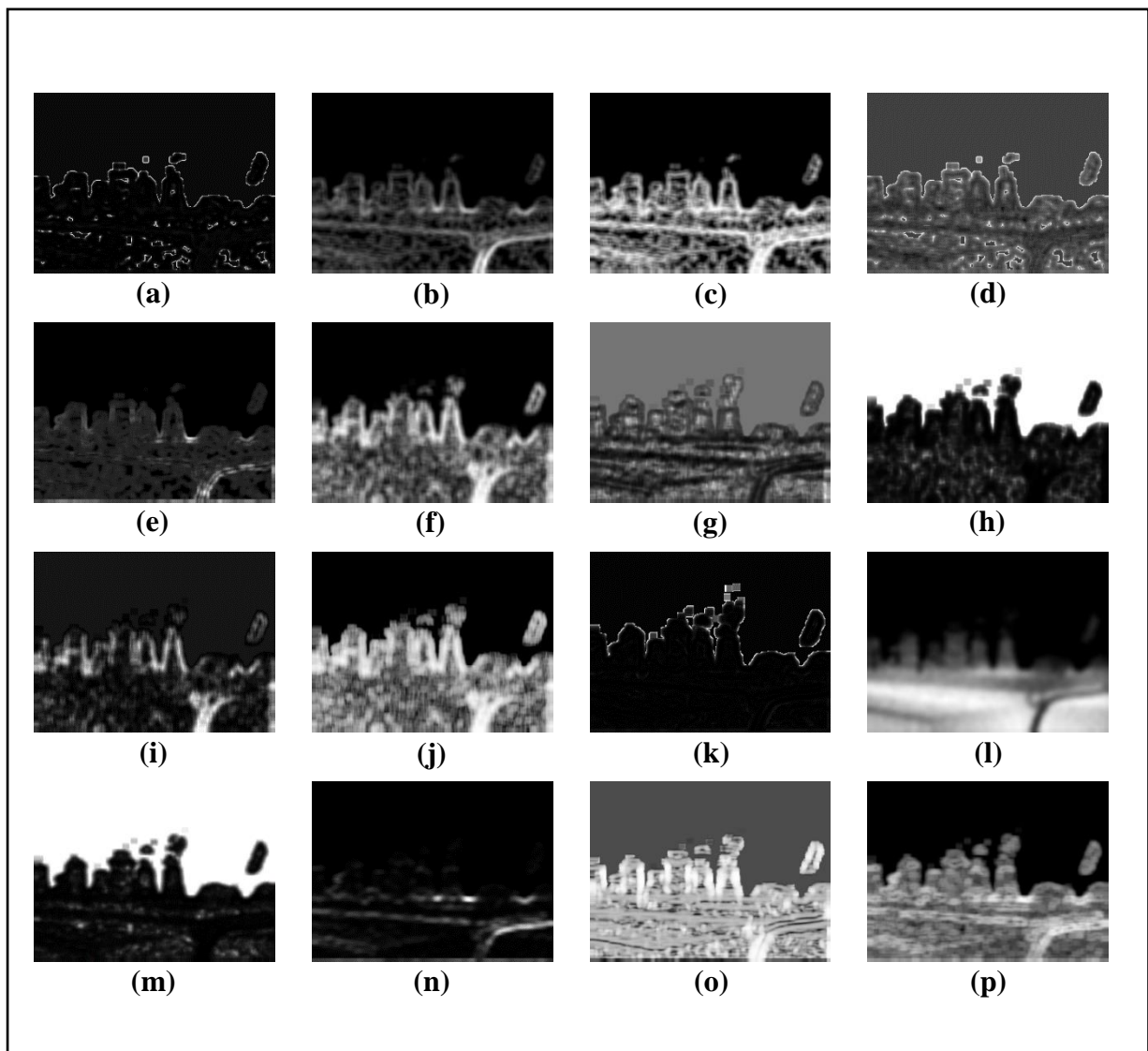
Figure 3.70: Feature Images for Sample Image-23 (Part-1)

(a) GrKurtosis4b, (b) GrMean4b, (c) GrNonZeros4b, (d) GrSkewness4b,

(e) GrVariance4b, (f) Horzl_Fraction6b, (g) Horzl_GLevNonU6b,

(h) Horzl_LngREmph6b, (i) Horzl_RLNonUni6b, (j) Horzl_ShrtREmp6b,

(k) Kurtosis, (l) Mean, (m) S(0,2)AngScMom6b, (n) S(0,2)Contrast6b ,

(o) S(0,2)Correlat6b, (p) S(0,2)DifEntrp6b
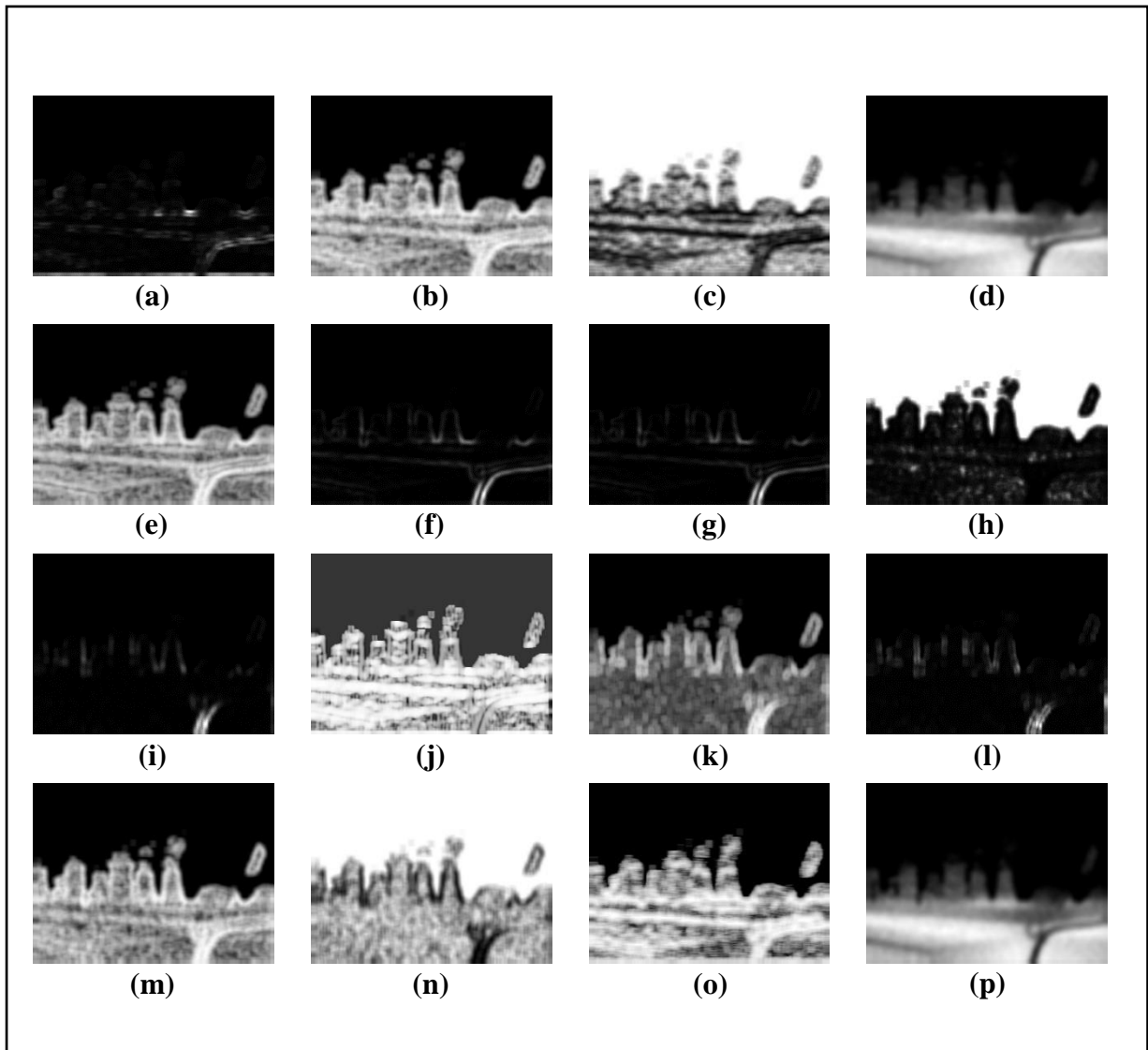
Figure 3.71: Feature Images for Sample Image-23 (Part-2)

(a) S(0,2)DifVarnc6b, (b) S(0,2)Entropy6b, (c) S(0,2)InvDfMom6b,

(d) S(0,2)SumAverg6b, (e) S(0,2)SumEntrp6b, (f) S(0,2)SumOfSqs6b,

(g) S(0,2)SumVarnc6b, (h) S(2,0)AngScMom6b, (i) S(2,0)Contrast6b,

(j) S(2,0)Correlat6b, (k) S(2,0)DifEntrp6b, (l) S(2,0)DifVarnc6b,

(m) S(2,0)Entropy6b, (n) S(2,0)InvDfMom6b ,
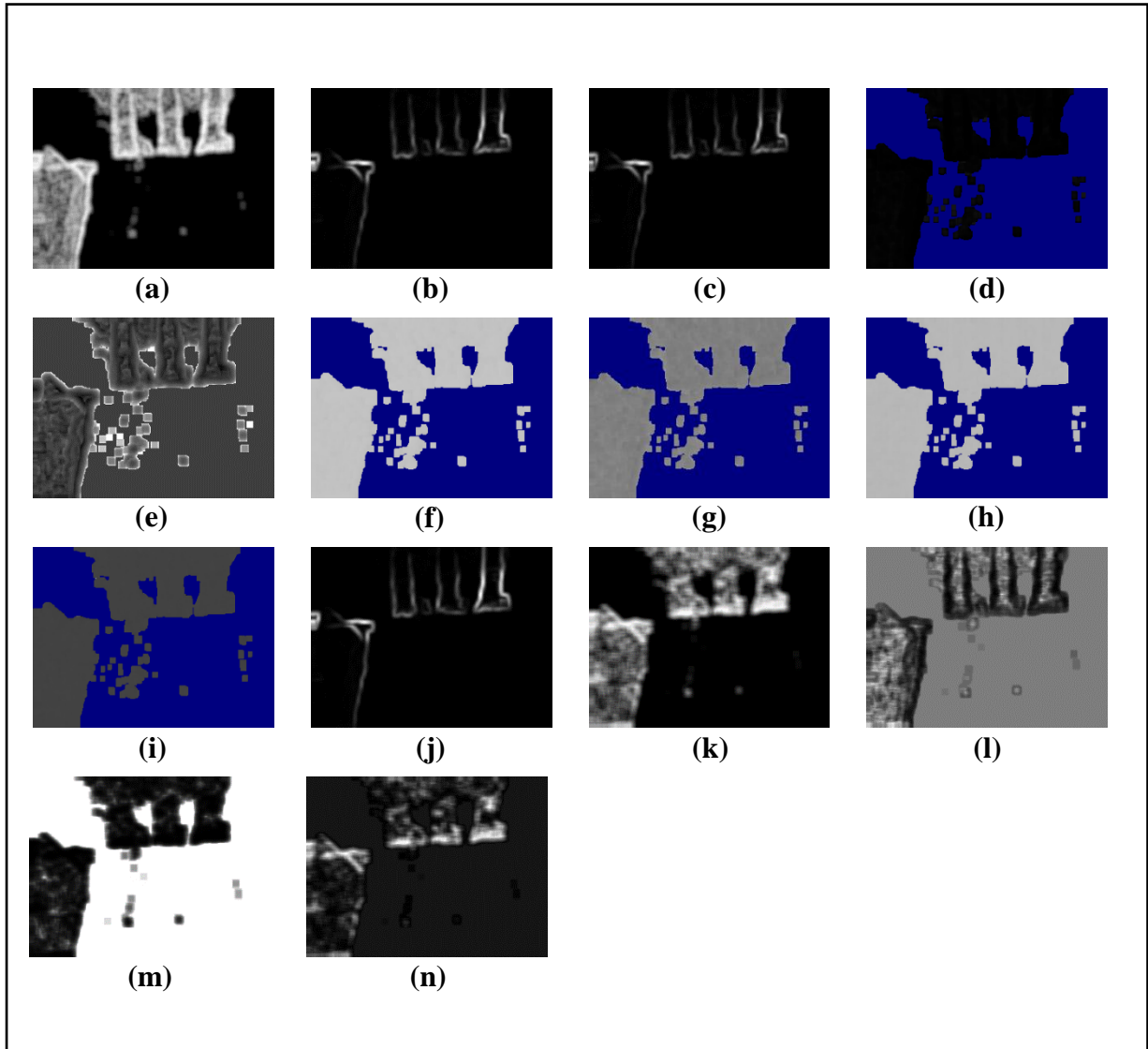
(o) Vertl_ShrtREmp6b, (p) S(2,0)SumAverg6b
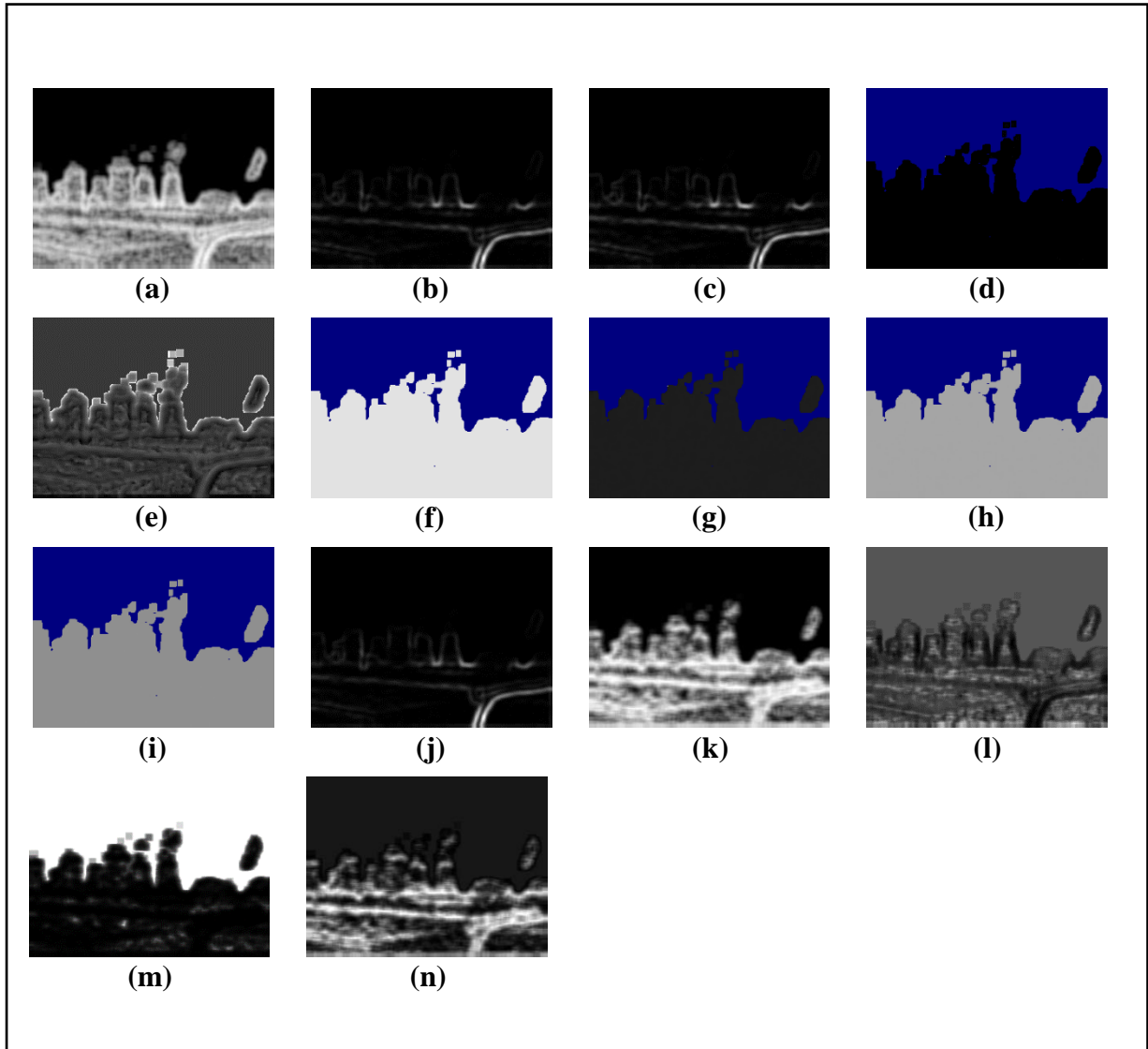
Figure 3.72: Feature Images for Sample Image-23 (Part-3)

(a) S(2,0)SumEntrp6b, (b) S(2,0)SumOfSqs6b, (c) S(2,0)SumVarnc6b, (d) Sigma,

(e) Skewness, (f) Teta1, (g) Teta2, (h) Teta3, (i) Teta4, (j) Variance, (k) Vertl_Fraction6b,

(l) Vertl_GLevNonU6b, (m) Vertl_LngREmph6b, (n) Vertl_RLNonUni6b

3.4.24 Collected Feature Images from Sample Image-24:
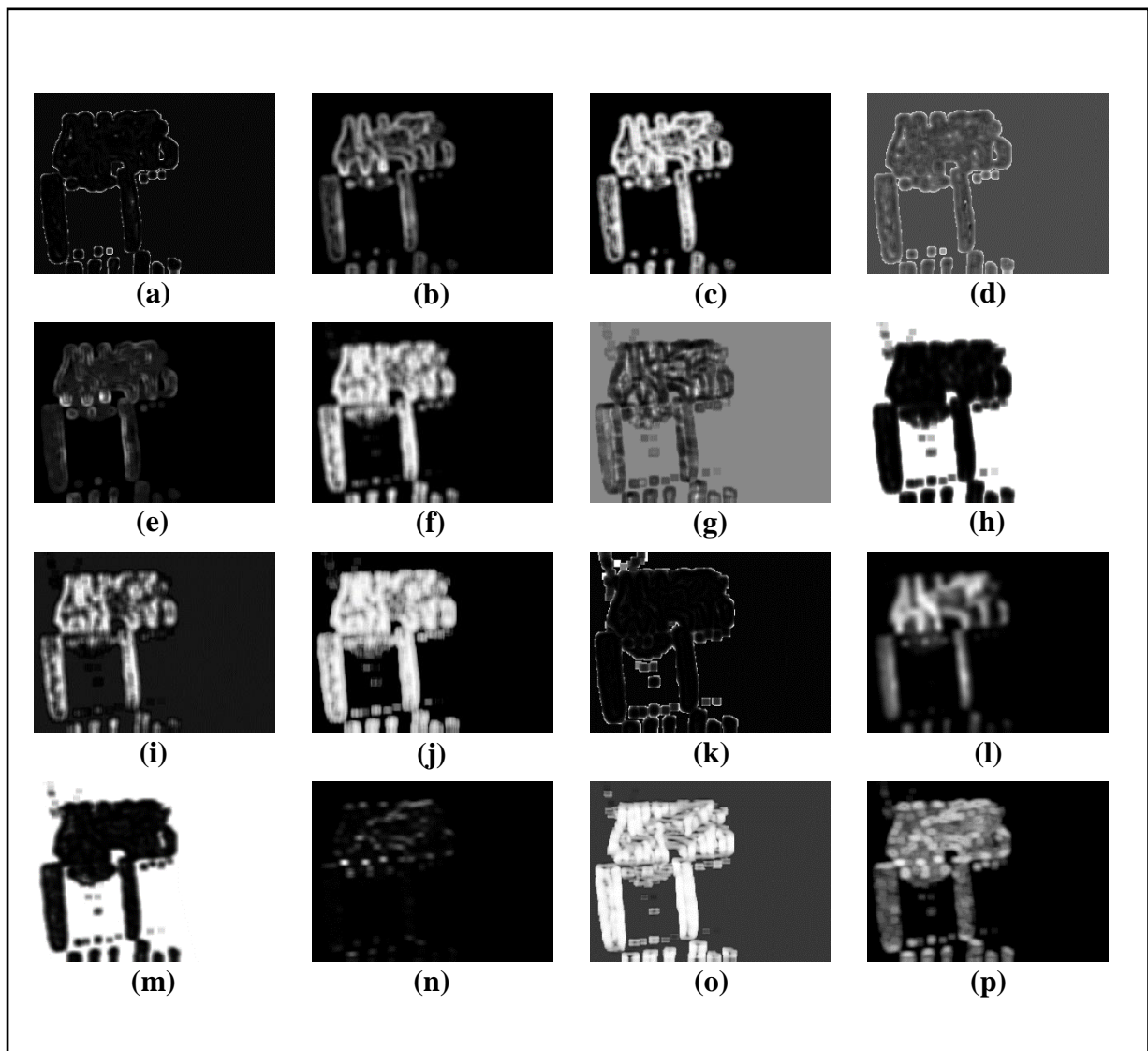
Figure 3.73: Feature Images for Sample Image-24 (Part-1)

(a) GrKurtosis4b, (b) GrMean4b, (c) GrNonZeros4b, (d) GrSkewness4b,

(e) GrVariance4b, (f) Horzl_Fraction6b, (g) Horzl_GLevNonU6b,

(h) Horzl_LngREmph6b, (i) Horzl_RLNonUni6b, (j) Horzl_ShrtREmp6b,

(k) Kurtosis, (l) Mean, (m) S(0,2)AngScMom6b, (n) S(0,2)Contrast6b ,
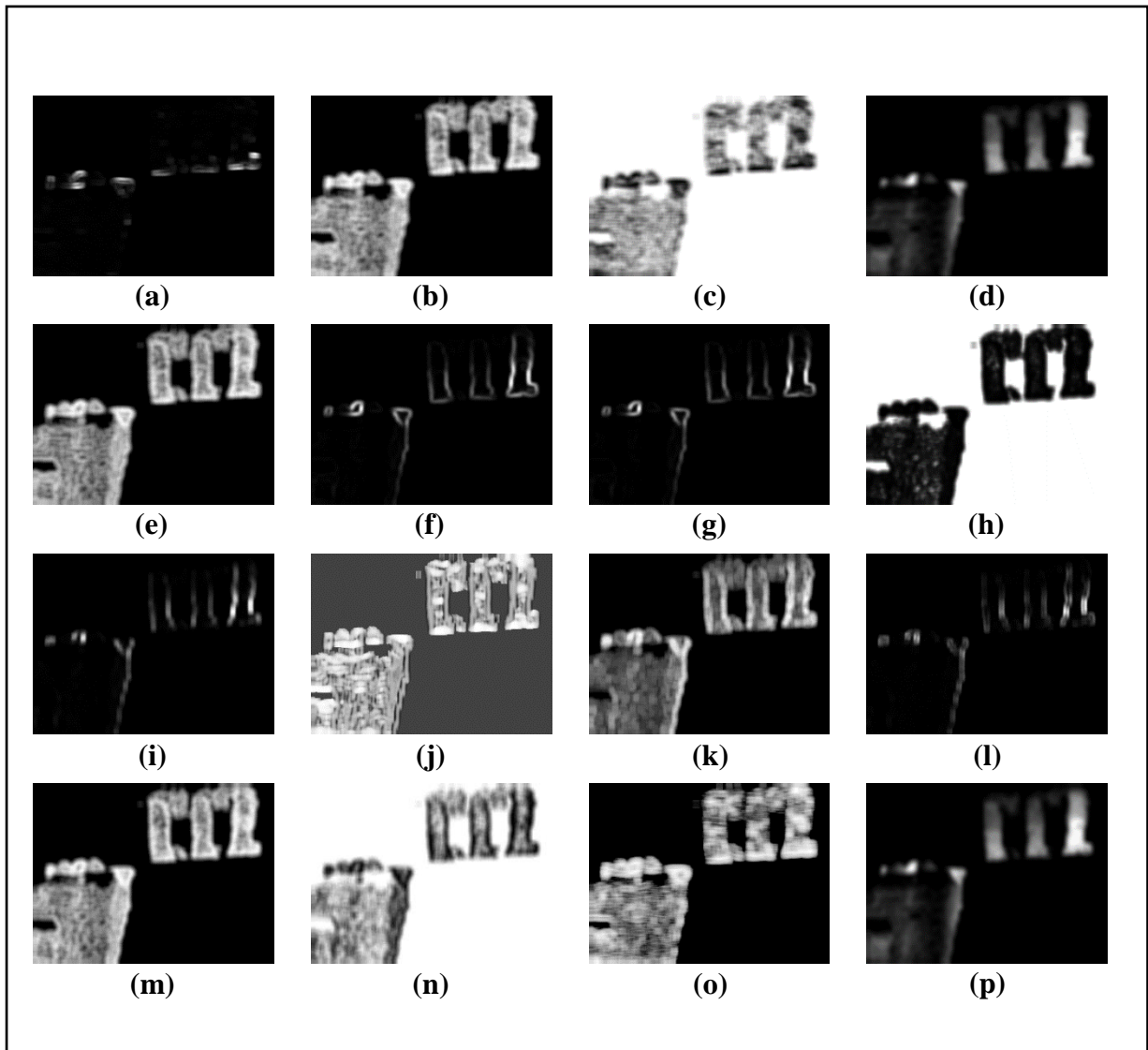
(o) S(0,2)Correlat6b, (p) S(0,2)DifEntrp6b
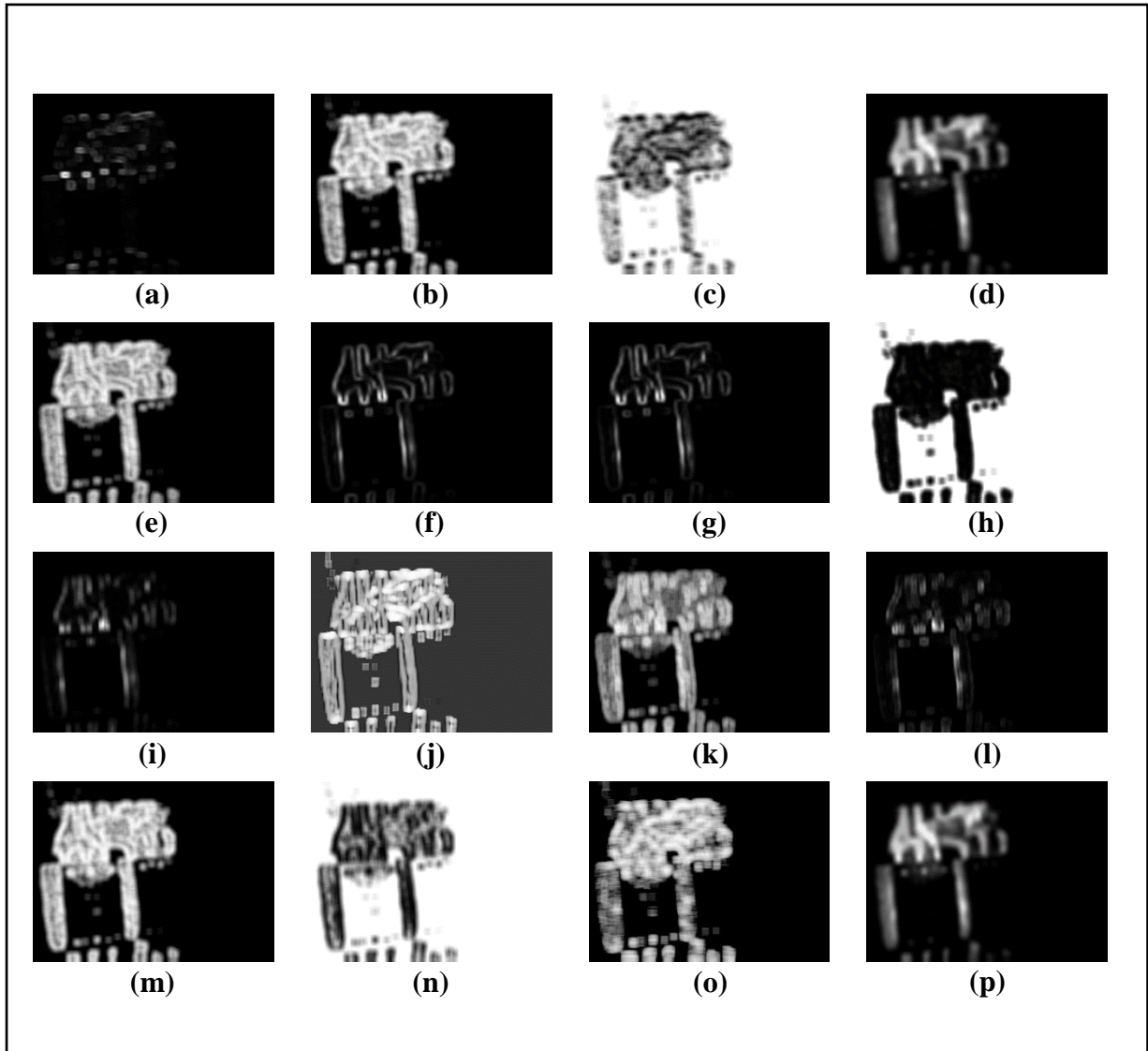
Figure 3.74: Feature Images for Sample Image-24 (Part-2)

(a) S(0,2)DifVarnc6b, (b) S(0,2)Entropy6b, (c) S(0,2)InvDfMom6b,

(d) S(0,2)SumAverg6b, (e) S(0,2)SumEntrp6b, (f) S(0,2)SumOfSqs6b,

(g) S(0,2)SumVarnc6b, (h) S(2,0)AngScMom6b, (i) S(2,0)Contrast6b,

(j) S(2,0)Correlat6b, (k) S(2,0)DifEntrp6b, (l) S(2,0)DifVarnc6b,

(m) S(2,0)Entropy6b, (n) S(2,0)InvDfMom6b ,

(o) Vertl_ShrtREmp6b, (p) S(2,0)SumAverg6b
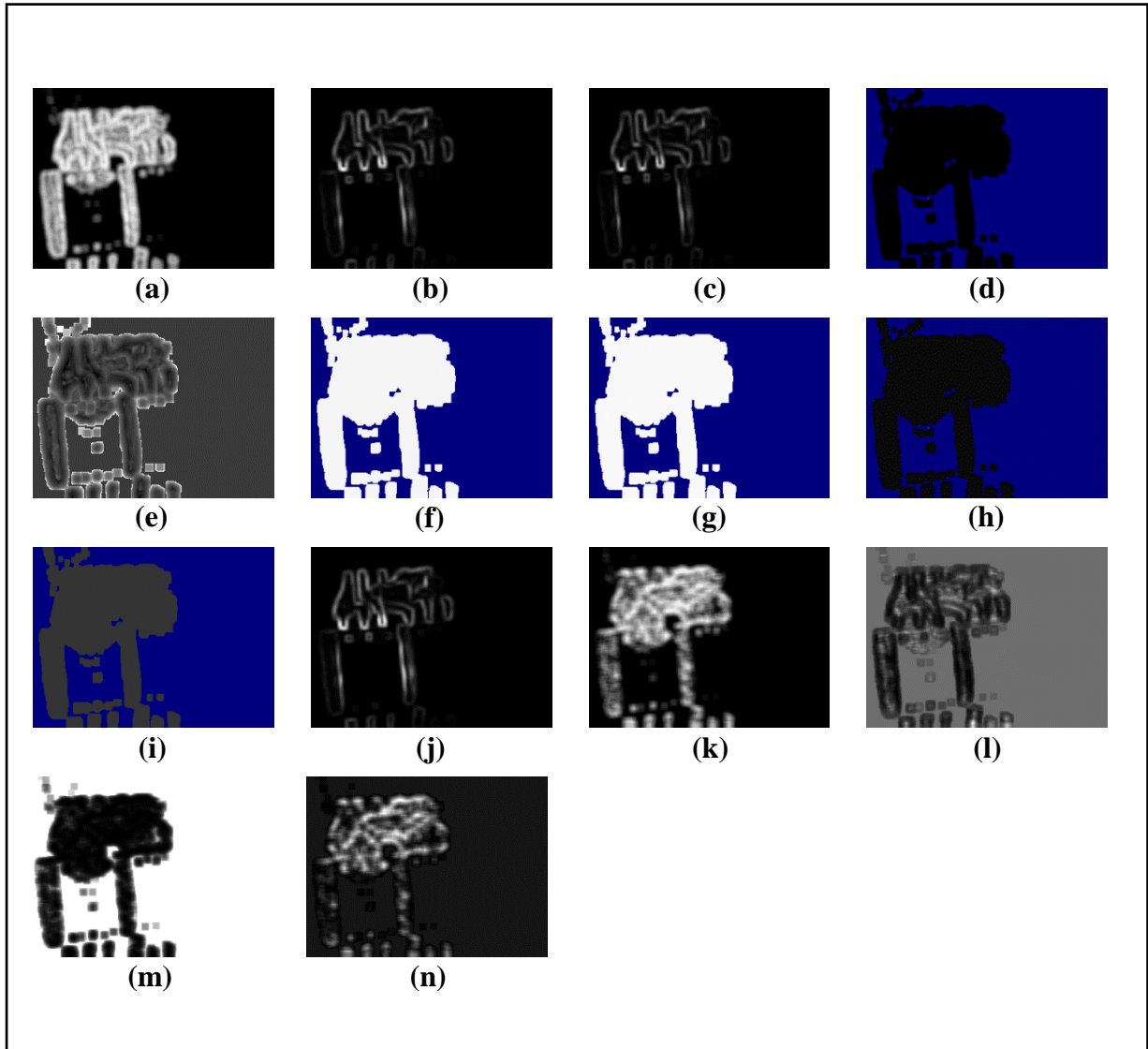
Figure 3.75: Feature Images for Sample Image-24 (Part-3)

(a) S(2,0)SumEntrp6b, (b) S(2,0)SumOfSqs6b, (c) S(2,0)SumVarnc6b, (d) Sigma,

(e) Skewness, (f) Teta1, (g) Teta2, (h) Teta3, (i) Teta4, (j) Variance, (k) Vertl_Fraction6b,

(l) Vertl_GLevNonU6b, (m) Vertl_LngREmph6b, (n) Vertl_RLNonUni6b

## 3.5.1 Report of Extracted Features from Sample Image-1:

Features	Normal Zone	Heated Zone	Features	Normal Zone	Heated Zone
Mean	5.1632076	98.798753	S(0,2)Entropy	0.5475274	2.4770276
Variance	121.97824	983.06519	S(0,2)DifVarnc	0.7732396	4.8379532
Skewness	2.8842268	0.92805	S(0,2)DifEntrp	0.2663532	0.8429614
Kurtosis	7.6293251	0.4327752	Horzl_RLNonUni	4351.8718	3605.2196
S(2,0)AngScMom	0.6772365	0.0033769	Horzl_GLevNonU	666.51386	222.06928
S(2,0)Contrast	1.6450688	22.224331	Horzl_LngREmph	1333.6083	1.9911937
S(2,0)Correlat	0.8627615	0.818577	Horzl_ShrtREmp	0.7287328	0.8650699
S(2,0)SumOfSqs	5.9934648	61.250036	Horzl_Fraction	0.1266202	0.8020719
S(2,0)InvDfMom	0.8908157	0.2847068	Vertl_RLNonUni	3815.9846	2825.485
S(2,0)SumAverg	3.7397773	52.190709	Vertl_GLevNonU	638.48267	199.95441
S(2,0)SumVarnc	22.32879	222.77581	Vertl_LngREmph	1335.7292	2.7613982
S(2,0)SumEntrp	0.4441669	1.7260629	Vertl_ShrtREmp	0.700816	0.8112942
S(2,0)Entropy	0.5675296	2.6296122	Vertl_Fraction	0.1199434	0.7193503
S(2,0)DifVarnc	1.4976897	10.548249	GrMean	0.1210267	1.2578357
S(2,0)DifEntrp	0.2946313	1.0042428	GrVariance	0.162679	0.8830626
S(0,2)AngScMom	0.6822969	0.0048749	GrSkewness	3.6309992	0.8883384
S(0,2)Contrast	0.8587957	10.139662	GrKurtosis	14.261927	1.7720491
S(0,2)Correlat	0.9304474	0.9163374	GrNonZeros	0.0926174	0.7903318
S(0,2)SumOfSqs	6.1737158	60.598522	Teta1	0.8640285	0.9218138
S(0,2)InvDfMom	0.9002373	0.3634948	Teta2	-0.7329176	-0.8349808
S(0,2)SumAverg	3.7830392	51.496329	Teta3	0.7623927	0.8377475
S(0,2)SumVarnc	23.836067	232.25443	Teta4	0.1018842	0.0714107
S(0,2)SumEntrp	0.4404296	1.7272561	Sigma	0.0931077	0.0835957

Table 3.1: Report of Extracted Features from Sample Image-1

3.5.2 Report of Extracted Features from Sample Image-2:

Features	Normal Zone	Heated Zone	Features	Normal Zone	Heated Zone
Mean	5.2910226	63.749537	S(0,2)Entropy	0.5925932	2.1451807
Variance	92.333573	336.54142	S(0,2)DifVarnc	0.8454416	2.1865012
Skewness	2.1923099	1.025335	S(0,2)DifEntrp	0.2964497	0.7205132
Kurtosis	3.503628	0.9429877	Horzl_RLNonUni	4141.3763	4102.0664
S(2,0)AngScMom	0.629138	0.010317	Horzl_GLevNonU	935.29184	549.08267
S(2,0)Contrast	1.1399717	6.0789855	Horzl_LngREmph	901.57384	3.574524
S(2,0)Correlat	0.8640412	0.8562864	Horzl_ShrtREmp	0.6998007	0.7448024
S(2,0)SumOfSqs	4.1923428	21.149651	Horzl_Fraction	0.1432646	0.6454847
S(2,0)InvDfMom	0.8801252	0.4409382	Vertl_RLNonUni	3966.9535	4394.9744
S(2,0)SumAverg	3.6714267	33.529167	Vertl_GLevNonU	935.14089	566.75154
S(2,0)SumVarnc	15.6294	78.51962	Vertl_LngREmph	880.08888	3.5326274
S(2,0)SumEntrp	0.4766293	1.5071399	Vertl_ShrtREmp	0.6839098	0.7642841
S(2,0)Entropy	0.6030832	2.1628256	Vertl_Fraction	0.1432611	0.6559522
S(2,0)DifVarnc	1.0064079	3.0095069	GrMean	0.1188609	0.7584288
S(2,0)DifEntrp	0.306756	0.7444395	GrVariance	0.1387847	0.4733614
S(0,2)AngScMom	0.6332963	0.0101334	GrSkewness	3.1112272	0.3409761
S(0,2)Contrast	0.958551	4.9920506	GrKurtosis	9.0131466	-0.3785999
S(0,2)Correlat	0.8843179	0.8816393	GrNonZeros	0.0983338	0.5990343
S(0,2)SumOfSqs	4.143038	21.088286	Teta1	0.8816367	0.9034385
S(0,2)InvDfMom	0.8844278	0.4374348	Teta2	-0.7227005	-0.7567405
S(0,2)SumAverg	3.6584111	33.480578	Teta3	0.7238125	0.7643433
S(0,2)SumVarnc	15.613601	79.361095	Teta4	0.11235	0.0913175
S(0,2)SumEntrp	0.4720463	1.5048735	Sigma	0.1118999	0.1107365

Table 3.2: Report of Extracted Features from Sample Image-2

3.5.3 Report of Extracted Features from Sample Image-3:

Features	Normal Zone	Heated Zone	Features	Normal Zone	Heated Zone
Mean	2.795171	53.845524	S(0,2)Entropy	0.3715716	1.9091954
Variance	30.834459	259.39609	S(0,2)DifVarnc	0.3427443	2.2273307
Skewness	3.5059597	1.1846977	S(0,2)DifEntrp	0.187588	0.6153277
Kurtosis	12.060534	1.1804645	Horzl_RLNonUni	1848.9975	1895.0159
S(2,0)AngScMom	0.7602183	0.0148917	Horzl_GLevNonU	746.98762	302.12836
S(2,0)Contrast	0.5917783	6.5526369	Horzl_LngREmph	1977.3713	4.236972
S(2,0)Correlat	0.7833709	0.8044794	Horzl_ShrtREmp	0.5931286	0.7493461
S(2,0)SumOfSqs	1.3658791	16.756895	Horzl_Fraction	0.0802884	0.6258153
S(2,0)InvDfMom	0.9343369	0.4662462	Vertl_RLNonUni	1805.5089	1140.2603
S(2,0)SumAverg	2.6788228	28.750153	Vertl_GLevNonU	725.81803	254.37621
S(2,0)SumVarnc	4.8717379	60.474941	Vertl_LngREmph	1671.5661	6.2532663
S(2,0)SumEntrp	0.3056808	1.4243096	Vertl_ShrtREmp	0.5972926	0.6375781
S(2,0)Entropy	0.3741628	2.059623	Vertl_Fraction	0.0771842	0.5146552
S(2,0)DifVarnc	0.5545702	3.5272616	GrMean	0.0459067	0.6578588
S(2,0)DifEntrp	0.1977296	0.7564991	GrVariance	0.0523219	0.5073927
S(0,2)AngScMom	0.76092	0.0202965	GrSkewness	5.0517064	0.7566459
S(0,2)Contrast	0.3693555	3.6729112	GrKurtosis	25.296247	0.2432106
S(0,2)Correlat	0.8722063	0.8862322	GrNonZeros	0.040324	0.515812
S(0,2)SumOfSqs	1.4451236	16.142134	Teta1	0.8840591	0.9195126
S(0,2)InvDfMom	0.9368113	0.565262	Teta2	-0.8030179	-0.8422254
S(0,2)SumAverg	2.7122019	28.359311	Teta3	0.8799232	0.8911581
S(0,2)SumVarnc	5.411139	60.895624	Teta4	0.0304971	0.0340187
S(0,2)SumEntrp	0.3073699	1.4206028	Sigma	0.1147401	0.0963519

Table 3.3: Report of Extracted Features from Sample Image-3

3.5.4 Report of Extracted Features from Sample Image-4:

Features	Normal Zone	Heated Zone	Features	Normal Zone	Heated Zone
Mean	8.9398173	91.412044	S(0,2)Entropy	1.0104303	2.2721895
Variance	147.55414	1304.3289	S(0,2)DifVarnc	0.6428473	2.8776722
Skewness	1.5201637	1.1218497	S(0,2)DifEntrp	0.3639765	0.6866624
Kurtosis	1.3499986	0.6191957	Horzl_RLNonUni	5416.9444	2759.3642
S(2,0)AngScMom	0.3373131	0.0067471	Horzl_GLevNonU	1435.1575	192.722
S(2,0)Contrast	1.628823	25.960759	Horzl_LngREmph	244.71361	3.1927438
S(2,0)Correlat	0.8958857	0.8456051	Horzl_ShrtREmp	0.6091564	0.8178721
S(2,0)SumOfSqs	7.8222807	84.072616	Horzl_Fraction	0.2236599	0.701559
S(2,0)InvDfMom	0.8024321	0.3779883	Vertl_RLNonUni	3596.9906	1432.7812
S(2,0)SumAverg	5.4743487	48.627669	Vertl_GLevNonU	1271.0233	153.09493
S(2,0)SumVarnc	29.6603	310.3297	Vertl_LngREmph	396.26027	5.8894458
S(2,0)SumEntrp	0.8390643	1.7210465	Vertl_ShrtREmp	0.5231767	0.6743768
S(2,0)Entropy	1.0655219	2.5452335	Vertl_Fraction	0.1910321	0.5388404
S(2,0)DifVarnc	1.3180824	15.072807	GrMean	0.1613336	1.0723855
S(2,0)DifEntrp	0.4321245	0.9945028	GrVariance	0.1781155	1.1370335
S(0,2)AngScMom	0.3462528	0.0106382	GrSkewness	2.5285506	1.019746
S(0,2)Contrast	0.8046576	4.9534684	GrKurtosis	5.6691836	1.0670321
S(0,2)Correlat	0.9496966	0.9698669	GrNonZeros	0.1359001	0.6337386
S(0,2)SumOfSqs	7.9980474	82.193083	Teta1	0.886011	0.9533278
S(0,2)InvDfMom	0.8343395	0.5308862	Teta2	-0.7743478	-0.9068505
S(0,2)SumAverg	5.5227309	47.836367	Teta3	0.7991479	0.9109442
S(0,2)SumVarnc	31.187532	323.81886	Teta4	0.0880025	0.042892
S(0,2)SumEntrp	0.833789	1.7096353	Sigma	0.0727355	0.047665

Table 3.4: Report of Extracted Features from Sample Image-4

3.5.5 Report of Extracted Features from Sample Image-5:

Features	Normal Zone	Heated Zone	Features	Normal Zone	Heated Zone
Mean	8.7380045	131.39734	S(0,2)Entropy	0.9611605	2.5281044
Variance	170.45968	2128.4014	S(0,2)DifVarnc	0.7385956	4.3795359
Skewness	1.8630754	0.4447316	S(0,2)DifEntrp	0.3648435	0.7795432
Kurtosis	2.9181021	-0.4941078	Horzl_RLNonUni	5409.1244	2950.3375
S(2,0)AngScMom	0.3956602	0.0030138	Horzl_GLevNonU	1218.255	118.53616
S(2,0)Contrast	1.5886921	41.090409	Horzl_LngREmph	388.8766	2.3322083
S(2,0)Correlat	0.9107893	0.8350207	Horzl_ShrtREmp	0.6273125	0.8667101
S(2,0)SumOfSqs	8.9041582	124.53198	Horzl_Fraction	0.2076685	0.7779445
S(2,0)InvDfMom	0.8180508	0.2951794	Vertl_RLNonUni	4124.3862	1766.402
S(2,0)SumAverg	5.3337282	69.714165	Vertl_GLevNonU	1105.5355	97.503753
S(2,0)SumVarnc	34.027941	457.0375	Vertl_LngREmph	535.49243	4.1612128
S(2,0)SumEntrp	0.7854522	1.8656387	Vertl_ShrtREmp	0.5727089	0.7565596
S(2,0)Entropy	0.9923604	2.8033738	Vertl_Fraction	0.1860642	0.6238996
S(2,0)DifVarnc	1.3175885	22.025897	GrMean	0.1645365	1.3487666
S(2,0)DifEntrp	0.4113657	1.108722	GrVariance	0.1880853	1.5716256
S(0,2)AngScMom	0.3985873	0.0049778	GrSkewness	2.6213713	1.3260732
S(0,2)Contrast	0.9055227	7.7997984	GrKurtosis	6.5152376	2.4285724
S(0,2)Correlat	0.9506286	0.9688736	GrNonZeros	0.1357957	0.7278732
S(0,2)SumOfSqs	9.1705102	125.29237	Teta1	0.8475766	0.960634
S(0,2)InvDfMom	0.8385886	0.4606569	Teta2	-0.7070723	-0.9068454
S(0,2)SumAverg	5.3968446	68.082056	Teta3	0.7588668	0.8909055
S(0,2)SumVarnc	35.776518	493.36968	Teta4	0.0996889	0.055642
S(0,2)SumEntrp	0.7862888	1.8699634	Sigma	0.0806129	0.0492335

Table 3.5: Report of Extracted Features from Sample Image-5

3.5.6 Report of Extracted Features from Sample Image-6:

Features	Normal Zone	Heated Zone	Features	Normal Zone	Heated Zone
Mean	10.814631	108.72736	S(0,2)Entropy	0.7810907	1.9266024
Variance	406.64607	363.56375	S(0,2)DifVarnc	1.1636996	0.9887108
Skewness	2.0222519	0.3473411	S(0,2)DifEntrp	0.310546	0.5117756
Kurtosis	2.7675805	-0.6966417	Horzl_RLNonUni	2777.647	2568.7715
S(2,0)AngScMom	0.5308621	0.0186448	Horzl_GLevNonU	378.56808	725.26382
S(2,0)Contrast	2.2686023	1.2203679	Horzl_LngREmph	659.33545	15.129255
S(2,0)Correlat	0.9477905	0.9728348	Horzl_ShrtREmp	0.6741438	0.4325823
S(2,0)SumOfSqs	21.725942	22.461978	Horzl_Fraction	0.1603293	0.3426345
S(2,0)InvDfMom	0.8559721	0.6966105	Vertl_RLNonUni	2336.2554	3897.1189
S(2,0)SumAverg	6.3336639	55.317088	Vertl_GLevNonU	332.68321	777.52803
S(2,0)SumVarnc	84.635166	88.627546	Vertl_LngREmph	642.85124	11.999712
S(2,0)SumEntrp	0.6690186	1.5549387	Vertl_ShrtREmp	0.6417348	0.5346677
S(2,0)Entropy	0.8386436	1.8604562	Vertl_Fraction	0.1482988	0.3957681
S(2,0)DifVarnc	2.0000332	0.7460648	GrMean	0.1645401	0.3432941
S(2,0)DifEntrp	0.3671755	0.4513298	GrVariance	0.2241536	0.2999652
S(0,2)AngScMom	0.5526387	0.0173703	GrSkewness	3.0673391	1.2395807
S(0,2)Contrast	1.2948808	1.6647878	GrKurtosis	9.6074841	0.7193861
S(0,2)Correlat	0.9689701	0.9627578	GrNonZeros	0.1218371	0.2978561
S(0,2)SumOfSqs	20.865042	22.350811	Teta1	0.9367574	0.8997454
S(0,2)InvDfMom	0.881853	0.6595487	Teta2	-0.8595366	-0.6832758
S(0,2)SumAverg	6.1783255	55.396897	Teta3	0.8615512	0.6821438
S(0,2)SumVarnc	82.165286	87.738455	Teta4	0.0628976	0.1007526
S(0,2)SumEntrp	0.6413284	1.5542135	Sigma	0.0450718	0.0639951

Table 3.6: Report of Extracted Features from Sample Image-6

3.5.7 Report of Extracted Features from Sample Image-7:

Features	Normal Zone	Heated Zone	Features	Normal Zone	Heated Zone
Mean	15.530382	195.79622	S(0,2)Entropy	0.882108	2.2910308
Variance	916.49367	1220.3095	S(0,2)DifVarnc	3.6158531	5.460635
Skewness	2.0589082	0.2082918	S(0,2)DifEntrp	0.3998722	0.7603144
Kurtosis	3.0520638	-0.7128159	Horzl_RLNonUni	5748.2301	6809.661
S(2,0)AngScMom	0.5369907	0.0185895	Horzl_GLevNonU	355.81112	569.6727
S(2,0)Contrast	11.424932	7.9598909	Horzl_LngREmph	396.5911	20.006938
S(2,0)Correlat	0.8830418	0.944484	Horzl_ShrtREmp	0.7856922	0.7074406
S(2,0)SumOfSqs	48.841955	71.690013	Horzl_Fraction	0.2063082	0.5181139
S(2,0)InvDfMom	0.8089007	0.5417412	Vertl_RLNonUni	4770.4405	7294.6951
S(2,0)SumAverg	8.4382667	99.355455	Vertl_GLevNonU	299.02267	551.58758
S(2,0)SumVarnc	183.94289	278.80016	Vertl_LngREmph	578.55396	8.6013576
S(2,0)SumEntrp	0.7171078	1.6852197	Vertl_ShrtREmp	0.7621941	0.7210354
S(2,0)Entropy	0.9518425	2.2605861	Vertl_Fraction	0.1835279	0.5344275
S(2,0)DifVarnc	10.074098	5.4828728	GrMean	0.3547529	0.6877728
S(2,0)DifEntrp	0.4877381	0.7296874	GrVariance	0.8222529	0.7559423
S(0,2)AngScMom	0.5600126	0.0167785	GrSkewness	3.2423976	1.8606971
S(0,2)Contrast	4.0430646	8.3052841	GrKurtosis	11.786149	6.4015008
S(0,2)Correlat	0.9589207	0.9426596	GrNonZeros	0.1845218	0.4911078
S(0,2)SumOfSqs	49.210521	72.420808	Teta1	0.9089878	0.9074188
S(0,2)InvDfMom	0.8412453	0.5275466	Teta2	-0.8351859	-0.7339448
S(0,2)SumAverg	8.5181772	99.229425	Teta3	0.8525984	0.7336529
S(0,2)SumVarnc	192.79902	281.37795	Teta4	0.0762178	0.0915525
S(0,2)SumEntrp	0.6862119	1.7003275	Sigma	0.0602727	0.0726545

Table 3.7: Report of Extracted Features from Sample Image-7

3.5.8 Report of Extracted Features from Sample Image-8:

Features	Normal Zone	Heated Zone	Features	Normal Zone	Heated Zone
Mean	37.531334	123.52621	S(0,2)Entropy	1.4609092	2.0727696
Variance	1221.6584	767.17088	S(0,2)DifVarnc	3.4411063	1.193311
Skewness	0.1072495	0.6795662	S(0,2)DifEntrp	0.5383404	0.5441718
Kurtosis	-1.7853013	-0.5985833	Horzl_RLNonUni	3591.8563	6750.4895
S(2,0)AngScMom	0.1775036	0.0110885	Horzl_GLevNonU	663.67605	1008.015
S(2,0)Contrast	4.5356278	3.0890711	Horzl_LngREmph	63.265027	8.1022425
S(2,0)Correlat	0.9682324	0.9673378	Horzl_ShrtREmp	0.6137872	0.5878877
S(2,0)SumOfSqs	71.387577	47.288141	Horzl_Fraction	0.3114372	0.4642784
S(2,0)InvDfMom	0.7325979	0.5916479	Vertl_RLNonUni	3904.242	5358.9648
S(2,0)SumAverg	18.793823	63.119683	Vertl_GLevNonU	624.46565	834.69869
S(2,0)SumVarnc	281.01468	186.06349	Vertl_LngREmph	166.72246	9.563041
S(2,0)SumEntrp	1.17569	1.6630834	Vertl_ShrtREmp	0.6443935	0.5376369
S(2,0)Entropy	1.4703653	2.1112997	Vertl_Fraction	0.3109502	0.4251103
S(2,0)DifVarnc	3.7178003	1.9524256	GrMean	0.4019317	0.4434392
S(2,0)DifEntrp	0.5451902	0.5768148	GrVariance	0.5229302	0.3919477
S(0,2)AngScMom	0.1808365	0.0129648	GrSkewness	2.1349856	1.4937671
S(0,2)Contrast	4.2173114	2.0791477	GrKurtosis	5.5408904	4.4593022
S(0,2)Correlat	0.97061	0.97804	GrNonZeros	0.2896126	0.3728401
S(0,2)SumOfSqs	71.747271	47.339422	Teta1	0.9605139	0.8795919
S(0,2)InvDfMom	0.7430708	0.6196651	Teta2	-0.8560398	-0.7648813
S(0,2)SumAverg	18.956098	63.080519	Teta3	0.8289762	0.8382269
S(0,2)SumVarnc	282.77177	187.27854	Teta4	0.0662672	0.0467486
S(0,2)SumEntrp	1.1673521	1.6624358	Sigma	0.0469308	0.0521481

Table 3.8: Report of Extracted Features from Sample Image-8

3.5.9 Report of Extracted Features from Sample Image-9:

Features	Normal Zone	Heated Zone	Features	Normal Zone	Heated Zone
Mean	13.925935	136.34302	S(0,2)Entropy	0.7855864	2.1205298
Variance	695.98978	746.35984	S(0,2)DifVarnc	2.3103429	1.0684018
Skewness	1.8775074	0.22899	S(0,2)DifEntrp	0.3449944	0.5587957
Kurtosis	2.008237	-1.1107625	Horzl_RLNonUni	3857.2029	3857.9376
S(2,0)AngScMom	0.5643084	0.0111363	Horzl_GLevNonU	333.63706	591.19824
S(2,0)Contrast	3.8777958	1.7251033	Horzl_LngREmph	1053.1258	9.6178755
S(2,0)Correlat	0.9484487	0.9811461	Horzl_ShrtREmp	0.7468284	0.5260609
S(2,0)SumOfSqs	37.611008	45.749171	Horzl_Fraction	0.1684881	0.4224175
S(2,0)InvDfMom	0.8490689	0.6267279	Vertl_RLNonUni	3519.2311	5145.8278
S(2,0)SumAverg	7.7441995	69.369145	Vertl_GLevNonU	327.59872	641.17574
S(2,0)SumVarnc	146.56624	181.27158	Vertl_LngREmph	516.55556	7.4177306
S(2,0)SumEntrp	0.6490359	1.6836906	Vertl_ShrtREmp	0.7268766	0.5907964
S(2,0)Entropy	0.8327465	2.0724669	Vertl_Fraction	0.1626727	0.475515
S(2,0)DifVarnc	3.434042	0.9336423	GrMean	0.2333964	0.4069321
S(2,0)DifEntrp	0.3898488	0.5195498	GrVariance	0.3846464	0.3255217
S(0,2)AngScMom	0.5799319	0.0102333	GrSkewness	2.9319352	0.8774077
S(0,2)Contrast	2.5528961	2.087654	GrKurtosis	8.7137393	-0.6763367
S(0,2)Correlat	0.9653249	0.9771191	GrNonZeros	0.1487562	0.3528534
S(0,2)SumOfSqs	36.811693	45.619912	Teta1	0.9430707	0.9067984
S(0,2)InvDfMom	0.8693571	0.5907971	Teta2	-0.8962186	-0.681835
S(0,2)SumAverg	7.5848721	69.441739	Teta3	0.9348532	0.6462301
S(0,2)SumVarnc	144.69387	180.392	Teta4	0.0198795	0.1288333
S(0,2)SumEntrp	0.626855	1.6831867	Sigma	0.0409818	0.0503784

Table 3.9: Report of Extracted Features from Sample Image-9

3.5.10 Report of Extracted Features from Sample Image-10:

Features	Normal Zone	Heated Zone	Features	Normal Zone	Heated Zone
Mean	4.7523048	59.013252	S(0,2)Entropy	0.6284426	2.1447981
Variance	63.124003	560.05136	S(0,2)DifVarnc	0.4883767	3.9933871
Skewness	2.1994674	1.9553065	S(0,2)DifEntrp	0.2702513	0.73124
Kurtosis	3.8116684	5.3184174	Horzl_RLNonUni	4238.6039	2869.6067
S(2,0)AngScMom	0.5690072	0.0083278	Horzl_GLevNonU	1329.4387	301.01536
S(2,0)Contrast	0.9796896	18.773878	Horzl_LngREmph	745.92545	2.2344612
S(2,0)Correlat	0.8355805	0.7614978	Horzl_ShrtREmp	0.6495081	0.8549664
S(2,0)SumOfSqs	2.9792379	39.357868	Horzl_Fraction	0.1533825	0.7752558
S(2,0)InvDfMom	0.8701152	0.3182132	Vertl_RLNonUni	2462.4458	1628.2926
S(2,0)SumAverg	3.4981247	32.267192	Vertl_GLevNonU	1070.6008	241.75899
S(2,0)SumVarnc	10.937262	138.6576	Vertl_LngREmph	1037.5748	4.0425659
S(2,0)SumEntrp	0.5235671	1.5515467	Vertl_ShrtREmp	0.5405154	0.7261585
S(2,0)Entropy	0.6603714	2.3588202	Vertl_Fraction	0.123492	0.6170921
S(2,0)DifVarnc	0.8476755	9.4661335	GrMean	0.0925808	1.0391891
S(2,0)DifEntrp	0.3225191	0.9597001	GrVariance	0.1040477	0.9172676
S(0,2)AngScMom	0.5764231	0.0137103	GrSkewness	3.4520811	1.0684442
S(0,2)Contrast	0.555605	6.8610572	GrKurtosis	11.189759	2.0378655
S(0,2)Correlat	0.9098032	0.9078074	GrNonZeros	0.0799444	0.673072
S(0,2)SumOfSqs	3.0799598	37.210469	Teta1	0.8692311	0.9511519
S(0,2)InvDfMom	0.8957964	0.4760533	Teta2	-0.7450225	-0.9033004
S(0,2)SumAverg	3.5473045	31.587702	Teta3	0.7875992	0.8943808
S(0,2)SumVarnc	11.764234	141.98082	Teta4	0.0872967	0.0511515
S(0,2)SumEntrp	0.5196758	1.5377936	Sigma	0.1052682	0.0788778

Table 3.10: Report of Extracted Features from Sample Image-10

3.5.11 Report of Extracted Features from Sample Image-11:

Features	Normal Zone	Heated Zone	Features	Normal Zone	Heated Zone
Mean	7.6807131	89.121837	S(0,2)Entropy	0.6763515	2.2956646
Variance	190.67708	1422.5946	S(0,2)DifVarnc	0.627104	5.8512849
Skewness	1.9319192	1.2209815	S(0,2)DifEntrp	0.2711437	0.7724485
Kurtosis	2.2851092	0.4828984	Horzl_RLNonUni	3261.6155	2802.5847
S(2,0)AngScMom	0.5813821	0.0096513	Horzl_GLevNonU	689.05471	228.3721
S(2,0)Contrast	0.966907	19.859389	Horzl_LngREmph	867.98989	3.8253119
S(2,0)Correlat	0.9518026	0.8948306	Horzl_ShrtREmp	0.6201708	0.8168351
S(2,0)SumOfSqs	10.030699	94.41617	Horzl_Fraction	0.1307458	0.6818596
S(2,0)InvDfMom	0.8889074	0.3778435	Vertl_RLNonUni	2606.882	1769.0413
S(2,0)SumAverg	4.9093488	47.548843	Vertl_GLevNonU	642.39139	182.35084
S(2,0)SumVarnc	39.155887	357.80529	Vertl_LngREmph	1044.0048	5.5684803
S(2,0)SumEntrp	0.5659554	1.708009	Vertl_ShrtREmp	0.5679911	0.7161731
S(2,0)Entropy	0.6913558	2.472692	Vertl_Fraction	0.1215734	0.5644478
S(2,0)DifVarnc	0.8659856	11.03342	GrMean	0.1100629	1.0595139
S(2,0)DifEntrp	0.2927059	0.9640181	GrVariance	0.1332466	1.0772027
S(0,2)AngScMom	0.5839168	0.0131408	GrSkewness	3.4560648	0.890669
S(0,2)Contrast	0.7002861	9.1363247	GrKurtosis	12.281715	0.4444002
S(0,2)Correlat	0.9655967	0.9500683	GrNonZeros	0.0904033	0.635553
S(0,2)SumOfSqs	10.177602	91.488274	Teta1	0.8937481	0.9725909
S(0,2)InvDfMom	0.8976489	0.4981649	Teta2	-0.7581163	-0.9088795
S(0,2)SumAverg	4.9448272	46.956842	Teta3	0.7670922	0.8793968
S(0,2)SumVarnc	40.010122	356.81677	Teta4	0.0965742	0.0578831
S(0,2)SumEntrp	0.5641583	1.6911102	Sigma	0.0614218	0.0515075

Table 3.11: Report of Extracted Features from Sample Image-11

3.5.12 Report of Extracted Features from Sample Image-12:

Features	Normal Zone	Heated Zone	Features	Normal Zone	Heated Zone
Mean	6.9596143	95.753597	S(0,2)Entropy	0.6144033	2.3091242
Variance	166.53088	1067.5812	S(0,2)DifVarnc	0.673612	4.9244149
Skewness	2.0438615	0.687498	S(0,2)DifEntrp	0.2434692	0.7173786
Kurtosis	2.8138019	-0.5361996	Horzl_RLNonUni	3183.857	3092.1209
S(2,0)AngScMom	0.6232108	0.0056112	Horzl_GLevNonU	637.91467	247.76238
S(2,0)Contrast	1.2453413	12.877404	Horzl_LngREmph	1215.2911	3.924756
S(2,0)Correlat	0.9275363	0.9025165	Horzl_ShrtREmp	0.6467984	0.7693305
S(2,0)SumOfSqs	8.5928577	66.049152	Horzl_Fraction	0.121459	0.6457713
S(2,0)InvDfMom	0.900236	0.435019	Vertl_RLNonUni	2125.7642	2161.5456
S(2,0)SumAverg	4.5675582	50.475287	Vertl_GLevNonU	562.29293	190.79199
S(2,0)SumVarnc	33.12609	251.3192	Vertl_LngREmph	1158.7537	5.6755242
S(2,0)SumEntrp	0.5114508	1.7252491	Vertl_ShrtREmp	0.554357	0.6964814
S(2,0)Entropy	0.632928	2.449101	Vertl_Fraction	0.1064835	0.5523449
S(2,0)DifVarnc	1.1418186	7.8289762	GrMean	0.1060271	0.8252696
S(2,0)DifEntrp	0.2768576	0.8432978	GrVariance	0.1417492	0.9098331
S(0,2)AngScMom	0.6216074	0.0083484	GrSkewness	3.8797222	1.3800292
S(0,2)Contrast	0.7311904	7.451889	GrKurtosis	16.245724	2.88177
S(0,2)Correlat	0.9590556	0.9438584	GrNonZeros	0.0822987	0.5402161
S(0,2)SumOfSqs	8.9290668	66.366866	Teta1	0.897054	0.9121678
S(0,2)InvDfMom	0.9132223	0.5225033	Teta2	-0.7907296	-0.824904
S(0,2)SumAverg	4.6523019	49.638709	Teta3	0.8061137	0.8423949
S(0,2)SumVarnc	34.985077	258.01557	Teta4	0.0857865	0.0691876
S(0,2)SumEntrp	0.5154278	1.7212268	Sigma	0.0604906	0.0719972

Table 3.12: Report of Extracted Features from Sample Image-12

3.5.13 Report of Extracted Features from Sample Image-13:

Features	Normal Zone	Heated Zone	Features	Normal Zone	Heated Zone
Mean	6.1202944	90.438206	S(0,2)Entropy	0.677614	2.3643186
Variance	120.77977	1113.6565	S(0,2)DifVarnc	0.7201035	5.3532535
Skewness	2.2279505	0.7679525	S(0,2)DifEntrp	0.2832771	0.7798991
Kurtosis	4.0141	-0.3973622	Horzl_RLNonUni	3309.3379	2296.9422
S(2,0)AngScMom	0.5814522	0.0060527	Horzl_GLevNonU	774.67408	184.8624
S(2,0)Contrast	1.2516841	14.853912	Horzl_LngREmph	1079.8776	3.5518395
S(2,0)Correlat	0.8983457	0.8930068	Horzl_ShrtREmp	0.6227553	0.7693546
S(2,0)SumOfSqs	6.1565729	69.415236	Horzl_Fraction	0.1311602	0.6598361
S(2,0)InvDfMom	0.8866606	0.4237059	Vertl_RLNonUni	2856.4283	1950.0756
S(2,0)SumAverg	4.1951319	48.267737	Vertl_GLevNonU	774.34311	162.39803
S(2,0)SumVarnc	23.374607	262.80703	Vertl_LngREmph	949.18809	4.4640269
S(2,0)SumEntrp	0.5521005	1.7252574	Vertl_ShrtREmp	0.5871349	0.7386148
S(2,0)Entropy	0.683493	2.4586065	Vertl_Fraction	0.1259087	0.6091755
S(2,0)DifVarnc	1.1308339	9.105462	GrMean	0.1090349	0.897429
S(2,0)DifEntrp	0.3008117	0.8683999	GrVariance	0.1357349	0.9919417
S(0,2)AngScMom	0.5783755	0.0075174	GrSkewness	3.5362868	1.2086855
S(0,2)Contrast	0.8059602	8.89282	GrKurtosis	12.762123	1.5405897
S(0,2)Correlat	0.9360086	0.9354097	GrNonZeros	0.0879189	0.5666986
S(0,2)SumOfSqs	6.297411	68.840242	Teta1	0.8826916	0.9566183
S(0,2)InvDfMom	0.8919993	0.4655217	Teta2	-0.7788732	-0.8780213
S(0,2)SumAverg	4.2442744	47.623656	Teta3	0.813308	0.8704864
S(0,2)SumVarnc	24.383684	266.46815	Teta4	0.0822705	0.0496474
S(0,2)SumEntrp	0.5572917	1.717699	Sigma	0.0808086	0.0638056

Table 3.13: Report of Extracted Features from Sample Image-13

3.5.14 Report of Extracted Features from Sample Image-14:

Features	Normal Zone	Heated Zone	Features	Normal Zone	Heated Zone
Mean	2.6198359	68.875596	S(0,2)Entropy	0.3233556	2.2416725
Variance	31.004889	669.61572	S(0,2)DifVarnc	0.2477178	3.6156072
Skewness	4.0225867	0.966844	S(0,2)DifEntrp	0.1483967	0.7844793
Kurtosis	16.435999	1.0250347	Horzl_RLNonUni	1523.8424	1386.5365
S(2,0)AngScMom	0.7915959	0.0057899	Horzl_GLevNonU	539.36421	117.209
S(2,0)Contrast	0.4284988	18.034529	Horzl_LngREmph	3604.8158	2.2738268
S(2,0)Correlat	0.8518222	0.7871547	Horzl_ShrtREmp	0.6115644	0.8454042
S(2,0)SumOfSqs	1.4458941	42.365345	Horzl_Fraction	0.0598915	0.7684015
S(2,0)InvDfMom	0.9490856	0.300234	Vertl_RLNonUni	1164.7653	960.21475
S(2,0)SumAverg	2.6413536	37.550224	Vertl_GLevNonU	504.74132	97.147455
S(2,0)SumVarnc	5.3550775	151.42685	Vertl_LngREmph	3206.8553	4.2047981
S(2,0)SumEntrp	0.2758013	1.6263028	Vertl_ShrtREmp	0.5451815	0.7774472
S(2,0)Entropy	0.3330977	2.4115592	Vertl_Fraction	0.0566586	0.6357887
S(2,0)DifVarnc	0.4067845	8.1332062	GrMean	0.0383745	1.0636408
S(2,0)DifEntrp	0.1617778	0.9638754	GrVariance	0.0462158	0.7790259
S(0,2)AngScMom	0.7950804	0.0087993	GrSkewness	5.8220664	0.8186365
S(0,2)Contrast	0.2618384	7.2424493	GrKurtosis	34.900618	2.4585167
S(0,2)Correlat	0.9125784	0.9109016	GrNonZeros	0.0325741	0.7018114
S(0,2)SumOfSqs	1.4975617	40.642967	Teta1	0.1858168	1.0268694
S(0,2)InvDfMom	0.9535783	0.4320367	Teta2	1523.8424	1386.5365
S(0,2)SumAverg	2.6579941	36.664046	Teta3	539.36421	117.209
S(0,2)SumVarnc	5.7284085	155.32942	Teta4	3604.8158	2.2738268
S(0,2)SumEntrp	0.2734627	1.6141179	Sigma	0.6115644	0.8454042

Table 3.14: Report of Extracted Features from Sample Image-14

3.5.15 Report of Extracted Features from Sample Image-15:

Features	Normal Zone	Heated Zone	Features	Normal Zone	Heated Zone
Mean	3.5978388	77.753717	S(0,2)Entropy	0.3197175	1.9589376
Variance	65.460524	1406.324	S(0,2)DifVarnc	0.1334492	3.6134539
Skewness	3.1460696	0.7787104	S(0,2)DifEntrp	0.1046405	0.5833894
Kurtosis	8.7411438	-0.9834228	Horzl_RLNonUni	2440.3543	833.0489
S(2,0)AngScMom	0.7766084	0.0213567	Horzl_GLevNonU	547.36184	79.603912
S(2,0)Contrast	0.7410436	20.08912	Horzl_LngREmph	2832.9094	7.2885086
S(2,0)Correlat	0.8913918	0.8920837	Horzl_ShrtREmp	0.6903348	0.7407476
S(2,0)SumOfSqs	3.4115455	93.077345	Horzl_Fraction	0.0745448	0.5342913
S(2,0)InvDfMom	0.9345784	0.5380877	Vertl_RLNonUni	403.13676	360.12949
S(2,0)SumAverg	3.1380825	41.994213	Vertl_GLevNonU	256.94938	59.922306
S(2,0)SumVarnc	12.905138	352.22026	Vertl_LngREmph	5266.3279	14.597327
S(2,0)SumEntrp	0.3089073	1.6127149	Vertl_ShrtREmp	0.3729379	0.5605441
S(2,0)Entropy	0.373077	2.149613	Vertl_Fraction	0.0361138	0.3887626
S(2,0)DifVarnc	0.6946598	14.119469	GrMean	0.0505964	0.8032441
S(2,0)DifEntrp	0.1926912	0.847999	GrVariance	0.0580063	1.2087225
S(0,2)AngScMom	0.7922599	0.0277864	GrSkewness	4.954553	1.5150571
S(0,2)Contrast	0.138307	4.74868	GrKurtosis	25.386685	2.1560533
S(0,2)Correlat	0.9802017	0.9735947	GrNonZeros	0.0447203	0.4583501
S(0,2)SumOfSqs	3.4929022	89.919034	Teta1	0.7689301	0.769689
S(0,2)InvDfMom	0.9706638	0.6552532	Teta2	-0.738833	-0.6006511
S(0,2)SumAverg	3.1689867	40.835269	Teta3	0.9821257	0.7112807
S(0,2)SumVarnc	13.833302	354.92746	Teta4	-0.0132371	0.1270934
S(0,2)SumEntrp	0.2891315	1.5804952	Sigma	0.0536665	0.0808876

Table 3.15: Report of Extracted Features from Sample Image-15

3.5.16 Report of Extracted Features from Sample Image-16:

Features	Normal Zone	Heated Zone	Features	Normal Zone	Heated Zone
Mean	4.7165484	95.540941	S(0,2)Entropy	0.3934206	1.9114561
Variance	143.60923	1538.2703	S(0,2)DifVarnc	0.4013436	3.9523544
Skewness	3.5862533	1.7974479	S(0,2)DifEntrp	0.1491078	0.5924189
Kurtosis	12.266972	2.0855009	Horzl_RLNonUni	3780.5278	1174.309
S(2,0)AngScMom	0.771203	0.0258768	Horzl_GLevNonU	419.54732	185.74856
S(2,0)Contrast	1.8324136	24.723492	Horzl_LngREmph	2499.0996	4.8500411
S(2,0)Correlat	0.8656756	0.8859259	Horzl_ShrtREmp	0.7788568	0.7223628
S(2,0)SumOfSqs	6.8208524	108.36588	Horzl_Fraction	0.0917882	0.5832734
S(2,0)InvDfMom	0.9222448	0.5285763	Vertl_RLNonUni	1059.1993	554.14968
S(2,0)SumAverg	3.4951857	50.461629	Vertl_GLevNonU	253.72394	103.47641
S(2,0)SumVarnc	25.450996	408.74003	Vertl_LngREmph	3330.6518	12.111823
S(2,0)SumEntrp	0.3366615	1.5624001	Vertl_ShrtREmp	0.5354316	0.5836386
S(2,0)Entropy	0.4289149	2.1194665	Vertl_Fraction	0.0543149	0.4121459
S(2,0)DifVarnc	1.7163146	18.512972	GrMean	0.0931729	0.7078947
S(2,0)DifEntrp	0.2281542	0.825186	GrVariance	0.1423572	1.5204395
S(0,2)AngScMom	0.7712119	0.0377601	GrSkewness	4.5169066	2.2182747
S(0,2)Contrast	0.4184432	5.1645145	GrKurtosis	22.077305	5.0092364
S(0,2)Correlat	0.9721902	0.9744346	GrNonZeros	0.0661237	0.3636916
S(0,2)SumOfSqs	7.5232906	101.00604	Teta1	0.858411	0.7919433
S(0,2)InvDfMom	0.9550156	0.6451651	Teta2	-0.8253006	-0.605617
S(0,2)SumAverg	3.6229896	49.266271	Teta3	0.9645012	0.7022478
S(0,2)SumVarnc	29.674719	398.85963	Teta4	-0.0010671	0.1249513
S(0,2)SumEntrp	0.338612	1.5277167	Sigma	0.0509823	0.0771001

Table 3.16: Report of Extracted Features from Sample Image-16

3.5.17 Report of Extracted Features from Sample Image-17:

Features	Normal Zone	Heated Zone	Features	Normal Zone	Heated Zone
Mean	1.7047005	224.69421	S(0,2)Entropy	0.1053658	1.7934177
Variance	36.906858	1678.1869	S(0,2)DifVarnc	0.615706	22.594497
Skewness	12.349439	-1.205115	S(0,2)DifEntrp	0.0666584	0.9601232
Kurtosis	174.71354	0.1453434	Horzl_RLNonUni	669.89817	520.5441
S(2,0)AngScMom	0.9481733	0.1661078	Horzl_GLevNonU	149.6401	24.87517
S(2,0)Contrast	0.4513227	18.419054	Horzl_LngREmph	12585.243	31.396201
S(2,0)Correlat	0.8655765	0.8915659	Horzl_ShrtREmp	0.661607	0.8603083
S(2,0)SumOfSqs	1.6787343	84.932028	Horzl_Fraction	0.0211062	0.4703255
S(2,0)InvDfMom	0.9839936	0.5822136	Vertl_RLNonUni	778.15135	643.2314
S(2,0)SumAverg	2.2738276	114.84277	Vertl_GLevNonU	180.80269	29.98229
S(2,0)SumVarnc	6.2636147	321.30906	Vertl_LngREmph	8487.8021	15.628099
S(2,0)SumEntrp	0.089197	1.3115284	Vertl_ShrtREmp	0.6672773	0.8867616
S(2,0)Entropy	0.1068313	1.7731062	Vertl_Fraction	0.0238162	0.5405233
S(2,0)DifVarnc	0.4461826	13.218466	GrMean	0.0258083	1.1447013
S(2,0)DifEntrp	0.0628587	0.8200174	GrVariance	0.063469	2.116446
S(0,2)AngScMom	0.948614	0.1557584	GrSkewness	12.220819	0.9378355
S(0,2)Contrast	0.6228138	35.486671	GrKurtosis	170.66703	-0.3985627
S(0,2)Correlat	0.7945398	0.7699253	GrNonZeros	0.0139837	0.4607911
S(0,2)SumOfSqs	1.5156551	77.119883	Teta1	0.9652516	0.9934341
S(0,2)InvDfMom	0.9828988	0.5024836	Teta2	-0.8805978	-0.9111542
S(0,2)SumAverg	2.2582629	115.8257	Teta3	0.890202	0.816713
S(0,2)SumVarnc	5.4398068	272.99286	Teta4	0.02381	0.0989753
S(0,2)SumEntrp	0.0882735	1.3038547	Sigma	0.0628795	0.0479072

Table 3.17: Report of Extracted Features from Sample Image-17

3.5.18 Report of Extracted Features from Sample Image-18:

Features	Normal Zone	Heated Zone	Features	Normal Zone	Heated Zone
Mean	4.2880579	74.943557	S(0,2)Entropy	0.5107103	2.0522624
Variance	68.566432	432.59923	S(0,2)DifVarnc	0.3055164	1.7484454
Skewness	2.8503318	0.9011907	S(0,2)DifEntrp	0.1926455	0.6250533
Kurtosis	7.7962244	0.3923598	Horzl_RLNonUni	1484.5385	1873.2717
S(2,0)AngScMom	0.6578804	0.0123758	Horzl_GLevNonU	556.44867	262.76442
S(2,0)Contrast	0.3692659	3.358375	Horzl_LngREmph	2039.253	5.8775328
S(2,0)Correlat	0.9452561	0.9356196	Horzl_ShrtREmp	0.5325199	0.6695374
S(2,0)SumOfSqs	3.3726683	26.082276	Horzl_Fraction	0.0807506	0.5369441
S(2,0)InvDfMom	0.9289829	0.5200932	Vertl_RLNonUni	1264.8741	1523.1591
S(2,0)SumAverg	3.4117708	38.980125	Vertl_GLevNonU	531.16084	227.2848
S(2,0)SumVarnc	13.121407	100.97073	Vertl_LngREmph	1767.7616	7.8536705
S(2,0)SumEntrp	0.4430627	1.5549032	Vertl_ShrtREmp	0.4966697	0.6312838
S(2,0)Entropy	0.5204525	2.0900763	Vertl_Fraction	0.0775011	0.4858063
S(2,0)DifVarnc	0.3383016	1.637359	GrMean	0.0588117	0.5272282
S(2,0)DifEntrp	0.2048214	0.6467969	GrVariance	0.069156	0.4260509
S(0,2)AngScMom	0.6619691	0.014605	GrSkewness	4.535985	0.7721487
S(0,2)Contrast	0.3311044	3.150087	GrKurtosis	20.426296	-0.4059992
S(0,2)Correlat	0.9516811	0.9400388	GrNonZeros	0.0498982	0.425016
S(0,2)SumOfSqs	3.4262377	26.26771	Teta1	0.8648332	0.7984617
S(0,2)InvDfMom	0.9347619	0.5694454	Teta2	-0.6440156	-0.5787645
S(0,2)SumAverg	3.4208547	38.887217	Teta3	0.6756726	0.7775203
S(0,2)SumVarnc	13.373846	101.92075	Teta4	0.0999288	0.0128971
S(0,2)SumEntrp	0.439346	1.556683	Sigma	0.0780147	0.0765947

Table 1: Report of Extracted Features from Sample Image-18

3.5.19 Report of Extracted Features from Sample Image-19:

Features	Normal Zone	Heated Zone	Features	Normal Zone	Heated Zone
Mean	6.3712832	131.29675	S(0,2)Entropy	0.4696342	2.1792008
Variance	240.95993	771.95877	S(0,2)DifVarnc	1.2499794	3.1946127
Skewness	3.064767	0.0022298	S(0,2)DifEntrp	0.217902	0.6992382
Kurtosis	8.565962	-0.0704733	Horzl_RLNonUni	2726.4434	3301.5811
S(2,0)AngScMom	0.7437534	0.0182575	Horzl_GLevNonU	299.00976	330.60451
S(2,0)Contrast	2.3330215	7.0440781	Horzl_LngREmph	1750.7499	8.0864326
S(2,0)Correlat	0.9001679	0.9199757	Horzl_ShrtREmp	0.7273016	0.6800623
S(2,0)SumOfSqs	11.684726	44.012104	Horzl_Fraction	0.0908166	0.5030967
S(2,0)InvDfMom	0.9216807	0.5544197	Vertl_RLNonUni	2188.3479	3283.9138
S(2,0)SumAverg	4.2194747	67.5984	Vertl_GLevNonU	284.74747	340.84196
S(2,0)SumVarnc	44.405884	169.00434	Vertl_LngREmph	1866.8227	7.5075164
S(2,0)SumEntrp	0.3852118	1.6506348	Vertl_ShrtREmp	0.6719378	0.6751592
S(2,0)Entropy	0.4831626	2.1624521	Vertl_Fraction	0.0858155	0.507598
S(2,0)DifVarnc	2.2055148	4.7243245	GrMean	0.1138175	0.6133214
S(2,0)DifEntrp	0.2364274	0.7181322	GrVariance	0.2150491	0.6460701
S(0,2)AngScMom	0.7459173	0.0165187	GrSkewness	4.8427841	1.4107646
S(0,2)Contrast	1.3217329	5.2713373	GrKurtosis	26.331936	3.239746
S(0,2)Correlat	0.9447293	0.9406498	GrNonZeros	0.0701615	0.4342885
S(0,2)SumOfSqs	11.956911	44.408723	Teta1	0.9277813	0.9410713
S(0,2)InvDfMom	0.9278328	0.5496011	Teta2	-0.7947145	-0.8231414
S(0,2)SumAverg	4.2660975	67.404254	Teta3	0.736977	0.7920178
S(0,2)SumVarnc	46.505912	172.36356	Teta4	0.1293455	0.0925133
S(0,2)SumEntrp	0.3830812	1.6545921	Sigma	0.0617044	0.0568085

Table 3.19: Report of Extracted Features from Sample Image-19

3.5.20 Report of Extracted Features from Sample Image-20:

Features	Normal Zone	Heated Zone	Features	Normal Zone	Heated Zone
Mean	8.4511909	111.23972	S(0,2)Entropy	1.0821951	2.3180527
Variance	77.702129	837.40414	S(0,2)DifVarnc	0.5922439	6.0572541
Skewness	1.4519132	-0.1173713	S(0,2)DifEntrp	0.3407399	0.7388119
Kurtosis	2.4743304	-0.4743995	Horzl_RLNonUni	1895.5685	2628.1155
S(2,0)AngScMom	0.2115851	0.0052367	Horzl_GLevNonU	1667.4082	178.31389
S(2,0)Contrast	0.6668788	11.755458	Horzl_LngREmph	241.59747	3.1804727
S(2,0)Correlat	0.92221	0.8800724	Horzl_ShrtREmp	0.367523	0.7904707
S(2,0)SumOfSqs	4.2864056	49.010623	Horzl_Fraction	0.17176	0.6859091
S(2,0)InvDfMom	0.8502076	0.3761831	Vertl_RLNonUni	2215.0095	2008.5944
S(2,0)SumAverg	5.2150079	57.235276	Vertl_GLevNonU	1800.3423	152.07155
S(2,0)SumVarnc	16.478744	184.28704	Vertl_LngREmph	155.1663	4.9663717
S(2,0)SumEntrp	0.923496	1.7226094	Vertl_ShrtREmp	0.3917372	0.7408339
S(2,0)Entropy	1.070147	2.4884782	Vertl_Fraction	0.1836037	0.5997877
S(2,0)DifVarnc	0.5472369	5.9605756	GrMean	0.1021592	0.8663352
S(2,0)DifEntrp	0.3229073	0.8673222	GrVariance	0.1189677	0.8139608
S(0,2)AngScMom	0.2101316	0.0092931	GrSkewness	3.4890848	1.154445
S(0,2)Contrast	0.7326911	8.9714564	GrKurtosis	12.653471	2.133955
S(0,2)Correlat	0.912087	0.9049642	GrNonZeros	0.0863669	0.5919854
S(0,2)SumOfSqs	4.1671346	47.200406	Teta1	0.8731143	0.9333249
S(0,2)InvDfMom	0.8398825	0.5282741	Teta2	-0.7339881	-0.7502257
S(0,2)SumAverg	5.1799493	57.770354	Teta3	0.7985153	0.6975361
S(0,2)SumVarnc	15.935847	179.83017	Teta4	0.0657455	0.1174576
S(0,2)SumEntrp	0.9227748	1.719381	Sigma	0.1081011	0.0894822

Table 3.20: Report of Extracted Features from Sample Image-20

3.5.21 Report of Extracted Features from Sample Image-21:

Features	Normal Zone	Heated Zone	Features	Normal Zone	Heated Zone
Mean	3.5436219	69.618084	S(0,2)Entropy	0.4167289	2.1426718
Variance	54.88855	842.48353	S(0,2)DifVarnc	0.3240749	4.4291803
Skewness	3.2472523	1.4119239	S(0,2)DifEntrp	0.1744173	0.7229653
Kurtosis	10.074998	1.0873126	Horzl_RLNonUni	2020.4752	1018.9382
S(2,0)AngScMom	0.726556	0.0151503	Horzl_GLevNonU	613.85614	123.48
S(2,0)Contrast	0.5204855	12.580456	Horzl_LngREmph	2358.238	4.8075949
S(2,0)Correlat	0.9045635	0.8880822	Horzl_ShrtREmp	0.6034221	0.7463825
S(2,0)SumOfSqs	2.7268692	56.203977	Horzl_Fraction	0.0817012	0.5964965
S(2,0)InvDfMom	0.9282074	0.4867212	Vertl_RLNonUni	1303.0475	951.83802
S(2,0)SumAverg	3.0698045	36.932666	Vertl_GLevNonU	503.6008	124.85999
S(2,0)SumVarnc	10.386991	212.23545	Vertl_LngREmph	2578.2509	4.9693408
S(2,0)SumEntrp	0.3624633	1.5901726	Vertl_ShrtREmp	0.5224972	0.7252714
S(2,0)Entropy	0.4404586	2.2131394	Vertl_Fraction	0.0680701	0.5861036
S(2,0)DifVarnc	0.4819657	8.0721655	GrMean	0.054378	0.8504033
S(2,0)DifEntrp	0.2090152	0.8214853	GrVariance	0.0650856	0.898227
S(0,2)AngScMom	0.7360686	0.0152267	GrSkewness	4.8256629	1.1376489
S(0,2)Contrast	0.345364	7.0288038	GrKurtosis	23.527785	1.2071698
S(0,2)Correlat	0.9370437	0.9365869	GrNonZeros	0.0458758	0.5544518
S(0,2)SumOfSqs	2.7428871	55.420759	Teta1	0.8778607	0.9806135
S(0,2)InvDfMom	0.9435821	0.5036049	Teta2	-0.7809832	-0.9592626
S(0,2)SumAverg	3.0747232	36.935276	Teta3	0.8691122	0.9449649
S(0,2)SumVarnc	10.626185	214.65423	Teta4	0.0328784	0.0349756
S(0,2)SumEntrp	0.3532615	1.585163	Sigma	0.0776911	0.0503177

Table 3.21: Report of Extracted Features from Sample Image-21

3.5.22 Report of Extracted Features from Sample Image-22:

Features	Normal Zone	Heated Zone	Features	Normal Zone	Heated Zone
Mean	11.1702	141.68412	S(0,2)Entropy	0.7655252	2.1775277
Variance	446.56944	582.23594	S(0,2)DifVarnc	1.1606864	2.8732519
Skewness	2.0007461	-0.4873049	S(0,2)DifEntrp	0.3348771	0.6773093
Kurtosis	2.7101538	-0.449484	Horzl_RLNonUni	2754.7415	3607.654
S(2,0)AngScMom	0.5688933	0.0135923	Horzl_GLevNonU	330.07644	611.51699
S(2,0)Contrast	1.9287706	2.754823	Horzl_LngREmph	1251.1344	10.165906
S(2,0)Correlat	0.9605323	0.9604117	Horzl_ShrtREmp	0.6695501	0.5320227
S(2,0)SumOfSqs	24.434817	34.793406	Horzl_Fraction	0.1448783	0.4164183
S(2,0)InvDfMom	0.8731867	0.6332854	Vertl_RLNonUni	3559.959	6855.1196
S(2,0)SumAverg	6.6047634	71.983617	Vertl_GLevNonU	359.22449	738.93535
S(2,0)SumVarnc	95.810497	136.4188	Vertl_LngREmph	505.86248	6.369125
S(2,0)SumEntrp	0.6336752	1.646094	Vertl_ShrtREmp	0.7189182	0.6769209
S(2,0)Entropy	0.7846183	2.0557674	Vertl_Fraction	0.1619462	0.5291458
S(2,0)DifVarnc	1.738474	1.8414625	GrMean	0.1617963	0.5119999
S(2,0)DifEntrp	0.332877	0.5426467	GrVariance	0.2189718	0.4592076
S(0,2)AngScMom	0.58114	0.0114315	GrSkewness	3.2639004	1.1769145
S(0,2)Contrast	1.3322404	4.7490072	GrKurtosis	12.266036	1.3865751
S(0,2)Correlat	0.9704239	0.9286942	GrNonZeros	0.1225862	0.4100502
S(0,2)SumOfSqs	22.522261	33.300278	Teta1	0.9178941	0.9640893
S(0,2)InvDfMom	0.8652967	0.5502263	Teta2	-0.8039011	-0.8093893
S(0,2)SumAverg	6.3730148	72.297729	Teta3	0.7835181	0.7631273
S(0,2)SumVarnc	88.756805	128.4521	Teta4	0.106624	0.0810396
S(0,2)SumEntrp	0.6146729	1.6394458	Sigma	0.0447963	0.0613316

Table 3.22: Report of Extracted Features from Sample Image-22

3.5.23 Report of Extracted Features from Sample Image-23:

Features	Normal Zone	Heated Zone	Features	Normal Zone	Heated Zone
Mean	12.028833	144.41223	S(0,2)Entropy	0.8091229	2.3421937
Variance	491.98559	966.71814	S(0,2)DifVarnc	0.967268	3.4884323
Skewness	1.9157295	-0.213945	S(0,2)DifEntrp	0.3353225	0.7456412
Kurtosis	2.3271087	-1.2374396	Horzl_RLNonUni	3365.8549	2481.5377
S(2,0)AngScMom	0.5449303	0.0117354	Horzl_GLevNonU	382.01899	351.75702
S(2,0)Contrast	1.3836416	2.2106151	Horzl_LngREmph	1153.4804	11.148404
S(2,0)Correlat	0.9747401	0.9810412	Horzl_ShrtREmp	0.6721412	0.5063985
S(2,0)SumOfSqs	27.388061	58.300419	Horzl_Fraction	0.152658	0.3974126
S(2,0)InvDfMom	0.867476	0.6479216	Vertl_RLNonUni	3785.2898	8207.2565
S(2,0)SumAverg	7.0565896	73.411238	Vertl_GLevNonU	399.19551	570.99128
S(2,0)SumVarnc	108.1686	230.99106	Vertl_LngREmph	535.44464	3.9582673
S(2,0)SumEntrp	0.6708767	1.7176896	Vertl_ShrtREmp	0.688338	0.7647365
S(2,0)Entropy	0.8252287	2.0989656	Vertl_Fraction	0.1634577	0.6403383
S(2,0)DifVarnc	1.2163156	1.433536	GrMean	0.1541609	0.5849243
S(2,0)DifEntrp	0.3357073	0.5198813	GrVariance	0.1888097	0.4850627
S(0,2)AngScMom	0.5525695	0.0068838	GrSkewness	2.9351274	0.9884884
S(0,2)Contrast	1.1208118	6.458234	GrKurtosis	8.9523743	0.9273262
S(0,2)Correlat	0.9784843	0.9436014	GrNonZeros	0.122713	0.4668843
S(0,2)SumOfSqs	26.046373	57.255287	Teta1	0.9094571	0.9748553
S(0,2)InvDfMom	0.8626519	0.4615157	Teta2	-0.7723671	-0.7674606
S(0,2)SumAverg	6.8977271	73.748124	Teta3	0.7408357	0.7003799
S(0,2)SumVarnc	103.06468	222.56292	Teta4	0.126351	0.0921872
S(0,2)SumEntrp	0.6582571	1.7151636	Sigma	0.0391267	0.0478165

Table 3.23: Report of Extracted Features from Sample Image-23

3.5.24 Report of Extracted Features from Sample Image-24:

Features	Normal Zone	Heated Zone	Features	Normal Zone	Heated Zone
Mean	4.2253291	77.726873	S(0,2)Entropy	0.4549429	2.2270913
Variance	82.09216	526.81147	S(0,2)DifVarnc	0.5942703	3.090814
Skewness	2.9721081	0.5354705	S(0,2)DifEntrp	0.2160249	0.7282169
Kurtosis	7.8998811	-0.545546	Horzl_RLNonUni	3828.0979	4076.3634
S(2,0)AngScMom	0.728708	0.0052687	Horzl_GLevNonU	655.07199	345.58254
S(2,0)Contrast	1.2041652	13.86759	Horzl_LngREmph	1409.6183	2.6092663
S(2,0)Correlat	0.8372125	0.7845366	Horzl_ShrtREmp	0.7427097	0.8298304
S(2,0)SumOfSqs	3.6985809	32.180847	Horzl_Fraction	0.1101038	0.7378369
S(2,0)InvDfMom	0.9090453	0.3403447	Vertl_RLNonUni	2378.0995	2407.2166
S(2,0)SumAverg	3.2413741	41.268853	Vertl_GLevNonU	554.33986	270.72019
S(2,0)SumVarnc	13.590158	114.8558	Vertl_LngREmph	1667.3943	4.8634738
S(2,0)SumEntrp	0.3681117	1.6038803	Vertl_ShrtREmp	0.6417378	0.7192239
S(2,0)Entropy	0.4678251	2.4134516	Vertl_Fraction	0.0920573	0.5860021
S(2,0)DifVarnc	1.1052884	6.6299781	GrMean	0.0900659	0.9425438
S(2,0)DifEntrp	0.2531545	0.9118532	GrVariance	0.1150458	0.6640255
S(0,2)AngScMom	0.7284766	0.0087065	GrSkewness	3.9220007	0.583016
S(0,2)Contrast	0.6408595	5.6950158	GrKurtosis	15.417465	0.3040634
S(0,2)Correlat	0.9200599	0.9109742	GrNonZeros	0.0715633	0.6646606
S(0,2)SumOfSqs	4.0083709	31.985179	Teta1	0.9129052	0.9468042
S(0,2)InvDfMom	0.9258621	0.4851489	Teta2	-0.8377276	-0.9052427
S(0,2)SumAverg	3.3339999	40.697161	Teta3	0.8831991	0.935367
S(0,2)SumVarnc	15.392624	122.2457	Teta4	0.0379606	0.027718
S(0,2)SumEntrp	0.3715094	1.6051547	Sigma	0.079902	0.0726631

Table 3.24: Report of Extracted Features from Sample Image-24

Chapter 4

Establishing the Best Feature Extraction Method and Effective Prediction Analysis using Machine Learning

4.1 Introduction

The contactless estimation of temperature dispersions with thermographic cameras permits effective and dependable observation and control of temperature-critical forms or programmed quality control within the automation industry. During the specialized execution of custom-fitted computerization arrangements, people got benefitted by using their own method along with the thermography to determine any faults or to maintain the machine in a unique and safer way. In this thesis, Machine learning (ML) is used which is a method of data analysis. It is a branch of AI basically with the idea of learning from analyzing data sets. After enhancing the images, using moments binary thresholding technique, several feature extraction methods have been used to extract some features from the collected thermal images. These features are used as data sets in ML. ML takes these data to identify the patterns and predicts without any human interaction. In this research, features play a vital role as input as they act like an individual variable and while making the results or the predictions features are being used. Although new features can be extracted using feature engineering methods, five feature extraction techniques have been used here that were previously invented by researchers. In Machine Learning, data sets are used at large scale mostly. The only drawback in this case is having only 48 sets of data (faulty and normal) from 24 collected thermal images and the system had to be trained using those. A discussion has been given later in this thesis book about the prediction of the study after training ML using those date sets.

4.2 Analyzing Data Set using Supervision Learning

ML is part of Artificial Intelligence, that gives frameworks the capacity to consequently learn and make strides from experience without being expressly programmed. The method of learning starts with perceptions or information (i.e., cases, experience or instruction) to hunt for patterns in the information and make better choices in the future based examples that it is offered. The aim is to permit the computers to learn naturally without human intercession or help and adjust activities appropriately. ML has four types of learning [13]:

- Supervised

- Unsupervised

- Semi-Supervised

- Reinforced

Supervised ML algorithms use the data that has been learned in the past. That past experience is used to predict any related future event. First, the known data set is analyzed and then the learning algorithm makes a function that predicts a certain output value. The data set which is used to teach the program is called the training data set. Through the training data set, the system can come up with a new target for any new inputs. Basically, in supervised learning the data set is labelled. The input and output, both data sets are labelled in this case.

As supervised learning is used here, for that reason, the input is labelled in two parts. One is for faulty region another one is for normal region. Features are got from both faulty and normal region which was mentioned in the data set. Since, ML can learn itself and it cannot take any string input, therefore binary numbers are used to label the inputs that are put in the system.

Teta1	Teta2	Teta3	Teta4	Sigma	Label
0.864029	-0.73292	0.762393	0.101884	0.09308	1
0.921813	-0.83499	0.837757	0.071406	0.083582	0
0.881637	-0.7227	0.723813	0.11235	0.11189	1
0.903439	-0.75674	0.764343	0.091318	0.110737	0
0.884059	-0.80302	0.879923	0.030497	0.11474	1
0.919513	-0.84223	0.891158	0.034019	0.096352	0
0.886011	-0.77435	0.799148	0.088003	0.072736	1

Table 4.1: A Sample of Auto Regression Labelled Data Set

In above table, a data set have been shown which was found using Auto Regression feature extraction method. Similarly, data set for Histogram Method has been labelled and so are for Gradient, GLCM and GLRLM. This data sets were mentioned in chapter 3 as well. Those data sets were used as input in the supervised learning algorithm.

The supervising task that are used is called classification. Here, the output is defined with labeling which is either 0 or 1. The objective is to predict these discreet values belonging to a specific lesson and evaluate them within the premise of precision.

4.2.1 Splitting Data into Testing Training Sets

To build a model in ML, a training data is utilized, that can offer assistance machines to examine or recognize a certain kind of information accessible in different formats like texts, numbers, and pictures or recordings to predict as per the learned patterns. Training data set is labelled and is also used to teach the ML algorithms about that data set for future predictions. Basically, it is sub-set to train models. In case of splitting the data set in testing training method, the data set should be large enough to produce meaningful statistical results and should be a part of the data set as well which means in case of testing any data cannot be used that is out of character. In this thesis study, the test set has to predict two conditions: 0 and 1, in other words faulty and normal respectively. A model was also created that generalizes with a new data. The test set serves its role as the new data. To train the model accurately and to get accurate testing results, machine is fed with curated dataset that allowed it to learn by

recognizing different characteristics. The accuracy of the model also depends on the quality and quantity of the training datasets. The more the training data, the more the accuracy [14]. As it is known that features were mainly fed to the machine as dataset for training. Having 48 data sets, from which 33 data have been used for training and rest 15 for testing, in other words 70% are taken as training data and 30% are taken as testing. Testing dataset cannot used to train the model, otherwise the accuracy will be really high as in 99% which indicates that there might be a problem in the using dataset that is used to feed the system. In this thesis study, the data have been split into x_train, x_test, y_train, y_test. Now, x_train and x_test consist the features that were extracted from the images. y_train, y_test are the labelled binary segments of faulty and normal part. As five features extraction methods have been used, there are five of each x and y testing-training sets.

x_train:

0.864029	-0.73292	0.762393	0.101884	0.09308
0.921813	-0.83499	0.837757	0.071406	0.083582
0.881637	-0.7227	0.723813	0.11235	0.11189
0.903439	-0.75674	0.764343	0.091318	0.110737
0.884059	-0.80302	0.879923	0.030497	0.11474
0.919513	-0.84223	0.891158	0.034019	0.096352
0.886011	-0.77435	0.799148	0.088003	0.072736
0.953328	-0.90685	0.910944	0.042892	0.047665

Table 4.2: A Sample of x_train Pseudo–Data Set (Auto Regression)

x_test:

0.936757	-0.85954	0.861551	0.062898	0.045072
0.899745	-0.68328	0.682144	0.100753	0.063995
0.908988	-0.83519	0.852598	0.076218	0.060273

Table 4.3: A Sample of x_test Pseudo–Data Set (Auto Regression)

y_train:

1	1	0	0	0	1	1	1	0	0
0	0	0	1	1	0	0	0	1	0

Table 4.4: A Sample of y_train Pseudo-Data Set (Auto Regression)

y_test:

1	1	0	0	0	0	1	1	1	1

Table 4.5: A Sample of y_test Pseudo-Data Set (Auto Regression)

4.2.2 Applying Random Forest as Classifier for Prediction Analysis

Random Forest is a supervised learning classifier which can give binary and continuous results. In this case, binary results as inputs will be needed that are labelled in binary form. Though it can give both classify and regression output, it is mainly used for classification. It is a modern version of decision tree. Forest is basically made out of trees, just like this the random forest classifier is made out of several decision trees. The random forest algorithm creates decision trees on the data sets and gets a result from each of the data and determines the best results by voting. Instead making nodes of all the features, it takes only the important features into consideration and makes nodes. It is really easy to measure importance of the features of the data set by using this algorithm on each prediction. Each of the nodes represents a test, each branch represents an outcome and the node that does not have any child is a leaf. By determining which feature is useful, the less important features can be eliminated to prevent over fitting of the data, also as they do not contribute enough to make a prediction it is unnecessary to use those features as well. Random Forest is very flexible and has a high accuracy rate even if a large scale of data is missing [15]. The flow chart of Random Forest algorithm is-

128
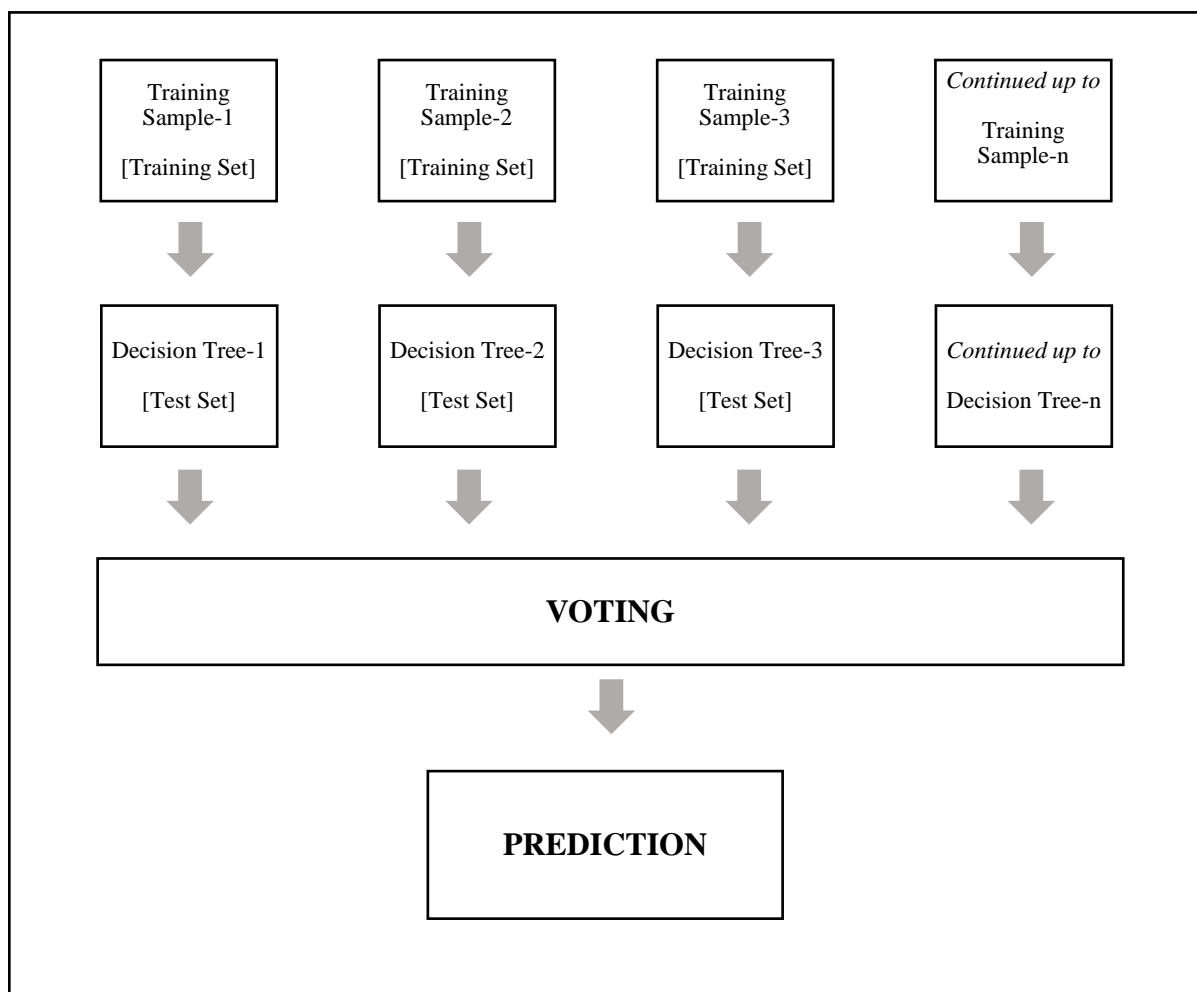
Figure 4.1: Flow Chart of Random Forest Classifier

The labelled data set have been used as input of Random Forest classifier. First, the data set has been split into training and testing data set, 70% was for training and 30% data was left for testing. After that, the training data had been fitted with the data set into the random classifier and made a prediction. The prediction was classified, in other words, it was in binary form. As five types of feature extraction methods have been used, there are 5 data sets containing 48 data of all features. The data were inputted one by one into ML for training then tested the data with the testing data set. Random Forest can give different results in different time because the dataset shuffles, so, if the data is not fixed in the system, there may come different results. Finally, after using random state and fixing the first 20 data, there can be the same results also with higher accuracy rate of prediction.

```
import pandas as pd
import numpy as np
import matplotlib.pyplot as plt
from sklearn.ensemble import RandomForestClassifier
from sklearn.model_selection import train_test_split
from sklearn import metrics
from sklearn.metrics import confusion_matrix
from sklearn.metrics import plot_confusion_matrix
from sklearn.datasets import make_classification
red = pd.read_csv('RLM (2).csv')
print(red.head())
x= red.drop(['Label'], axis=1).values
y= red['Label'].values
x_train, x_test, y_train, y_test = train_test_split(x, y, test_size =0.3, random_state=20)
clf=RandomForestClassifier(n_estimators=100)
clf.fit(x_train,y_train)
y_pred=clf.predict(x_test)
print("Prediction:",metrics.accuracy_score(y_test, y_pred))
```

Figure 4.2: Pseudo Code of Random Forest Classifier

After fitting all the testing, training data of all the five data sets in Random Forest classifier, y_predict can be got for every data set which is basically the output. The output is in binary form and the prediction rate of most of the feature extraction method is above 90%.

y_predict:

1	1	0	0	0	1	1	0	0	1

Table 4.6: A Sample of y_predict Pseudo-Data Set (Auto Regression)

4.2.3 Prediction Rate of Different Feature Extraction Method

After applying Random Forest on testing data, following prediction rates have been found.

Feature Extraction Method	Prediction Rate %
GLCM	94.33
GLRLM	93.33
Auto Regression	60.00
Histogram	93.33
Gradient	92.5

Table 4.7: Prediction Rate of Feature Extraction Methods after Applying Random Forest

4.3 Performance Analysis of ML using Confusion Matrix

Confusion matrix is a NxN matrix which is used in case of performance analysis on classified model. Here N is the number of the target classes. This matrix compares the actual value with the predicted value and gives the idea of how well the ML performed. There are two target values- 1. Positive and 2. Negative. The column of the confusion matrix represents the actual values and the row represents the predicted value by the ML. Basically a confusion matrix has four values-

- **TR (True Positive):** The predicted and the actual values are the same in this case. The actual value is positive and the predicted value is positive as well.

- **TN (True Negative):** The predicted and the actual values are the same in this case. The actual value is negative and the predicted value is negative as well.

- **FP (False Positive):** The predicted value was falsely indicated by ML. In this case the actual value was negative but ML predicted the value as positive. This is also known as Type-1 error.

- **FN (False Negative):** This predicted value was also falsely indicated by ML. In this case the actual value was positive but ML predicted the value as negative. This is also known as Type-2 error. [16]

The y_predict value and y_test value has been fitted in the confusion matrix and used it to determine the accuracy of the predicted value and also plotted the confusion matrix. True Negative (TN), True Positive (TP), False Negative (FN), False Positive (FP) values of the matrix for GLCM, GLRLM, Auto Regression, Histogram and Gradient were also established.

```python
from sklearn.model_selection import train_test_split
from sklearn import metrics
from sklearn.metrics import confusion_matrix
from sklearn.metrics import plot_confusion_matrix
from sklearn.datasets import make_classification
red = pd.read_csv('RLM (2).csv')
print(red.head())
x= red.drop(['Label'], axis=1).values
y= red['Label'].values
x_train, x_test, y_train, y_test = train_test_split(x, y, test_size =0.3, random_state=20)
clf=RandomForestClassifier(n_estimators=100)
clf.fit(x_train,y_train)
y_pred=clf.predict(x_test)
print("Prediction:",metrics.accuracy_score(y_test, y_pred))
plot_confusion_matrix(clf, x_test, y_test)
plt.show()
tn, fp, fn, tp = confusion_matrix(y_test, y_pred).ravel()
print(tn, fp, fn, tp)
pre= (tp/(tp+fp))
acc= ((tn+tp)/(tp+fp+fn+tn))
err= ((fp+fn)/(tp+fp+fn+tn))
tpr= tp/(tp+fn)
fpr= fp/(tn+fp)
```

Figure 4.3: Pseudo Code for Confusion Matrix

(a) GLCM **(b) GLRLM** **(c) Auto Regression**

(d) Gradient **(e) Histogram**
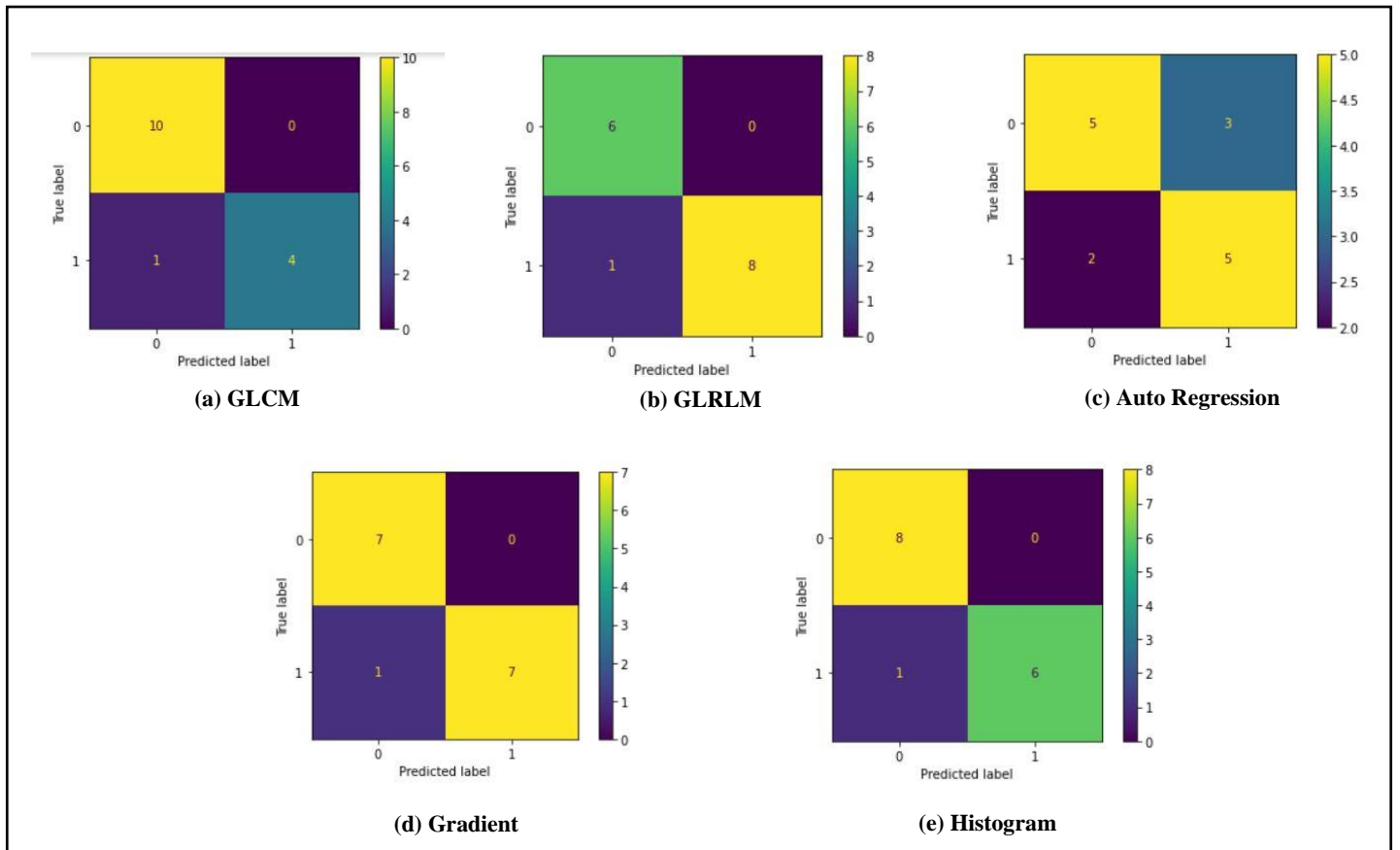
Figure 4.4: Confusion Matrix of Different Texture Feature Extraction Methods

Feature Extracting Method	TN	FP	FN	TP
GLCM	10	0	1	4
GLRLM	6	0	1	8
Auto Regression	5	3	2	5
Gradient	7	0	1	7
Histogram	8	0	1	6

Table 4.8: TN, FP, FN, TP Value for Different Feature Extraction Methods' Prediction

Mainly, a confusion matrix is established to determine the accuracy of the system whether the system has correctly predicted the values or what the rate of the accuracy is or how many it has predicted correctly and how many was predicted falsely. There are some definite equations that have been used to determine the Accuracy, Error Rate, TPR, FPR and Precision.

133

$$Accuracy = \frac{TP + TN}{TP + TN + FP + FN}$$

$$Precision = \frac{TP}{TP + FP}$$

$$Error = \frac{FP + FN}{TP + TN + FP + FN}$$

$$TPR = \frac{TP}{TP + FN}$$

$$FPR = \frac{FP}{TN + FP}$$

Using the above-mentioned equations, the accuracy, precision, error, TPR and FPR of the prediction are determined that is found by using Random Forest classifier.

Feature Extracting Method	Precision	Accuracy	Error	TPR	FPR
GLCM	1	94.33	5.9	80.0	0
GLRLM	1	93.33	6.6	88.8	0
Auto Regression	0.625	60.00	33.33	71.42	37.5
Gradient	1	93.33	6.66	85.714	0
Histogram	1	92.50	6.710	87.50	0

Table 4.9: Precision, Accuracy, Error, TPR, FPR Value for Different Feature Extraction Methods' Prediction

4.4 Summary

In this chapter, it is discussed about the effective prediction using Random Forest algorithm. The Random Forest flow chart that uses decision tree for all the samples is also included here. Prediction analysis is determined by applying testing training on the dataset which is shown in the above table. The testing training splitting samples are also added in previous 3 tables. The confusion matrix plot is given for each feature extraction technique. Also the performance parameters like TP, TN, FP, FN values were also determined and showed in this chapter. A pseudo code was added for cross checking for random forest and confusion matrix. All the

prediction and performance analysis were done on the five-feature extraction methods. If the collected dataset is enough, then using above mentioned method it is possible to predict the faulty part of the electrical equipment and the accuracy rate will be between 60% to 94% and error rate to be 5.9% to 33.33%. In short, if having enough information about the data set, in other words, the best features and efficient data, then the faulty part of the electrical component can approximately be determined and can built an ML with high accuracy and important features.

Chapter 5

Results and Discussion

5.1 Performance Result

After getting the picture in RGB form and enhancing it, applying the moments binary thresholding technique then extracting the features using different features extraction methods, the features of the faulty and normal part of the images are gathered. Those features have been used as input in ML and Random Forest as classifier. To find out the accuracy rate of those prediction, a performance analysis is done on the predicted results.

Feature Extracting Method	Prediction Rate (%)	Precision	Accuracy (%)	Error (%)	TN	FP	FN	TP	TPR (%)	FPR (%)
GLCM	94.33	1	94.33	5.9	10	0	1	4	80.0	0
GLRLM	93.33	1	93.33	6.6	6.6	0	1	8	88.8	0
Auto Regression	60.00	0.625	60.00	33.33	5	3	2	5	71.42	37.5
Histogram	93.33	1	93.33	6.66	8	0	1	6	85.714	0
Gradient	92.5	1	92.50	6.710	7	0	1	7	87.50	0

Table 5.1: Final Results based on Random Forest Prediction (Machine Learning)

5.2 Discussion

Confusion matrix has been applied on the prediction of all the feature extracting methods and got into a conclusion by looking at the above results that GLCM gives the most accurate result and most précised results and Auto Regression gave the least précised results. In case of the error, Auto Regression gave the highest error rate on the other hand GLCM gave the lowest error rate. From the results it is stated that if given enough data, the faulty part of an electrical component can be predicted and if GLCM technique is used as feature extracting method then usage of redundant features will be eliminated as well.

Chapter 6

Conclusion and Future Scope

6.1 Conclusion

In this thesis work, the primary objective was to analyze features extraction techniques from a good number of electrical equipment for condition monitoring to find the best feature extraction method. For that purpose, 24 thermal images of different electrical equipment were collected. Then by using Fluke Connect Software, the images were converted into grayscale that later had been enhanced. Original grayscale images also went through Image Segmentation process for further use and 'Moments' thresholding technique was applied here by ImageJ Software. After that, those segmented images were used to detect the heated and normal zone as two different ROI and by loading corresponding enhanced grayscale images upon it, the texture features were extracted. GLCM, GLRLM, Gradient, Histogram and Auto Regression techniques were used by MaZda Software for finding several features. Then by using Machine Learning technique, the performance parameters of each feature methods were calculated. The final results had been made where it is shown that GLCM Feature Extraction Technique is the most convenient for the users.

6.2 Future Scope

A promising device with IR Camera can be made and installed for condition monitoring where the actual features found from the GLCM Method will be fed. That device should be able to read the heat signature and find texture features continuously and compare them with the actual features that were previously fed and if found any discrepancy, it should be able to isolate that electrical equipment while notifying the user. Thus, the hassle of using multiple feature extraction method will be eradicated. User can rely upon only one feature extraction method and hereby, the safety of electrical equipment can be ensured. It should also be mentioned that

the samples that have been compared to the samples which are required to do a prefect prediction and calculation in ML is really low. In the future, if we get a chance and get some more samples to feed our system that will increase the chance of correct prediction also the error would be reduced as well. Moreover, the process used in this thesis work can be repeated with more different electrical equipment to get the best outcome for choosing right feature extraction methods in future.

References

[1] Lucas, Jim. (2019, February 27). What Is Infrared? LiveScience. Retrieved from www.livescience.com/50260-infrared-radiation.html#:~:text=Infrared%20radiation%20(IR)%2C%20or,are%20the%20sun%20and%20fire.

[2] Penn State Department of Meteorology. (n.d.). The Four Laws of Radiation. Retrieved from https://learningweather.psu.edu/node/18.

[3] Kaur, Dilpreet, and Yadwinder Kaur. "Various image segmentation techniques: a review." International Journal of Computer Science and Mobile Computing 3.5 (2014): 809-814.

[4] Szczypinski, Piotr M., Michal Strzelecki, and Andrzej Materka. "Mazda-a software for texture analysis." 2007 international symposium on information technology convergence (ISITC 2007). IEEE, 2007.

[5] Agwu, Kenneth K., and C. Ohagwu. "Histogram-based texture characterization and classification of brain tissues in non-contrast CT images of stroke patients." Pattern Recognition-Analysis and Applications (2016): 81-108.

[6] Nailon, William Henry. "Texture analysis methods for medical image characterisation." Biomedical imaging 75 (2010): 100.

[7] Tang, Xiaoou. "Texture information in run-length matrices." IEEE transactions on image processing 7.11 (1998): 1602-1609.

[8] Galloway, Mary M. "Texture analysis using gray level run lengths." Computer graphics and image processing 4.2 (1975): 172-179.

[9] Kumar, Indrajeet, Jitendra Virmani, and H. S. Bhadauria. "Optimization of ROI size for development of computer assisted framework for breast tissue pattern

characterization using digitized screen film mammograms." Machine Learning in Bio-Signal Analysis and Diagnostic Imaging. Academic Press, 2019. 127-157.

[10]   Subramanya, M. B., and Jitendra Virmani. "A DEFS Based System for Differential Diagnosis Between Severe Fatty Liver and Cirrhotic Liver Using Ultrasound Images." Machine Learning in Bio-Signal Analysis and Diagnostic Imaging. Academic Press, 2019. 53-72.

[11]   Al-Kilidar, Suhair HS, and Loay E. George. "Texture Classification Using Gradient Features with Artificial Neural Network." Journal of Southwest Jiaotong University 55.1 (2020).

[12]   Agwu, Kenneth K., and C. Ohagwu. "Histogram-based texture characterization and classification of brain tissues in non-contrast CT images of stroke patients." Pattern Recognition-Analysis and Applications (2016): 81-108.

[13]   Bansal, S. (2021, March 22). Supervised and Unsupervised learning. Retrieved from https://www.geeksforgeeks.org/supervised-unsupervised-learning/

[14]   Google Developers. (2020, October 2). Training and Test Sets: Splitting Data. Retrieved from https://developers.google.com/machine-learning/crash-course/training-and-test-sets/splitting-data/

[15]   Navlani, A. (2018, May 16). Understanding Random Forests Classifiers in Python. Retrieved from https://www.datacamp.com/community/tutorials/random-forests-classifier-python/

[16]   Nitin1901. (2020, August 21). Confusion Matrix in Machine Learning. Retrieved from https://www.geeksforgeeks.org/confusion-matrix-machine-learning/